Vol. 63 • No. 5
May 2020

Microwave Journal

horizon house®
Founded in 1958
mwjournal.com


ANALOG DEVICES
AHEAD OF WHAT'S POSSIBLE™
COMMUNICATIONS
RADAR
ELECTRONIC WARFARE
We Have You Covered from Alpha to Zulu
The industry's most complete portfolio of ICs and modules—from RF to bits.
RF/µW Amplifiers/ TR Modules
Analog Beamforming
Frequency Conversion
Converters and Transceivers
ADC
DAC
Power
Find your competitive advantage at analog.com/ADEF


K&L MICROWAVE
a DOVER company
Your 5G/LTE Testing Solution
LOS ANGELES 2020
CONNECTIVITY MATTERS
Visit us at IMS 2020
Booth #1123
Amplifiers and Signal Generators
+ Plus +
K&L Microwave Filters
= Equals =
Cost Effective
Custom Test Solutions
K&L Triplexer
Tx1 Filter
Tx2 Filter
Rx Filter
D.U.T
Low PIM Termination
Spectrum Analyzer
For more information please visit:
www.klmicrowave.com/catalog/KLIMDWeb.pdf
Microwave Products Group
a DOVER company
K&L MICROWAVE
POLE ZERO
BSC
DowKey Microwave
ENABLING COMMUNICATION AND SIGNAL CONTROL
www.klmicrowave.com • www.klfilterwizard.com • 410-749-2424 • sales@klmicrowave.com •


Relax
We've got you covered
Your supplier of high performance, precise equipment for AWGN
NOISEWAVE
The new wave in NOISE
Ph. (973) 386-1119 • Fax (973) 386-1131 • info@noisewave.com • www.noisewave.com

apitech™

www.apitech.com

RF & Microwave Components, Subsystems & Solutions

SPACE • COMMUNICATIONS • INDUSTRIAL • DEFENSE

RF & Microwave components and technologies from our Inmet & Weinschel brands. Delivering quality innovation for more than 60 years.

- Coaxial Fixed Attenuators
- Programmable Attenuators and Subsystems
- RF Switching and Signal Distribution Units
- RF Switch and Attenuation Matricies
- Coaxial Terminations
- Bias Tees, DC Blocks and Power Dividers
- Gain Equalizers and Phase Shifters
- Adapters, Connectors and Accessories
- Surface Mount Attenuators, Terminations, Resistors

Microwave Journal
May 2020
Vol. 63 • No. 5
5G & MTT-S IMS Show Issue
mwjournal.com

CONTENTS

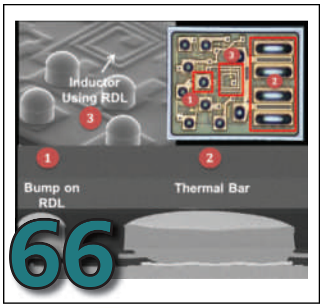

online spotlight

Look for this month's exclusive article online at mwjournal.com

Publisher's Note

Cover Feature

MVP: Most Valuable Product

Special Report

Technical Features

Application Note

63 YEARS OF PUBLISHING EXCELLENCE

Microwave Journal

CONTENTS

mwjournal.com

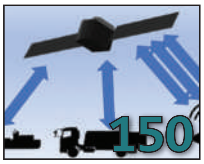

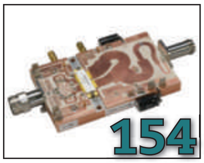

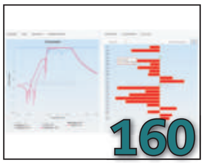

Product Features

Tech Briefs

Microwave Journal (USPS 396-250) (ISSN 0192-6225) is published monthly by Horizon House Publications Inc., 685 Canton St., Norwood, MA 02062. Periodicals postage paid at Norwood, MA 02062 and additional mailing offices.

POSTMASTER: Send address corrections to Microwave Journal, PO Box 1028, Lowell, MA 01853 or e-mail mwj@e-circ.net.com. Subscription information: (978) 671-0446. This journal is issued without charge upon written request to qualified persons working in the RF & microwave industry. Other subscriptions are: domestic, $120.00 per year, two-year subscriptions, $185.00; foreign, $200.00 per year, two-year subscriptions, $370.00; back issues (if available) and single copies, $10.00 domestic and $20.00 foreign. Claims for missing issues must be filed within 90 days of date of issue for complimentary replacement.

STAFF

Publisher: Carl Sheffres
Associate Publisher: Michael Hallman
Editor: Patrick Hindle
Technical Editor: Gary Lerude
Managing Editor: Jennifer DiMarco
Associate Technical Editor: Cliff Drubin
Copy Editor: Kelley Roche
Multimedia Staff Editor: Barbara Walsh
Contributing Editor: Janine Love
Electronic Marketing Manager: Chris Stanfa
Senior Digital Content Specialist: Lauren Tully
Audience Development Manager: Carol Spach
Traffic Manager: Edward Kiessling
Director of Production & Distribution: Robert Bass
Art Director: Janice Levenson
Graphic Designer: Ann Pierce

EUROPE

Office Manager: Nina Plesu

CORPORATE STAFF

CEO: William M. Bazzy
President: Ivar Bazzy
Vice President: Jared Bazzy

EXECUTIVE EDITORIAL OFFICE
685 Canton Street, Norwood, MA 02062
Tel: (781) 769-9750
FAX: (781) 769-5037
e-mail: mwj@mwjournal.com

EUROPEAN EDITORIAL OFFICE
16 Sussex Street, London SW1V 4RW, England
Tel: Editorial: +44 207 596 8730 Sales: +44 207 596 8740
FAX: +44 207 596 8749

SUBSCRIPTION SERVICES
Send subscription inquiries and address changes to:
Tel: (978) 671-0446
e-mail: mwj@e-circ.net

BPA WORLDWIDE

www.mwjournal.com

Printed in the USA

Microwave Journal CONTENTS

mwjournal.com

Source: Los Angeles Convention Center

IEEE MTT-S International Microwave Symposium & Exhibition

Departments

Matchmaker

0402DC Series Designer's Kit (C472-2):
20 samples each of 112 inductance values,
including 0.1 nH increments from 2.8 nH to 10 nH

Looking for the perfect high-Q inductor for impedance matching in RF/microwave antenna circuits? This kit has it!

Coilcraft 0402DC Series wirewound chip inductors offer the industry's highest Q factors in an 0402 (1005) size for super low loss in high frequency circuits. And with 112 values from 0.8 to 120 nH, including **0.1 nH increments from 2.8 nH to 10 nH**, you'll have exactly what you need for all your RF and Microwave applications.

The 0402DC also features wirewound construction for extremely high self resonance – up to 28.8 GHz – and offers DCR as low as 25 mΩ, significantly lower than other inductors this size.

Equip your lab with the ultimate impedance matching resource. Our C472-2 Designer's Kit has 20 samples of all 112 values! Purchase one online at **www.coilcraft.com/0402DC.**

Coilcraft®

coilcraftdirect.com
No min order. Next day delivery.

WWW.COILCRAFT.COM

Microwave Journal Online

Visit us @ mwjournal.com

E LEARNING CENTER

Optimizing Peak-to-Average Power Ratio for Wireless Systems
Sponsored by: Boonton and Tabor Electronics 5/6

The Rebirth of HF
Sponsored by: Rohde & Schwarz 5/13

Executive Interviews

Jakub Kucera, cofounder and CEO of test and measurement firm **AnaPico**, discusses the company's founding, growing portfolio of instruments, and its successful strategy tapping Switzerland's reputation for quality, engineering and manufacturing.

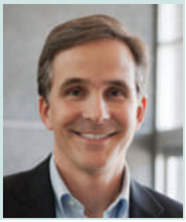

James Thompson, executive VP of engineering and CTO of **Qualcomm Technologies**, discusses Qualcomm's culture of innovation, from CDMA to 5G; its advocacy of mmWave in the smartphone; and the vision of a 5G-AI-cloud computing world.

FEATURED e-Books

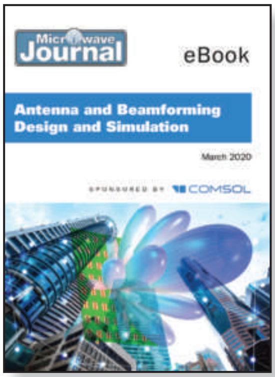

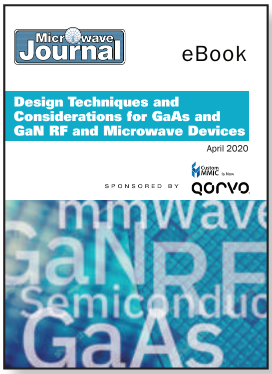

mwjournal.com/ebooks

WHITE PAPERS

Roos Instruments — Modular ATE for the World's Most Advanced Technology
ATE Strategy For mmWave Mass Market Production

Gate Drive Measurement Considerations

ROHDE&SCHWARZ — Make ideas real
Minimize Measurement Uncertainty for EIRP OTA Measurements

The Rebirth of HF

Norsat International Inc.
Topic: Radio Over Satellite

Join Us Online

Follow us
@Pathindle
@MWJGary
@MWJEditor

Join us at the RF and Microwave Community

Become a fan at facebook.com/microwavejournal

Catch *Frequency Matters*, the industry update from *Microwave Journal*,
microwavejournal.com/FrequencyMatters

COM

JUNE

MICROWAVE WEEK 2020

IMS
Connecting Minds. Exchanging Ideas.

ARFTG

RFIC: June 21-23
IMS: June 21-26
ARFTG Conference June 26

LOS ANGELES 2020
CONNECTIVITY MATTERS

21-26

IEEE MTT-S IMS 2020

Los Angeles, Calif.

The IEEE MTT-S International Microwave Symposium (IMS) brings together technologists involved in all aspects of microwave theory and practice. Attendees experience a full week of events including technical paper presentations, workshops and tutorials, as well as numerous social events and networking opportunities.

www.ims-ieee.org

Catch our exclusive conference information, news, social networking, photos, videos and more at: mwjournal.com/IMS2020

2

Call for Papers Deadline

The International Semiconductor Conference (CAS), an IEEE event since 1995, is targeting not only semiconductor electronics, but also micro- and nanotechnologies including micro-nanosystems.

www.imt.ro/cas

15

Call for Papers Deadline

ASDAM 2020

Washington, DC

The International Conference on Advanced Semiconductor Devices and Microsystems (ASDAM) 2020 is devoted to the latest results of research and development in the field of new semiconductor devices and microsystems. Its goal is to bring together leading experts from institutes and universities as well as companies interested in the progress of high technology devices and microsystems.

elu.sav.sk/asdam

Hear From Industry Experts: Frequency Matters Podcasts

In the latest episodes, Microwave Journal editors Pat Hindle and Gary Lerude talk with Qorvo about the A&D/5G Infrastructure market, Anokiwave about the 5G/SATCOM mmWave market and Marki Microwave about the evolution of the company from a hybrid mixer company to a cutting edge MMIC company.

FOR DETAILS, VISIT MWJOURNAL.COM/EVENTS

Coming**Events**

CALL FOR PAPERS

2020 IEEE BiCMOS and Compound Semiconductor Integrated Circuits and Technology Symposium (BCICTS)
May 9

APMC 2020
May 31

IEEE IMaRC 2020
July 15

IEEE Women in Engineering Forum USA East
September 1

mwjournal.com

JUNE

IEEE MTT-S IMS 2020
June 21-26 • Los Angeles, Calif.
http://ims-ieee.org

Sensors Expo & Conference
June 22-24 • San Jose, Calif.
www.sensorsexpo.com

95th ARFTG Conference
June 26 • Los Angeles, Calif.
www.arftg.org

JULY

SEMICON WEST 2020
July 21-23 • San Francisco, Calif.
www.semiconwest.org

IEEE EMC+SIPI 2020
July 27-31 • Reno, Nev.
www.emc2020.emcss.org

AUGUST

AUVSI's Xponential
August 9-12 • Boston, Mass.
www.xponential.org

Space Tech Expo USA 2020
August 10-12 • Long Beach, Calif.
www.spacetechexpo.com

5G Antenna Systems
August 26 • Dallas, Texas
www.antennasonline.com

SEPTEMBER

RFIT 2020
September 2-4 • Hiroshima, Japan
www.rfit2020.org

EuMW
September 13-18 • Utrecht, The Netherlands
www.eumweek.com

EDI CON China 2020
September 27-28 • Bejing, China
www.ediconchina.com

OCTOBER

EDICON Online
October 6, 13, 20 & 27
www.ediconononline.com

MWC Los Angeles
October 28-30 • Los Angeles, Calif.
www.mwclosangeles.com

NOVEMBER

AMTA 2020
November 1-6 • Newport, R.I.
www.amta2020.org

Global MilSatCom
November 3-5 • London, U.K.
www.globalmilsatcom.com

2020 IEEE BiCMOS and BCICTS
November 7-11 • Monterey, Calif.
https://bcicts.org/

IEEE Women in Engineering Forum USA East
November 12-14 • Providence, R.I.
http://attend.iee.org/wie-forum-usa-east-2020

Space Tech Expo Europe 2020
November 17-19 • Bremen, Germany
www.spacetechexpo.eu

DECEMBER

WAMICON 2020
December 1-3 • Clearwater, Fla.
www.wamicon.org

AOC International Symposium & Convention 2020
December 8-10 • Washington D.C.
www.crows.org/mpage/2020HOME

Has Amplifier Performance or

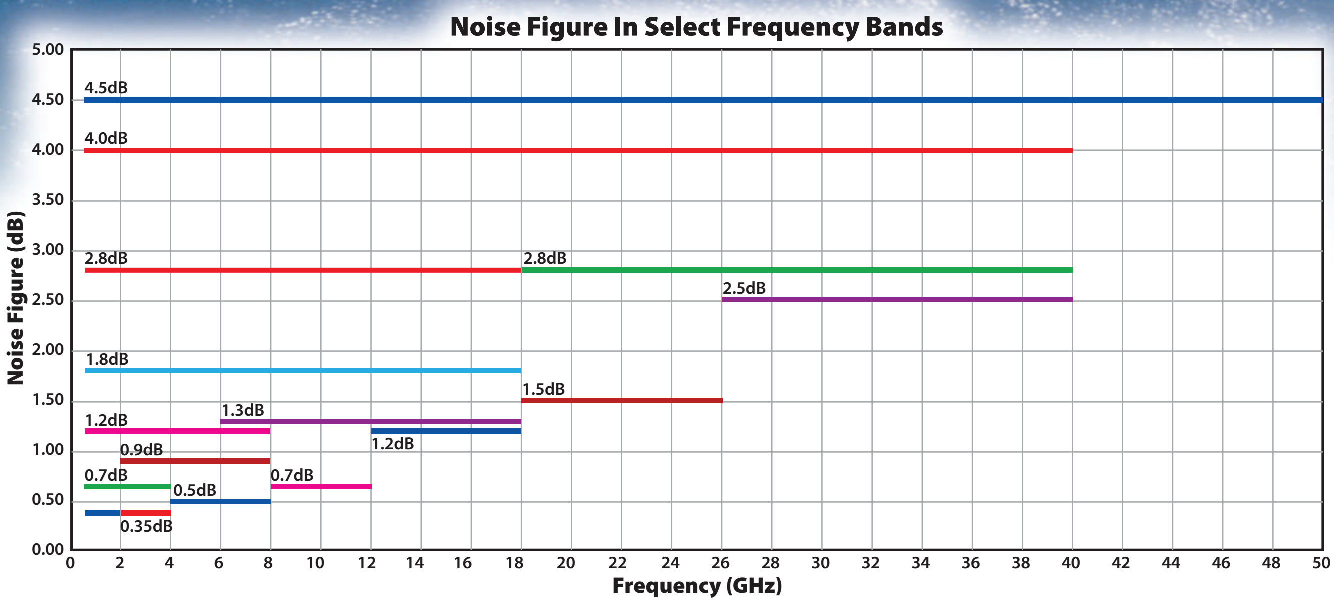

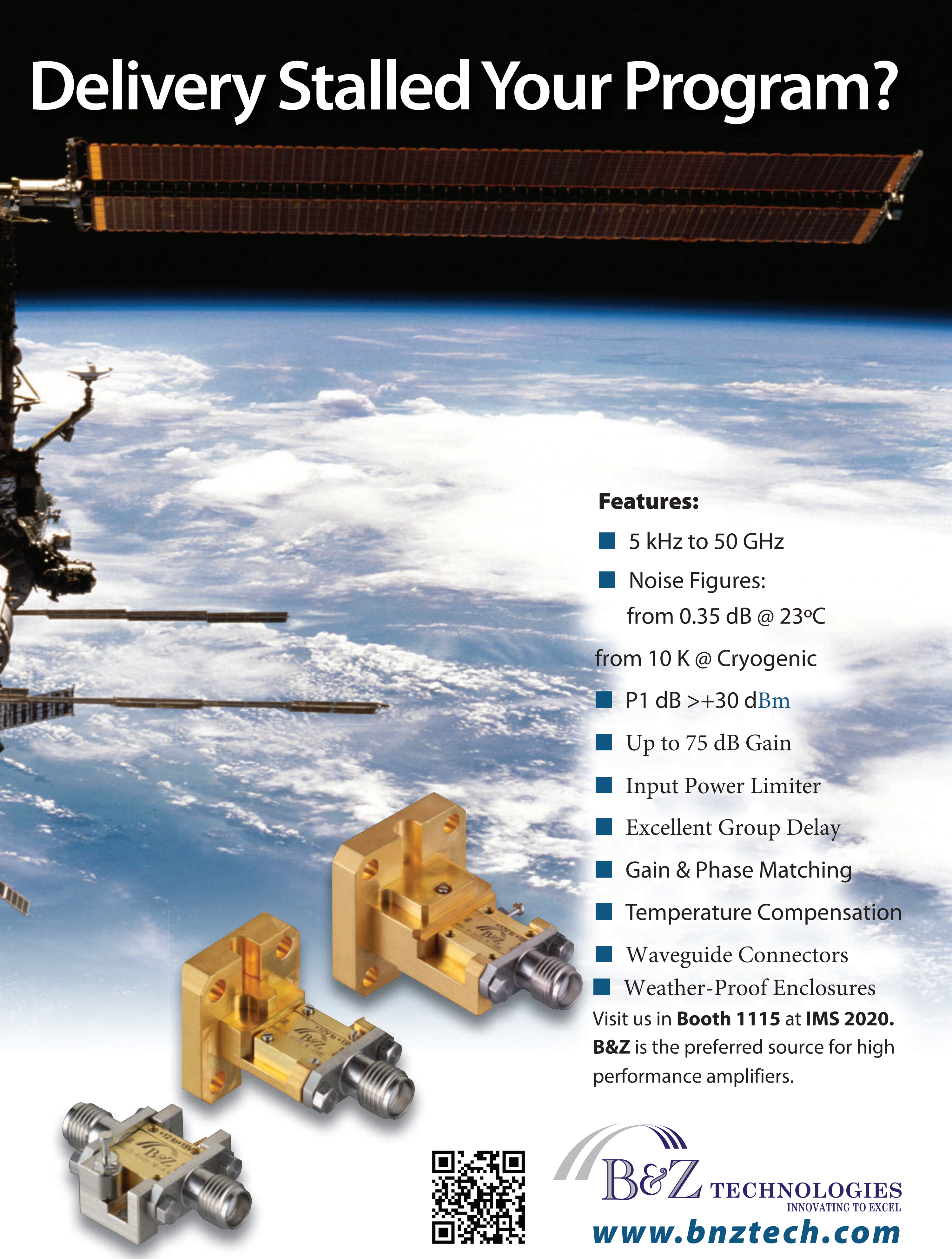
Delivery Stalled Your Program?
Features:
5 kHz to 50 GHz
Noise Figures:
from 0.35 dB @ 23°C
from 10 K @ Cryogenic
P1 dB >+30 dBm
Up to 75 dB Gain
Input Power Limiter
Excellent Group Delay
Gain & Phase Matching
Temperature Compensation
Waveguide Connectors
Weather-Proof Enclosures
Visit us in Booth 1115 at IMS 2020.
B&Z is the preferred source for high performance amplifiers.
B&Z TECHNOLOGIES
INNOVATING TO EXCEL
www.bnztech.com

Navigating These Uncertain Times

Carl Sheffres
Microwave Journal *Publisher*

It seems like just yesterday that I was making travel arrangements to Asia to visit clients and partners in preparation of our EDI CON China event in May. Needless to say, that trip did not happen and the event has been postponed to the Fall. Instead, I sit here in my home office (actually, my dining room table) on the first Sunday of April wondering, like most people, when this crisis will begin to subside.

As you read this column a month or so later, my hope is that life has begun to normalize, despite the human and economic pain that has been endured. Many of you work for companies that are considered essential and many more are working remotely. Our industry carries on, providing products and technology for critical wireless and defense applications.

By now, we should know the status of more industry events, including IMS. Live events have always been an integral part of the year for many of us. We plan our marketing campaigns around them, our travel plans and our sales meetings. Some of you present papers on the great work that you are doing and many of us are able to listen and learn. We look forward most to catching up with industry friends and colleagues. We could use that more now than ever.

At Microwave Journal, our goal is to deliver information in multiple formats; print and digital, live and virtual. We organize several live exhibitions, including European Microwave Week (EuMW) on behalf of the European Microwave Association and the aforementioned EDI CON China. EuMW is scheduled for September 13-18 in Utrecht, The Netherlands. EDI CON China will take place in the fall as well.

We launched EDI CON Online last year with great success and have expanded the conference to four days, with tracks covering 5G/IoT/Automotive (October 6), PCB/Interconnect Design (October 13), Signal Integrity/Power Integrity (October 20) and Radar/Antennas (October 27). IEEE has approved the technical sessions for Continuing Education Units (CEUs) and Professional Development Hours (PDHs). This event is produced in conjunction with our sister media resource, Signal Integrity Journal. If you have not yet checked out this peer-reviewed portal of SI/PI knowledge, I encourage you to do so. It is not too late to subscribe to the July print edition either.

We have seen a distinct uptick in webinar activity in this time of social distancing. The number of companies that are utilizing this tool has increased significantly, as has audience engagement. The same is true for white papers and eBooks. We are seeing more quality content coming from the industry and more downloads from readers. We are offering companies the opportunity to present their latest offerings via 30-minute webinars in place of the launches they had planned for some now-cancelled live events. Our long-running video series titled "Frequency Matters" has continued twice monthly, with editors Pat Hindle and Gary Lerude broadcasting from their homes via the Zoom platform. They have launched a new podcast series as well, the latest featuring experts from Marki Microwave discussing the evolution of their company. Look for more innovative content in the year ahead.

This issue of Microwave Journal serves as both the show issue for the IEEE MTT-S International Microwave Symposium and has editorial focus on 5G. It features a cover story from Qualcomm on "The Evolution of Cellular Technology: The Long Road to 5G." That road has recently gotten longer, with the pandemic delaying pilot deployments across the globe.

Lastly, I remind you that this "magazine" is available in print, digital, online and mobile formats. You can always update your profile and preferences on our website under "My Account" at the top. While you are there, make sure to register, in order to access all of the content that we publish.

We will survive this crisis together. In the meantime, stay healthy and safe. I hope to catch up with you soon. ■

ATC 531Z Broadband Multilayer Capacitors

Low Insertion Loss from 16 KHz to 30 GHz

Advantages:

- Broadband Performance
- Low insertion Loss
- Flat Frequency Response
- Excellent Return Loss
- Unit-to-Unit Performance Repeatability
- Rugged Ceramic Construction

Features:

- EIA 0201Case Size
- Capacitance: 100 nF
- Operating Frequency: 16 KHz to 30 GHz
- Insertion Loss: <0.5 dB typ.
- Low Loss X5R Dielectric
- Voltage Rating: 16 WVDC
- Solderable SMT Terminations
- RoHS Compliant

531Z Insertion Loss (S21)

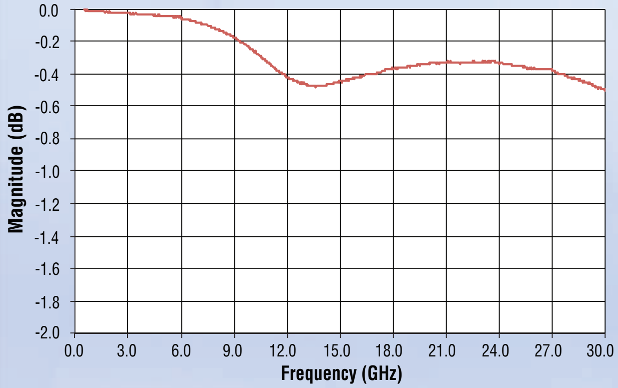

531Z Return Loss (S11)

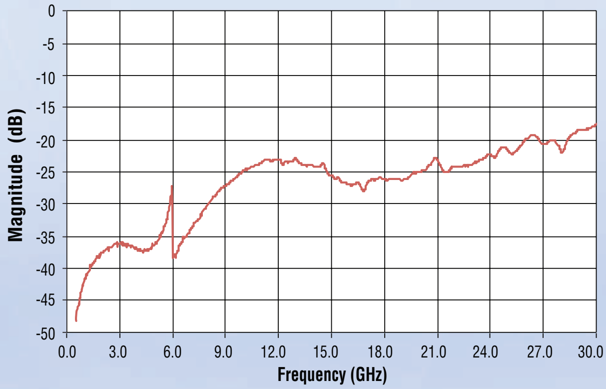

RoHS Compliant

AMERICAN TECHNICAL CERAMICS
AN AVX GROUP COMPANY

THE ENGINEERS' CHOICE
ISO 9001 REGISTERED COMPANY

www.atceramics.com

THE ENGINEERS' CHOICE®

The Evolution of Cellular Technology: The Long Road to 5G

Gary Lerude
Microwave Journal, Norwood, Mass.

This is the story of Qualcomm, a company that started in sunny San Diego in the summer of 1985, and its impact on the evolution of cellular technology. Qualcomm's success reflects its pioneering role inventing technologies with the potential to radically shape our lives, then successfully bringing them to life. What has made Qualcomm unique is its seemingly insatiable pursuit of innovation, based on a culture where ideas brew rapidly. This began with the collective vision of the founders, Irwin Jacobs and six colleagues—Andrew Viterbi, Adelia Coffman, Andrew Cohen, Franklin Antonia, Harvey White and Klein Gilhousen—who left Linkabit to start "QUALity COMMunications," initially pursuing government R&D contracts (see ***Figure 1***).

FROM 1G TO DIGITAL COMMUNICATION

The early cellular networks in the U.S. were based on the Advanced Mobile Phone System (AMPS) standard, an analog technology which boosted cellular capacity compared to the erstwhile mobile telephone system (MTS). Once Americans knew the convenience of carrying a phone while on the move, they no longer wanted the limitation of landline telephones. This opened the initial sluicegate of cellular phone usage, prompting mobile operators to scramble to install more cell towers to add capacity. However, the operators soon realized that adding cell towers was too costly to be sustainable, so they asked the Federal Communications Commission (FCC) to allocate additional spectrum. New spectrum was only a short-term fix, though, challenging operators to find a long-term solution to meet the continuously growing demand.

Fig. 1 **Early Qualcomm brochure showing the company founders and employees.**

Cellular was analog, while the booming computer world was digital. For the cellular industry to evolve and become a technology for the masses, it had to find a path to the digital world. At that time, not many foresaw the fledgling cellular technology converging with the computer industry to create today's digital world. Few had explored digital communication as a viable solution for cellular, which created an opportunity for Qualcomm to apply its experience developing digital communications for military and satellite systems. This led the cellular industry to be introduced to a technology called code division multiple access (CDMA).

CDMA, A NOVEL IDEA

To support the growth of cellular, the Cellular Telecommunications Industry Association (CTIA) saw the need for a digital wireless standard to increase capacity and improve quality. Responding, Qualcomm pitched a novel and little understood technology based on CDMA. CDMA used spread-spectrum techniques, a complex and very different approach from how the airwaves were being used by better known access technologies: frequency-division multiple access (FDMA) and time-division multiple access (TDMA). With CDMA, multiple users with unique codes share a single, wide bandwidth channel, which significantly increases capacity (see ***Figure 2***).

Many operators had difficulty visualizing CDMA, much less believing it could work in the "real world." Some "experts" argued it was too nascent to scale commercially. While the theoretical ben-

smiths interconnect

CEX Series

High Frequency Chip Equalizers

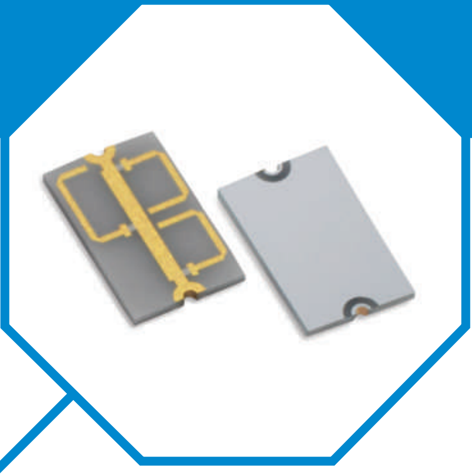

Design flexibility ensures precise gain compensation over frequency

- Configurable design approach providing optimized solutions for gain variation over frequency
- Multiple slope options (1-4 dB) and excellent slope linearity (±0.25 dB or better)
- Frequency offering up to 40 GHz supporting a wide array of markets and applications

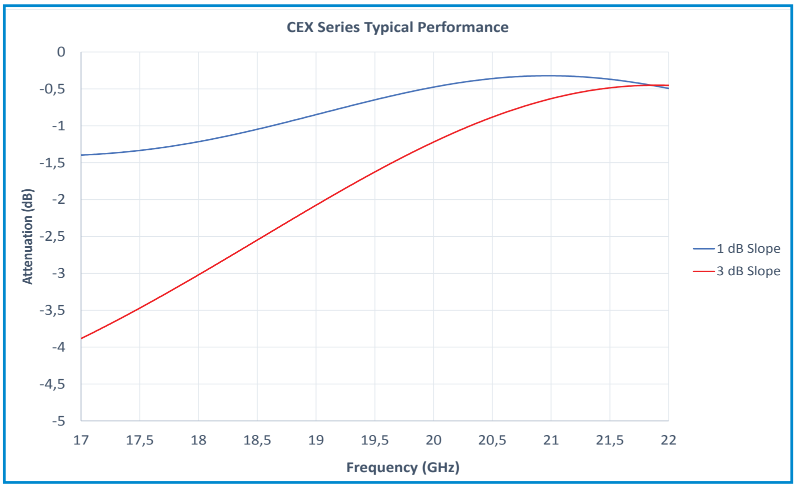

Excellent slope linearity, insertion loss and VSWR within the specified frequency band

more > smithsinterconnect.com

efits of CDMA were impressive, several technical hurdles limited it from being considered for cellular communication. First was transmit power, also referred to as the "near-far problem." The transmit power from a CDMA user near a tower could block everyone further away. The second challenge was known as the "single channel problem." Using the same channel on all towers, devices located between towers could cause interference to users connected to the other tower. A third issue was system acquisition time, how long it took for a device to find the network after powering on.

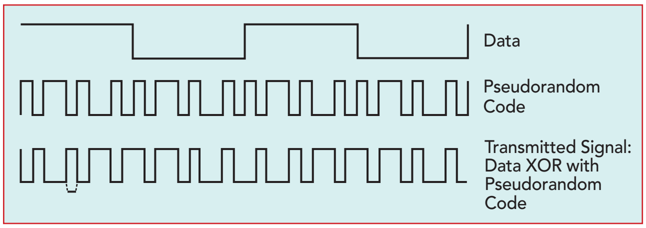

Fig. 2 **With CDMA, each user's data has a unique code that enables many users to share a single, wide bandwidth channel.**

Qualcomm developed solutions to overcome these and other challenges, innovations such as fast power control, soft handover and a common pilot signal using GPS. However, by the time Qualcomm introduced these solutions, TDMA had established a strong foothold. The Telecommunications Industry Association (TIA) and the CTIA had announced TDMA as the cellular standard for digital communication. This was a major blow to Qualcomm, leading industry experts to predict an early exit for the company and CDMA; they believed CDMA would be limited to military and satellite communications or academia. However, Jacobs and his team believed CDMA was the right long-term solution for cellular standards because it would provide much higher capacity as well as better quality of service. For operators, this meant satisfied users and the capacity to serve more of them. Qualcomm continued researching and improving CDMA, and with persistence and persuasive demonstrations to policy drivers and regulators, the company successfully convinced the FCC to allow any operator the option to deploy CDMA.

This was a big win, and it was not long before some operators did. However, if CDMA were to become the digital communication standard in the U.S., Qualcomm did not have much time. Turning a policy win into commercial success required wide availability of cellular phone components in volume, which was challenging because of the complexity to implement CDMA. While manufacturing was not a Qualcomm core competency, the company made a strategic decision to apply its expertise with CDMA to design the ASICs which would implement the most complex elements of the technology. To further bootstrap the ecosystem, Qualcomm established a joint venture to produce mobile phones (see ***Figure 3***), which helped convince the supply chain that CDMA technology was ready for the mass

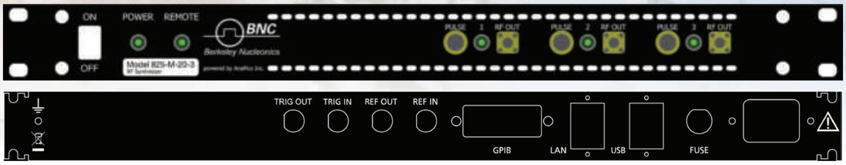

Model 825-M-20

Model 875

market. The decision to design its own ASICs and phones paid long-term dividends, adding valuable system knowledge which Qualcomm transformed into a leading market position in cellular modems and processors.

Although the market outlook for CDMA was improving, Qualcomm still faced challenges, including a significant cash crunch. To raise funding, the company released an initial public offering (IPO) of stock on December 16, 1991 and the price rose more than 50 percent within two weeks. However, the market's optimism was short-lived; in January, the CTIA endorsed TDMA as the preferred cellular standard, largely erasing the gains from the IPO. Disappointed, yet undaunted, Qualcomm continued to develop and promote CDMA. By the end of 1993, the TIA had adopted CDMA as the digital cellular standard for 2G in the U.S., leading to it being selected by several operators in the U.S. and Korea. In Europe, GSM was the 2G digital standard, having been developed by the European Telecommunications Standards Institute (ETSI) and adopted in 1987 by 13 European countries as a mandatory standard for Europe.

3G AND THE MOBILE INTERNET

When the International Telecommunication Union finalized the requirements for IMT-2000—popularly known as "3G"—CDMA's position as the preferred technology expanded beyond the U.S. and Korea. As part of 3G, Qualcomm advanced CDMA with higher speeds and capacity in an evolved standard called cdma2000. Europe and Japan developed a 3G CDMA standard called wideband CDMA (WCDMA). Even though the cdma2000 was slightly different than WCDMA, the two standards bodies worked to harmonize key aspects. After years of technology investment and development, CDMA had been adopted as the global cellular standard, confirming Qualcomm's early vision.

▲ Fig. 3 **Qualcomm QCP-2700 cellular phone, which operated on the 800 MHz analog and 1900 MHz CDMA networks.** ***Source:*** **Ben Schumin, Wikimedia Commons.**

Although voice calls were the primary cellular service during the 1990s, Qualcomm had been laying the foundation for high speed data applications. "Evolution data optimized" (EV-DO) introduced an IP packet-based network design to enable high speed mobile broadband services. EV-DO adopted networking technology from the computer industry, departing from the circuit-switched standard long used for telephone service. Among other innovations, EV-DO provided an enhancement called "opportunistic scheduling," which is still used in advanced cellular technologies. Opportunistic scheduling uses smaller data packets, exchanged "opportunistically" between a device and the base station when radio conditions are optimum. An upgrade to EV-DO enabled mobile terminals to communicate with the network using multiple RF carriers (see ***Figure 4***). To enable these capabilities, Qualcomm envisioned combining the cellular modem with a powerful processor with graphics, making the mobile phone a handheld computer. The success of the EV-DO structure was affirmed when key aspects were integrated into high speed packet access (HSPA).

Motivating its technology development, Qualcomm realized that wireless technologies are only successful when they embrace the entire ecosystem. As well as increasing the data capacity of the network,

ADVERTORIAL:

The Competitive Advantage of Specialty Materials

Resonators, Filters, and other RF to mmWave Passives

The microwave and millimeter-wave (mmWave) industries are in a period of rapid flux. The increasingly cluttered sub-6 GHz spectrum is causing many emerging and evolving applications to transition to higher frequencies, including satellite communications, terrestrial wireless communications, aerospace communications, and military/defense communications and sensing. This transition is now leading to unforeseen interference and cosite issues that are, in turn, pushing radar and radionavigation system manufacturers to either move to even higher frequencies or to use more complex modulation techniques to mitigate the growth in spectrum congestion from new wireless technologies and services of interference.

All the while, there are a greater number of applications that rely ever more heavily on radionavigation, communication, and sensing technologies including unmanned, naval, land mobile, and commercial/military aerospace systems. High performance resonator technology is now becoming increasingly valuable for virtually every application including bandpass filtering, notch filtering, electromagnetic compliance (EMC), passive intermodulation (PIM) filtering, and broadband duplexing/multiplexing.

The key considerations for high quality filters are the resonator technology and overall filter design and manufacturing expertise. Though clever filter design can overcome some of the limitations of low quality resonator materials, inferior resonator materials can lead to other detrimental factors, especially at microwave and mmWave frequencies. Many of the applications that employ microwave and mmWave filters also require these devices to be thermally, and otherwise, environmentally stable. High quality resonator materials and design are necessary to ensure that a filter performs as designed in all environments. Filter complexity is also significantly reduced through the use of high quality resonators, directly reducing the size and cost of a filter relative to filters designed with low quality resonators.

For these reasons, and many others, it is even more crucial for systems integrators and microwave/mmWave system manufacturers to have access to a supplier that leverages the use of both high quality dielectric resonators/substrates as well as the filter and passive component design expertise necessary to realize the benefits of such high quality materials. This is why MCV Microwave has made addressing the customer's microwave and mmWave resonator, filter, and other passive components challenges it's mission since 1995. **With truly vertically integrated filter and component manufacturing, MCV is the ideal supplier to support quick-turn high-reliability (Hi-Rel) defense/aerospace and 5G/IoT commercial wireless communication applications.**

About MCV

MCV Technologies, Inc. DBA MCV Microwave (ITAR registered) is one of the few companies to earn ISO Standard 9001:2015 certification for the design and manufacture of Advanced Dielectric Resonators, RF/Microwave FIlters, connector assemblies and adaptors as well as having been successfully audited and certified to AS9100 Rev. D standard for the aerospace industry to meet the International Aerospace Quality Group (IAQG) quality initiatives.





MCV MICROWAVE

To learn how MCV Microwave's products and designs can solve your filtering challenges, please contact MCV Microwave at:
+1 858-450-0468 | sales@mcv-microwave.com.

CERTIFIED ISO 9001:2015 COMPANY — CERTIFIED AS 9100D COMPANY — ITAR International Traffic in Arms Regulations Compliant

EV-DO/HSPA was a precursor to digitally connecting the world, whether people or "things." This capability enabled a class of new applications with a growing presence today: high speed browsing, multimedia exchange with rich media experience, low latency gaming and multicasting. Mobility with access to the Internet removed the limitation of desktop browsing and gaming, creating a more social and interactive experience we now view as normal.

The IP-based architecture of EV-DO/HSPA offered a flexible and cost-effective way to roll out applications and services. This proved a significant benefit to operators, enabling them to offer and monetize services. On-demand video and music streaming were being introduced, which accelerated data consumption on mobile devices.

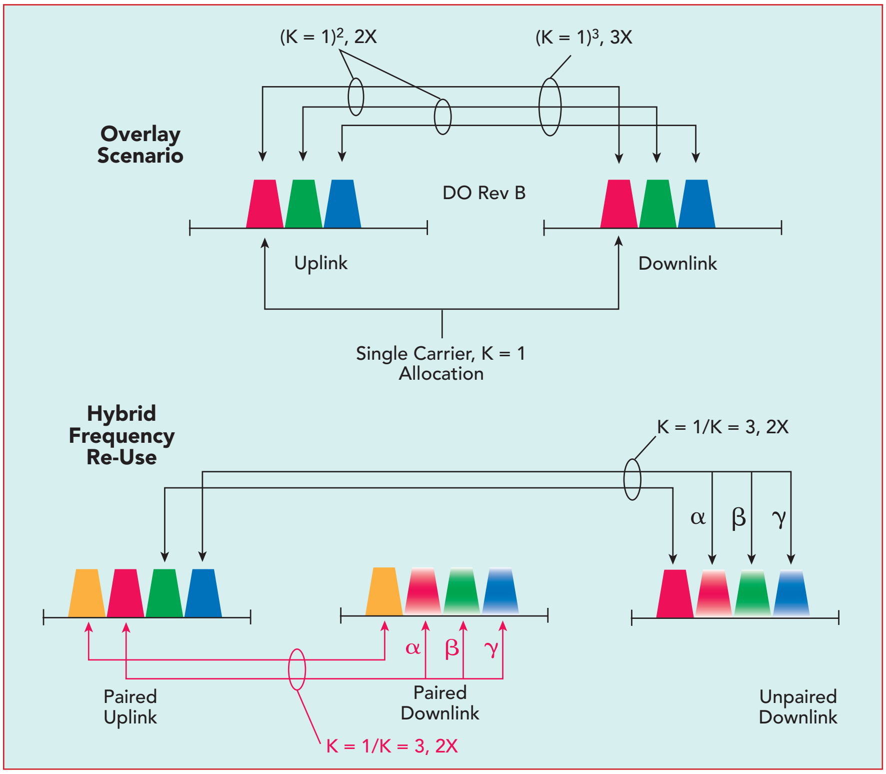

Fig. 4 **Multi-carrier capability introduced by EV-DO.**[1]

3G shifted what consumers expected from their phones, renamed handsets. Internet connectivity was rapidly becoming a necessity, and EV-DO had created the enabling technology. Its IP-based architecture was best suited to support high data rates and could be deployed in tandem with voice services, giving consumers both.

4G AND THE SMARTPHONE

CDMA had proven to be very efficient for channels up to 5 MHz bandwidth. For channels greater than 10 MHz, another access technology—orthogonal frequency-division multiplexing (OFDM)—was more efficient. OFDM uses multiple, narrowband subcarriers spread over a wide channel bandwidth. Recognizing the need to strengthen its capability in OFDM, Qualcomm acquired Flarion Technologies in 2006, which provided the framework for 4G/LTE.

The proliferation of voice, broadband internet and other data services, with the convergence of these industries, offered opportunities for new services and significantly more capacity to support them. Low power computing became exceedingly important as the cellular modem, embedded camera, graphics and multimedia were bundled to support multimedia applications. This was another capability Qualcomm had anticipated, first introducing mobile devices with integrated, low power computing in 2002.


Proven mmWave RF Solutions that Connect and Protect™
Unmanned Vehicles
Space and Satcom
Electronic Warfare
Phased Array Radar
QORVO CMD299K4
QORVO QPA2611
QORVO QPA2211
For Mission Critical Aerospace and Defense Applications
Since its inception, Qorvo® has focused on helping our customers overcome their toughest design challenges in aerospace and defense applications. Our MMIC design experience, portfolio of GaN/GaAs solutions combined with our extensive knowledge of the entire RF/microwave signal chain enable us to make your next system design a reality.
To find out how Qorvo solutions are All Around You®, visit www.qorvo.com
Custom MMIC Is Now
QORVO®

Higher data rates—well over 50 Mbps—and faster connection times were the driving forces that led to the 4G era. Smartphones, such as the iPhone, and the apps they spawned required higher data capacity. Additional antennas were integrated for both uplink and downlink, introducing the use of MIMO to significantly increase data speeds by creating multiple orthogonal data streams, called layers. MIMO could improve spectral efficiency without requiring more spectrum, scaling the network to support higher data speeds.

Launched in 2010, 4G enabled operators to offer OFDM-based services in conjunction with their existing 3G networks, creating the opportunity to expand their business models as wireless internet service providers. This convergence of networks and devices supporting both CDMA and OFDM enabled operators to assign the most appropriate access technology—3G CDMA, 4G, Bluetooth or Wi-Fi—depending on the requested service and location. The result was a more seamless experience for users. The rapid proliferation of 4G led to a "connected world" with billions of devices communicating with each other, exchanging data and offering users unprecedented lifestyle changes. The term "internet of things" (IoT) was coined as users found themselves connected to the things in the world around them, enabled by cellular IoT connections in homes, businesses, transportation, energy infrastructure, farms, hospitals and retail stores. 4G's all-IP architecture, inherent security and rapid global adoption further incentivized application developers to create innovative businesses using mobile devices, with Uber and Lyft as oft-cited examples.

UBIQUITOUS CONNECTIVITY

As 4G continued to develop capabilities, defined by the roadmaps for LTE-Advanced and LTE-Advanced Pro, the need for a next-generation cellular network, named 5G, was initially met with skepticism. Qualcomm was an early proponent. As with CDMA, it saw 5G as an innovation platform for a new decade, one that could power a significant shift in how the world uses mobile devices. To support the continuing upsurge in applications and foster use cases not yet conceived, Qualcomm believed 5G could unify a diverse range of spectrum and deployment scenarios, one that would scale across these varied applications.

In 2015, the initial requirements for 5G were published as the IMT-2020 standard, and the telecommunications industry began defining the wireless networking solution to meet a core set of requirements, including ultra-fast data rates, ultra-low latency and ubiquitous connectivity to many devices, virtually anywhere. Qualcomm worked with the mobile ecosystem of standards bodies, regulatory committees, operators, mobile device and infrastructure manufacturers and technology partners to define the standards that became the first embodiment of 5G. The 5G new radio (5G NR) is designed to handle a wide

range of services, deployments and spectrum bands; to do so, it uses many of the capabilities established in 3G and 4G: carrier aggregation, OFDM and MIMO. In release 15, the first standard defining the implementation of 5G, the 3GPP defined a foundation for NR that comprises five capabilities that were pioneered by Qualcomm (see ***Figure 5***): a flexible, slot-based framework; scalable OFDM air interface; advanced channel coding; massive MIMO; and the use of mmWave spectrum for mobile and fixed wireless access. Historically, mobile communication has used spectrum below 3 GHz. 5G expands that to higher frequencies: "mid-bands" to 6 GHz and "high-bands" above 24 GHz. Adding mmWave radios at existing 4G cell sites enables operators to significantly increase data rates, with shared sites enabling faster deployment at lower cost.

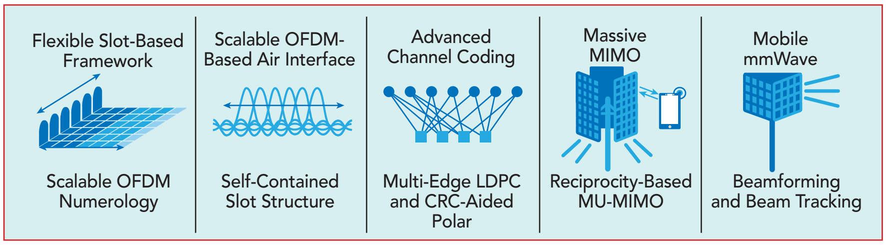

Fig. 5 **Elements of the 5G NR.**

mmWave was always considered unsuitable for mobile communication because of the perceived technical challenges, such as limited range, line-of-sight links and large parabolic antennas. However, Qualcomm saw mmWave as essential to realize the potential of 5G, analogous to its early belief in CDMA, and was a strong advocate. Field tests in 2015 showed robust non-line-of-sight propagation using multi-beam techniques; by 2018, Qualcomm, Ericsson, Nokia and Samsung had demonstrated 5G NR interoperability at the mmWave and mid-band frequencies; in 2019, mmWave radios began rolling out in commercial networks. In parallel, Qualcomm developed antenna front-end modules for the handset, the first and only supplier to offer a mmWave front-end. The antenna front-end module is controlled by its Snapdragon 5G modem to optimize handset performance, including battery life.

The evolution of 5G has already begun with 3GPP release 16, which will address once inconceivable vertical services, such as high-performance industrial automation and cellular vehicle-to-everything (C-V2X). Again, Qualcomm anticipated the need: in 2007, it began R&D on device-to-device proximity services, a foundation for C-V2X, integrated access and backhaul and IoT relays. Looking forward, AI will play an increasingly important role in devices and networks. Primarily concentrated in the cloud today, AI intelligence will be distributed between the device and the cloud, what is called the "intelligent wireless edge." With its

5G Technology – 600 MHz & 3500 MHz PIM Test Analyzers

For future 5G technology Rosenberger introduces low-PIM components as well as PIM test solutions for all applications – new rack and portable desktop analyzers, and band filter units for 600 MHz & 3500 MHz measurements.

The portable desktop analyzer offers high flexibility for measurements in production lines, R&D and test labs.

Rosenberger rack analyzers are designed to make PIM tests in production or test lab environments as modular, precise, and efficient as possible.

Due to the cost-effective broadband design up to 11 different band filters can be added to the broadband base unit. A fast band selection is possible via an optional switch matrix.

www.rosenberger.com/pia

Rosenberger

TABLE 1 EVOLUTION OF CELLULAR TECHNOLOGY

Generation	Analog	2G	3G	4G	5G
Services	Voice	Voice Text Messaging	Wireless Internet	Mobile Broadband	Enhanced Mobile Broadband Ultra-Reliable, Low-Latency Connections Massive # of Connections
Radio Access Technology	Analog FDMA	GSM TDMA CDMA	CDMA & WCDMA EVDO & HSPA	OFDMA	Scalable OFDMA

advanced network architecture, 5G can provide the framework to connect AI-powered devices with each other and the cloud, to enhance user experience, network efficiency and improve data security and privacy.

SUMMARY

The evolution of cellular technology, from analog to 5G (see ***Table 1***), has been a long road, requiring vision and persistence. Arguably, no company more than Qualcomm has played such a pivotal role in developing and commercializing mobile technology, leading to the connected world we enjoy today.

The 5G story will be one of momentum, evolution and transformation, leading to an even more connected world, expanding beyond consumers to industrial applications and health care. IHS Markit estimates 5G will enable $13.2 trillion in global economic output in 2035, with the 5G value chain generating $3.6 trillion and supporting 22.3 million jobs.[2]

Despite their belief in CDMA, Qualcomm's founders could not have imagined its impact on the world when the company was formed. ■

Read *Microwave Journal*'s interview with Qualcomm's Chief Technology Officer, James Thompson, at www.microwavejournal.com.

ACKNOWLEDGMENT

This article would not have been written without the assistance of Suranjeeta Choudhury and her team at Qualcomm, who provided technical and historic insight.

References

1. Rashid Attar, Donna Ghosh, et al., "Evolution of cdma2000 Cellular Networks: Multi-carrier EV-DO," *IEEE Communications Magazine*, February 2006.
2. *IHS Markit*, "The 5G Economy, How 5G will Contribute to the Global Economy," November 2019.


Technology innovation
from a reliable foundry
We're proud to offer foundry access to our fellow U.S. defense contractors. We provide the key technologies and support to give you discriminating performance at an affordable price. Join us in working with some of the highest performing GaAs and GaN processes in the world for your small development or full production projects.
baesystems.com/foundry
BAE SYSTEMS

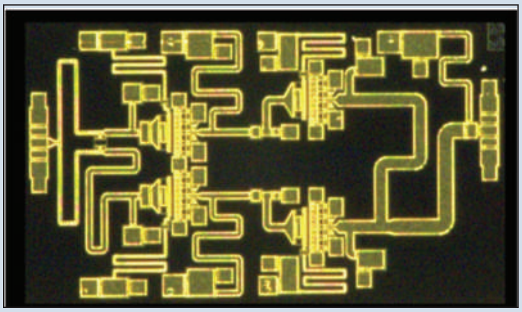
Image courtesy of Mitsubishi Electric

EDA Update Improves EM and PA Stability Analyses and Transmission Line Synthesis

Cadence
El Segundo, Calif.

Cadence has released the latest version of the AWR Design Environment®, Version 15 (V15), the first release since the company acquired AWR Corporation from National Instruments. This latest version, available for current customers and evaluators, includes new features, add-on modules and enhancements to the AWR Microwave Office® circuit design software, AWR Visual System Simulator™ (VSS) system design software, AXIEM® 3D planar method of moments and Analyst™ 3D finite element method electromagnetic (EM) simulators.

New capabilities introduced in V15 help designers address the challenges developing and integrating RFICs, MMICs, device and module packaging and PCB assemblies for 5G, automotive and aerospace and defense applications. These systems increasingly use advanced RF front-end components and antennas that must be designed to achieve spatial and spectral efficiency with minimal power consumption. To meet these needs, the latest release of the AWR Design Environment expands support for power amplifier (PA) and antenna/array design, EM modeling and RF/microwave integration within heterogenous systems.

PAST IS PRESENT…AND FUTURE

Today's RF technology stems from a long and steady effort among platform integrators, semiconductor manufacturers and electronic design automation (EDA) suppliers. In the late 1980s, the U.S. Department of Defense launched the MIMIC program to develop "affordable, available and broadly applicable" microwave and mmWave subsystems for military systems. The program targeted computer-aided engineering as an essential capability for the development of GaAs MMICs. The MIMIC program and complementary efforts yielded an industrial base for design and semiconductor development, confirmed by technology adoption in military systems and subsequently commercial communications. Cadence, formed in 1988, joined the MIMIC program to develop "smart" microwave libraries, combining electrical models for MMIC components with their physical layouts.

Electronic design has become a complex process, involving an array of analysis, verification and manufacturing tools, reusing design IP to reduce complexity and improve the likelihood of first-pass success. Systems increasingly have embedded radios—Wi-Fi, Bluetooth, cellular or some other standard—and the RF components enabling this wireless connectivity are among the most challenging to design. A holistic approach to the design of the entire system is required.

Cadence is addressing these challenges through the Intelligent System Design™ strategy, delivering its computational software capabilities across all design elements of electronic systems. At the core of this strategy is design excellence, an optimized EDA portfolio of tools with best-in-class RF, microwave and mmWave circuit, system and EM analysis; IP for semiconductor, package and PCB design; and scalable access in the cloud.

THE WIRELESS REVOLUTION WILL BE INTEGRATED

Enabled by wireless, RF will be integrated in an unprecedented number of connected smart devices

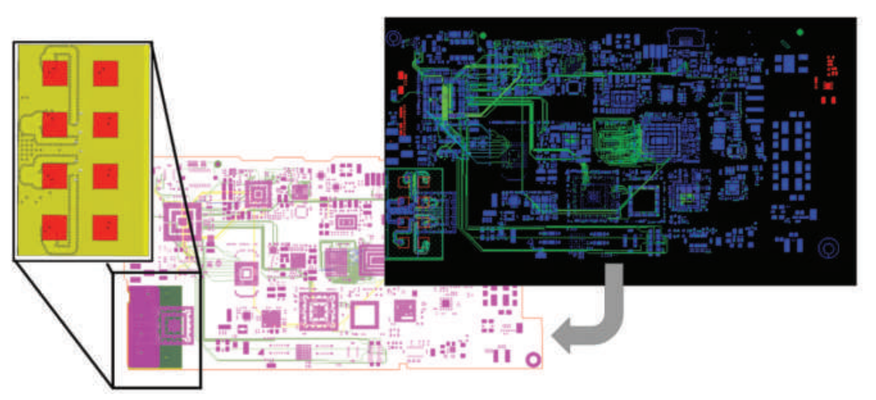

Fig. 1 AWR EM analysis of a 28 GHz, 2 x 4 element antenna array on a 5G handset PCB design imported from Cadence Allegro.

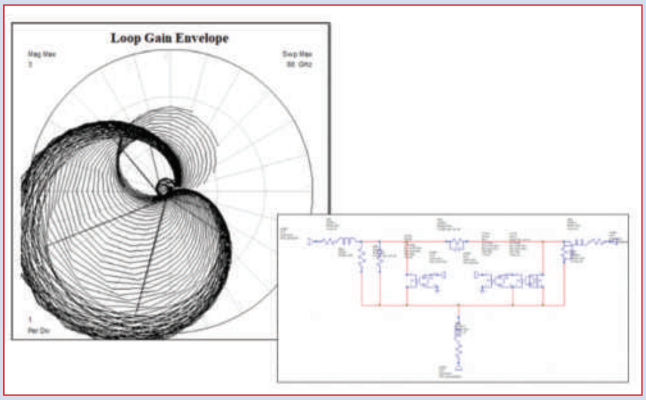

Fig. 2 Loop-gain envelope stability analysis enables the stability and margin of each device within an amplifier to be determined.

and systems. Developing these systems requires a significant advance in multi-domain analyses, simulation capacity, design automation and seamless interoperability between RF/microwave EDA and the broader portfolio of mixed-signal IC, PCB, system-in-package and system-on-chip (SoC) design tools. The "more than Moore" pace of electronic design is enabled by technology integration using densely populated, heterogeneous substrates. These tightly stacked components behave as mechanical systems with sophisticated electronics, transporting RF and high speed signals through a complex network of interconnects. To function properly, mixed-technology systems require co-design and co-optimization across multiple domains: RF, analog and digital simulation aided by large-scale EM and thermal analysis, with robust design verification and signoff. AWR's V15 offers the following features to aid this design process:

Faster EM Analysis of Mixed Technologies

The meshing and solver technologies in the AXIEM EM simulator have been enhanced for speed and capacity to characterize RFICs, MMICs and laminate structures using the latest via meshing technology for "healing" to reduce mesh size (see ***Figure 1***). Complex PCB and SoC components contain manufacturing features that do not impact RF performance, yet they slow EM analysis. Shape pre-processing rules have been expanded to better address large via arrays on user-specified layers inside or outside a specified region. The AXIEM DC solver includes a new sparse symmetric matrix technology that achieves a 10x savings in time and memory.

Power for the PA Designer

Stability analysis is critical to PA design and optimization. The commonly used K and μ factors cannot detect instabilities in multi-stage amplifiers or devices connected in parallel. Other stability analyses, such as normalized determinate function, overcome these limitations at the cost of computation run time, rendering them too slow for optimization. V15 supports a new loop-gain envelope technique, reducing the simulation time of this rigorous stability analysis from hours to seconds, making it ideal for stability optimization (see ***Figure 2***). Loop-gain envelope stability analysis offers several benefits, the stability and margin of each device within a MMIC amplifier is quantified. Analysis speed is increased by analytically applying the input and output terminations. With this speed improvement, optimization of phase margin for each device within a MMIC is possible, the magnitude of source

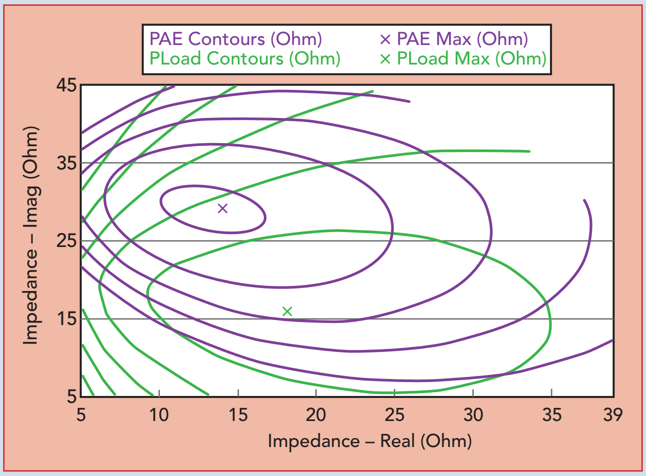

▲ **Fig. 3** Power and PAE load-pull performance contours on a rectangular grid using V15.

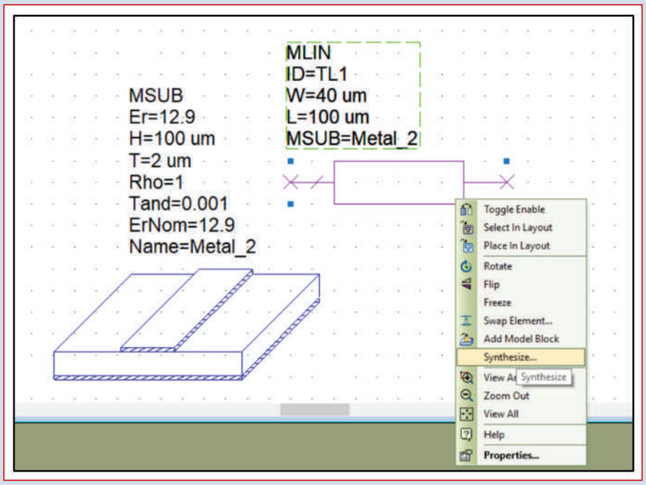

▲ **Fig. 4** Designers can directly synthesize microstrip, stripline and coplanar waveguide transmission lines from design parameters.

and load gamma is selectable to quickly determine stability with different loading.

Baseband impedance variation versus frequency in wideband PAs can impact linearity, resulting in intermodulation levels that vary asymmetrically with instantaneous signal bandwidth, behavior associated with baseband memory effects. PA developers have achieved significant improvements in linearity when active, baseband injection architectures such as envelope tracking are employed. Using V15, designers can optimize PA linearity through video band load-pull analysis—along with fourth and fifth harmonic load-pull capability—and plotting performance contours versus load impedance on rectangular graphs (see ***Figure 3***).

Synthesis Accelerates Designs

The characteristic impedance and electrical length of transmission lines—λ/4 impedance transformers, Wilkinson power dividers and combiners, hybrid couplers, filters—are important design parameters for passive RF/microwave circuits. Using V15, designers can directly synthesize these microstrip, stripline or coplanar waveguide structures for a given substrate, based on the desired electrical characteristics (see ***Figure 4***). Similarly, the electrical characteristics can be calculated directly from the physical properties without manually invoking the TX-LINE calculator and inputting the results. The latest synthesis wizard enables users to generate matching networks using components from the Microwave Office supplier library for surface-mount PCB designs or process design kits, extending synthesis to MMIC designs.

SUMMARY

V15 of the Cadence AWR Design Environment brings RF/microwave simulation to Cadence's portfolio of EDA solutions. New capabilities address stability analysis, video band and fourth and fifth harmonic load-pull and faster harmonic balance. Network synthesis supports optimization using supplier components, single and coupled transmission line synthesis and faster planar EM meshing and solver technology. The Cadence Intelligent System Design strategy envisions a future where electronic design is multi-faceted and relies on multi-physics and a host of design disciplines, with integrated RF, microwave and mmWave content a common factor.

VENDORVIEW

Cadence
El Segundo, Calif.
www.awr.com
www.cadence.com

NEXT GENERATION MILLIMETERWAVE COMPONENTS

SAGE Millimeter is now Eravant, a change that renews our commitment to the millimeterwave industry. Since 2011, we have been delivering quality products and energizing the customer experience to respond to the next generation of RF engineers.

As we continue to grow into an industry leader, we want a new identity that reflects our vision for enabling tomorrow's technology.

Check out our new website and customer portal at www.eravant.com

www.sagemillimeter.com

www.sagemillimeter.com 3043 Kashiwa St. Torrance, CA 90505
T: 424-757-0168 F: 424-757-0188 sales@SAGEMillimeter.com

RF Amplifiers and Sub-Assemblies for Every Application

Delivery from Stock to 2 Weeks ARO from the catalog or built to your specifications!

- Competitive Pricing & Fast Delivery
- Military Reliability & Qualification
- Various Options: Temperature Compensation, Input Limiter Protection, Detectors/TTL & More
- Unconditionally Stable (100% tested)

ISO 9001:2000 and AS9100B CERTIFIED

OCTAVE BAND LOW NOISE AMPLIFIERS

Model No.	Freq (GHz)	Gain (dB) MIN	Noise Figure (dB)	Power-out @ P1-dB	3rd Order ICP	VSWR
CA01-2110	0.5-1.0	28	1.0 MAX, 0.7 TYP	+10 MIN	+20 dBm	2.0:1
CA12-2110	1.0-2.0	30	1.0 MAX, 0.7 TYP	+10 MIN	+20 dBm	2.0:1
CA24-2111	2.0-4.0	29	1.1 MAX, 0.95 TYP	+10 MIN	+20 dBm	2.0:1
CA48-2111	4.0-8.0	29	1.3 MAX, 1.0 TYP	+10 MIN	+20 dBm	2.0:1
CA812-3111	8.0-12.0	27	1.6 MAX, 1.4 TYP	+10 MIN	+20 dBm	2.0:1
CA1218-4111	12.0-18.0	25	1.9 MAX, 1.7 TYP	+10 MIN	+20 dBm	2.0:1
CA1826-2110	18.0-26.5	32	3.0 MAX, 2.5 TYP	+10 MIN	+20 dBm	2.0:1

NARROW BAND LOW NOISE AND MEDIUM POWER AMPLIFIERS

Model No.	Freq (GHz)	Gain (dB) MIN	Noise Figure (dB)	Power-out @ P1-dB	3rd Order ICP	VSWR
CA01-2111	0.4 - 0.5	28	0.6 MAX, 0.4 TYP	+10 MIN	+20 dBm	2.0:1
CA01-2113	0.8 - 1.0	28	0.6 MAX, 0.4 TYP	+10 MIN	+20 dBm	2.0:1
CA12-3117	1.2 - 1.6	25	0.6 MAX, 0.4 TYP	+10 MIN	+20 dBm	2.0:1
CA23-3111	2.2 - 2.4	30	0.6 MAX, 0.45 TYP	+10 MIN	+20 dBm	2.0:1
CA23-3116	2.7 - 2.9	29	0.7 MAX, 0.5 TYP	+10 MIN	+20 dBm	2.0:1
CA34-2110	3.7 - 4.2	28	1.0 MAX, 0.5 TYP	+10 MIN	+20 dBm	2.0:1
CA56-3110	5.4 - 5.9	40	1.0 MAX, 0.5 TYP	+10 MIN	+20 dBm	2.0:1
CA78-4110	7.25 - 7.75	32	1.2 MAX, 1.0 TYP	+10 MIN	+20 dBm	2.0:1
CA910-3110	9.0 - 10.6	25	1.4 MAX, 1.2 TYP	+10 MIN	+20 dBm	2.0:1
CA1315-3110	13.75 - 15.4	25	1.6 MAX, 1.4 TYP	+10 MIN	+20 dBm	2.0:1
CA12-3114	1.35 - 1.85	30	4.0 MAX, 3.0 TYP	+33 MIN	+41 dBm	2.0:1
CA34-6116	3.1 - 3.5	40	4.5 MAX, 3.5 TYP	+35 MIN	+43 dBm	2.0:1
CA56-5114	5.9 - 6.4	30	5.0 MAX, 4.0 TYP	+30 MIN	+40 dBm	2.0:1
CA812-6115	8.0 - 12.0	30	4.5 MAX, 3.5 TYP	+30 MIN	+40 dBm	2.0:1
CA812-6116	8.0 - 12.0	30	5.0 MAX, 4.0 TYP	+33 MIN	+41 dBm	2.0:1
CA1213-7110	12.2 - 13.25	28	6.0 MAX, 5.5 TYP	+33 MIN	+42 dBm	2.0:1
CA1415-7110	14.0 - 15.0	30	5.0 MAX, 4.0 TYP	+30 MIN	+40 dBm	2.0:1
CA1722-4110	17.0 - 22.0	25	3.5 MAX, 2.8 TYP	+21 MIN	+31 dBm	2.0:1

ULTRA-BROADBAND & MULTI-OCTAVE BAND AMPLIFIERS

Model No.	Freq (GHz)	Gain (dB) MIN	Noise Figure (dB)	Power-out @ P1-dB	3rd Order ICP	VSWR
CA0102-3111	0.1-2.0	28	1.6 Max, 1.2 TYP	+10 MIN	+20 dBm	2.0:1
CA0106-3111	0.1-6.0	28	1.9 Max, 1.5 TYP	+10 MIN	+20 dBm	2.0:1
CA0108-3110	0.1-8.0	26	2.2 Max, 1.8 TYP	+10 MIN	+20 dBm	2.0:1
CA0108-4112	0.1-8.0	32	3.0 MAX, 1.8 TYP	+22 MIN	+32 dBm	2.0:1
CA02-3112	0.5-2.0	36	4.5 MAX, 2.5 TYP	+30 MIN	+40 dBm	2.0:1
CA26-3110	2.0-6.0	26	2.0 MAX, 1.5 TYP	+10 MIN	+20 dBm	2.0:1
CA26-4114	2.0-6.0	22	5.0 MAX, 3.5 TYP	+30 MIN	+40 dBm	2.0:1
CA618-4112	6.0-18.0	25	5.0 MAX, 3.5 TYP	+23 MIN	+33 dBm	2.0:1
CA618-6114	6.0-18.0	35	5.0 MAX, 3.5 TYP	+30 MIN	+40 dBm	2.0:1
CA218-4116	2.0-18.0	30	3.5 MAX, 2.8 TYP	+10 MIN	+20 dBm	2.0:1
CA218-4110	2.0-18.0	30	5.0 MAX, 3.5 TYP	+20 MIN	+30 dBm	2.0:1
CA218-4112	2.0-18.0	29	5.0 MAX, 3.5 TYP	+24 MIN	+34 dBm	2.0:1

LIMITING AMPLIFIERS

Model No.	Freq (GHz)	Input Dynamic Range	Output Power Range Psat	Power Flatness dB	VSWR
CLA24-4001	2.0 - 4.0	-28 to +10 dBm	+7 to +11 dBm	+/- 1.5 MAX	2.0:1
CLA26-8001	2.0 - 6.0	-50 to +20 dBm	+14 to +18 dBm	+/- 1.5 MAX	2.0:1
CLA712-5001	7.0 - 12.4	-21 to +10 dBm	+14 to +19 dBm	+/- 1.5 MAX	2.0:1
CLA618-1201	6.0 - 18.0	-50 to +20 dBm	+14 to +19 dBm	+/- 1.5 MAX	2.0:1

AMPLIFIERS WITH INTEGRATED GAIN ATTENUATION

Model No.	Freq (GHz)	Gain (dB) MIN	Noise Figure (dB)	Power-out @ P1-dB	Gain Attenuation Range	VSWR
CA001-2511A	0.025-0.150	21	5.0 MAX, 3.5 TYP	+12 MIN	30 dB MIN	2.0:1
CA05-3110A	0.5-5.5	23	2.5 MAX, 1.5 TYP	+18 MIN	20 dB MIN	2.0:1
CA56-3110A	5.85-6.425	28	2.5 MAX, 1.5 TYP	+16 MIN	22 dB MIN	1.8:1
CA612-4110A	6.0-12.0	24	2.5 MAX, 1.5 TYP	+12 MIN	15 dB MIN	1.9:1
CA1315-4110A	13.75-15.4	25	2.2 MAX, 1.6 TYP	+16 MIN	20 dB MIN	1.8:1
CA1518-4110A	15.0-18.0	30	3.0 MAX, 2.0 TYP	+18 MIN	20 dB MIN	1.85:1

LOW FREQUENCY AMPLIFIERS

Model No.	Freq (GHz)	Gain (dB) MIN	Noise Figure dB	Power-out @ P1-dB	3rd Order ICP	VSWR
CA001-2110	0.01-0.10	18	4.0 MAX, 2.2 TYP	+10 MIN	+20 dBm	2.0:1
CA001-2211	0.04-0.15	24	3.5 MAX, 2.2 TYP	+13 MIN	+23 dBm	2.0:1
CA001-2215	0.04-0.15	23	4.0 MAX, 2.2 TYP	+23 MIN	+33 dBm	2.0:1
CA001-3113	0.01-1.0	28	4.0 MAX, 2.8 TYP	+17 MIN	+27 dBm	2.0:1
CA002-3114	0.01-2.0	27	4.0 MAX, 2.8 TYP	+20 MIN	+30 dBm	2.0:1
CA003-3116	0.01-3.0	18	4.0 MAX, 2.8 TYP	+25 MIN	+35 dBm	2.0:1
CA004-3112	0.01-4.0	32	4.0 MAX, 2.8 TYP	+15 MIN	+25 dBm	2.0:1

CIAO Wireless can easily modify any of its standard models to meet your "exact" requirements at the Catalog Pricing.

Visit our web site at **www.ciaowireless.com** for our complete product offering.

Ciao wireless

Ciao Wireless, Inc. 4000 Via Pescador, Camarillo, CA 93012
Tel (805) 389-3224 Fax (805) 389-3629 sales@ciaowireless.com

Multi-Function Capabilities and Operational Readiness of Semiconductor Technology

BAE Systems successfully demonstrated new, powerful small form factor semiconductor technology designed to sense radio frequency (RF) and communication signals in congested and contested battle environments in conjunction with an unmanned aerial system.

In a recent military exercise attended by representatives from multiple research labs and military service branches, BAE Systems successfully demonstrated new, powerful small form factor semiconductor technology. The Hedgehog technology, which was used in this exercise to sense RF and communication signals in congested and contested battle environments in conjunction with an unmanned aerial system, is a collection of general-purpose, reconfigurable MATRICs™ chips in a software-defined radio (SDR) system.

The Hedgehog demonstration was in support of the Defense Advanced Research Projects Agency (DARPA) Distributed RF Analysis and Geolocation on Networked System (DRAGONS) research. The DRAGONS program is designed to deliver a drone-integrated, small form factor signal identification and geolocation capability.

The demonstration highlighted the ability for forward operators to deploy technology to secure tactical signals intelligence and geolocation data in near real-time with low size, weight and power requirements. The technology provides agility, a broad frequency range and high instantaneous bandwidth—all key capabilities that are not currently available from other SDRs.

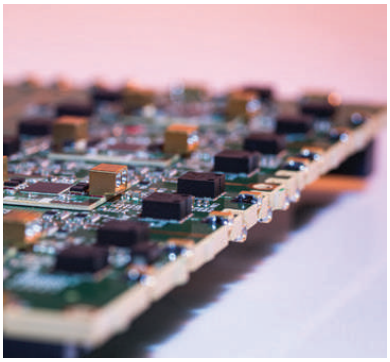

Source: BAE Systems

Hedgehog is a SDR designed for unprecedented agility, frequency range and wide instantaneous bandwidth. Its RF front-end is a collection of general-purpose microwave array technology for reconfigurable integrated circuits transceivers, or MATRICs™ transceivers, that can be reconfigured for integration into a variety of systems. Digitization and processing is provided by the Xilinx radio frequency system on a chip (RFSoC). This first integration of the MATRICs transceiver with an RFSoC delivers unrivaled tuning ability in a low size, weight and power device. Its extremely agile frequency hopping capabilities provide endless functionality, and unique protection from hacking, jamming and interception. BAE Systems' MATRICs chips are less expensive and time consuming to develop than traditional application-specific chips and can be integrated into a variety of systems to help address future requirements of electronic warfare, communications and signal intelligence systems.

"On-The-Move" Ground Radar Demonstration

Northrop Grumman Corporation recently completed a successful government customer demonstration of the highly adaptable multi-mission radar (HAMMR) system at Eglin Air Force Base, Fla. "GaN has the promise of increased market share in 2013 and is forecast to be a significant force by 2020," notes Lance Wilson, research director at Mobile Networks. "It bridges the gap between two older technologies, exhibiting the high-frequency performance of gallium arsenide combined with the power-handling capabilities of Silicon LDMOS. It is now a mainstream technology that has achieved measurable market share and in the future will capture a significant part of the market."

During the successful live fire demonstration, Northrop Grumman used the HAMMR system, mounted on a high mobility multipurpose wheeled vehicle as an integrated air and missile defense (IAMD) sensor to detect and track an unmanned aerial vehicle target.

"This first-of-its-kind demonstration validated the sense on-the-move capability in concept for the Department of Defense's IAMD enterprise and proved that this capability can be developed and fielded to warfighters much sooner than anticipated," said Mike Meaney, vice president of land and maritime sensors at Northrop Grumman.

Northrop Grumman's HAMMR is a short- to medium-range X-Band 3D radar that uses the proven active electronically scanned array AN/APG-83 F-16 fighter radar in a ground-based, sense on-the-move role. HAMMR provides robust multi-mission 3D performance for air surveillance, weapon cueing and counter-fire target acquisition missions in either a 360-degree or sector-only staring mode. HAMMR delivers the unprecedented ability to provide force protection while operating on the move, significantly increasing warfighter survivability.

Flat-Panel Technology Could Transform Antennas, Wireless and Cell Phone Communications

Researchers at Los Alamos National Laboratory are reinventing the mirror, at least for microwaves, potentially replacing the famil-

For More Information Visit mwjournal.com for more defense news.

iar 3D dishes and microwave horns we see on rooftops and cell towers with flat panels that are compact, versatile and better adapted for modern communication technologies. The flat-panel reflector can be controlled electronically, which means its characteristics can be reconfigured on the fly. This opens the window for beam steering, customized focusing and other functions that are difficult to achieve with conventional antenna designs.

Most reflectors are reciprocal. With a bathroom mirror, for example, if you can see someone reflected in it, they can see you too. The new reflector design breaks reciprocity, effectively turning it into a one-way mirror. The reflectors are composed of an array of finely structured electronic components on a planar surface. Applying signals to the components allows the 2D reflector to perform much like a 3D antenna and, in some cases, do things a conventional antenna cannot.

This device is known as a "metasurface," because its characteristics can be electronically changed to act in different ways without modifying the physical shape of the surface. "We have demonstrated the first dynamic metasurface capable of achieving extreme non-reciprocity by converting microwaves into plasmons, which are electric charge waves on the reflector's surface," said Diego Dalvit of the T-4 group at Los Alamos. "This is key to controlling the way the reflectors function."

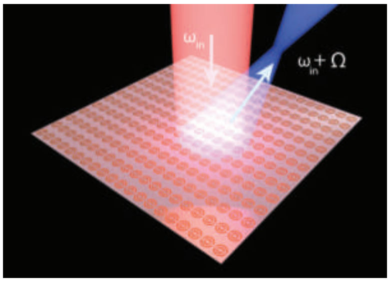

Source: Los Alamos National Laboratory.

By applying electrical signals to the reflector components, the researchers modulated the metasurface to control the direction and frequency of reflected light. The non-reciprocal response of the reflector can help prevent antennas from picking up echoes from their outgoing broadcasts and protect delicate circuitry from powerful, potentially damaging incoming signals. Miniaturized versions could improve chip-based circuitry by ensuring that signals go only to the intended components and do not lead to inadvertent signals in other parts of the circuit, a problem that chip designers often worry about.

The new Los Alamos reflector platform opens opportunities in various applications, including adaptive optics that can account for distortions that disrupt signals, one-way wireless transmission and novel antenna designs.

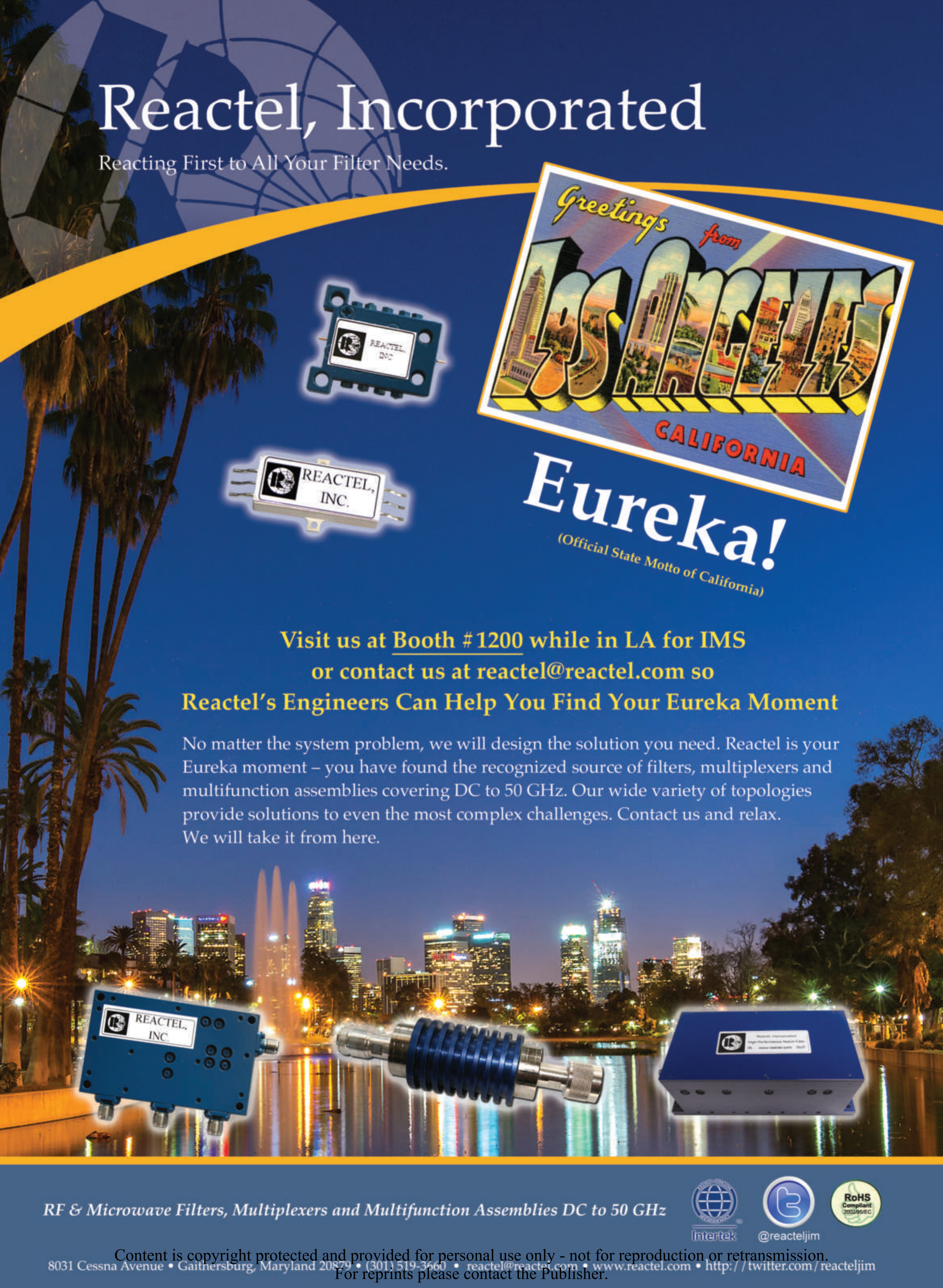

Reactel, Incorporated
Reacting First to All Your Filter Needs.
Greetings from
LOS ANGELES
CALIFORNIA
Eureka!
(Official State Motto of California)
REACTEL, INC.
REACTEL, INC.
Visit us at Booth #1200 while in LA for IMS
or contact us at reactel@reactel.com so
Reactel's Engineers Can Help You Find Your Eureka Moment
No matter the system problem, we will design the solution you need. Reactel is your Eureka moment – you have found the recognized source of filters, multiplexers and multifunction assemblies covering DC to 50 GHz. Our wide variety of topologies provide solutions to even the most complex challenges. Contact us and relax. We will take it from here.
REACTEL, INC.
RF & Microwave Filters, Multiplexers and Multifunction Assemblies DC to 50 GHz
Intertek
@reacteljim
RoHS Compliant
8031 Cessna Avenue • Gaithersburg, Maryland 20879 • (301) 519-3660 • reactel@reactel.com • www.reactel.com • http://twitter.com/reacteljim

5G Will Shift C-V2X into High Gear

Soon cars will start to communicate with each other to increase overall road safety and traffic. According to recent figures published by ABI Research, a total of 41 million 5G connected cars will be on roads by 2030. That number will rise to 83 million 5G connected cars by 2035. By then, 5G connected cars will make up more than 75 percent of the total C-V2X equipped cars.

"These numbers underline the huge momentum for cellular connectivity, and particularly 5G, in the automotive sector," says Leo Gergs, research analyst for 5G markets at ABI Research. "As a consequence, we will see a rising number of automotive OEMs start developing C-V2X modules for their cars during 2020. We can then expect the first 5G connected cars on the roads in 2022."

While leading car manufacturer Ford already announced new car models equipped with C-V2X for 2021, other automotive heavyweights like Audi, BMW and Volkswagen have all partnered up with the likes of Ericsson, Huawei and Nokia to commence large-scale trial projects to test the capabilities of cellular technology for connected car use cases. The results of these proof-of-concept projects are auspicious and show that, through enhancing traffic efficiency, 5G can reduce fuel consumption by up to one third. "More importantly, however, the sharing of sensor data will make overtaking much safer and will be critical to protecting vulnerable road users (such as pedestrians or cyclists). Therefore, bringing 5G-based cellular connectivity into cars will be critical in making the vision of zero road traffic deaths a reality," Gergs emphasizes.

In total, ABI Research has quantified the contribution of 5G to global GDP to reach U.S.$17 trillion by 2035. A large part of that global GDP will be through increasing the safety of road traffic, which will reduce health care expenditure drastically and take pressure off doctors and hospitals.

5G's Year One: Fast Start and Healthy Growth

Customers are making 5G the fastest growing generation of cellular wireless technology in terms of new subscriptions, according to 5G Americas. According to data from Omdia, there are now over 17.7 million 5G connections globally as of Q4 2019, which represents 329 percent growth over Q3 2019—and is five million subscribers ahead of previous projections.

Chris Pearson, president at 5G Americas said, "We truly had a great year in 2019, as 5G adoption has surpassed most forecasts. With the first year of 5G completed, 2020 is shaping up to be focused on the growth of new 5G devices, increasing coverage, increasing network densification and probably the first 5G standalone deployments."

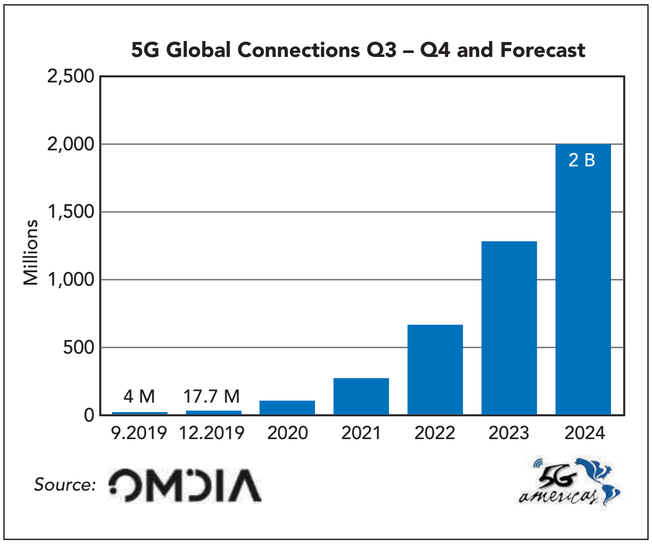

The rapid ascent of 5G compares favorably with the initial year for previous cellular communication technologies like LTE, which has now reached 5.3 billion connections after ten years of operation. While LTE became commercially available in the last quarter of 2009, it was used by only around 1,000 customers in Western Europe initially. In 2010, North America added 20,000 more LTE customers, bringing the total to 23,250 connections globally. It took roughly ten quarters, or until Q1 2012, for 4G LTE to reach 17.9 million connections—roughly where 5G is today. 3G did not reach that mark until December 2010, after 11 Quarters and 2G reached it in December 1995, after 14 quarters.

The rapid growth of 5G has been fueled by an explosion of 3GPP-standard commercial 5G networks deployed globally. There are now five 5G commercial networks, a number which is expected to nearly quadruple to 200 by the end of 2020, according to data from TeleGeography.

Regionally by the end of 2019, North America had 587,000 5G connections and 483 million LTE connections. In Q4 2019, North America continued with robust subscription additions of 434,000 5G connections (284 percent Q3 to Q4) and 13 million LTE connections (2.7 percent Q3 to Q4) across the region. Latin America and the Caribbean ended 2019 with 1,237 5G subscriptions (314 percent Q3 to Q4) and 366 million LTE subscriptions (27 percent Q3 to Q4 growth), respectively.

Looking forward, Omdia projects 5G connections will reach 91 million globally by the end of 2020, of which North America will account for 13.9 million. Latin America and the Caribbean will account for an additional 1.5 million subscribers by the end of the year. At the same time, global 4G LTE connections are expected to reach 5.9 billion, of which 513 million (6.2 percent annual growth) will come from North America and 397

For More Information Visit mwjournal.com for more commercial market news.

million (8.6 percent annual growth) will come from Latin America and the Caribbean.

COVID-19 Pandemic Impact on 5G

The COVID-19 pandemic has forced a delay in the crucial standardization work that would make 5G available for enterprise use cases. The relevant standardization body, 3GPP, has formally announced a deferral of this standardization until at least June 2020, which would delay commercial rollout of industrial 5G until at least 2022. Given that most industrial enterprises are looking to upgrade their communication technology in 2021, this delay will result in 5G missing out on at least 25 percent of the revenue opportunities within industrial enterprises, which given the importance of industrial use cases for overall 5G revenues, this translates into 5G losing up to 10 percent of total 5G revenues. In the long run, this could result in a shortfall of several U.S. billion dollars in contribution to the global economy, states global tech market advisory firm, ABI Research.

"This is a blow to the standards bodies and the timeline of 5G," says Leo Gergs, principal analyst at ABI Research. "The cancellation of leading industry events, such as Mobile World Congress in Barcelona, caused more complicated workflows for the 3GPP. As a result, the freeze of Release 16 (which is of key importance for 5G applications in industrial and logistics environments) has been delayed until June. This would, in turn, push the rollout of 5G into warehouses, shipping ports and factory floors until at least 2022."

Even though, in the short-term, this current pandemic is putting the timely enterprise rollout of 5G at risk in the long-term, enterprise verticals will consider 5G for automating workflows in factories and other industrial environments to keep supply chain disruptions at a minimum. "However, we will also see 5G applications for life-critical verticals, such as agriculture/food production, to pick up pace, while a growing number of countries will consider enhancing their healthcare sector with 5G-enabled capabilities," Gergs points out.

Situations like these underline the importance of a technologically up-to-date healthcare system, as well as more automation in factories and production outlets. However, the current situation around COVID-19 will most probably induce a shift in the verticals that investigate 5G deployment. "While it puts 5G applications in industrial surroundings in a difficult position, current experiences will ignite considerations for 5G applications in healthcare and agriculture/food production. The telco ecosystem must prepare for this shift," Gergs recommends.


Interconnect Solutions That Ensure
Precise Tests & Measurements

Around the **Circuit**

Barbara Walsh, Multimedia Staff Editor

MERGERS & ACQUISITIONS

Qorvo® announced that it has completed its acquisition of **Decawave**. The Decawave team has become the Ultra-Wideband Business Unit within Qorvo Mobile Products. Dublin, Ireland-based-Decawave was founded in 2007 and has deployed more than 8 million chipsets in more than 40 different market verticals—from smartphones to drones. Decawave's impulse radio ultra-wideband technology allows for position accuracy of a few centimeters and with extremely low latency.

COLLABORATIONS

Rohde & Schwarz and **Decawave** have jointly developed test and measurement capabilites for production line testing of UWB functions in chipsets and complete devices. As part of the cooperation, Decawave provided knowledge of the required test strategy and test methods, as well as the Decawave DW3000 as test device. Rohde & Schwarz has added UWB test capabilities to their R&S CMP200 radio communication tester, making it the only test platform on the market able to provide R&D and production RF tests for both 5G FR2 and UWB functions.

Keysight Technologies Inc. announced a collaboration with **VIOMI** to accelerate the market introduction of innovative 5G-enabled IoT devices for consumers in China. VIOMI selected Keysight's 5G solutions to validate the RF performance of the company's IoT devices for home applications. The deployment of massive IoT networks is expected to create a $1.2B global opportunity by 2024 according to a report published by Research and Markets earlier this year. Keysight's 5G device test solutions are well-positioned to address the 5G IoT endpoint installed base market, which Gartner predicts will more than triple between 2020 and 2023.

Modelithics welcomes **Vishay Intertechnology** into the Modelithics Vendor Partner (MVP) Program at the Sponsoring level. As a Sponsoring MVP, Vishay is supporting RF and microwave designers by sponsoring free extended 90-day trials (with approval) of all Modelithics models available for Vishay components, as well as collaborating with Modelithics to develop new design data and models for selected components. In addition, to becoming a Sponsoring MVP, Vishay and Modelithics are collaborating to develop three new Microwave Global Models™ for Vishay's CH02016F, CH0402F and CH0603F resistors.

Taoglas® and **MixComm** are partnering to co-develop a 5G new radio mmWave smart antenna subsystem covering 26.5 to 29.5 GHz. The antenna will support small cells, repeaters and customer-premises equipment for infrastructure and 5G IoT devices. The antenna subsystem is based on Taoglas' KHA16.23C smart antenna and integrates MixComm's newly announced 5G 28 GHz beamforming front-end IC, the SUMMIT 2629. The KHA16.23C is a 2D array in a multi-layer PCB containing 16 antenna elements and integrating the MixComm RFICs, with layers for power optimization, thermal control, digital control and RF feed lines—in a footprint of 53 mm x 84 mm.

Gapwaves announced a collaboration with **Uhnder** to develop a high-resolution radar for a last mile autonomous delivery vehicle. Gapwaves has developed a waveguide antenna technology for mmWave applications such as automotive radar and 5G telecom. Its gap waveguide technology achieves the low loss of waveguide and is compatible with high volume, cost-effective manufacturing. For automotive radar applications, its antenna provides a wide field of view and high isolation, which has garnered industry interest and license agreements with tier 1 automotive radar manufacturers. Uhnder has developed a unique digital radar-on-chip, combining advanced CMOS with digital code modulation.

ACHIEVEMENTS

AT&T was the winning bidder for 39 GHz spectrum licenses in the FCC's recent Spectrum Frontiers auction (auction 103), which granted licenses for spectrum at 37, 39 and 47 GHz. AT&T's licenses cover more than 99 percent of the U.S. population. AT&T said it improved its 39 GHz spectrum holdings to 786 MHz, an increase of 102 percent. Added to its 24 GHz spectrum, AT&T's average mmWave spectrum has increased to more than 1.04 GHz nationwide. AT&T said its existing spectrum allowed the company to add more coverage last year than any other wireless provider and the new spectrum will continue the progress.

Cobham Advanced Electronic Solutions announced accelerated demand for its technology to be used for rapid sequencing of coronavirus samples for analysis and to aid in diagnosing and treating coronavirus patients. Cobham's application specific integrated circuits (ASIC) are used in advanced devices used to deliver the genomic sequence of the SARS-CoV-2 virus that causes the COVID-19 disease, enabling insights into how the virus is transmitted and how it evolves. CAES ASICs are also a key technology used by a leading global provider of computed tomography scanners used to help diagnose respiratory conditions. Cobham has recently seen an increase of approximately 30 percent in demand for its medical ASIC products.

For the tenth consecutive year, **Mini-Circuits** has received a 4-Star Supplier Excellence Award from longtime customer **Raytheon Integrated Defense Systems**. Raytheon's Integrated Defense Systems business instituted the annual Supplier Excellence Awards program to recognize suppliers who have provided outstanding service and partnership in exceeding customer requirements. Award candidates are judged on certain criteria, including overall quality and on-time delivery. Mini-Circuits was

For More Information

For up-to-date news briefs, visit mwjournal.com

one of 86 companies recognized by Raytheon's Integrated Defense Systems business for 4-Star honors.

Northrop Grumman has completed a live fire demonstration of the highly adaptable multi-mission radar (HAMMR) system at Eglin Air Force Base, Fla., where it detected and tracked an unmanned aerial vehicle target. HAMMR is a short- to medium-range X-band 3D radar that "borrows" the F-16's AN/APG-83 active electronically scanned array (AESA). HAMMR uses the AESA radar to provide multi-mission 3D performance for air surveillance, weapon cueing and counter-fire target acquisition missions in either a 360-degree or sector-only staring mode. During the successful demonstration at Eglin, HAMMR was mounted on a high mobility multipurpose wheeled vehicle to make an integrated air and missile defense system.

Georgia Tech has developed a room-temp process to bond GaN to diamond in order to improve GaN device cooling to achieve higher output power, improved reliability and reduced manufacturing costs. The technique, called surface-activated bonding, uses an ion source in a high-vacuum environment to clean the surfaces of the GaN and diamond, which activates them by creating "dangling" bonds. Introducing small amounts of silicon into the ion beams helps form strong atomic bonds at room temperature, enabling direct bonding of the GaN with single-crystal diamond to fabricate HEMTs. Performed at room temperature, the new process reduces the thermal stress applied to the device.

Autotalks completed Wi-Fi 5 pre-certification for its evaluation kit based on its second generation vehicle-to-everything (V2X) chipset. Autotalks' dual-mode (dedicated short range communications and cellular vehicle-to-everything (C-V2X)) chipset recently achieved this milestone for its dual-band Wi-Fi (2.4 GHz and 5 GHz) supporting standards 802.11a/b/g/n/ac. The testing was done by an authorized test laboratory of the Wi-Fi Alliance™, using Autotalks evaluation kits. As automakers increasingly embed V2X units in the vehicles' telematics control unit, the addition of out-of-vehicle Wi-Fi functionality to Autotalks' V2X chipset can facilitate a range of out-of-vehicle connectivity services.

Researchers from the **Fraunhofer Institute for Applied Solid State Physics IAF** have developed compact and energy-efficient high-frequency/high-bandwidth RF filters to meet the increasing demand of RF components for mobile devices. During the project PiTrans, the researchers have managed to grow Aluminum Scandium Nitride with the required industrial specifications and to realize novel electroacoustic devices for smartphones. The number of RF components built into a single smartphone has increased significantly in recent years and there is no end in sight.

CONTRACTS

Raytheon Co. will produce and deliver SM-3® Block IB

Around the **Circuit**

interceptors under a $2.1 billion, multi-year **U.S. Missile Defense Agency** contract. It is the first multi-year contract for the SM-3 program and covers fiscal years 2019–2023. SM-3 is the only ballistic missile interceptor that can be launched on land and at sea. It is deployed worldwide and has achieved more than 30 exoatmospheric intercepts against ballistic missile targets. The Block IB variant achieved full-rate production in 2017. The company has delivered more than 400 SM-3 rounds over the lifetime of the program.

Science Applications International Corp. (SAIC) won the Federal Supply Group – 80 Tailored Logistics Support Program contract from the **Defense Logistics Agency**. The single-award, indefinite-delivery, indefinite-quantity contract has a ceiling value of $950 million. On this contract, SAIC will take over supply chain management for the FSG 80 commodity, which includes paints, preservation and sealing compounds and adhesives. Many of these items have short shelf lives and require temperature-controlled storage. The company will provide services including, but not limited to, procurement, demand planning, inventory and distribution management, shelf-life management and direct delivery of the commodity to more than 5,000 **Department of Defense (DoD)** locations.

Oshkosh Defense LLC announced that it has been awarded delivery orders totaling $346.4 million from the **U.S. Army Contracting Command - Warren** to modernize vehicles in the U.S. Army and U.S. Army Reserve Heavy Tactical Vehicle (FHTV) fleets. Under the delivery orders, Oshkosh will recapitalize heavy expanded mobility tactical trucks and palletized load system (PLS) trucks as well as manufacture new PLS trailers. The FHTV fleet is designed to accommodate many mission packages, allowing it to support multi-domain operations as the battlefield continues to evolve.

CACI International Inc. announced it has been awarded a six-year single-award task order, with a ceiling value of nearly $249 million, to provide operations, planning and training support to **U.S. Africa Command (AFRICOM)**. Through the task order, CACI will provide high-level mission expertise to AFRICOM, its component commands and partners. CACI experts, located both at AFRICOM headquarters in Germany and across Africa, will assist the command with planning and executing peacetime, crisis and contingency operations. CACI will also use collaboration tools and techniques to increase efficiency and effectiveness.

The U.S. Space Force's Space and Missile Systems Center (SMC) at Los Angeles Air Force Base has awarded **Lockheed Martin** a $240 million contract to develop a prototype payload for its new protected tactical SATCOM (PTS) system. PTS is a next-generation capability connecting warfighters with more agile and jam-resistant satellite communications (SATCOM). The complete system will deploy a constellation of dedicated geostationary satellites, commercially hosted payloads and coalition partner


ANALOG DEVICES
AHEAD OF WHAT'S POSSIBLE™
MODULES AND SUBSYSTEMS
BEAMFORMING SOLUTIONS
INERTIAL, ATTITUDE, AND STABILIZATION
Accelerating Time from Concept to Product
More competitors. More demands. More rapidly emerging threats.
Analog Devices has a depth of industry *and* technical expertise that is unmatched. Together with an unrivaled portfolio of RF and microwave solutions, you can now reduce the prototype phase of design by months and get to market faster than you ever thought possible.
Get to market faster at analog.com/ADEF

satellites integrated through a ground control network to provide U.S. and coalition forces protected communications in a data hungry battlespace. SMC's acquisition begins with a rapid prototyping phase for a new mission payload hosting the protected tactical waveform.

Amentum has been awarded a new contract by **Naval Surface Warfare Center Dahlgren Division** worth up to $87 million. Under the contract, Amentum will provide systems engineering support to naval weapons systems, weapon control systems and warfare systems for ballistic missile and guided missile submarines and surface ships, including Aegis, Ship Self-Defense System, DDG-1000 Guided Missile Destroyers, Guided Missile Frigates and U.S. Coast Guard cutters. The cost plus fixed-fee contract has one base year and four one-year option periods.

Teledyne Defense Electronics, doing business as **Teledyne Microwave Solutions**, has been awarded a $34,963,200 firm-fixed-price requirements contract by the **U.S. Navy**. The contract is for the repair of traveling wave tubes in support of the Advanced Electronic Guidance and Instrumentation System/Combat System. Work on the model 10 kW TWTs will be performed at the Teledyne MEC 160,000 square foot production facility in Rancho Cordova, Calif. and is expected to be complete by March 2025. This contract includes a five-year base period with no options. Annual working capital funds (Navy) will be obligated as individual task orders as issued and funds will not expire at the end of the current fiscal year.

SAB Biotherapeutics announced it has been awarded a contract from the **U.S. DoD** to develop and test a Rapid Response Antibody Program, valued at up to $27 million. This progressive and competitive, three-stage, multi-year contract calls for the development of a state-of-the-art, pharmaceutical platform technology capable of rapidly and reliably producing antibody-based Medical Countermeasures for biological threats.

Comtech Telecommunications Corp. announced that during its second quarter of fiscal 2020, its Santa Clara, Calif.-based subsidiary, **Comtech Xicom Technology Inc.**, which is part of Comtech's Commercial Solutions segment, received a contract valued at $1.3 million for rack-mounted Ku-band high-power traveling wave tube amplifier systems for a military satellite communications ground system.

Phase Four, makers of RF plasma engines for in-space propulsion, has been awarded a Small Business Innovation Research Phase I contract by Air Force tech accelerator **AFWERX**, in partnership with the **Air Force Research Laboratory** and the **National Security Innovation Network**. As part of this partnership Phase Four will work with the Air Force to adapt its revolutionary Maxwell in-space propulsion system to meet the needs of defense users. Affordable and reliable in-space propulsion is an essential requirement for both commercial and defense next-generation satellite constellations.

Around the **Circuit**

REP APPOINTMENTS

Advanced RF Technologies Inc. (ADRF) announced that **Windy City Wire (WCW)** has become a preferred distributor of its in-building wireless solutions for commercial and public safety use cases. Per the agreement, WCW will only distribute ADRF distributed antenna system (DAS) and repeater products to customers. ADRF's commercial and public safety solution suite, including its PSR-X series repeaters, FiRe repeater and ADXV DAS, will be available for purchase through WCW sales representatives and accessible 24/7 through their e-commerce platform. Additionally, ADRF products will be available in WCW's 19 warehouses and offices located in major cities around the nation to accelerate product delivery.

Adding to its broad range of technology suppliers for component solutions from RF, microwave and mmWave through Terahertz frequencies, **Impulse Technologies** now represents **Sakura Tech Corp.** Since 1991, Impulse Technologies has supplied everything from antennas through frequency synthesizers for a wide range of markets including aerospace, commercial, industrial, medical, military and scientific research applications. Impulse enhances its extensive product lines and global reach with excellent professional services, including engineering, export licensing, repair and test. Sakura Tech offers accurate and reliable imaging sensors based on wideband microwave and mmWave radar technologies.

RFMW announced global distribution of **Custom MMIC** products beginning immediately. **Qorvo**'s recent acquisition of Custom MMIC folds their portfolio of high performance MMIC devices into an expanding list of customer solutions with amplifiers, control devices, mixers and multipliers for next-generation long range military phased radar and electronic warfare systems, in addition to advanced aerospace and satellite communications and other RF/microwave signal chains through V-band. Founded in 2006 as a fabless RF and microwave MMIC designer, Custom MMIC has been entrusted by government and defense industry original equipment manufacturer with their biggest microwave circuit challenges, gaining industry recognition as one of the most innovative and responsive MMIC vendors.

Richardson RFPD announced that it has entered into a global franchise agreement with **MixComm Inc.** MixComm is a New Jersey-headquartered start-up that bases its technology on RFSOI and mmWave breakthroughs developed at Columbia University's CoSMIC lab. MixComm's products address the critical challenges that currently constrain 5G mmWave success including limited range that increases cost and diminishes customer satisfaction, excessive thermal and electrical power consumption budgets and low integration and excessively large antenna arrays that drive high module cost. Under the new agreement, Richardson RFPD will distribute MixComm's upcoming mmWave products to customers worldwide. MixComm's first production device is a 5G 28 GHz beamforming "SUMMIT 2629™" front-end IC.

AMCOM COMMUNICATIONS
The RF Power House

New Driver Amplifiers

ISO 9001

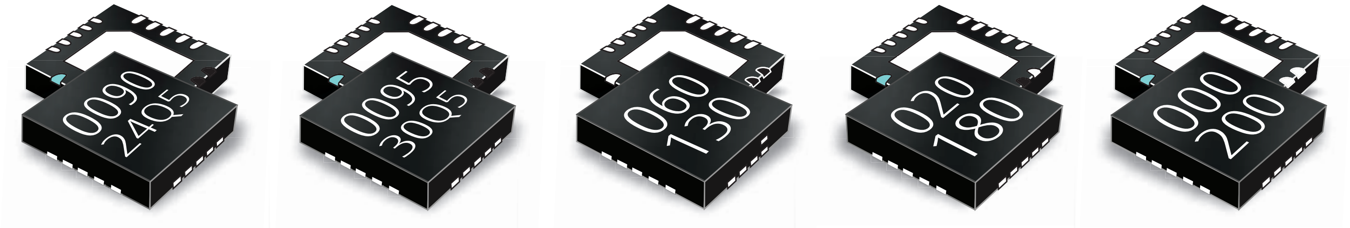

AM009024WM-QN5-R
is an ultra-broadband GaAs MMIC power amplifier. It has 22dB gain, and 24dBm output power over the 0.05 to 9GHz .

AM009530WM-QN5-R
is an ultra-broadband GaAs MMIC power amplifier. It has 20dB gain, and 30dBm output power over the 0.05 to 9.5GHz .

AM06013033WM-QN5-R
is a broadband GaAs MMIC which operates between 6 and 13 GHz with 28 dB gain and 33 dBm output power.

AM02018026WM-QN5-R
Broadband GaAs MMIC Distributed Power Amplifier which operates between 2 and 18 GHz with 23 dB gain, and 26 dBm output power.

AM00020026WM-QN5-R
Broadband GaAs MMIC Distributed Power Amplifier which operates between DC and 20 Ghz with 13 dB gain, and 26 dBm output power.

Custom MMIC Circuit Design and Production

We offer custom design of MMIC circuits with output power from a few watts to over fifty watts. Power amplifiers, Low Noise Amplifiers, Phase Shifters, Attenuators, Up-converters, Down-converters, and Switches. Smart compact design in ceramic or plastic packages. Frequencies up to 40GHz. Our design team has successfully developed over 100 MMIC circuits.

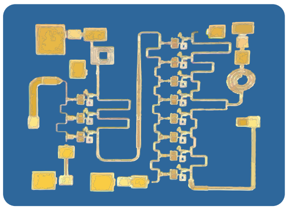

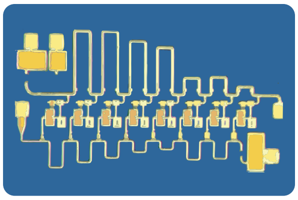

IMS
Connecting Minds. Exchanging Ideas.

Visit us at Booth 1205

We are excited to participate in this years International Microwave Symposium (IMS) show that will be held in Los Angeles, CA June 21-26th. We have lots to show you.

GaAs MMIC PAs

Model	Freq(GHz)	Gain(dB)	P1dB(dBm)	Psat(dBm)	Eff(%)	Vd(V)
AM003536WM-XX-R	0.01-3.5	23	35	36	20	20
AM002535MM-XX-R	0.03-2.5	24	34	35	25	20
AM012535MM-XX-R	0.03-2.5	20	33	33.5	20	20
AM009023WM-XX-R	0.05-9	21	21	23	20	12
AM008030WM-XX-R	0.05-10	18	30	31	20	12
AM012020WM-XX-R	0.1-2	30	16	17	8	8
AM011037WM-XX-R	0.2-1.0	31	37	37.5	40	8
AM103026MM-XX-R	0.9-3.2	22	25	26	10	14
AM132740MM-XX-R	1.3-2.7	26	38	39	30	14
AM142540MM-XX-R	1.4-1.8	25	39	40	35	14
AM153040WM-XX-R	1.4-3.4	18	37	38	30	12
AM143440WM-XX-R	1.5-1.8	20.5	38.5	39	35	12
AM143438WM-XX-R	1.5-1.8	20.5	37.5	38	30	12
AM153540WM-XX-R	1.5-3.5	18	39	39.5	35	14
AM183030WM-XX-R	1.6-3.3	30.5	30.5	31.5	20	8
AM183031WM-XX-R	1.6-3.3	31.5	31.5	32.5	25	8

GaN MMIC PAs

Model	Freq(GHz)	Gain(db)	Psat(dBm)	Eff(%)	Vd(V)
AM00010037WN-00-R	DC-10	13	37	25	28
AM00010037WN-SN-R	DC-10	13	37	23	28
AM003042WN-00-R	0.05-3	24	42	35	40
AM003042WN-XX-R	0.05-3	23	42	33	40
AM206041WN-00-R	1.8-6.5	32	42	27	28
AM206041WN-SN-R	1.8-6.5	30	41	23	28
AM408041WN-00-R	3.75-8.25	33	42	27	28
AM408041WN-SN-R	3.75-8.25	31	41	23	28
AM07512041WN-00-R	7.75-12.25	28	42	27	28
AM07512041WN-SN-R	7.75-12.25	27	41	22	28
AM08012041WN-00-R	7.5-12	22	42	20	28
AM08012041WN-SN-R	7.5-12	21	41	20	28

Visit our website today to view our full product line.

www.amcomusa.com

CELEBRATING 23 YEARS OF BUSINESS

Phone 301.353.8400 - www.amcomusa.com - info@amcomusa.com

INVITED PAPER

Advancements in III-V Technology and Performance: A Twenty-Year Retrospective

David Danzilio and Dennis Williams
WIN Semiconductors Corp., Taoyuan City, Taiwan

As WIN Semiconductors marks its twentieth anniversary, we look back at how III-V technology has evolved to meet continually changing market requirements and achieve production scale.

Over the last 20 years, products based on III-V semiconductor technology have transitioned from defense-oriented niche applications to an enabling technology used in mobile devices, wireless networks, satellite communications and optoelectronics. Common to all these uses is the need for economically viable solutions with best-in-class front-end performance, including operating frequency, power, efficiency and linearity. In all these applications, the performance advantages of compound semiconductors have enabled GaAs to become the dominant front-end technology for the mobile communications that connect billions of people across the globe.

The broad adoption of compound semiconductor technologies by the wireless industry is well illustrated by its remarkable revenue growth (see ***Figure 1***). This figure, courtesy of Strategy Analytics, illustrates the impact of two macro trends on annual GaAs component revenues. The first growth phase, from 1990 to 1999, was driven by the Microwave and Millimeter Wave Integrated Circuit (MIMIC) and Microwave and Analog Front-End Technology (MAFET) programs funded by the U.S. Department of Defense, to mature critical GaAs technologies. These programs largely benefited U.S. GaAs manufacturers, helping component revenue increase from some $250 million in 1990 to $2.5 billion in 1999.

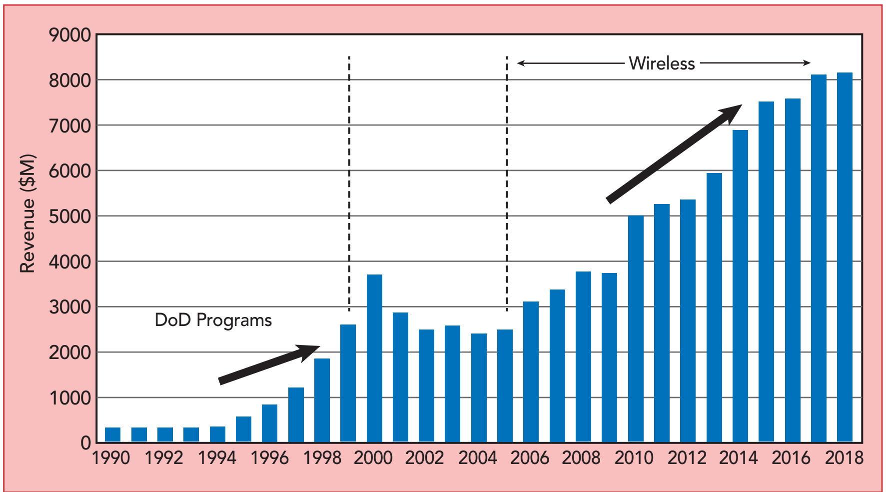

Fig. 1 **RF GaAs component revenue from 1990 through 2018.** ***Source:*** **Strategy Analytics.**

The second growth phase, from 2006 to 2017, was driven by the global adoption of GaAs technology in wireless communications systems and mobile devices. Early in this period, smartphone manufacturers recognized that GaAs power amplifiers (PA) provided the optimum combination of higher linearity and transmit power with the low power consumption needed in battery-operated devices. At the same time, WIN Semiconductors provided pure-play foundry access to a portfolio of GaAs technologies. The superior performance and value of GaAs front-ends combined with rapid production scaling enabled the industry to support annual smartphone shipments exceeding 1 billion units, with RF GaAs revenue more than $8 billion in 2017.

PURE-PLAY FOUNDRY MODEL

An underappreciated element in the market uptake of III-V products was the success of the pure-play foundry model. When WIN Semiconductors started in 1999, the III-V wafer foundry business was exclusively a side business of the established GaAs component manufacturers. This made good economic sense for the foundry owner, selling excess wafer capacity to an external component company increased fab utilization, and the added revenue offset some of the fixed costs of a capital-intensive factory. This was

a viable foundry model as long as there was no direct competition between the wafer supplier, an integrated device manufacturer, and the foundry customer, also an integrated device manufacturer.

Inevitably, component suppliers with similar product expertise will compete for the same market opportunities. This competition typically results in lost business for the foundry customer, because fabless component suppliers are at a significant disadvantage when they compete with their foundry suppliers. A wafer foundry business based on selling excess capacity inevitably creates business risk for the foundry customer and is not sustainable. Today, nearly all integrated device manufacturers have terminated their foundry businesses; the few that remain limit engagement to "strategic customers."

To support the demand driven by the wireless industry, the GaAs component market needed access to high performance compound semiconductor technology from a pure-play foundry. WIN Semiconductors entered the III-V wafer foundry market to meet this need. To prove the pure-play model could succeed with compound semiconductors, WIN had to provide technologies that offered a market advantage: in PA performance, multifunctional integration and flexible large-scale manufacturing.

MOBILE DEVICES: EFFICIENCY MATTERS

By the mid-2000s, broad deployment of 3G networks and mobile data services moved handsets from a business tool to a consumer device. CDMA networks imposed new linearity requirements, difficult to achieve with Si PAs. The battery limitations of mobile devices required the front-end PA to meet this linearity specification at the required power level—typically 28 dBm—while operating at the highest possible power-added efficiency (PAE). These challenging mobile PA requirements created an opportunity for high performance GaAs HBT technology. HBT quickly became the "best value" mobile PA technology, as it provided high gain (10 dB per stage), linearity (ACPR ≤-40 dBc) and PAE (>65 percent), ensuring long battery life.

CDMA mobile PAs have a simultaneous set of requirements, where the primary trade-off is between linearity and efficiency at a set output power. This trade-off is shown in ***Figure 2***, which overlays 1.95 GHz load-pull contours of PAE and linearity for an HBT2 power cell at 28 dBm output and biased at 3.4 V. HBT2 was WIN's workhorse platform for mobile PAs from 2004 through 2008. The Smith chart shows that the loads for peak ACLR and PAE are similar, with an optimal trade-off at the intersection of the peak ACLR and the contour corresponding to 50.8 percent PAE. The output match for peak linearity is only 5 percentage points away from the peak PAE match, which is a unique characteristic of GaAs HBTs. This reduces the "cost" of efficiency to achieve linearity, enabling a compact two-stage GaAs HBT PA to meet all CDMA requirements while maintaining approximately 50 percent PAE.

With the growing popularity of high-end smartphones with large, power-hungry displays—and thin form factors limiting battery capacity—handset manufacturers expect component suppliers to reduce power consumption. To be competitive, component suppliers create differentiation by offering better performance or greater functionality with reduced current consumption. In the RF front-end, PA efficiency, linearity and functionality are the primary differentiators, and securing market share on the next smart-

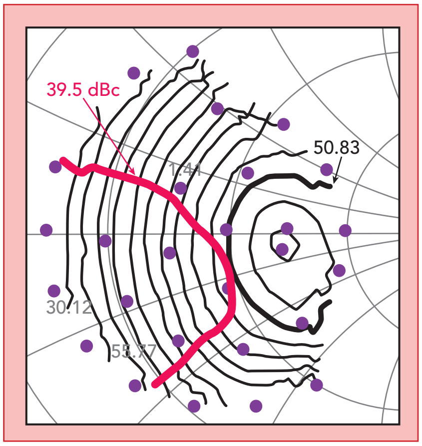

▲ **Fig. 2** Impedance for peak ACLR with high PAE.

ULTRA-LOW PHASE NOISE OCXOs 10 and 100 MHz

FOR:

- TELECOMMUNICATION EQUIPMENT
- TEST & MEASUREMENT EQUIPMENT
- DIGITAL TV BROADCASTING
- HI-END AUDIO EQUIPMENT
- RADARS, FREQUENCY SYNTHESIZERS

MV269M 100 MHz

√ SMALL PACKAGE 21 X 13 X 9.5 (DIL 14)
√ SIN AND HCMOS OUTPUTS

Phase noise, dBc/Hz

10 Hz	<-102
100 Hz	<-135
1 kHz	<-163
10 kHz	<-175
100 kHz	<-178

MV317 100 MHz

√ LOW G-SENSITIVITY <1E-9/G (TYPICAL), OPTIONS UP TO <2E-10/G

Phase noise (typical), dBc/Hz

10 Hz	<-102
100 Hz	<-135
1 kHz	<-164
10 kHz	<-180
100 kHz	<-185

MV359 DUAL FREQUENCY 10 and 100 MHz

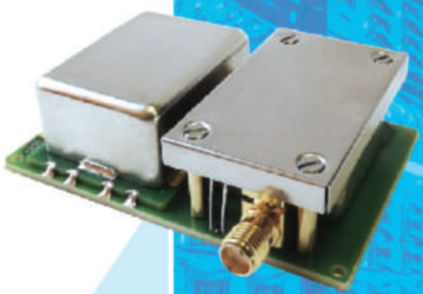

√ ALLAN DEVIATION 5E-13 PER SEC.
√ TEMPERATURE STABILITY ±1E-9

Phase noise, dBc/Hz

	for 10 MHz	100 MHz
1 Hz	<-120	<-98
10 Hz	<-145	<-125
100 Hz	<-160	<-135
1 kHz	<-165	<-160
10 kHz	<-170	<-175
100 kHz	<-170	<-180

MORION US

MORION US, LLC
1750 MERIDIAN AVE. #5128
SAN JOSE, CA 95150

+1 408 329-8108
SALES@MORION-US.COM
WWW.MORION-US.COM

phone platform frequently comes down to PA efficiency and the proven ability to improve performance with each design cycle.

WIN Semiconductors has responded to these expectations with successive generations of GaAs HBT transistor designs and process platforms that increase linear PA efficiency. Since 2012, WIN Semiconductors has used letter designations for production epitaxial designs, and ***Figure 3*** compares the C, D and F epi used on the HBT4 platform. Epi C rolled out in 2012 for LTE, epi D in 2014 for improved linearity and epi F in 2015 for the higher voltage operation required for envelope tracking (ET). Comparing data from identical cell layouts and testing, all improved linear PAE, with the maximum PAE at -40 dBc ACPR. Further RF performance improvement can be achieved by shrinking device geometries. Figure 3 also shows an additional 2.5 points of PAE obtained using the HBT5 platform with epi F.

WIN Semiconductors' HBT technologies have sustained increased linear PAE, supporting the transition from 3G to 4G and meeting increasingly difficult front-end specifications. Until 2013, average power tracking was the de-facto standard for cellular PA designs. ET was introduced to further reduce PA power consumption, and ***Figure 4*** shows the 10-year increase in PAE for WIN Semiconductors' HBT technologies characterized for ET. HBT7-H is WIN Semiconductors' most advanced HBT platform, planned for release mid-year 2020.

WIN Semiconductors continues to improve HBT technology to meet the emerging demands for 5G handset PAs, which will operate to 6 GHz. ***Figure 5*** shows the improvement in unit cell small-signal gain for several generations of HBT platforms, using the same epi. The HBT7 release will be accompanied by new epi layer designs to improve performance in the higher frequency 5G bands.

MULTI-MARKETS: POWER & EFFICIENCY MATTER

Multi-market applications for III-V technologies encompass a diverse set of functions—PAs, low noise amplifiers, RF switching, single-chip front-ends, mixers—and performance specifications—power, linearity, efficiency, noise figure and switching speed. Operating frequencies range from 1 to >100 GHz, and the diversity of products using GaAs and GaN technologies is staggering: macrocell and small cell base stations; mmWave phased arrays for 5G fixed wireless access and mobile; backhaul links; terminals for low earth orbit (LEO) and geostationary earth orbit (GEO) satellites; S-, C- and X-band radar; mmWave components in optical networks. New functions, specifications and frequencies are constantly evolving with these markets.

No single transistor technology or process node has the capability to provide the best product performance across this diverse range of functions and operating frequencies. A range of GaAs PHEMT and

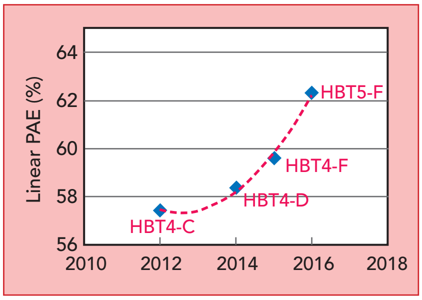

Fig. 3 Linear PAE improvement for WIN HBT processes.

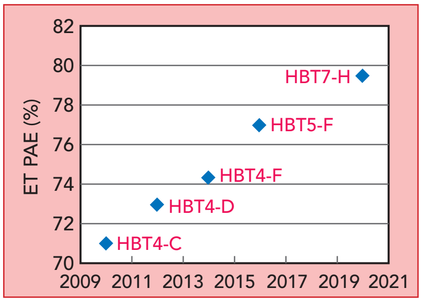

Fig. 4 Improvements in HBT PAE with ET.

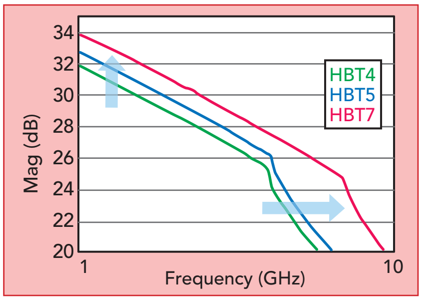

Fig. 5 Small-signal gain vs. frequency for recent HBT platforms.

ALTUM RF

2–20 GHz GaN DISTRIBUTED POWER AMPLIFIER

THE ARF1307C7 IS HOUSED IN A 7X7MM AIR-CAVITY SURFACE-MOUNT CERAMIC PACKAGE AND DESIGNED FOR HIGH BANDWIDTH APPLICATIONS. IT FEATURES 17 dB SMALL-SIGNAL GAIN, 10 W OF OUTPUT POWER AND 11 dB OF POWER GAIN.

IT IS VERSATILE FOR A RANGE OF APPLICATIONS, INCLUDING TEST & MEASUREMENT, AEROSPACE & DEFENSE, AND ISM.

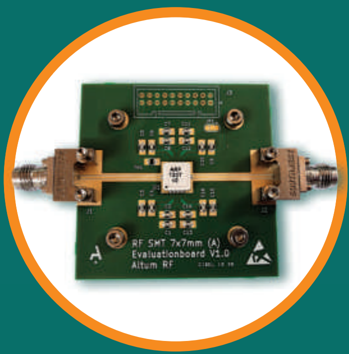

ALTUMRF.COM

ESTABLISHED BY LEADING EXPERTS IN THE RF/MICROWAVE INDUSTRY, ALTUM RF DESIGNS HIGH-PERFORMANCE MILLIMETER-WAVE TO DIGITAL SOLUTIONS FOR NEXT GENERATION MARKETS AND APPLICATIONS.

MEET US IN THE IMS2020 STARTUP PAVILION (BOOTH 6)

INFO@ALTUMRF.COM | +31 (0) 40 2390 888

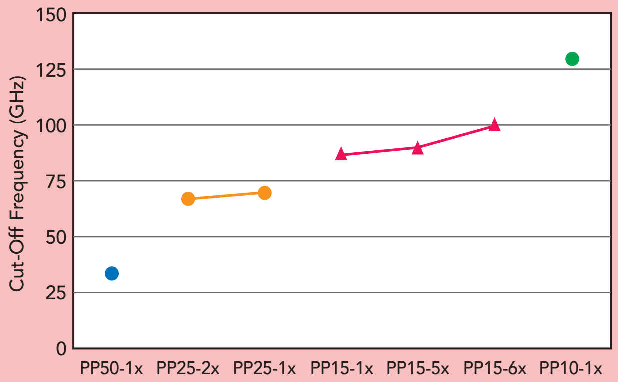

Lg (μm)	0.50	0.25	0.25	0.15	0.15	0.15	0.10
V_B	20	20	14	10	16	13	10
V_{DD}	8	8	6	5	6	6	4

Fig. 6 GaAs PHEMT cut-off frequency.

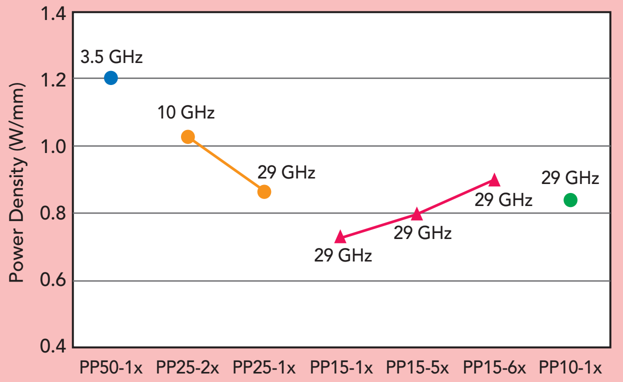

Lg (μm)	0.50	0.25	0.25	0.15	0.15	0.15	0.10
V_B	20	20	14	10	16	13	10
V_{DD}	8	8	6	5	6	6	4

Fig. 7 GaAs PHEMT transistor power density.

RF GaN HEMT technologies have proven the best options for designers. The primary figure of merit for these technologies is the cut-off frequency (f_t), an indication of transistor capability. f_t reflects multiple device geometry and process parameters, the most pertinent being operating frequency, output power, operating voltage and gate length (l_g). ***Figures 6*** and ***7*** show transistor f_t and saturated output power in several of WIN's GaAs PHEMT processes optimized for multi-market applications. The tables with each figure show the main transistor characteristics for each process, with the processes arranged by decreasing l_g and, for the same l_g, earliest to latest process. Each process was optimized for a specific multi-market requirement: PP50-1x for 10 to 20 W PAs operating below 5 GHz; PP25-2x for 10 W MMICs operating through 10 GHz; PP25-2x with higher f_t for 30 GHz applications. With an f_t above 90 GHz, the PP15 family supports PA MMICs through 60 GHz, and the 0.1 μm PP10 process is used for applications through 100 GHz.

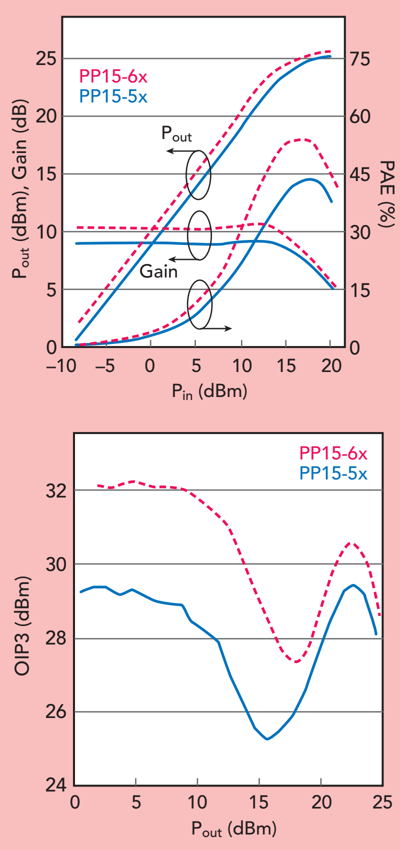

Fig. 8 29 GHz swept power and OIP3 for PP15-6x and PP15-5x PHEMT processes.

Figure 6 illustrates the trend between smaller gate length and increasing f_t. This is not the only path, as seen with the three PP15 processes. Originally released in 2001, PP15-1x operates at 5 V VDD and provides a saturated output power (P_{sat}) of 0.7 W/mm (see Figure 7). Responding to the need for higher output power, the PP15-5x process was released in 2011, achieving a P_{sat} of 0.8 W/mm at 6 V bias and a modest improvement in f_t. Most recently, linearity has become a differentiator, which drove the development of PP15-6x. Released in 2018, this technology maintains 6 V operation, increases f_t to 100 GHz, raises P_{sat} to 0.9 W/mm and significantly improves linearity.

Figure 8 compares the transistor power performance and output third-order intercept (OIP3) for both the PP15-6x and PP15-5x processes, measured at 29 GHz and 6 V VDS. PP15-6x has 1 dB more gain, 10 points higher PAE and increased P_{sat}. The 29 GHz OIP3, measured with a two-tone input signal separated by 10 MHz and using the optimal input and output impedances, shows this latest generation achieves an OIP3 improvement of 2 to 3 dB relative to PP15-5x.

TABLE 1

WIN GaN HEMT PROCESSES

Process	Gate Length (μm)	V_B (V)	f_t (GHz)	Drain Voltage (V)	P_{sat} (W/mm)	Peak PAE (%)
NP45-11	0.45	>170	15	48	10.5 @ 2.7 GHz	68
NP25-02	0.25	>120	25	28	4.3 @ 5.8 GHz	76
NP15-00	0.15	>120	35	20	3.3 @ 29 GHz	43

GAN FOR HIGHEST POWER DENSITY

The continued market demand for higher RF power spurred the development and adoption of GaN HEMTs, which deliver impressive RF power and are the principal PA technology where the highest power density and PAE are primary requirements. To support PA designs from 1 to >30 GHz, WIN has developed three GaN processes manufactured on 100 mm SiC substrates, to provide maximum thermal dissipation (see ***Table 1***).

With a bandgap of 3.39 eV, GaN HEMTs have considerably higher breakdown (VB) and operating voltages compared to GaAs, with a bandgap of 1.34 eV. GaN HEMTs also use a source-coupled field plate to reduce the peak electric field and improve breakdown. The field plate enables GaN transistors to operate at drain biases from 20 to >48 V. Fundamentally, the material properties of GaN enable transistor designs with high electron density, and the field plate contributes to the high breakdown and operating voltages to achieve power densities >10 W/mm. ***Figure 9*** shows the 2.7 GHz swept power characteristics of a 4 × 250 μm GaN HEMT from the NP45-11 process. This 1 mm transistor delivers a saturated output power >10 W with 68 percent PAE.

FUNCTIONALITY, FLEXIBLE INTEGRATION

To reduce chip counts and simplify assembly, multifunction technologies with functionality beyond the core amplifier are being adopted. Since every MMIC is designed to meet a unique set of requirements, WIN Semiconductors has developed a portfolio of added functions that can be used when needed. These on-chip functions enable electrostatic discharge (ESD) protection, control of PA performance, interface with external control signals or integration of receive low noise amplifiers (LNA) and T/R switches to realize a single-chip front-end.

Perhaps the most basic function is ESD protection. Because of historical process limitations, PHEMT technologies have used large area Schottky diodes for ESD protection. These diodes, which use the same Schottky contact as the PHEMT gate elec-

Reliability Is Essential

HASCO's Ruggedized, Armored RF and Microwave Test Cables provide supreme durability, repeatable measurements, low insertion loss and excellent phase and amplitude stability with flexure.

Ruggedized Test Cables for Laboratory, Production, Test and Measurement application[redacted].
Standard lengths in stock.

SPECIFICATION	HLL185R (1.85mm)	[redacted]	[redacted]228R (2.92mm)	HLL283R (SMA)
• Frequency Range	DC - 67 GHz	DC - 50 GHz	DC - 40 GHz	DC - 26.5 GHz
• Insulation Resistan[redacted]	5,000MΩ	5,000MΩ	5,000MΩ	[redacted]
• Insertion Loss	≤4.0dB @ 67 GHz	≤2.8dB @ 50 GHz	≤2.0dB [redacted]	≤[redacted]
• VSWR	1.50:1 MAX	[redacted]	[redacted]	[redacted]
• Impedence	50 Ohms	[redacted]	[redacted]	[redacted]
• Min. Bend Radius	1.2"	[redacted]	[redacted]	[redacted]
• Velocity of Propagation	76%	76%		
• RF Leakage	>90 dB	>90 dB	[redacted]	[redacted]
• Phase Stability	≤±0.15dB @ 67 GHz	≤±0.1dB @ 50 GHz	≤±[redacted] @ 40 G[redacted]	≤[redacted]
• Phase Stability over Flexure	≤±6.5° @ 67 GHz	≤±5° @ 50 GHz	≤±4° @ 40 GHz	≤±2.7° @ 26.5 GHz
• Dielectric Withstanding Voltage	1,000V Max at Sea Level	1,000V Max at Sea Level	1,000V Max at Sea Level	1,000V [redacted] at Sea Level
• Capacitance	27pf/ft=88pf/m	27pf/ft=88pf/m	27pf/ft=88pf/m	27pf/ft=88pf/m
• Temperature Range	-45°C - +85°C	-55°C - +125°C	-55°C - +125°C	-55°C - +125°C

HASCO Components

Phone +1 (888) 498-3242
sales@hasco-inc.com
www.hasco-inc.com

Intertek
RoHS compliant

Order Online for Same-Day Shipping

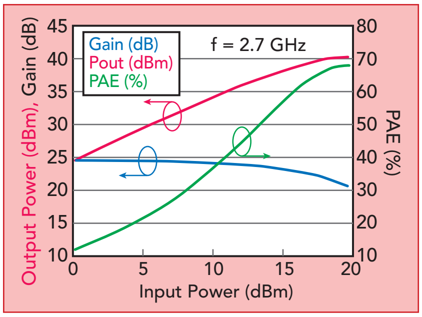

▲ Fig. 9 Swept power and efficiency at 2.7 GHz for a 1 mm NP45-11 GaN HEMT.

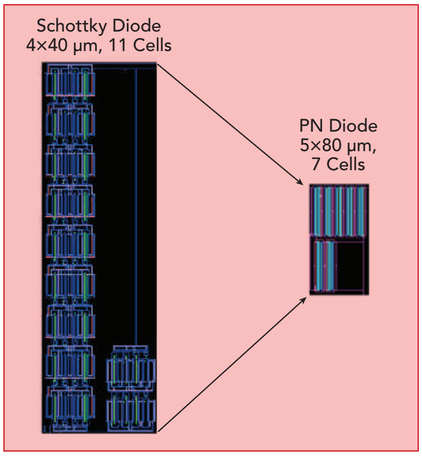

▲ Fig. 10 Size of Schottky and PIN diode ESD protection circuits.

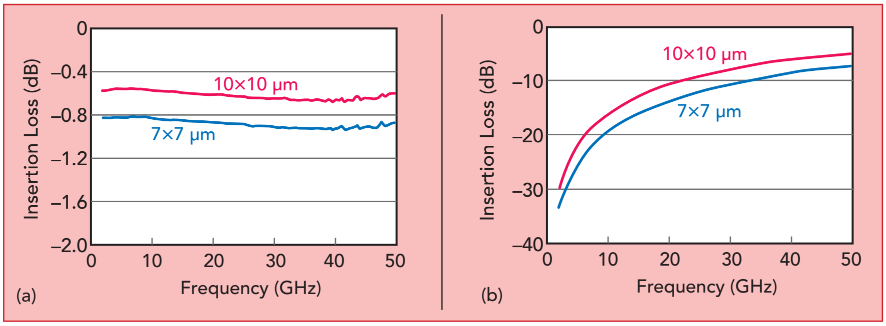

▲ Fig. 11 PIN diode insertion loss (a) and isolation (b) vs. frequency.

trode, are limited to approximately 800 V protection using the human body model (HBM). Depending on the level of protection required, these large area diodes can use substantial chip area. To reduce the size, WIN Semiconductors has incorporated monolithic PN junction diodes into its PHEMT processes. They provide up to 3 kV HBM protection and are much smaller than a Schottky, reducing the area by some 80 percent (see ***Figure 10***).

The same process used for PN diodes can be used for PIN diodes. When integrated with a PHEMT process, PIN diodes can provide ESD protection, a power limiter for an LNA or a mmWave T/R switch in a single-chip front-end. ***Figure 11*** shows the measured insertion loss and isolation for two shunt PIN diodes from the PIH1-10 mmWave PHEMT platform. 7 × 7 and 10 × 10 μm diodes have insertion losses of 0.6 and 0.9 dB, respectively.

On-chip logic is particularly important for active antenna arrays, to simplify the interface with the beamformer IC. A growing library of logic cells, such as the two-bit decoder shown in ***Figure 12***, has been incorporated into the baseline PIH1-10 technology as process options, to be used if required by the application. These libraries of logic and ESD reference circuits provide designers enhanced tools to add functionality to high performance mmWave front-ends.

Depending on the III-V device used, PHEMT or GaN HEMT, a power transistor can be used as a low noise amplifier or an RF switch. Although adding on-chip functionality, it will entail a performance compromise: an on-chip LNA or RF switch built with a transistor optimized for power density may not have best-in-class noise figure or insertion loss. Nonetheless, it may be a favorable trade-off, by reducing RF losses, parts count or by simplifying assembly and lowering cost. To help designers understand the tradeoffs, WIN Semiconductors characterizes its GaAs PHEMT and GaN HEMT technologies for LNA and switch performance, incorporating models into the PDKs. Design versatility is enhanced by offering optional enhancement/depletion transistors, for logic and digital bias control, and PN or PIN diodes, for ESD protection, input limiting and power switching. These options of-

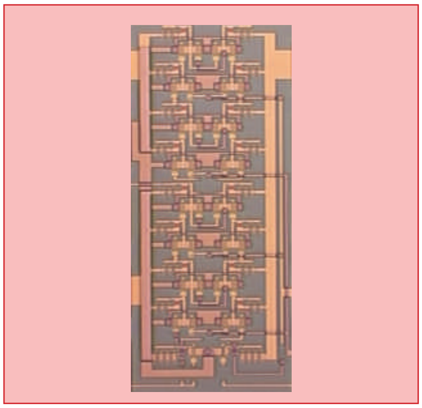

Fig. 12 Two-bit GaAs decoder.

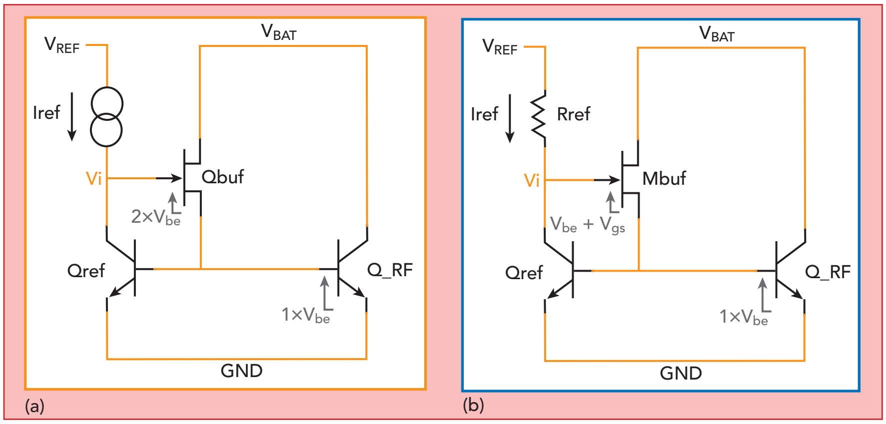

Fig. 13 Stand-alone HBT (a) and BiHEMT (b).

fer multiple solutions for designing complex circuits and achieving challenging specifications.

With GaAs HBT MMICs, increasing the functionality is achieved by adding enhancement/depletion mode PHEMT devices to the HBT process. This functionality is available with WIN's BiHEMT (bipolar + HEMT) platform. Combining both technologies on the same MMIC provides a high linearity and efficient HBT PA, low loss D-mode PHEMT switch and low F_{min} E-mode LNA with control logic. BiHEMT control logic operates at lower voltage, enabling the V_{enable} control voltage to be reduced from 1.2 V, for the HBT process, to 0.75 V for the depletion mode PHEMT (see ***Figure 13***). The integration advantages of the BiHEMT process have been demonstrated by the market's adoption of single-chip front-end modules for Wi-Fi, which integrate the LNA, switch and PA (see ***Figure 14***). Single-chip front-ends now comprise between 30 and 50 percent of mobile Wi-Fi production volumes.

As mobile devices become thinner, interior board space is increasingly valuable, driving the front-end supply chain to smaller packages —or no package. Similarly, losing 1 dB of power to packaging in a mmWave phased array is expensive. These packaging challenges flow down to the front-end semiconductor technology, and WIN Semiconductors has responded with a portfolio of flexible Cu pillar bump assembly interfaces that minimize package footprint and reduce mmWave losses. Cu bumps are particularly useful for GaAs HBT and BiHEMT technologies, as they form RF/DC connections and provide an improved thermal environment for the transistors in the PA (see ***Figure 15***). The cross-section shows a copper redistribution layer (RDL) used to form high-Q inductors or to position a bump input/output (I/O) above the underlying circuitry. To implement this packaging capability, WIN Semiconductors has internal Cu pillar bump facilities co-located with its wafer fabs.

At the 28 to 39 GHz bands now being used for 5G links, over-designing the power and LNA to offset package losses is expensive, and the problem becomes more severe at the higher bands used for high capacity wireless backhaul (71 to 86 and 92 to 114 GHz). Bond wire inductances can impair PA performance by >1 dB. I/O bumps at these frequencies are feasible; however, to use them, designs must shift from microstrip to coplanar waveguide. Unfortunately, the industry has limited experience with coplanar design, prompting WIN to develop a process technology to pattern the backside

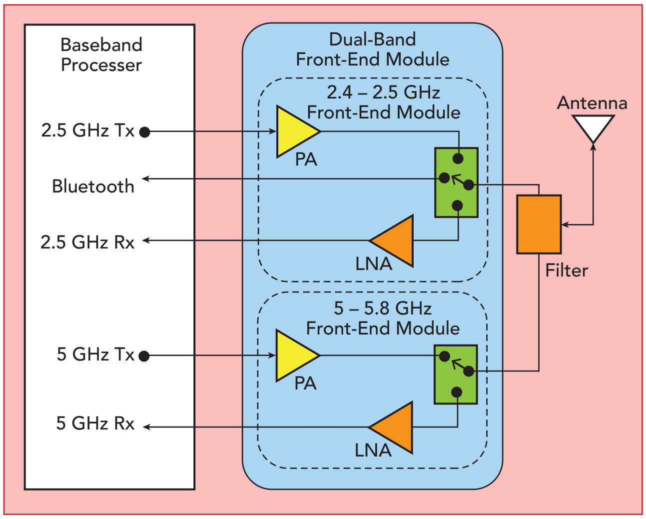

Fig. 14 Wi-Fi module using a single-chip BiHEMT front-end.

ground plane to isolate the input/output ports and create through-chip RF transitions (see ***Figure 16***). A MMIC design uses microstrip on the topside, with through-chip transitions on the RF I/O ports and standard wire bonds for DC connections. The ground plane is removed on the backside of the RF transition for the I/O connections. The design rules for this patterning technique are flexible; when coupled with a compatible board design and die bonding process, the approach can eliminate RF bond wires from the assembly.

SUMMARY

Compound semiconductors have evolved from performance-driven to the "best value" front-end technology for smartphones, wireless networks and multi-market applications. III-Vs, particularly GaAs, have become the preferred front-end solution, combining best available performance with a flexible amplifier trade-space. This characteristic enables a simpler path to satisfy difficult MMIC performance requirements. With multiple degrees of freedom to optimize and advance transistor capabilities, GaAs and GaN have demonstrated decades of RF, microwave and mmWave performance improvement. These technologies now offer increased on-chip functionality and advanced integration options to support diverse packaging environments, applications and systems.

Over the last 20 years, the annual market for GaAs components has grown to over $9 billion. This expansion has come despite the challenges of increasingly difficult specifications and unrelenting competition from advanced Si processes. As the industry's leading pure-play III-V wafer foundry, WIN Semiconductors has responded with sustained technology advancement, operational excellence and manufacturing scale. This capability is WIN Semiconductors' core strength and underpins the continued growth of the GaAs and GaN component market. ■

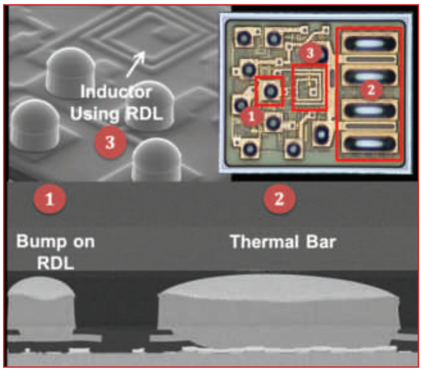

Fig. 15 Cu bumps used for I/O, thermal management and high Q inductors.

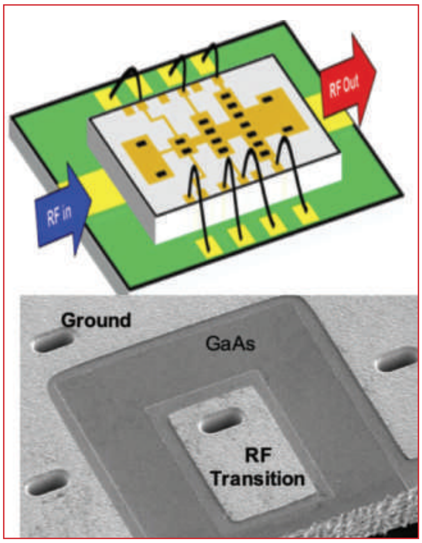

Fig. 16 Patterned ground plane for through-chip RF transitions.

Editor's Note: This article is based on US Patent Application No. 62/469,752, March 10, 2017. It describes a new micro-electromechanical-system (MEMS) switch technology in a three-part article over the next three issues. Part I reports on MEMS switch topologies including a new defective ground structure (DGS) and metamaterial inspired capacitive contact MEMS switch; Part II reports methods to reduce stiction effects in a resistive contact MEMS switch; and Part III discusses methods to reduce static friction (or stiction) effects in a capacitive contact MEMS switch for applications in modern electronic circuits and 5G communications.

INVITED PAPER

A Microelectromechanical Switch with Metamaterial Contacts, Part I: Concepts and Technology

Shiban K. Koul and Chaitanya Mahajan
C.A.R.E, Indian Institute of Technology, Delhi, India

Ajay K. Poddar and Ulrich L. Rohde
Synergy Microwave, N.J., USA

A new MEMS switch with improved isolation, insertion loss and reduced liability for stiction is reported for the applications in high frequency electronics and communication systems. MEMS switches are suitable for signal routing for transmit and receive applications, switched line phase shifters for phased array antennas, wide band tuning networks and high precision instrumentation applications. Typical MEMS switches are categorized by the contact methods, capacitive (metal-insulator-metal) and resistive (metal-to-metal).

MEMS switches are typically a silicon-based integrated circuit technology with moving mechanical parts that are released by means of etching sacrificial silicon dioxide layers. MEMS switches include a signal line having an input port and output port between first and second ground planes, and a beam for controlling the activation. In this article, the variation of the switch architecture includes one or more DGS formed in the first and second ground planes, and a corresponding secondary deflectable beam positioned over each DGS. For reducing the vulnerability of stiction, the switch incorporates an artificial engineering structure known as metamaterial for creating the repulsive Casimir interactions to mitigate the stiction related issues in switches.[1-6]

Compared with PIN diodes or field effect transistor switches, MEMS switches offer lower cost and improved performance (power consumption, isolation, insertion loss and linearity). However, MEMS switches can encounter several drawbacks: high actuation voltages, high insertion loss and poor return loss. In addition to this, MEMS switches are susceptible to electromechanical failure after many switching cycles, especially under hot switching conditions. For instance, the switch may fail due to stiction buildup. When the moveable part of the switch is pulled into contact with another component of the system (e.g., a signal line); the static friction can cause the switch to become stuck and non-functional. It may require a high voltage to overcome the stiction force. But at low voltage, the switch can remain "welded" to the component.

MEMS SWITCHES

MEMS switches are usually categorized by the contact methods: capacitive (metal-insulator-metal) and resistive (metal-to-metal). Capacitive switches use a thin layer of dielectric material to separate two conducting electrodes when actuated. The dielectric layer prevents direct metal-to-metal contact. Therefore, stiction of contacts due to thermal energy is less of a concern. However, the thin layer of dielectric material will only conduct signals with reasonable insertion loss when the coupling between conductor electrodes is above a certain frequency. Moreover, the isolation bandwidth of capacitive switches is limited by the ratio between the ON and OFF capacitances. Metal-to-metal switches use physical contact of metal with low contact resistance to achieve low insertion loss when actuated. Therefore, the metal-to-metal MEMS switches can be operated from DC to RF frequency with isolation defined by the coupling capacitance of the electrodes when the switch is open. The metal-to-metal contact is made by surface asperities and the true contact area is much smaller than the apparent contact area. For the metal-to-metal contact to have low contact resistance, some plastic deformation of the asperities is required.


Portable Handheld Field Solutions
Expand your choice of 5G spectrum analysis capabilities
-Coax or Waveguide
24 to 40 GHz
M28H2ADC
M28H2ADC-K
26 GHz (24.25 to 27.5 GHz)
28 GHz (27.5 to 28.35 GHz)
38 GHz (37 to 38.6 GHz)
39 GHz (38.6 to 40 GHz)
Innovation in Millimeter Wave Solutions
www.omlinc.com
(408) 779-2698
OML

In general, as the pull-down force increases, the asperity deformation increases and the contact resistance decreases. However, adhesion of the contact point is proportional to the contact area and the temperature associated with the degree of deformation, so lower contact resistance is often accompanied with stronger adhesion. RF switches carry RF signals, so in certain operation conditions, such as impedance mismatch, a high level of RF power will pass through the switches. In such cases, the heat generated by RF power may cause micro-melting of asperities and could potentially short the contact points.

Before the integration of metal-to-metal switches into 5G mmWave communication systems become a reality, the adhesion (stiction) problem and reliability associated with the contacts needs to be resolved. The possible techniques for reducing the surface adhesion is either by selecting contact materials with less adhesion by applying chemical surface treatment or eliminating contamination with plasma cleaning.

Figure 1 illustrates a typical example of a cantilevered out-of-plane MEMS switch. Figure 1a is a cross-sectional view of the switch along X-axis; Figure 1b is a top view of the switch; and Figure 1c is a cross-sectional view of the switch along Y-axis. The typical MEMS switch is formed over a coplanar waveguide 101 in which a signal line 110 is formed between ground planes 102, 104 on a substrate 105 as shown in Figure 1. The signal line 110 includes an input port 112 and an output port 114 formed on opposing ends of the substrate 105. The cantilever switch includes a post 120 or anchor affixed to the substrate 105 and includes an extension extending over the substrate in a direction perpendicular to the signal line 110. The extension of the cantilever includes a bottom layer 125 of dielectric material, such as silicate and a top layer of conductive material 130, such as gold. The cantilever further includes a contact bump or dimple 135 positioned underneath the bottom dielectric layer 120 and in alignment with the signal line ports 112, 114. Thus, when the cantilever is bent downward, the dimple 135 contacts the signal line 110, thereby connecting the input and output ports 112, 114.

In addition to this, the MEMS switch depicted in Figure 1 also includes an electrostatic actuator (not shown) for actuating the cantilever by applying or removing a DC bias voltage between the cantilever and the ground 102, 104 of the coplanar waveguide 101. The cantilever bends downward and upward, in a direction toward and away from the signal line, respectively, in response to the applied voltage from the actuator. Other RF MEMS switches may rely on a lateral movement in order to bring the moveable part of a cantilevered switch toward or away from a contact. Each moving part and contact may be metal (resistive switch), or one may be metal while the other is dielectric (capacitive switch).

NEW MEMS SWITCH USING CAPACITIVE CONTACTS (METAL-INSULATOR-METAL)

Figures 2 and ***3*** show the side view and top view of capacitive

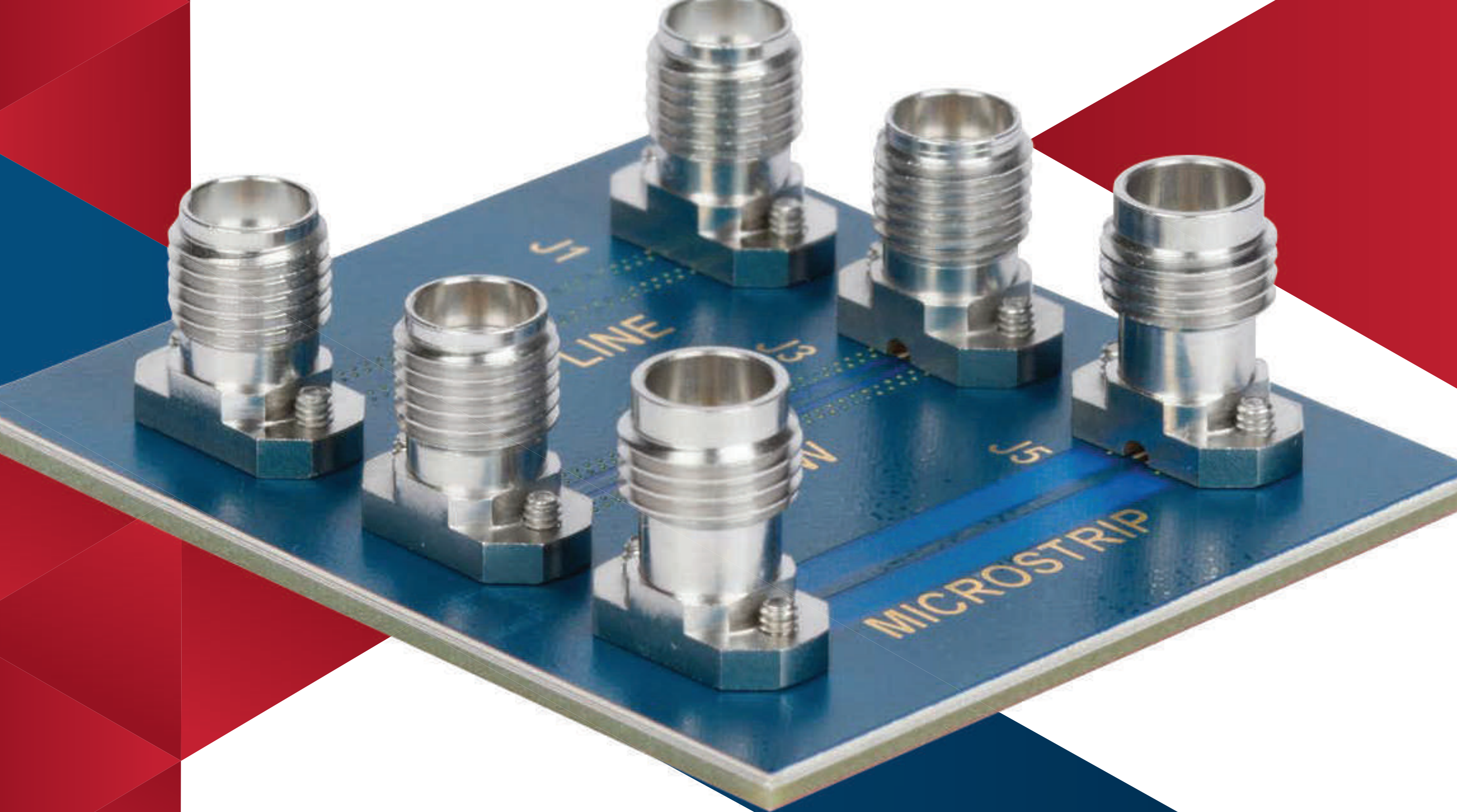
J1
LINE
J3
J5
MICROSTRIP

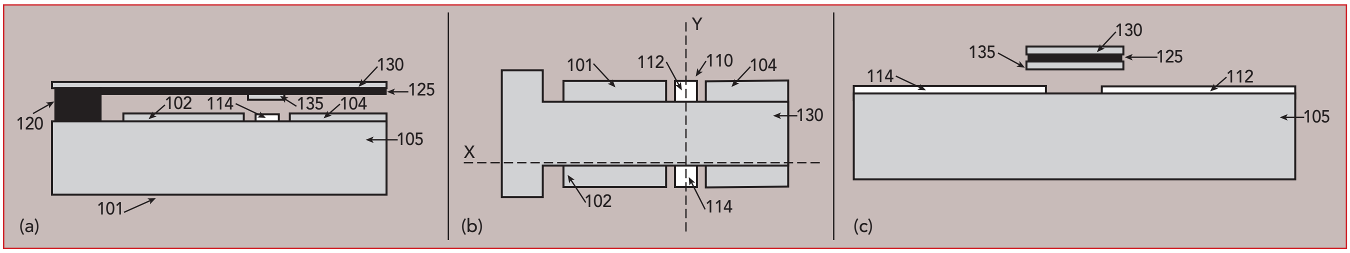

▲ Fig. 1 A typical MEMS switch: (a) cross-sectional view along X-axis, (b) top view and (c) cross-sectional view along Y-axis.

contacts shunt MEMS switch with a doubly supported cantilever beam 210 formed above a coplanar waveguide formed on a substrate 201. As shown in Figure 2, the first end 212 and second end 214 of the beam 210 are supported by respective ground planes 202 and 204 formed in the coplanar waveguide. The middle of the beam 210 is suspended over a signal line 220 formed in the coplanar waveguide. The beam 210 is connected to an actuator (not shown) configured to apply a DC bias voltage across the beam 210 and the ground planes 202, 204. The DC bias voltage causes the beam 210 to deflect downward. The signal line 220 includes a conductive layer 222 covered by a thin dielectric layer 224, such as silicon nitride.

The dielectric layer is selected about 0.2 μm thick. When the beam 210 deflects downward and contacts the signal line 220, a large shunt capacitance is obtained. The large shunt capacitance blocks RF signals from propagating along the signal line 220 of the coplanar waveguide (ON-state). When the DC bias is removed, the beam 220 deflects upward and returns to its original position, the shunt capacitance drops and the RF signal resumes propagating in unattenuated form (OFF-state).

In Figure 2, the beam 210 is made of molybdenum, and has a length of about 325 μm, a width of about 60 μm and a thickness of about 1.2 μm. The signal line 220 extends through the coplanar waveguide and has a width (in the direction of the beam length) of about 60 μm. The beam 210 is suspended about 2.5 μm above the signal line 220, thereby forming a 2.5 μm air

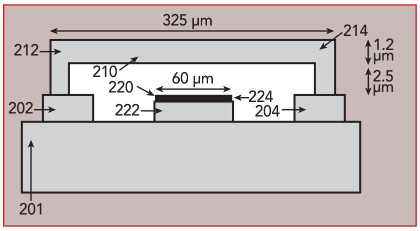

▲ Fig. 2 Shows Side-View of switch using a doubly supported cantilever beam designed above a coplanar waveguide.

SIGNAL MICROWAVE

Leading in Innovation

1.0 mm (110 GHz) Edge Launch Connectors with Test Boards Using our innovative design techniques these 110 GHz connectors and boards were developed and tested in just 4 months.

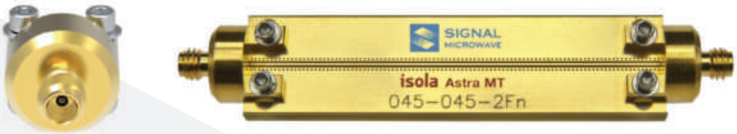

Narrow Body Edge Launch Connectors (40 GHz and 70 GHz)
Our innovative low-profile design allowed us to easily make a narrow body version targeted to 100 ohm differential designs.

Narrow Profile Standard Profile

2.92 mm Field Replaceable Connectors

- Low VSWR: DC – 27.0 GHz....1.10:1
  27.0 – 40.0 GHz...1.15:1
- Temp Range -55°C to +105°C

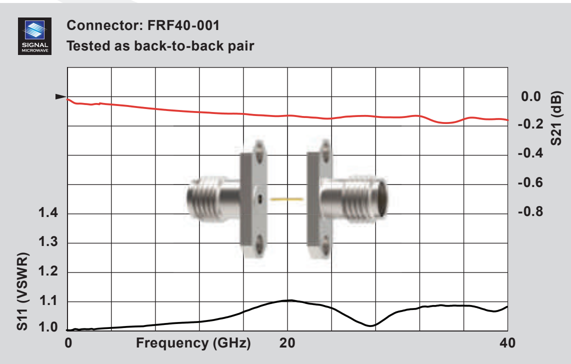

2.92 mm Vertical Launch Connectors

- Solderless connectors anywhere on the board
- Developed for the Signal Integrity Industry by modifying a field replaceable connector to interface directly to the board
- Compression fit, screw-on mounting
- No soldering Required

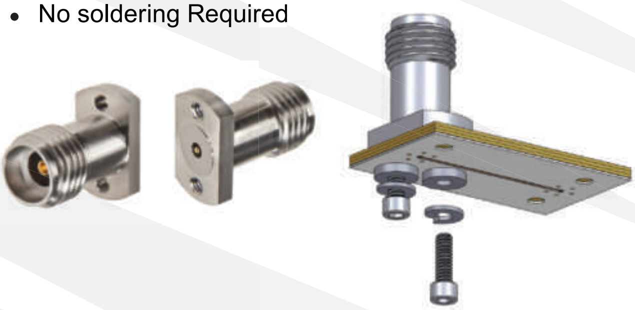

Image made using COMSOL Multiphysics® software and provided courtesy of COMSOL.

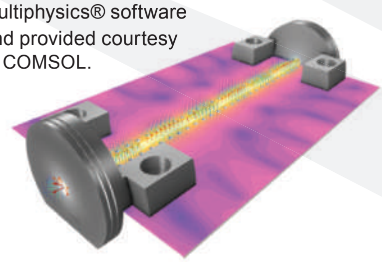

PCB Design Resources for Board Mount Connectors

- Innovative designs created by first focusing on connectors from the board side, then designing the transition to the interface.
- 3D models for simulation available at no charge to assist customers in their own development efforts.
- Innovative board launch design methodology allows for efficiently created reference designs which are made available at no charge to the customer.

For a copy of our new product brochure email us at info@signalmicrowave.com

Visit us at **IMS booth 2723**

Signal Microwave, LLC
Tempe, Arizona
info@signalmicrowave.com
www.signalmicrowave.com
(480) 322-4992

SIGNAL MICROWAVE

gap. The dielectric layer has a thickness of about 0.2 μm.

As shown in Figure 3, the beam 210 is perforated, having a grid of small perforations 301 in the middle and a large perforation 302, 303 at each end. The perforations yield improved downward deflection of the beam 210. It can be seen that vertical displacement of the beam 210 when the DC bias voltage is applied, which extends from no displacement at the respective ends 212, 214 of the beam, to about 0.91 μm in the middle of the beam 210. The DC bias for the switch has been observed to be about 37 V.

Figure 4 shows the plot of the isolation characteristics of the switch in Figure 2 when the switch is open, across a band of mmWave signals from 75 to 130 GHz. The typical isolation is about -12.4 dB at 75 GHz, and about -19.7 dB at 130 GHz. The typical insertion loss of the switch when closed is about 0.74 dB and return loss is about 10.04 dB. The actuation voltage needed for the switch can be further reduced by providing a different perforation arrangement.

In the example of ***Figure 5***, the MEMS switch includes a rectangular beam 510 made of gold and having a perforated structure. The middle portion 516 of the beam 510 forms a perforated grid or lattice. Each corner of the lattice structure then extends in a serpentine pattern toward the first and second ends 512, 514 of the beam 510. The serpentine patterns on either end are then connected to one another, thereby forming first and second serpentine structures on either end of the beam 510. The serpentine structure permits for deflection of the beam with a lower bias voltage. The dimensions of the switch shown in Figure 5 are largely comparable to that of Figure 3 except that the beam of Figure 5 is slightly longer (about 345 μm), and slightly wider (about 65 μm). The beam still deflects downward up to 0.9 μm but with only a 17 V bias voltage. The MEMS switch of Figure 5 exhibits improved isolation characteristics.

Figure 6 shows isolation characteristics of the switch of Figure 5 when the switch is open, across the 75 to 130 GHz band. Isolation is about -22 dB at 75 GHz, about -14.7 dB at 130 GHz and drops to as little as about -24.8 dB at 86 GHz. Insertion loss of the switch when closed is only about 0.6 dB and return loss is about 15.15 dB.

NEW DGS CAPACITIVE MEMS SWITCH

The isolation characteristics of these new shunt switches can be further improved by incorporating DGS, particularly in the mmWave frequency band of 75 to 130 GHz. A two-dimensional DGS is formed in each of the ground planes 702 and 704 of the MEMS switch shown in ***Figure 7***. The DGS essentially behaves as a band stop filter, thereby affecting the transmission characteristics of the switch. Figure 7 includes a beam 710 having the same structural arrangement as the beam 510 of Figure 5 and formed on a ground plane structure 701 measuring about 320 μm long by about 400 μm wide. The ground plane structure 701 includes a sig-

Micro Lamb[redacted]
Simple and Easy to Use!

MLBS-Synthesizer Test Box – 600 MHz to 20 GHz
Standard models cover the 0.6 to 2.5 GHz, 2 to 8 GHz, 8 to 20 GHz and 2 to 20 GHz frequency bands. All versions of the MLSP synthesizer product family can be easily inserted into the test box. Tuning consists of a control knob, key pad, USB and Ethernet connections. Units provide +10 dBm to +13 dBm output power levels and are specified over the lab environment of +15°C to +55°C and are CE certified.

Units are provided with a power cord, USB cable, Ethernet cable, CD incorporating a users manual, quick start guide and PC interface software.

MLBF-Filter Test Box – 500 MHz to 50 GHz
Standard models utilize any Bandpass or Bandreject filter manufactured by Micro Lambda today. Bandpass filter models cover 500 MHz to 50 GHz and are available in 4, 6 and 7 stage configurations. Bandreject (notch) filter models cover 500 MHz to 20 GHz and are available in 10, 12, 14 and 16 stage configurations. Units are specified to operate over the lab environment of +15°C to +55°C and are CE certified.

Units are provided with a power cord, USB cable, Ethernet cable, CD incorporating a users manual, quick start guide and PC interface software.

See our complete line of wideband, low noise components

MLSP-series Synthesizers
600 MHz to 20 GHZ

MLSW-series Synthesizers
600 MHz to 16 GHz

MLTO-series TO-8 Oscillators
2 to 16 GHz

MLSMO-series Surface Mount Oscillators
2 to 16 GHz

www.microlambdawireless.com

MICRO LAMBDA WIRELESS, INC.

"Look to the leader in YIG-Technology"

46515 Landing Parkway, Fremont CA 94538 • (510) 770-9221 • sales@microlambdawireless.com

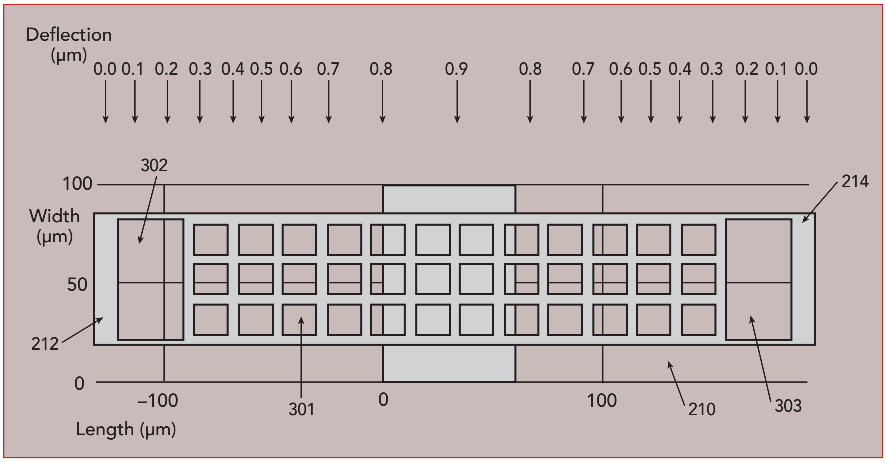

Fig. 3 Shows the Plan-View of switch with a doubly supported cantilever beam above a coplanar waveguide.

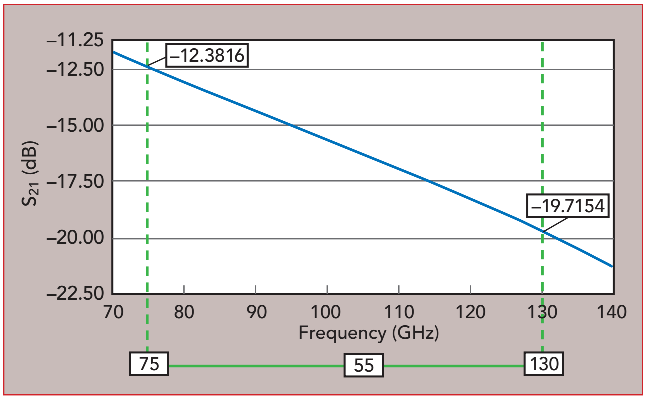

Fig. 4 Shows the isolation plot of MEMS switch depicted in Figures 2 and 3.

nal line 720 between two ground planes 702, 704. In the example of Figure 7, the DGS forms four spiral shaped slots 731, 732, 733, 734 in a two-by-two grid and having mirror symmetry along the lengthwise axis of the signal line 720. Each of the spiral shaped slots have a common, uniform width.

Figure 8 shows insertion loss and return loss of the switch in Figure 7 when the switch is closed. The typical insertion loss is 2.2 dB at 75 GHz and 10.4 dB at 130 GHz, but drops as low as 16.6 dB at 105 GHz. Return loss is about 24 dB at 75 GHz and about 11.2 dB at 130 GHz but increases to about 9.5 dB at 105 GHz. ***Figure 9*** shows isolation for the DGS inspired MEMS switch illustrated in Figure 7 when the switch is open. Isolation is about -17.1 dB at 75 GHz and about -11.5 at 130 GHz and drops as far as about -32.5 dB at 82 GHz. Although isolation characteristics of the switch of Figure 7

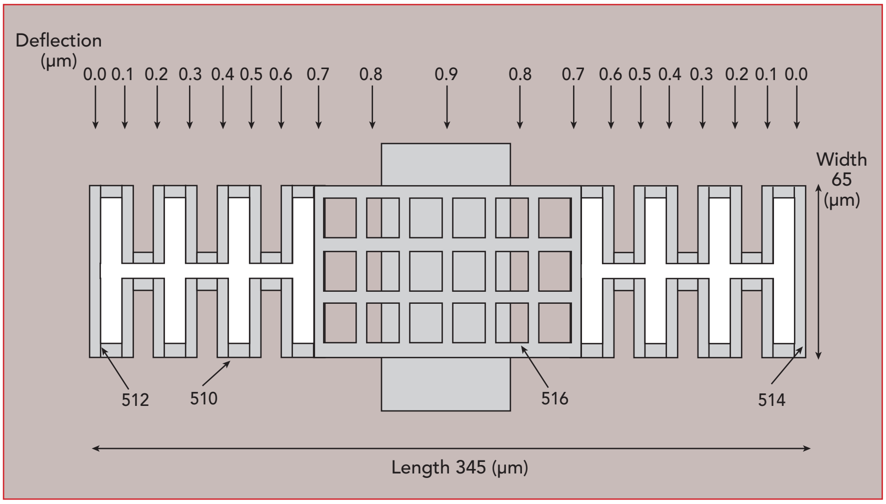

Fig. 5 Plan-View of capacitive shunt switch using a serpentine structure in the cantilever beam.

show improvement, higher insertion loss limits the applications. To overcome the insertion loss, variation to the DGS structures are incorporated to ***Figure 10***.

The MEMS switch shown in Figure 10 is similar in structure to that of Figure 7. As illustrated in Figure 10, the MEMS switch has two ground planes 1102, 1104 bisected by a signal line 1120 and has four DGS structures 1131, 1132, 1133 and 1134 formed in the ground planes. The length of the ground planes and signal line are about 340 μm, and the cumulative width of the switch is about 404 μm. MEMS switch as shown in Figure 10 differs from Figure 7 in that each of the DGS structures includes a secondary MEMS switch 1141, 1142, 1143, 1144 positioned above the DGS structure. The shape of both the secondary switch and DGS may be rectangular, but the secondary switch may be longer while the DGS structure may be wider. In the example of Figure 10, each DGS structure is a perforated lattice, and is about 105 μm in length and about 85 μm in width, overlaid by a secondary switch that is about 139 μm in length and 65 μm in width. The MEMS switch described in Figure 10 includes a substrate 1101 on which the ground plane is formed. The ground plane has a thickness or height of about 2 μm.

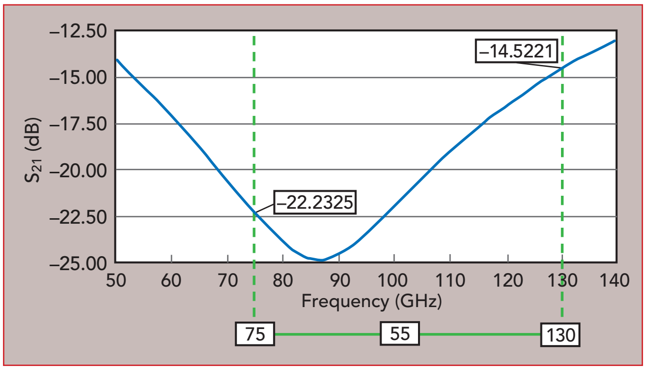

Fig. 6 **Shows the isolation plot of MEMS shunt switch in Figure 5.**

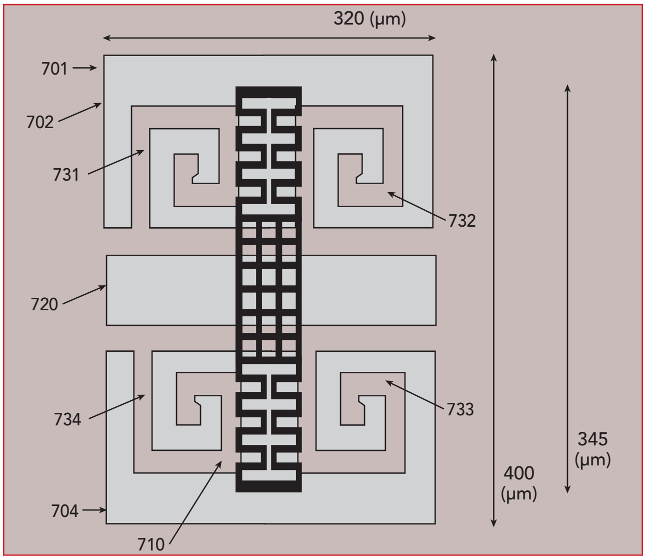

Fig. 7 **Shows the Plan-View of the DGS inspired MEMS switch.**

Although not shown, the slots of the DGS structure 1131 are formed in the ground plane and may have a depth equal to the height of the ground plane 1102. A secondary switch 1141 is formed above the DGS structure 1131. As depicted in Figure 10, the secondary switch 1141 includes a beam 1151 supported by two feet 1162, 1164. The supporting feet have a height of about 1 μm, thereby raising the beam 1151 about 1 μm above the DGS and ground plane. Thus, there is an air gap of about 1 μm between the non-deflected beam and the DGS positioned below. The beam thickness or height of the beam 1151 may be about 1.2 μm.

The beam 1151 shown in Figure 10 is connected to an actuator (not shown) to supply a bias voltage, which runs from the beam 1151 to the ground plane 1102 via the feet 1162, 1164. Applying the bias voltage causes the beam 1151 to deflect downward toward the ground plane 1102, thereby affecting the capacitive characteristics of the DGS structure 1131. The amount of voltage applied to the switch 1101 may be continuously variable and thus the capacitive characteristics of the DGS structure (and its effect on the main MEMS switch of the device) can be varied or tuned.

It has been found that the switch arrangement of Figure 10 behaves like a metamaterial (engineered material). This can be seen by first analyzing the transmission and reflection phases of a signal line formed in a coplanar waveguide without the DGS structure of Figure 10, and then analyzing the transmission and reflection phases of the same signal line with the DGS structure of Figure 10.

For a simple coplanar line without DGS, the transmission and reflection phase are analyzed. The results are shown in ***Figure 11***; the transmission and reflection phases of a signal transmitted across a coplanar

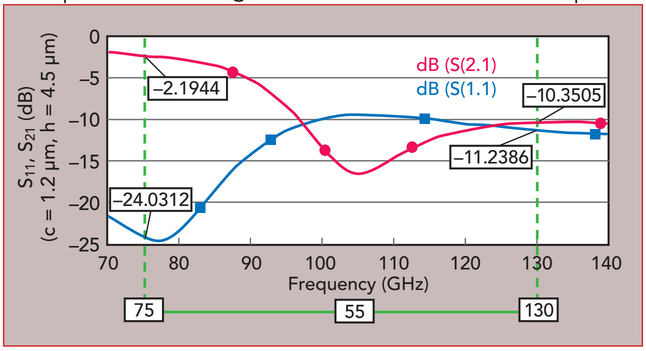

▲ Fig. 8 Shows the return loss and insertion loss of MEMS switch in Figure 7.

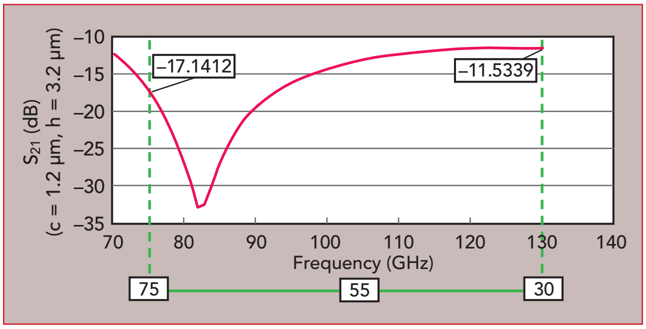

▲ Fig. 9 Shows the isolation of MEMS switch in Figure 7.

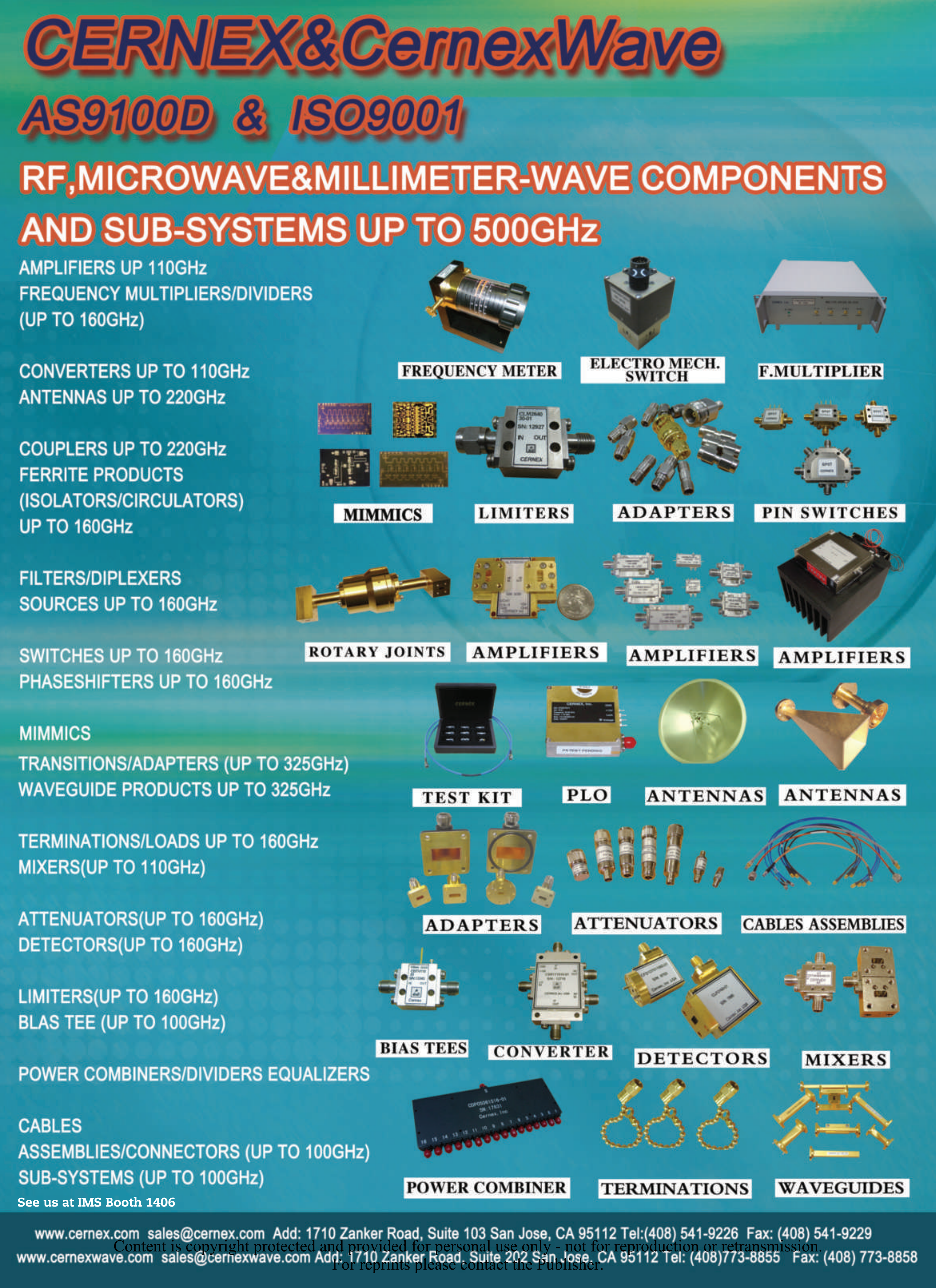
CERNEX&CernexWave
AS9100D & ISO9001
RF,MICROWAVE&MILLIMETER-WAVE COMPONENTS
AND SUB-SYSTEMS UP TO 500GHz
AMPLIFIERS UP 110GHz
FREQUENCY MULTIPLIERS/DIVIDERS
(UP TO 160GHz)
CONVERTERS UP TO 110GHz
ANTENNAS UP TO 220GHz
COUPLERS UP TO 220GHz
FERRITE PRODUCTS
(ISOLATORS/CIRCULATORS)
UP TO 160GHz
FILTERS/DIPLEXERS
SOURCES UP TO 160GHz
SWITCHES UP TO 160GHz
PHASESHIFTERS UP TO 160GHz
MIMMICS
TRANSITIONS/ADAPTERS (UP TO 325GHz)
WAVEGUIDE PRODUCTS UP TO 325GHz
TERMINATIONS/LOADS UP TO 160GHz
MIXERS(UP TO 110GHz)
ATTENUATORS(UP TO 160GHz)
DETECTORS(UP TO 160GHz)
LIMITERS(UP TO 160GHz)
BLAS TEE (UP TO 100GHz)
POWER COMBINERS/DIVIDERS EQUALIZERS
CABLES
ASSEMBLIES/CONNECTORS (UP TO 100GHz)
SUB-SYSTEMS (UP TO 100GHz)
FREQUENCY METER
ELECTRO MECH. SWITCH
F.MULTIPLIER
MIMMICS
LIMITERS
ADAPTERS
PIN SWITCHES
ROTARY JOINTS
AMPLIFIERS
AMPLIFIERS
AMPLIFIERS
TEST KIT
PLO
ANTENNAS
ANTENNAS
ADAPTERS
ATTENUATORS
CABLES ASSEMBLIES
BIAS TEES
CONVERTER
DETECTORS
MIXERS
POWER COMBINER
TERMINATIONS
WAVEGUIDES
See us at IMS Booth 1406
www.cernex.com sales@cernex.com Add: 1710 Zanker Road, Suite 103 San Jose, CA 95112 Tel:(408) 541-9226 Fax: (408) 541-9229
www.cernexwave.com sales@cernexwave.com Add: 1710 Zanker Road, Suite 202 San Jose, CA 95112 Tel: (408)773-8855 Fax: (408) 773-8858

waveguide without the DGS structure over a band of mmWave frequencies from 50 to 140 GHz. As shown, any shift in the transmission phase of the signal is met with a substantially equal (within about 20 degrees) shift in the reflection phase.

Figure 12 shows transmission and reflection phases of a signal over the same band of frequencies for the same coplanar waveguide but with the DGS structure incorporated into the waveguide at a height of 2.2 μm, which is the distance from the top surface of the substrate (the basin of the slots of the DGS structure) to the bottom surface of the secondary switch positioned above the DGS structure. The transmission and reflection phases do not shift equally across the band of frequencies, and even shift in opposite directions, eventually crossing one another at 85 GHz and then crossing back at 96 GHz.

Figure 13 shows transmission and reflection phases for the same coplanar waveguide but with the DGS structure at a height of 2.8 μm. The transmission and reflection phases shift substantially equally until about 110 GHz, but then begin shifting in opposite directions at frequencies above 115 GHz and even cross one another at about 128 GHz. The resonance frequency of the DGS structure thus varies depending on the height of the air gap between the ground plane and the beam.

Figure 14 shows a plot of isolation characteristics for five secondary switches positioned over DGS structures at varying heights. The resonant frequency of the structure is shown to shift to higher frequencies as the air gap between the ground plane and beam increases.

An example MEMS shunt switch with DGS structures and overlaid secondary switches is shown in complete form in ***Figure 15***, which includes a signal line 1720 positioned between a first ground plane 1702 and a second ground plane 1704, the signal line separated from each ground plane by first and second spaces 1703, 1705, respectively. A primary shunt switch 1710 is posi-

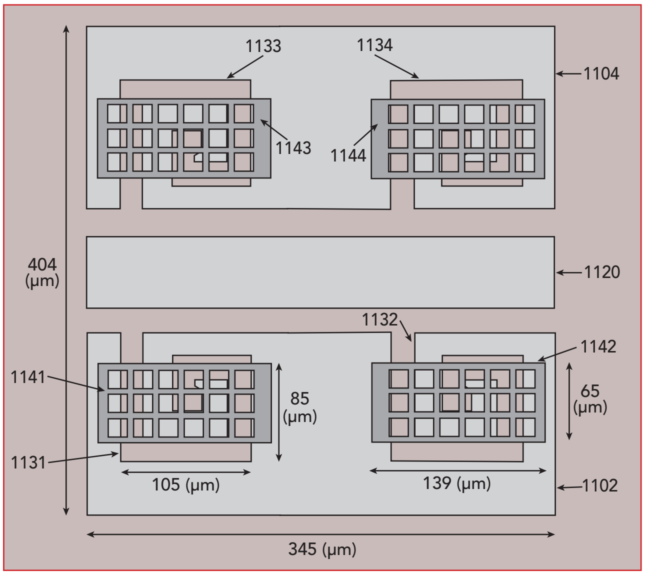

Fig. 10 Shows the Plan-View of a switch, secondary MEMS switches are placed above the DGS.

tioned on top of, is connected to and bridges the first and second ground planes 1702, 1704. The primary shunt switch 1710 runs perpendicular to, and is suspended over, the signal line 1720. When a bias voltage is applied to the primary shunt switch 1710, the switch 1710 deflects downward toward the signal line 1720. When the bias voltage is not applied, the switch 1710 deflects back upward to its original position.

A first DGS structure 1731 and a second DGS structure 1732 are formed in the first ground plane 1702. A third DGS structure 1733 and a fourth DGS structure 1734 are formed in the second ground plane 1704. The first and third DGS structures 1731, 1733 have mirror symmetry along a lengthwise x-axis of the primary switch 1710 and are a similar shape. The second and fourth DGS structures 1732, 1734 also have mirror symmetry along a lengthwise x-axis of the primary switch 1710 and are a similar shape.

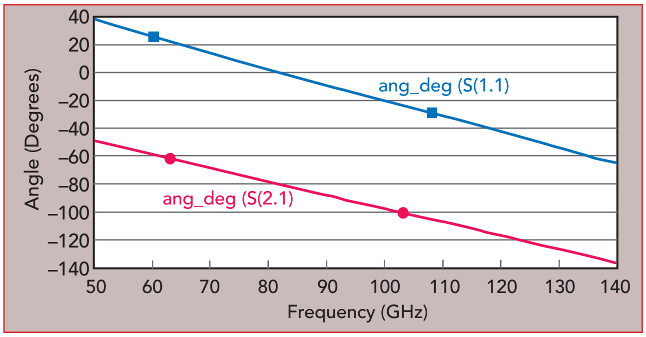

▲ Fig. 11 Transmission and reflection phase for the coplanar line of a switch without DGS.

In the example of Figure 15, the first and third DGS structures 1731, 1733 are a different size from the second and fourth DGS structures 1732, 1734. The second slots of the first and third DGS structures 1731, 1733 are about 85 μm long, whereas the second slots of the second and fourth DGS structures 1732, 1734 are about 100 μm long. The third slots of the first and third DGS structures 1731, 1733 are also shorter than those of the second and fourth DGS structures 1732, 1734. This contrasts with the four DGS structures shown in each of Figures 7 and 10, which all have the same dimensions.

Each DGS structure is overlaid by a respective secondary shunt switch 1741, 1742, 1743, 1744. Each secondary shunt switch is connected to its respective ground line and is suspended over its respective DGS structure with an air gap in between. The secondary shunt switches are rectangular, each of the secondary switches positioned lengthwise parallel to the signal line 1720 and perpendicular to the primary shunt switch 1710. The secondary switches positioned above the first DGS structure 1731 and the third DGS structure 1733 have a mirror symmetry with the secondary switches positioned above the second DGS structure 1732 and the fourth DGS structure 1734 along a lengthwise x-axis of the primary switch 1710. Additionally, the secondary switches positioned above the first DGS structure 1731 and the second DGS structure 1732 have a mirror symmetry with the secondary switches positioned above the third DGS structure

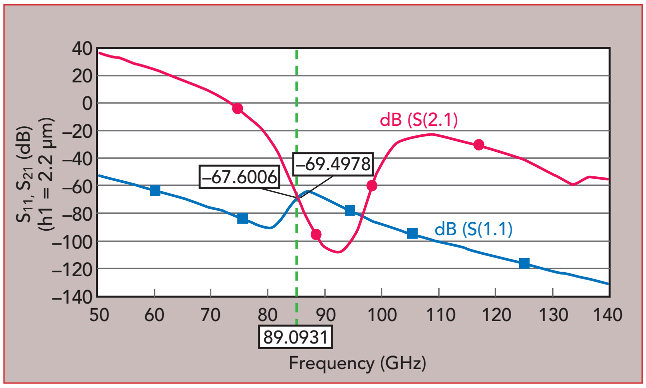

Fig. 12 Plots of the transmission and reflection phase for the coplanar waveguide with DGS in Figure 10 for a height 2.2 μm.

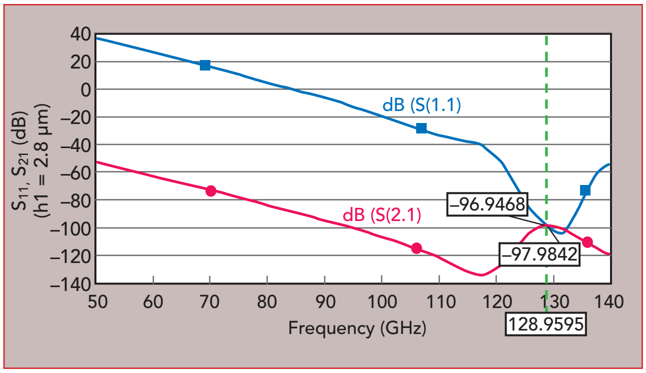

Fig. 13 Plots of the transmission and reflection phase for the coplanar waveguide with DGS in Figure 10 for a height 2.8 μm.

1733 and the fourth DGS structure 1734 along a lengthwise y-axis of the signal line 1720. The secondary shunt switches 1741, 1742, 1743, 1744 are also perforated. In the example of Figure 15, the switches have a grid-like lattice perforation.

Figure 16 shows a side-view of the switch of Figure 15. The switch in Figure 15 is formed on a substrate 1701. A ground plane 1702 is formed over the substrate 1701, and the primary switch 1710 is formed on top of the ground plane 1702. The primary switch 1710 has two feet 1712 (the second foot is obstructed by foot 1712 in Figure 17) supporting a beam 1716. Two secondary switches 1731, 1732 are positioned on either side of the primary switch 1710. Each of the secondary switches also includes two feet 1752, 1754 supporting a beam 1756. DGS structures (not shown) are formed in the ground plane 1702 at re-

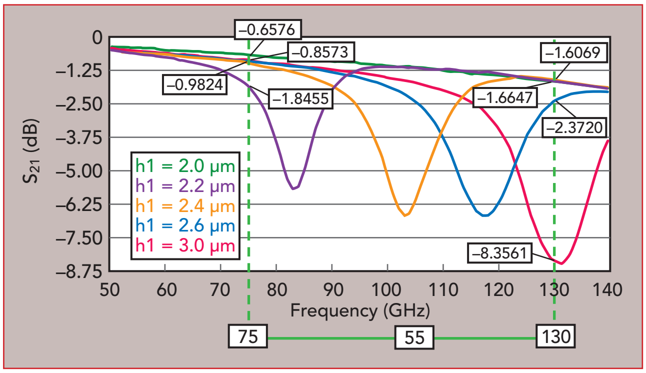

Fig. 14 Plots of isolation characteristics for five secondary switches positioned over DGS structures at varying heights.

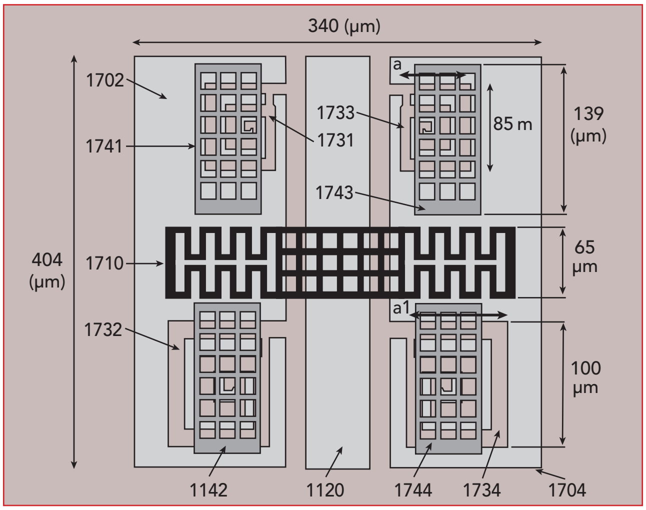

Fig. 15 **A top view of a metamaterial inspired switch having a DGS and secondary switches in accordance with an aspect of the new structure.**

spective positions underneath the secondary switches 1731, 1732.

In the example of Figures 15 and 16, the substrate and ground planes have a length of about 404 µm, and a width of about 340 µm. The ground planes have a thickness of about 2 µm. The primary switch 1710 extends the length of the substrate, the primary switch feet 1712 and beam 1716 have a width of about 65 µm. The feet 1712 have a height of about 2.5 µm, and the beam 1716 has a thickness of about 1.2 µm. The secondary switches 1731 have a length of about 139 µm, and the secondary switch feet 1752, 1754 and beam 1756 have a width of about 65 µm. The feet 1752 have a height of about 1 µm, and the beam 1756 has a thickness of about 1.2 µm. Thus, the entire switch in Figure 15 can be formed on top of the substrate 1701 within a 5.7 µm space.

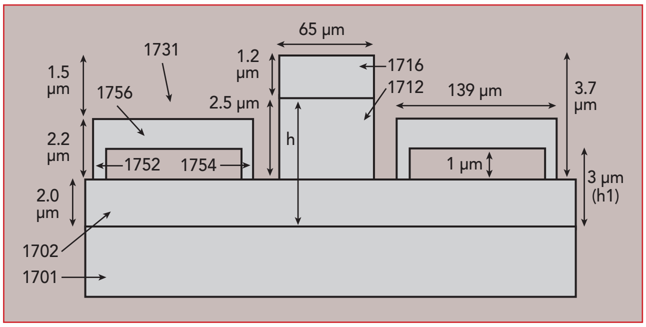

Fig. 16 **Side view of the switch shown in Figure 15.**

NEW METAMATERIAL MEMS SWITCH

Figure 17 shows an example layout of a metamaterial inspired MEMS switch, showing the connections between the primary switch 1910 and secondary switches 1941-1944, a first actuator 1962 and a second actuator 1964. The first actuator 1962 is connected to the primary switch 1910 and configured to provide a bias voltage to the primary switch. The second actuator 1964 is connected to each of the secondary switches 1941-1944 and is configured to provide a bias voltage to the sec-


DELTA
Electronics Mfg. Corp.
SMP - SMPM - SMPS
High Performance
Connectors to 65 GHz
SMP
SMPM
SMPS
Interconnects
that Guide &
Protect us
978-927-1060
sales@deltarf.com
deltarf.com

ondary switches.

In operation, the primary switch shown in Figure 17 may be either ON (bias voltage provided from the first actuator 1962) or OFF (no bias voltage provided by the first actuator 1964). When the primary switch is ON, the primary switch beam deflects downward, resulting in a large shunt capacitance that blocks RF signals from propagating along the signal line 1920. When the primary switch is OFF, the primary switch beam deflects back upward (at rest), reducing the shunt capacitance and permitting RF signals to propagate along the signal line 1920.

When the primary switch 1910 is OFF, the secondary switches 1941-1944 may be turned ON in order to negate the effects of the DGS structures toward insertion and return loss. A bias voltage is applied from the second actuator 1964 to each of the secondary switches 1941-1944, thereby causing the switches to deflect downward toward the DGS structures and create a shunt capacitance blocking the effects of the DGS structure.

Figure 18 shows the amount of downward deflection at several points of the secondary switches (measured in μm) when the secondary switches are actuated. ***Figure 19*** shows return loss and insertion loss characteristics for the MEMS switch

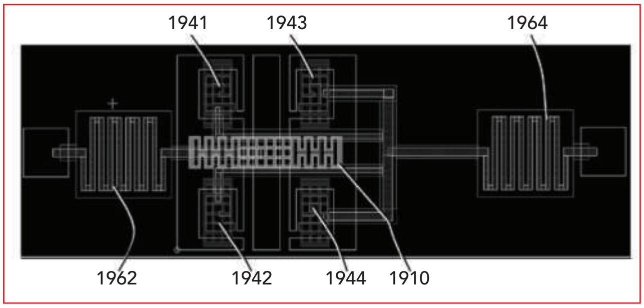

Fig. 17 Example layout of the metamaterial inspired MEMS switch.[1]

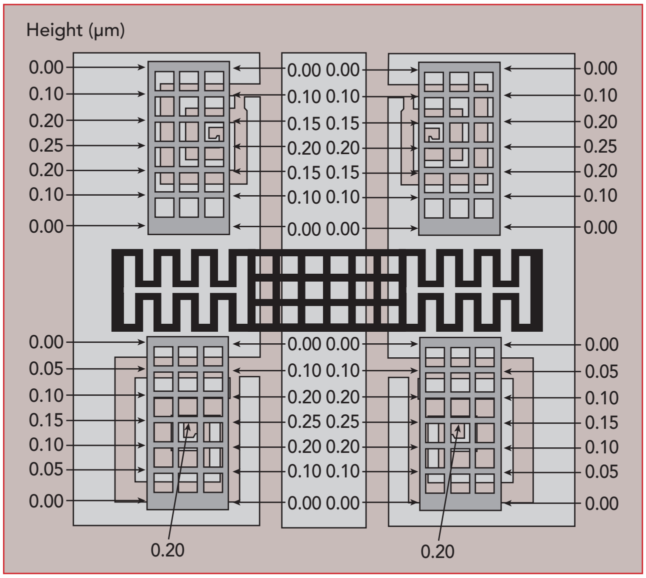

Fig. 18 The amount of downward deflection at several points of the secondary switches (measured in μm) when the secondary switches are actuated.[1]

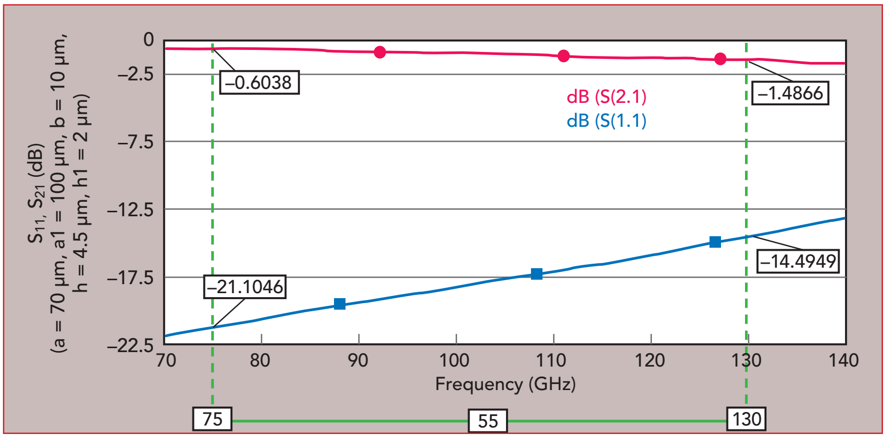

Fig. 19 Plot of return loss and insertion loss of the switch described in Figure 17 with the secondary switches activated.

illustrated in Figure 17 when the primary switch is OFF, and the secondary switches are ON. At 75 GHz, insertion loss is as low as about 0.6 dB and return loss is as low as about 21.1 dB. At 130 GHz, insertion loss is still relatively low at about 1.5 dB, and return loss is also relatively low at 14.5 dB. Returning to Figure 17, when the primary switch 1910 is ON, the secondary switches 1941-1944 may be turned OFF in order to get the benefit of the DGS structures toward isolation. No bias voltage is applied from the second actuator to the secondary switches 1941-1944, so the switches remain separated from the DGS structures underneath by the airgap.

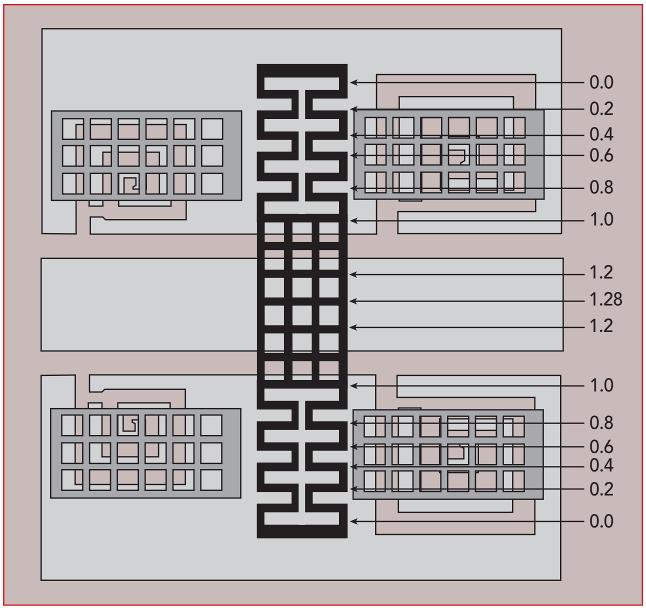

Fig. 20 The amount of downward deflection at several cross-sections of the primary switches (measured in µm).

Figure 20 shows the amount of downward deflection at several cross-sections of the primary switches (measured in µm) when the primary switch is actuated. Deflection along the entire width of the primary switch is uniform for any given point along the length of the switch.

Figures 21 and ***22*** show the isolation characteristics for the MEMS switch in Figure 17 when the primary switch is ON and the secondary switches are OFF. In Figure 21, the same DGS structure is used. This leads to a significant improvement in isolation at a relatively narrow band (e.g., less than about 10 GHz, between 90 and 100 GHz). At 75 GHz isolation is about -23.1 dB and at 130 GHz, isolation is about -23.9 dB. But at about 95 GHz, isolation is improved to about -52 dB.

Figures 22 and ***23*** show plots of isolation and insertion loss characteristics for MEMS switch utilizing different structures. The metamaterial construction leads to an overall improvement of isolation over a wider band of frequencies. The structure represented in Figure 15 yields improved isolation at about 84 GHz (about -51 dB) and at about 112 GHz (about -59 dB) and is not worse than about -24 dB between 75 and 130 GHz. The insertion loss characteristics of the DGS switch is poor compared to the regular switch and metamaterial versions. Switch Type 2 is the first version of the new MEMS Switch using Capacitive Contacts.

As seen from the attenuation characteristics of Figures 19 and 21, providing DGS structures with capacitive MEMS shunt switches above the DGS structures is an effective way of incorporating the benefits of DGS for improved isolation when RF signals are blocked, while at the same time negating the detriments caused by the DGS to insertion loss and return

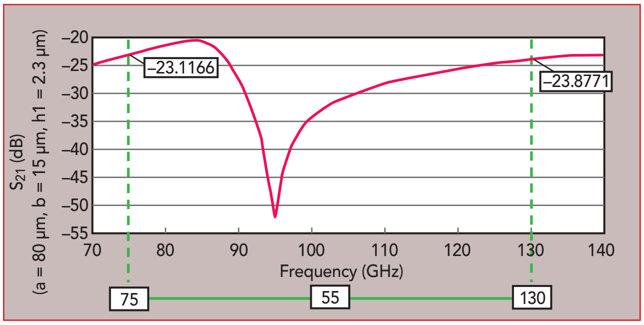

Fig. 21 The isolation characteristics of the switch of Figure 17 having varying air gap heights.

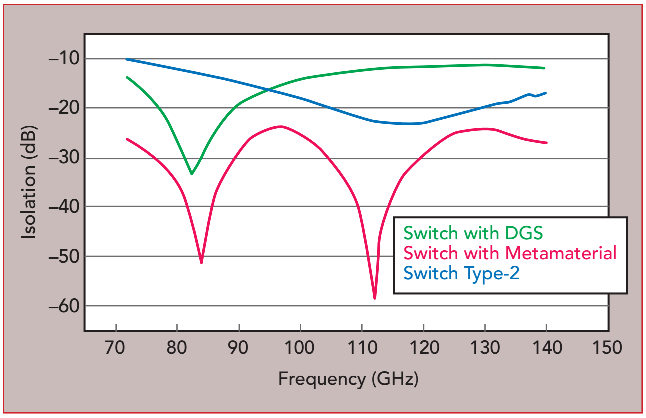

▲ **Fig. 22 Isolation characteristics for switches with different topologies.**

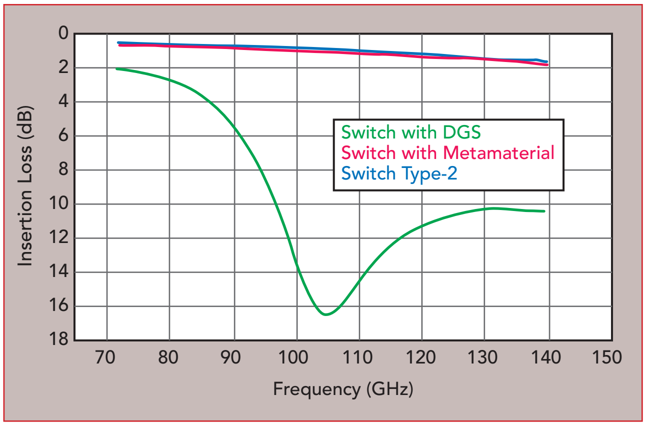

▲ **Fig. 23 Insertion loss characteristics for switches with different topologies.**

loss when RF signals are propagating. In this respect, incorporation of DGS structures and corresponding shunt switches are an improvement to RF MEMS design and operation. ***Table 1*** provides a summary of the actuation voltage, isolation and insertion loss characteristics for the above-described switch designs with air gaps (and cantilever beam heights) of about 2.5 μm.[1]

Figure 24 shows isolation characteristics for several switches having different DGS and secondary switch arrangements, in which both switches are actuated. Actuating the secondary switch results in improved isolation characteristics over a narrow band of frequencies. The band at which the improved isolation occurs varies depending on the air gap height between the switches and DGS structures. As the air gap increases, the frequency band at which the best isolation for the switch occurs shifts upward. For an air gap of 2.2 μm, isolation of about -52 dB is achieved at about 85 GHz and for an air gap of 3.0 μm isolation of about -44 dB is achieved at about 122 GHz. This demonstrates the relative flexibility of the proposed combination of DGS structures with secondary switches for providing improved isolation across a wide range of high frequencies.

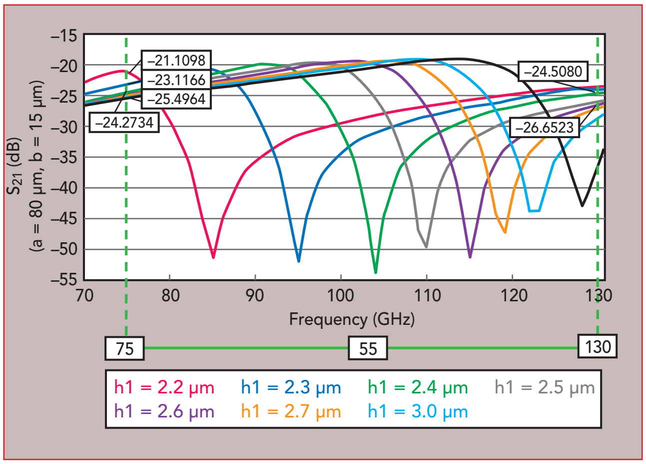

▲ **Fig. 24 Isolation characteristics for various MEMS switch designs.**

CONCLUSION

In Part I of this three-part series, it is shown that both the DGS structures and secondary switches can achieve improvements in insertion loss and isolation. These improvements contrast with the tradeoffs conventionally seen when using either only a shunt switch (good insertion loss, poor isolation) or only a DGS structure (improved isolation, but worse insertion loss). The proposed combination of a primary shunt switch, DGS structures and secondary shunt switches is shown to behave like a metamaterial. In addition to this solution, it also improves resistance to stiction of the MEMS switch using metamaterial layers within the design of the switch contacts which will be covered in detail in Parts II and III.■

TABLE 1

COMPARISON OF MEMS SWITCHES PERFORMANCE

Parameters	Shunt Switch (Figs. 2-3)	Shunt Switch (Fig. 5)	Shunt Switch + DGS w/o Switches (Fig. 7)	Shunt Switch + DGS w/ Switches (Fig. 17)
Actuation Voltage	37 V	17 V	17 V	17 V
Isolation (75-130 GHz)	-12 to -19 dB	-15 to -24 dB	-11 to -32 dB	-24 to -59 dB
Insertion Loss	0.74 dB	0.6 dB	-2 to -11 dB	0.6 dB
Material	Molybdenum	Gold	Gold	Gold
Cantilever Height	2.5 μm	2.5 μm	2.5 μm	2.5 μm

References

1. Shiban Koul, Ajay Poddar and Ulrich Rohde, "Microelectromechanical Switch with Metamaterial Contacts," *US Patent Pub. No. 02161415A1*.
2. Astrid Lambrecht, "The Casimir Effect: a Force from Nothing," *Physics World, September 2002*.
3. F. Intravaia and C. Henkel, *New Frontiers of Casimir Force Conference*, Santa Fe, New Mexico, 2009.
4. U. Leonhardt and T. G. Philbin, "Quantum Levitation by Left-Handed Metamaterials," *New J. of Physics*, August 2007.
5. Mercado et. al.,"A Mechanical Approach to Overcome RF MEMS Switch Stiction Problem," *ECTC 2003*.
6. Chaitanya Mahajan, "Design and Analysis of RF MEMS Switches (70 GHz to 130 GHz), M.Tech dissertaion, CARE, IIT Delhi, May 2018.

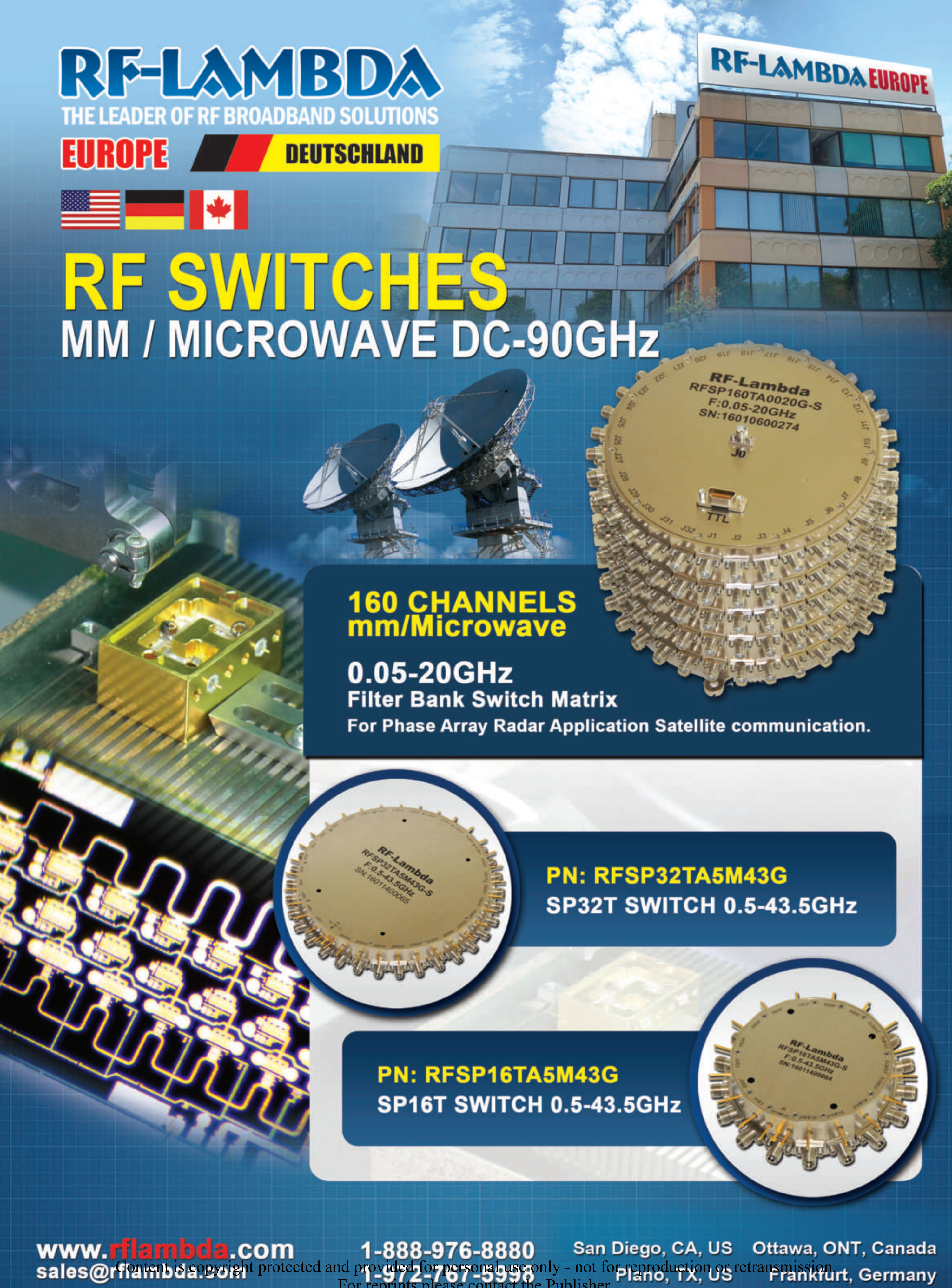

RF-LAMBDA
THE LEADER OF RF BROADBAND SOLUTIONS
EUROPE
DEUTSCHLAND
RF-LAMBDA EUROPE
RF SWITCHES
MM / MICROWAVE DC-90GHz
RF-Lambda
RFSP160TA0020G-S
F:0.05-20GHz
SN:1601060274
J0
TTL
160 CHANNELS
mm/Microwave
0.05-20GHz
Filter Bank Switch Matrix
For Phase Array Radar Application Satellite communication.
RF-Lambda
RFSP32TA5M43G-S
F:0.5-43.5GHz
PN: RFSP32TA5M43G
SP32T SWITCH 0.5-43.5GHz
PN: RFSP16TA5M43G
SP16T SWITCH 0.5-43.5GHz
RF-Lambda
RFSP16TA5M43G-S
F:0.5-43.5GHz
www.rflambda.com
sales@rflambda.com
1-888-976-8880
1-972-767-5998
San Diego, CA, US
Plano, TX, US
Ottawa, ONT, Canada
Frankfurt, Germany

INVITED PAPER

Liquid Crystals: A Power and Cost-Efficient Electronically Steerable Antenna Solution for 5G

Mohammad Reza Dehghani, Ahmed H. Akgiray, Arshad Mehmood and Onur Hamza Karabey
ALCAN Systems, Darmstadt, Germany

Electronically steerable antennas (ESA) are key components for 5G, especially at mmWave frequencies. Typical ESAs are phased arrays based on silicon beamforming integrated circuits (IC). Notwithstanding the flexibility silicon-based ESAs offer, two potential obstacles to widespread deployment are power consumption and equipment cost. These result in high operating and capital expenses for network operators. As an alternative to silicon-based active phased arrays, liquid crystal (LC)-based passive phased arrays are being introduced for 5G applications.

5G is being deployed worldwide using both sub-6 GHz (e.g., Deutsche Telekom, O2, Sprint, Vodafone and Three) and mmWave (e.g., AT&T, Verizon and SK Telekom) frequency ranges. This fifth generation will be a mobile network and, unlike its predecessors (4G, 3G and 2G), it aims to be an "everything network," i.e., available "everywhere" for "everyone," able to provide high data rates with low power consumption.

One of the key hardware components of the physical layer is the antenna. Until now, typical antenna solutions have been either parabolic antennas for high gain links (e.g., point-to-point backhaul) or sectorial antennas for base stations (e.g., point-to-multipoint). These antennas offer no beam steering features for backhaul or only a few degrees in just one dimension (1D), for base station vertical tilting. For 5G, ESAs are required, especially at mmWave frequencies.

5G ANTENNA REQUIREMENTS

5G frequency bands are divided into sub-6 GHz and mmWave (i.e., greater than 24 GHz). Because of their propagation properties, the sub-6 GHz range is more suitable for larger, less dense cells in rural areas. For these cases, 1D antenna steering (e.g., azimuth) might be adequate.

5G offers highly reliable networks with high data rate services. High data rates require large bandwidths available at higher frequencies, such as mmWaves. This is underscored by a recent announcement by the International Radio Union (ITU) after World Radiocommunication Conference 2019 (WRC-19). Five additional mmWave frequency bands (4.25 to 27.5, 37 to 43.5, 45.5 to 47, 47.2 to 48.2 and 66 to 71 GHz) are identified to facilitate diverse 5G usage scenarios.[1] Recent frequency band auctions in the U.S., Japan and the European Union allocating the 26 GHz band for 5G and early 5G deployments at mmWave frequencies in the U.S. and Asia demonstrate increased interest in mmWaves for applications such as fixed wireless access (FWA) and 5G hot spots within the 5G cellular network.[2]

Urban areas with high mobile traffic, i.e., with a high demand for capacity per subscriber and large numbers of subscribers, require high data rates—hence, large bandwidth. This leads inevitably to increasing frequencies up to mmWave, where large swaths of frequency spectrum are available. Due to high path losses at these frequencies and because of high mobile traffic, an (ultra) dense cellular network with many pico- and femtocells must be deployed to serve many users with high throughput. To reduce the

impact of mmWave path loss and to reduce interference in these dense cellular networks, narrow beamwidth high gain antennas with 2D beam steering or beamforming and multi-beam capabilities are required.

LC-BASED PHASED ARRAY

As previously detailed by Christian Weickhmann et al.,[3] LC antenna technology combines liquid crystal display (LCD) technology with microwave LCs and array antenna design (see ***Figure 1***). The phased array consists of a feed network, an LC phase shifter stack and a radiator stack. Using this approach, all parts can be designed independently and in a modular fashion. The LC phase shifter stack is fabricated using standard LCD processes. This allows for large-scale fabrication accommodating virtually any aperture size, including segments or antenna groups. The LC phase shifter stack consists of two glass sheets separated by spacers, where the LC material is filled in between. Depending on the chosen device topology, the LC layer thickness may vary from a few to tens of micrometers. An inverted microstrip line (IMSL) implements the phase shifting functionality, as shown in ***Figure 2***, with the typical LC layer thickness of the IMSL approximately 100 µm. Other phase shifter topologies with LC layer thicknesses of just a few micrometers enable lower loss and more compact size,[4,5] essential to reduce response time to milliseconds.[6]

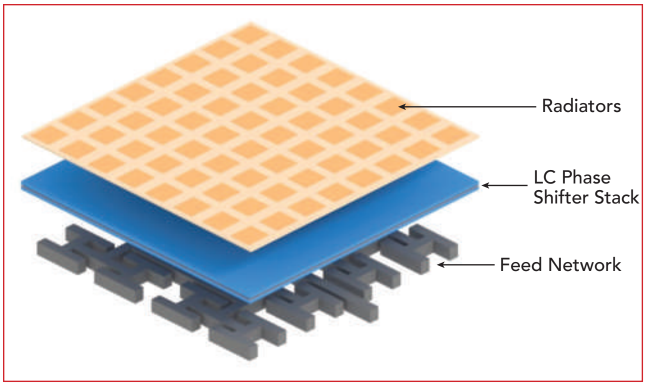

Fig. 1 LC-based phased array.

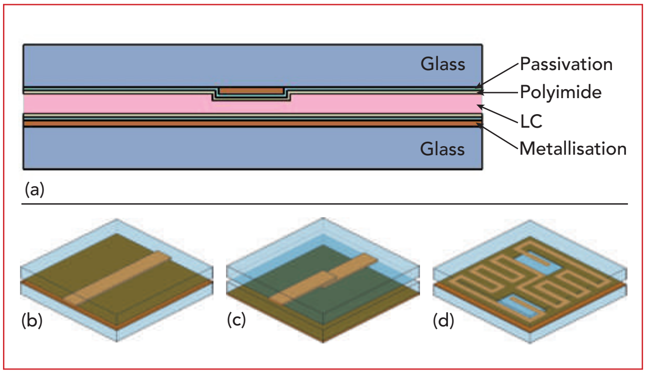

Fig. 2 LC phase shifter stack: cross-section (a), IMSL (b), loaded line (c) and layout with input and output (d).

In the LC phase shifter stack, the inner surfaces of the glass layers are metallized and then coated with a polyimide (PI) layer to anchor the LC and enforce an orientation of the material. Usually, the RF signal, due to its polarization, experiences low effective permittivity. When a voltage is applied between ground and signal, the LC reorients according to the magnitude of the applied voltage (see ***Figure 3***). If the applied bias voltage (V_b) is higher than a threshold voltage (V_{th}), the molecules tend to orient toward the applied electrostatic field. The resultant orientation is determined by the equilibrium between the applied electrical force and elastic force in the bulk LC, due to the alignment layer. Hence, continuous tunability of the LC material is possible. The more the LC orients along the bias field, the higher the effective permittivity for the traversing RF signal. When the bias voltage is turned off, the molecules align back to the initial orientation because of the alignment layer. Other topologies are possible, which offer more design choices, but the operating principle is the same.

A top view of an LC-based array (see ***Figure 4***) shows each unit cell has independent phase shifters. Hence, when they are fed from a feed network on one side and coupled into radiating elements on the other side, a classic phased array is formed, where each individual radiator has its corresponding independent phase shifter. The phase shifters can achieve any phase value, enabling continuous beam steering, unlike a semiconductor digital phase shifter. Various panel sizes are possible: TV-screen apertures for satellite reception, CD-sized panels for conformal layouts or multi-antenna modules for terrestrial applications like 5G. ALCAN has developed and patented a low-cost electronics solution developed exclusively for phased arrays.

The LC technology is passive and biasing, using very low power. Controlling up to 512 radiating elements consumes less than 0.5 W. Depending on topology and design choices, an insertion loss of 2 to 3 dB is achieved and the beam steering time is in milliseconds.[6] This steering time is longer than that of an array using beamformer ICs, which might seem to be a limitation; however, a steering time on the order of a few milliseconds is compatible with a latency of a 1 ms or less. Latency is the time between a stimulation and the corresponding response, which is mainly a signal processing issue, while the steering time is the time necessary to change the direction of a beam.

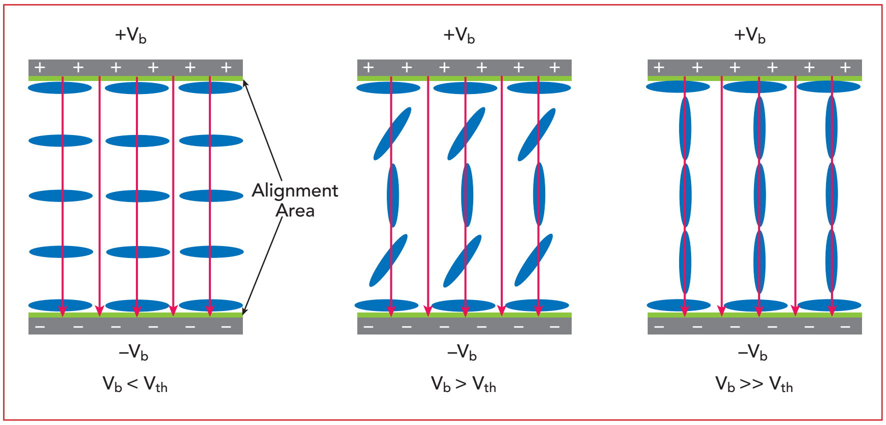

Fig. 3 Tuning the LC phase shifter.

Fast steering is required for two main scenarios: one is for tracking

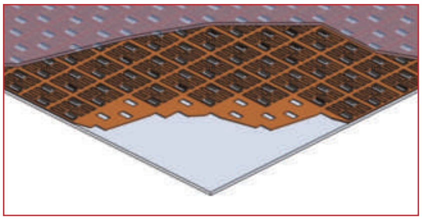

Fig. 4 LC-based phased array, where each radiator is fed with an independent phase shifter.

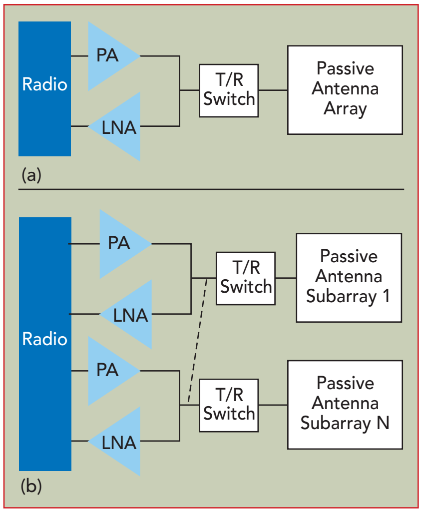

Fig. 5 Fully analog beam steering array (a) and hybrid beam steering (b) architectures.

high-speed vehicles such as trains and airplanes, which is achievable with LC technology.[7] The second is for optimal resource allocation when the antenna is used as a macro base station and schedules/switches between different users, on the order of symbol/slot durations similar to sub-6 GHz macro base stations. Operating at mmWave, however, the base station antenna is used mainly as a small cell hotspot or FWA access point, where the number of users is less and fast switching is not necessary.

Other LC-based antennas based on holographic beamforming use LCs in a metamaterial approach within leaky wave antennas. These are based on resonant meta-atoms and suffer from fundamental limitations, such as limited bandwidth. These solutions require tens of thousands of elements, equivalently meta-atoms, to interface with matching structures,[8] and they have complex design and control schemes.[9] In application, several thousand tunable devices must be controlled, which is a hurdle to scale antenna size and reduce cost.

ANTENNA ARCHITECTURES FOR 5G APPLICATIONS

Two antenna solutions are possible depending on the application and type of link: (1) fully analog beam steering antenna arrays for point-to-point (PtP) links and (2) hybrid analog/digital beam steering antenna arrays with multi-beam capability for point-to-multipoint (PtMP) links, such as massive MIMO (mMIMO) base stations (see ***Figure 5***). In the hybrid architecture, one RF chain is used for each subarray; in the analog architecture, a single RF chain is used for the entire array. The RF chain (RF front-end) comprises of one power amplifier (PA), one low noise amplifier (LNA) and a T/R switch meeting the 5G power levels and TDD requirements.

The fully analog architecture shown in Figure 5a is suitable for single beam (single user, PtP) cases and offers the best cost and simplicity. For PtMP scenarios, the architecture in Figure 5b provides the best trade-off between beamforming flexibility and RF front-end cost and complexity. Compared to silicon-based beamforming antennas, the LC smart antenna and its hybrid beamforming architecture require fewer RF components. Using LC phase shifter technology to achieve the phase shift for each element with the passive subarrays is a much lower cost and consumes less power compared to a typical MMIC approach. The beamforming architecture does not require an LNA, PA and T/R switch for every element, rather one per subarray.

MMIC-based phased arrays typically use off-the-shelf beamforming ICs available from companies such as Analog Devices, Anokiwave and Qorvo. An 8 × 8 antenna using one of those commercial ICs consumes around 20 W compared to only 5.5 W for the LC antenna solution. ***Table 1*** compares the performance of an ALCAN 8 × 8 array with a single beam analog architecture compared to several silicon MMIC-based 8 × 8 arrays, assuming operating at 28 GHz.

The differences become more significant for larger arrays, especially power consumption, because the power consumption of the LC solution does not increase linearly

TABLE 1
LC VS. MMIC TRANSMIT PHASED ARRAY

Company and Technology	Gapwaves Si[10]	Anokiwave Si[11]	ALCAN MLC	ALCAN MLC
Array Size (Elements)	8 × 8	8 × 8	8 × 8	10 × 10
Subarray (Elements)	1×4 Vertical	No Subarray	No Subarray	No Subarray
Front-End Modules	4 + 1	16	1	1
Average Tx Module Output (dBm)	8	14	30 (PA)	33 (PA)
Passive Gain (dBi)	24	22	22.75	24.75
EIRP (dBmi)	44	50	45.25	50.25
Total Power Consumption (W)	13	20	5.5	8.2
Beam Steering (°)	±45 Az ±10 El	±60 Az ±60 El	±60 Az ±60 El	±60 Az ±60 El

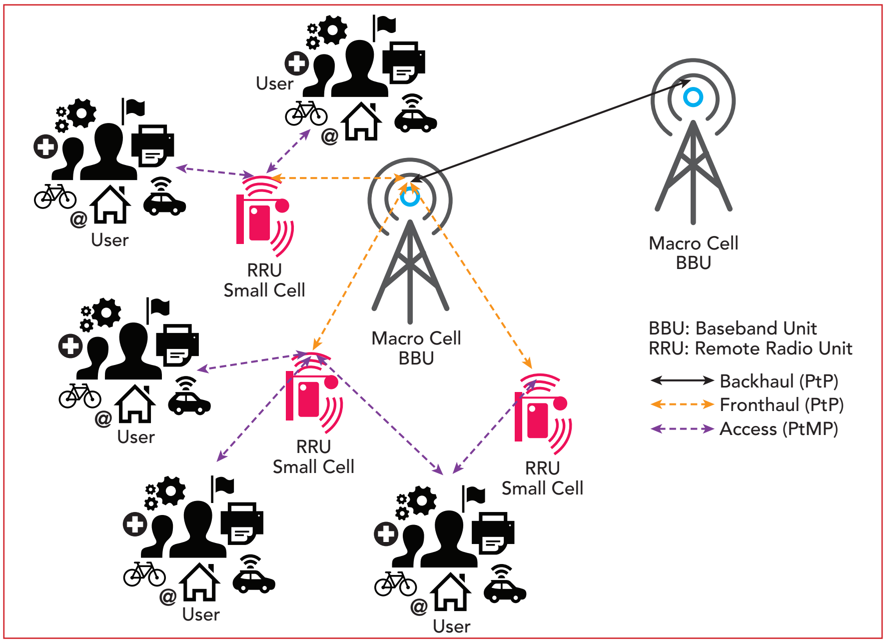

Fig. 6 Notional 5G heterogeneous network.[14]

with an increasing number of array elements. For example, for a 16 × 16 element array with four beams and a minimum equivalent isotropically radiated power (EIRP) of 60 dBm, the LC antenna's overall power consumption is around 19 W, compared to 65 W for antenna arrays based on silicon-based ICs.[11]

In a simplified case[12] for a random Dallas suburb with 800 houses per square kilometer, nine cell sites with inter-site distance of 500 m are required to ensure 1 Gbps service per user. Each cell site requires at least three access antennas with 120 degree coverage to provide full 360 degree coverage around the cell, leading to a minimum of 27 access antennas per square kilometer. The maximum authorized EIRP for an outdoor base station access antenna is 75 dBm, and operators

tend to use this maximum level to ensure the highest coverage and capacity.[13] For silicon MMIC-based solutions, an antenna with an EIRP of 75 dBm consumes more than 200 W, while the LC antenna only consumes around 35 W and can be powered by a solar panel with an aperture of 48 × 66 cm.

LC-based antennas benefit from a cost-efficient phase shifting technology that leverages the existing mass production capabilities of LCD production lines with a low marginal cost of producing an additional type of LC panel. This economy of scale enables ALCAN to reduce LC phase shifter cost by 100×, to around $300/m^2, compared to semiconductor phase shifters, which are estimated to cost around $30,000/m^2 using 30 cm diameter wafers. Depending on the antenna application, LC-based phased array antennas—including the RF front-end with a PA, LNA and T/R switch for each array or subarray—consume up to 5× less power and are up to 10× lower cost compared to semiconductor-based phased array antennas, especially at mmWave frequencies.

APPLICATIONS

A terrestrial mobile network (see ***Figure 6***) generally uses two types of links: PtP and PtMP. PtP links provide backhaul and fronthaul connections between the macros and small cells, and they mainly employ high gain antennas with narrow beam widths. PtP links require beam steering for aligning the antennas during installation of the link, dynamic alignment to compensate for antenna twisting and swaying and network reconfiguration.

A PtMP link is used to connect between the base station and several simultaneous users, providing them with access to the network and the internet. Here, wider beams are required than with PtP links, to handle beam steering scenarios such as following on-the-move users until a handoff to a neighboring node or auto-aligning the link to establish FWA service between the base station and customer premises equipment. Antenna solutions with multiple beams are increasingly deployed to increase access capacity via MIMO arrays.

A new trend called self-backhauling or "integrated access and backhaul," uses a single antenna to form both PtP and PtMP links. For such use cases, modular mMIMO antennas with hybrid beamforming architectures seem to offer the best, most compatible, solutions. ESAs are also required at the user equipment (UE), especially at mmWave frequencies to overcome path losses. UEs need high gain antennas and narrow beams, and beam steering is required to align the UE's narrow beam with the access point's beam, and the system must maintain alignment if the UE is moving, e.g., CV2X between the base station and a vehicle.

CONCLUSION

For 5G, ESAs are becoming a basic requirement both for network nodes and UEs. At mmWave, where

Planar Monolithics Industries, Inc.

Integrated RF/Microwave Assemblies & Modules

PMI offers the highest quality multi-function modules and integrated microwave assemblies for industrial and military applications in frequency ranges up to 50 GHz. Built to your specifications with functions that include amplification, attenuation, filtering, switching, phase shifting, power detection, modulation, coupling, limiting and digital/analog control. PMI offers many other standard models with various options that are available at:
https://www.pmi-rf.com/categories/integrated-mic-mmic-assemblies

- Amplifiers - Solid State
- Attenuators - Variable/ Programmable
- Bi-Phase Modulators
- Couplers (Quadrature, 180, Directional)
- Detectors - RF / Microwave
- DLVAs, ERDLVAs & SDLVAs
- Filters & Switched Filter Banks
- Form, Fit, Functional Products & Services
- Frequency Converters
- Frequency Sources
- Frequency Discriminators & IFM
- Frequency Synthesizers
- Gain & Loss Equalizers
- Integrated MIC/MMIC Assemblies (IMAs)
- IQ Vector Modulators
- Limiters - RF / Microwave
- Log Amps
- Miscellaneous Products
- Monopulse Comparators
- Multifunction Integrated Assemblies (IMAs)
- Phase Shifters & Bi-Phase Modulators
- Power Dividers/Combiners (Passive & Active)
- Pulse Modulators - SP1T
- Rack & Chassis Mount Products
- Receiver Front Ends & Transceivers
- Single Side Band Modulators
- SMT & QFN Products
- Switch Matrices
- Switch Filter Banks
- Switches - Solid-State
- Systems - Radar Sense & Avoid
- Systems - Fly Eye Radar
- Threshold Detectors
- USB Products

PTRAN-100M18G-SDLVA-SFB-3UVPX-10HP-MAH-MX

https://www.pmi-rf.com/product-details/ptran-100m18g-sdlva-sfb-3uvpx-10hp-mah-mx

PMI Model No. PTRAN-100M18G-SDLVA-SFB-3UVPX-10HP-MAH-MX is a transceiver that covers the frequency range of 100 MHz to 18.0 GHz and fits into a 3U open VPX form factor utilizing the high speed VITA 67 RF connector. This unit up-converts a 100 MHz to 4.0 GHz transmit signal to the 2.0 to 18.0 GHz range and down-converts a 100 MHz to 18.0 GHz received signal to the 100 MHz to 4.0 GHz intermediate frequency range for analog to digital conversion. A receive filter bank incorporates a 2-way absorptive switch to select an input, along with two 6-way switches allowing one of six filter paths to be chosen. A filter bank is used also on the transmit path, with two 6-way switches allowing one of six filter paths to be chosen. The unit is designed to attach to an FPGA controller card allowing for a total solution in a 10 HP (2”) form factor.

- 100 MHz to 18.0 GHz Transceiver
- Integrated Up and Down Converters
- IF up to 4 GHz
- Time Gated SDLVA for Pulse Blanking
- -80 to -10 dBm Input Dynamic Range
- Customizable Switched Filter Banks
- 0 to +10 dBm Transmit Power
- 100 ns Switching Speed
- Less than 30W Power Consumption
- Customizable Switch Filter Banks
- Over 100 dB of Isolation between Tx and Rx
- 300% smaller than individual single function components
- Fits into a 3U open VPX form factor utilizing the high speed VITA 67 RF connector.
- CW Immunity
- Unit Size: 6.299” x 3.937” x 1.915”

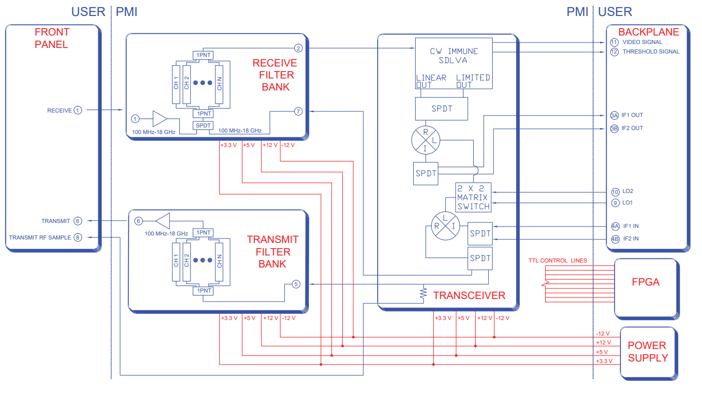

PRX-20-1G18G-850M-SFF

https://www.pmi-rf.com/product-details/prx-20-1g18g-850m-sff

PMI has developed a channelized receiver covering 1 to 18 GHz instantaneously in 20 channels. IF frequencies between 1 and 4.4 GHz are output and ready to be digitized. The receiver is designed to cover a 60 dB dynamic range using a built-in internal 10 MHz reference to lock the internal LO’s used in down-converting the signal into the necessary frequency bands. The reference is also output at a +20 dBm level to be used for synchronization. All of this state-of-the-art functionality is packaged in a 10” x 8” x 3” package consuming around 50 Watts of power.

- 1.0 to 18.0 GHz Channelized Receiver
- -58 to +2 dBm Input Dynamic Range
- 60 dB Output Spurious Free Dynamic Range
- 20 Output Channels, IF Frequencies of 850 MHz BW from 1 to 4.4 GHz (4 Filtered Thru Path and 16 Down-Converted Paths)
- Overall Gain of 0 dB +/-3 dB
- 10 MHz Output Reference with output stability of +/-1 PPM
- Input and Output SMA RF Connectors and 9 Pin D-Sub male for Power
- Less than 50 W Power Consumption
- Unit size : 10.0” x 8.0” x 3.0”

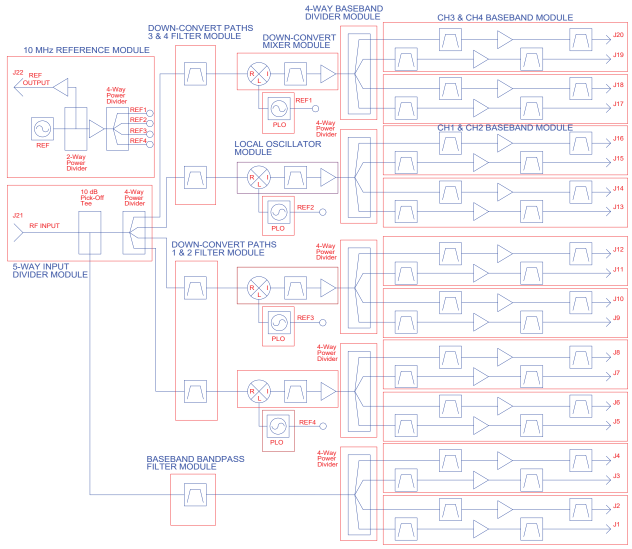

West Coast Operation:
4921 Robert J. Mathews Pkwy, Suite 1
El Dorado Hills, CA 95762 USA
Tel: 916-542-1401, Fax: 916-265-2597

East Coast Operation:
7311-F Grove Road
Frederick, MD 21704 USA
Tel: 301-662-5019, Fax: 301-662-1731

sales@pmi-rf.com • www.pmi-rf.com

ISO9001:2015 REGISTERED

they will be deployed in large numbers, they must be small in size, to be unobtrusive in urban areas; be low-cost, to be economically justifiable; be energy efficient, to consume minimal power; and have low mass, to ease installation and maintenance.

The main features that differentiate LC-based phased arrays from other antenna solutions are 1) energy efficiency, with low power consumption (a few watts) and little heat dissipation; and 2) low-cost compared to traditional active phased array antennas, because they do not use MMIC-based phased shifters. LC phased arrays are a "pure" passive solution with continuous beam steering.

Depending on the application, LC-based phased arrays support beamforming architectures that are either fully analog, for single beam ESAs, or hybrid analog/digital, for multi-beam ESAs. They have response times of milliseconds, which are compatible with a 1 ms latency requirement for most 5G use cases, such as small cells, FWA and UE. LC-based arrays are extremely flat, compatible with low profile applications.■

Acknowledgment

The authors would like to thank Professor Rolf Jakoby, Institut für Mikrowellentechnik und Photonik (IMP) at Technische Universität Darmstadt, and André Doll, 5G antenna senior advisor and former CTO of RFS, for their valuable contributions to this article. We also extend our gratitude to the IMP labs at TUDA for their test facilities.

References

1. "WRC-19 Identifies Additional Frequency Bands for 5G," *ITI News*, November 2019, Web. news.itu.int/wrc-19-agrees-to-identify-new-frequency-bands-for-5g/.
2. F. Pujol, C. Manero and S. Remis, "5G Observatory Quarterly Report 5," *European Commission DG Communications Networks*, October 2019.
3. C. Weickhmann et al., "A Low-Cost, Flat, Electronically Steerable Array Antenna for New Massive NGEO Constellations Ground Terminals and Future 5G," EuCAP, April 2019, Krakow, Poland.
4. F. Goelden, A. Gaebler, M. Goebel, A. Manabe, S. Mueller and R. Jakoby, "Tunable Liquid Crystal Phase Shifter for Microwave Frequencies," *Electronics Letters*, Vol. 45, No. 13, June 2009, pp. 686–687.
5. R. Jakoby, O. H. Karabey and W. Hu, "Phase Shift Device," U.S. Patent 10141620, issued November 27, 2018.
6. F. Goelden, A. Gaebler, S. Mueller, A. Lapanik, W. Haase and R. Jakoby, "Liquid-Crystal Varactors with Fast Switching Times for Microwave Applications," *Electronics Letters*, Vol. 44, March 2008, pp. 480–481.
7. R. E. Hattachi and J. Erfanian "NGMN 5G White Paper," *NGMN Alliance*, February 2015.
8. M. C. Johnson, S. L. Brunton, N. B. Kundtz and J. N. Kutz, "Sidelobe Canceling for Reconfigurable Holographic Metamaterial Antenna," *IEEE Transactions on Antennas and Propagation*, Vol. 63, No. 4, February 2015, pp. 1881–1886.
9. A. Bhattacharya, "Modeling Metamaterials - Metamaterial Development using Electromagnetic Simulation," *Physics' Best*, April 2014, pp. 30–32.
10. C. Bencivenni, T. Emanuelsson and M. Gustafsson, "Gapwaves Platform Integrates 5G mmWave Arrays" *Microwave Journal*, Vol. 62, No. 2, February 2019, pp. 22–38.
11. "Introduction to All Silicon Millimeter-Wave 5G Arrays," *Anokiwave Inc.*, March 2019, Web. www.anokiwave.com/contact/overview_request/mmWave_array_wp_request.php.
12. B. Peterson, "RF Front-end Technology and Tradeoffs for 5G mmWave Fixed Wireless Access," *Microwave Journal*, Vol. 61, No. 11, November 2018.
13. "Use of Spectrum Bands Above 24 GHz for Mobile Radio Services, In the matter of GN Docket No. 14-177, IB Docket No. 15-256, RM-11664, WT Docket No. 10-112, IB Docket No. 97-95," *Federal Communications Commission*, July 2016, Retrieved from mentor.ieee.org/802.18/dcn/16/18-16-0058-00-0000-fcc-mmwave-r-o-and-fnprm.pdf
14. M. R. D. Kodnoeih, *Development of Next-Generation 5G Directive Antennas at Millimeter Waves*, PhD thesis, UNIVERSITE DE NANTES, France, 2018.

INVITED PAPER

The Role of Satellites in 5G Networks

Pasternack
Irvine, Calif.

This article provides an overview of current satellite topologies, their key enabling technologies and how satellite communication can supplement 5G networks.

Cellular macro and micro base station densification is already underway to support 5G, with complex radio techniques to support 5G data rates, capacity and coverage. The 3GPP release 16 has a release date of June, with release 17 expected during the second half of 2021. Improvements to V2X, industrial IoT, multi-SIM devices, reliability and low latency performance, access to unlicensed spectrum to 71 GHz, efficiency and interference and other features are expected to be fleshed out. An addition to the large list of 24 items discussed at the 3GPP meeting in Spain late last year, 5G new radio (NR) support from non-terrestrial access (NTN) technologies such as satellites and high altitude platforms are being defined. Satellite technology can be a contributing asset to the framework of 5G globally, due to the inherent benefits of the platform.

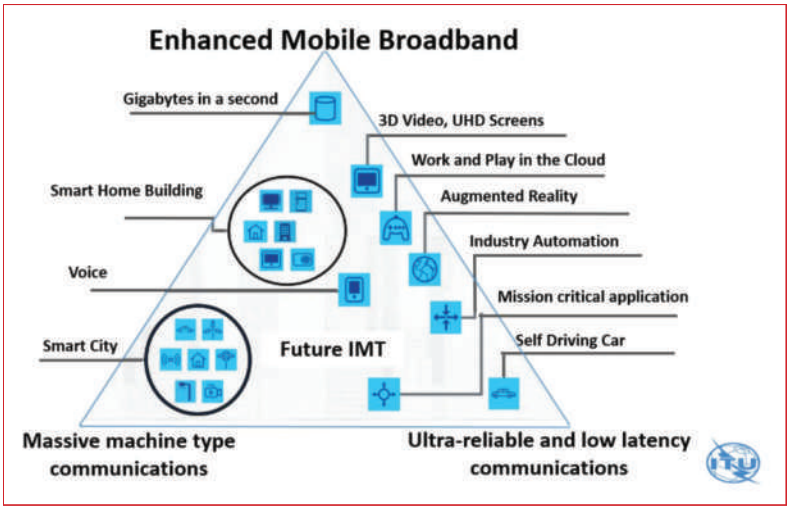

▲ Fig. 1 5G generic use cases. *Source:* ITU.

5G BACKHAUL

With a multitude of radio access technologies enabling 5G, backhaul has necessarily evolved, decomposing the baseband unit (BBU) and remote radio head found in LTE networks into separate functional blocks: a centralized unit (CU), distributed unit (DU) and radio unit (RU). Cooperative radio techniques such as carrier aggregation, downlink coordinated multi-point transmission/reception and MIMO make the most of the limited sub-6 GHz spectrum, while massive MIMO (mMIMO) improves network capacity and coverage at each cell site with high spectral efficiency. Solutions such as dense mmWave small cell deployments move up the spectrum to access large bandwidth. These various solutions enable 5G enhanced mobile broadband (eMBB), ultra-reliable and low latency communications (uRLLC) and massive machine type communications (mMTC), the 5G capabilities defined by the International Telecommunications Union (see ***Figure 1***).

As shown in ***Figure 2***, the current strategy for the 5G radio access network (RAN), termed the gNodeB (gNB), comprises a two-tier architecture with a distributed tier (DU) providing low latency, for factory automation and medical services, and a centralized tier (CU) handling the power hungry

processing. The separation of the RU and DU exposes the common public radio interface (CPRI), which is enhanced for 5G and called the enhanced CPRI (eCPRI) interface. In some scenarios, the DU can be integrated with the RU to function as a small cell.

SATELLITE CONVERGENCE WITH 5G

The use of a satellite-terrestrial architecture to supplement the 5G RAN is being explored through several testbeds. The EU Horizon 2020 is a collaboration involving companies across Europe, with the goal to develop a "Satellite and Terrestrial Network for 5G." Another project, funded by the European Space Agency, is the "Demonstrator for Satellite-Terrestrial Integration in the 5G Context (SATis5G)." SpaceX, OneWeb and Amazon are developing low earth orbit (LEO) constellations to provide connectivity anywhere on the globe. High throughput satellite (HTS) technology in geostationary orbit (GEO) is another player in the convergence of the satellite-terrestrial network with 5G, offering spot beam and multicast capabilities. The cellular standards organization 3GPP is also working on defining the role of satellite communications in 5G through studies of non-terrestrial networks with satellites in LEO, medium earth orbit (MEO) and GEO.[1]

From the launch in 2004 of Anik F2, with a throughput of 4 Gbps, to the 2017 launch of EchoStar XIX, with a throughput of 200 Gbps, HTS technology has evolved dramatically. Soon, Tbps speeds will be feasible with Ka-Band transponders and optimization techniques to decrease the cost per bit. There is a goal for "plug and play" capability for the satellite network to support 5G through satellite network virtualization, allowance of the cellular network to control satellite radio resources, development of link aggregation for small cell connectivity, optimized security through key management and authentication between cellular and satellite access technologies and integration of the multicast benefits of satellite technologies.[2]

As shown in ***Figure 3***, the organizations involved in the H2020 project have identified four use cases for satellite integration with 5G networks, where the satellites connect to:

- Trunks and head-ends for terrestrial networks in isolated, hard-to-reach areas.
- User premises, providing direct service to underserved areas.
- Moving platforms.
- Hybrid architectures, complementing terrestrial capabilities with services such as multicasting.

Fixed Backhaul

Fixed satellite backhaul to base stations or individual small cells can support eMBB where no cost-effective terrestrial backhaul exists. Often, this is in underdeveloped and underserved regions of the globe with little cellular infrastructure and wireless access. In addition to eMBB, satellites can support mMTC for IoT applications such as smart farming.

Content to Premises

Bringing ubiquitous high speed coverage to homes across a country is difficult, let alone providing global coverage. A viable approach for hard-to-reach areas is a line-of-sight link from space, as installing fiber optic cables over the last mile is costly, time-consuming and may not be viable with the density of users. In 2017, around 10 million rural homes in the U.S. did not have access to broadband with download speeds of at least 25 Mbps.[3] In these cases, routing fiber to a wireless access point on a tower is generally the best option, or broadband service may use microwave backhaul from the wireless internet service provider to a fiber connection. Often, residents outside of the limited coverage area have no connection. In these underserved or underdeveloped regions, a hybrid xDSL terrestrial and satellite broadband link can provide service for homes and offices using distributed small cells connecting to the satellite. Adding caching and storage capabilities to the cells can provide near-seamless connectivity. With phased array antennas, the cells can simultaneously receive multicast and unicast streams from several orbital locations.

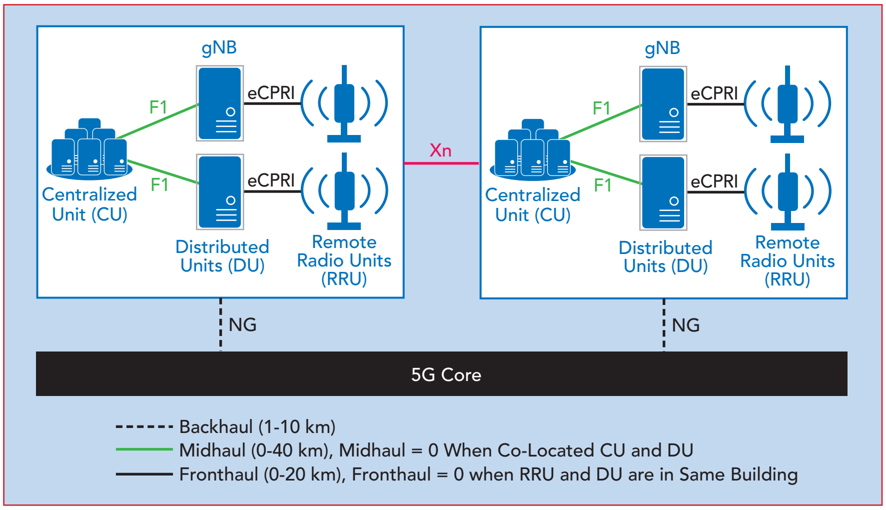

Fig. 2 Generalized 5G backhaul architecture.

Fig. 3 Satellite integration with the 5G network. *Source:* SaT5G-project.

Moving Platforms

Satellite links are practical for moving platforms, providing the capability to connect anywhere on the ground or in the air, regardless of the speed of the platform. Terrestrial infrastructure to do this must be relatively elaborate, with complex handoff capability to support moving platforms such as planes, ships, trucks, cars and railway cars. In many cases, hybrid multiplay support may be feasible, although more remote moving platforms such as planes and ships would likely require a fixed satellite backhaul. Sat5G envisions three major use cases for this application: 1) updating content for on-board systems, 2) broadband access and 3) business and technical data transfer for the moving platform company.

Complementary Services for Low Density Areas

This case entails using the satellite to provide live or on-demand multimedia content, offloading it from the ground 5G infrastructure in areas with low population densities and where service costs are high. Satellite multicasting sends the same data packet to multiple user terminals in a broad geographic area, which avoids taxing the capacity of the 5G infrastructure. The major limitation for this application is the high latency of GEO satellite links. To provide timely video sessions, caching optimization techniques with knowledge of the popularity of specific content by region, with online prefetching through the satellite, can be used.[4]

SATELLITE-TERRESTRIAL NETWORKS

A satellite in a 5G satellite access network will have one of two architectures, referred to as bent pipe gNB or regenerative gNB (see ***Figure 4***). The bent pipe simply redirects user data to the ground gNBs using NR protocols, while regenerative satellites have fully functional gNBs. Newer satellites with digital payloads can regenerate an incoming signal, while legacy relay satellites merely shift the incoming signals from the uplink to downlink frequencies, amplifying and transmitting without altering the original content. As shown in the figure, the F1 logical interface in the regenerative satellite represents the connection between a CU and DU in 5G. This helps explain the allocation functions to each of the blocks in the signal chain, where satellites have the potential to provide high bandwidth, low to high latency 5G cellular services to regions across the globe for a variety of use cases.[5]

While it is not yet specified by 3GPP, future ground stations may connect multiple satellites from various orbital positions, simultaneously benefiting from the low latency of LEO satellites, the location/positional capabilities of MEO satellites and the coverage and high throughput of GEO satellites. This will require a user terminal able to receive the satellite signal, likely using an active phased array.

HTS ENABLING TECHNOLOGIES

Satellite technology has evolved from the traditional fixed satellite service (FSS) to HTS technologies, which continue to provide more capabilities and services.

Spot Beams and Frequency Reuse

Where FSS beams are few and extremely large—spanning a continent—HTS satellites yield great-

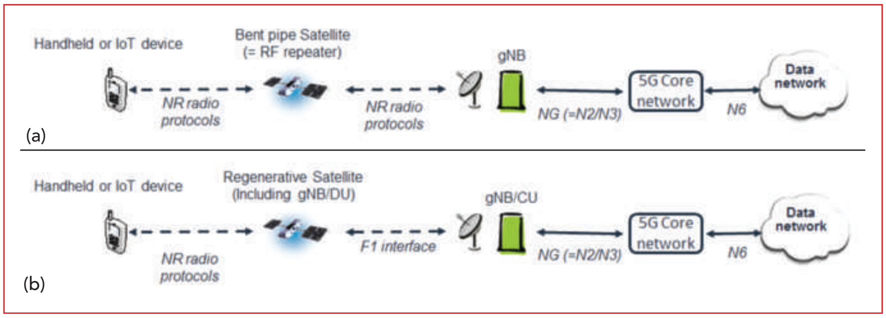

Fig. 4 Bent pipe (a) and regenerative satellite (b) integration in the 5G access network. *Source:* 3GPP TR 22.822.

SKYWORKS®

RF Solutions for Next-generation Wireless Connectivity

Aerospace and Defense

For high-reliability, space, instrumentation, avionics, land mobile radio and overall military communication applications.

Part Number	Description	Freq. Range (GHz)
SKYH22001 SKYH22002	Hermetically Sealed Broadband Low-Noise Amplifier	0.300 to 3.800 0.100 to 6.000
SKY16603-632LF	High Linearity Limiter Module	0.600 to 6.000

Small Cell Infrastructure

For applications including CBRS, FDD and TDD 2G/3G/4G LTE systems, small cell, micro and macro base stations, active antenna arrays and massive MIMO.

Part Number	Description	Freq. Range (GHz)
SKY67183-396LF	High Performance Wideband Low-Noise Amplifier	0.400 to 6.000
SKY67189-396LF	Broadband Low-Noise Amplifier	0.400 to 6.000
SKY66317-11	High Efficiency Wideband 5G n41 Small Cell Amplifier	2.496 to 2.690
SKY66318-11	High Efficiency Wideband 5G n78 Small Cell Amplifier	3.300 to 3.600
SKYFR-001657	Low Insertion Loss, Low Profile Circulator in a 7 mm Package	3.400 to 3.600
SKYFR-001753	Low Profile Circulator with Excellent Performance in a 7 mm Package	4.400 to 5.000

Internet of Things (IoT)

For fitness/smart watches, trackers, wireless headphones, in-home appliances, smart thermostats, alarms, lighting, sensors, access points, routers, automotive infotainment, telematics applications and more.

Part Number	Description	Freq. Range (GHz)
SKY66403/4/5/7	2.4 GHz Zigbee® / Thread / Bluetooth® FEMs	2.400 to 2.483
SKY66118-11	2.4 GHz, 20 dBm Zigbee® / Thread / Bluetooth® FEM	2.400 to 2.483
SKY66420/1/2/3	Sub-1 GHz RF FEMs for LoRa, SigFox, Wireless MBUS Applications	0.860 to 0.930

Wi-Fi Connectivity

For wireless audio and video streaming, 802.11ax / WiFi-6 networking, routers, gateway applications and more.

Part Number	Description	Freq. Range (GHz)
SKY85333-11	2.4 GHz WiFi-6 Front-end Module	2.400 to 2.500
SKY85747-11	5 GHz High-Power WiFi-6 Front-end Module	5.150 to 5.925

For more information about all of our solutions, please visit us at www.skyworksinc.com.

sales@skyworksinc.com | USA: 781-376-3000 | Asia: 886-2-2735 0399 | Europe: 33 (0)1 43548540 | Nasdaq: SWKS |

er than 20x the throughput within the same frequency allocation, by using multiple spot beams balanced with frequency reuse (see ***Figure 5***). Each spot beam provides more power to a targeted area than the wide beam from an FSS satellite. This enables optimal spectrum usage regardless of the satellite transponder's operating band (e.g., C-, K- or Ka-Band). To mitigate the risk of interference and signal loss, the spot beams are laid out so neighboring beams are not close in frequency. There is a trade-off between the frequency separation between the spot beams and satellite throughput: the closer in frequency, the more frequency reuse can occur, which gives the satellite more capacity. The concept is like the data rate and capacity increase achieved with mMIMO, where hundreds of active antenna elements and beamforming point multiple beams to users at various locations. However, there is a significant difference between this and spatial diversity: where terrestrial mMIMO systems reduce co-channel interference by increasing the beams, satellites are not in a rich scattering environment, so co-channel interference is a concern. This is mitigated with "four color" frequency reuse (FR4): orthogonality between adjacent beams with disjoint frequencies of different polarizations. The orthogonality is typically preserved to the user terminal.

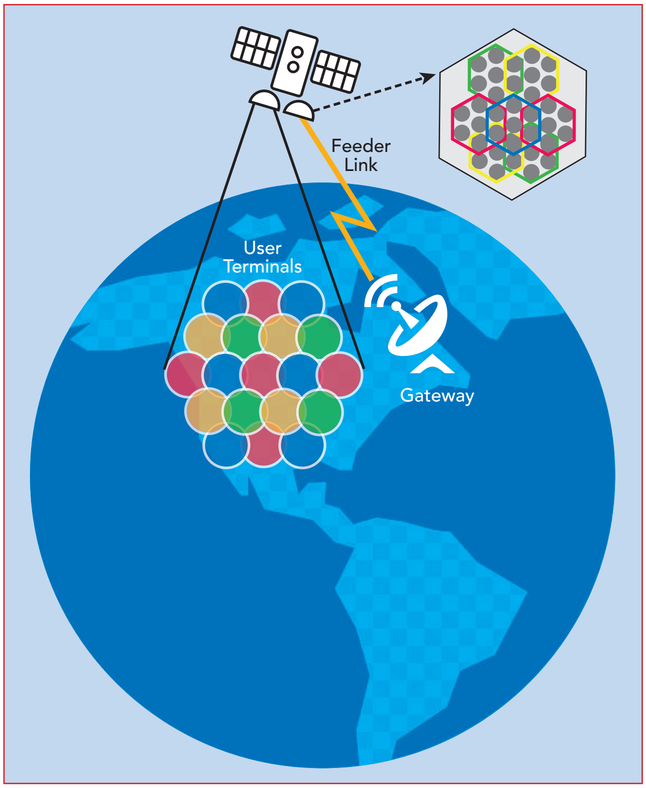

▲ Fig. 5 Spot beams and frequency separation improve HTS coverage and capacity.

Multicast

HTS technology is inherently capable of multicast, where one message does not have to be sent individually to a thousand users a thousand different times—rather, just once, providing more efficient use of the spectrum and data resources. Compared to terrestrial wireless services, the coverage area of a satellite beam is large, and the channel codes are long to overcome noise, with the transmitted signal containing information from multiple users. The frame, which may be coded using a DVB-S2X framing protocol, is decoded by a group of users, yielding a multicast transmission.[6] As the number of devices receiving the broadcast increases, so do the bandwidth savings. One example of a multicast service is video conferencing, where each participant is a single source multicast to all other participants (i.e., multipoint-to-multipoint). While this is typically a bandwidth hungry process for terrestrial systems, it is relatively straightforward with HTS.

Up the Spectrum

Most recent HTS launches have used Ka-Band transponders. The shift to higher frequencies is to get greater bandwidth, which enables more spot beams. Future generations of satellites will provide terabit per second capacities, which will likely require Q- and V-Band feeder links to be able to aggregate more


STRONG, CONSISTENT
WIDEBAND
POWER
ALL THE WAY THROUGH YOUR BAND
Wideband High Power Amplifiers (WHPAs)
WIDEBAND
2-18 GHz
Pout: 30 dBm
K BAND
15-27 GHz
Pout: 29 dBm
Ka BAND
17-43 GHz
Pout: 22 dBm
Ka BAND
24-40 GHz
Pout: 22 dBm
Q BAND
33-47 GHz
Pout: 29 dBm
W BAND
75-83 GHz
Pout: 27 dBm
erzia.com/microwave/WHPA

TABLE 1

3GPP REQUIREMENTS FOR LOW LATENCY, HIGH RELIABILITY SERVICES[7]

Scenario	*Maximum End-to-End Latency (mS)*	*User Data Rate (Mbps)*
Discrete Automation	10	10
Process Automation: Remote Control	60	1–100
Process Automation: Monitoring	60	1
Electricity Distribution: Medium Voltage	40	10
Electricity Distribution: High Voltage	5	10
Intelligent Transport Systems: Infrastructure Backhaul	30	10

user traffic and split the coverage into thousands of spot beams.

LEO LOW LATENCY

LEO constellations offer capabilities not viable with single GEO satellites. The major LEO advantages are reduced latency and the increased coverage a LEO constellation provides. A GEO satellite at 35,000 km altitude has an end-to-end propagation delay of 280 ms, a MEO satellite at 10,000 km altitude has a delay of 90 ms and a LEO satellite at 350 to 1,200 km altitude has a delay of 6 to 30 ms. The lower latency of LEO satellites can support a limited range of low latency 5G services; however, the synchronization chain of most low latency 5G services requires much tighter round trip delays and respective timing errors (see *Table 1*).

With ubiquitous global coverage, a LEO constellation is best suited to serve mMTC applications. While HTS GEO satellites use a spot beam architecture with frequency reuse to provide targeted service to predesignated areas, a LEO constellation with adequate ground infrastructure can cover the entire globe. While the first LEO constellation, Iridium, went bankrupt shortly after it was launched in 1998, it subsequently provided low data rate services for more than a decade and the constellation was upgraded with a new generation of satellites.[8]

Several technologies enable a LEO constellation to function, including digital payloads, advanced modulation, frequency reuse, GaN power amplifiers (PA) with high power densities and active phased arrays for beam agility.

LEO Communications

LEO constellations involve "round robin" communications

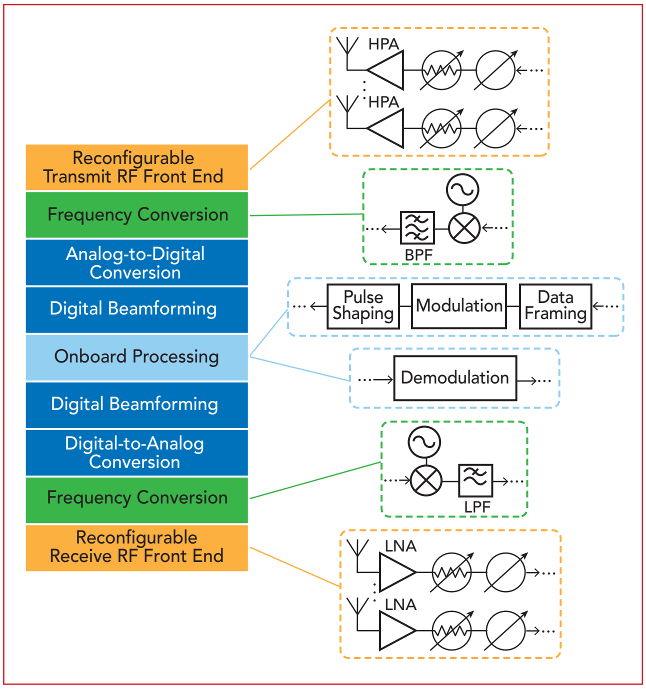

Fig. 6 **Regenerative satellite onboard signal processing.**

between the ground and satellite, ground stations (G2G), satellites (S2S) and the satellite and ground. These physical links are classified into ground-to-satellite and inter-satellite links. Inter-satellite and ground station communication is another differentiating factor between LEOs and HTS. This net of LEO satellite communication enables tight control of the data transfer among the user and the control and telemetry (e.g., status, diagnostics, configuration).

Instead of maintaining a fixed position in the sky like a GEO, a LEO satellite quickly passes over a ground segment, requiring multiple satellites for consistent coverage of an area. Complex handoffs are required by the ground stations, accomplished with either mechanically-steered reflector antennas or active phased arrays with high gain and directivity. For status updates, beam hopping between a satellite and users to reach remote areas without infrastructure can be supported with G2G links. Tracking of space debris using satellites with cameras and sensors is possible with tight S2S coordination.[5]

On-Board Processing

Increasing a satellite's throughput requires adjustments in HTS GEO and LEO satellite architectures. The main change is with the architecture, where a previous bent pipe becomes a regenerative topology. The bent pipe satellite uses transponders with fixed bandwidths that are not finely adjustable, requiring a user to purchase a segment rather than only using what is required for the application. This results in inefficient management of bandwidth and satellite resources.

Many current satellites use regenerative transponders. Software-defined payloads can be accomplished with on-board processing (OBP) technology or digital transparent processors (DTP). DTPs divide each incoming channel into subchannels of variable width without modifying the form of the received signals. More sophisticated OBP performs beamforming, interference suppression, automatic level control and frequency multiplexing/demultiplexing (see ***Figure 6***). This processing is possible with technologies such as array-fed reflectors or direct radiating arrays, ASICs, high speed serializer/deserializer, digital signal processors and data converters.[9] While in orbit, modular and flexible payloads can adjust to changing service needs, configuring to support new applications.

GaN SSPAs

Traveling wave tube amplifiers (TWTA) have historically been used for the PAs in ground stations because of their high output power, necessary to overcome atmospheric propagation losses from the ground to the GEO satellites. A LEO constellation has the benefit of shorter distances, requiring lower transmit power. However, the size constraints in a smaller LEO satellite make the power density of the PA a significant requirement. A solid-state power amplifier, even with relatively low

efficiency compared to a TWTA, is often preferred because of its lower launch weight and cost. GaN PAs offer an attractive solid-state option, providing better linearity, lighter weight, a smaller form factor and, in some cases, equivalent efficiency as a TWTA.

Phased Array Antennas

The active phased array is being implemented in space surveillance and tracking systems, where thousands of transmit/receive modules monitor and track space debris. Fitting this technology into smaller ground terminals to track LEO constellations can replace a gimballed antenna with electronic beam steering, changeable scan rates and interference cancellation, and it offers better reliability than a mechanically-steered antenna.

CONCLUSION

Both HTSs and LEO constellations can augment terrestrial 5G networks to ensure seamless connectivity to remote and urban locations, by providing hybrid multiplay and fixed backhaul services. HTS technology is already providing broadband internet around the globe and will likely continue serving this role, while increasing capacity to multi-Tbps with Q- and V-Band feeder links and smaller spot beams. The LEO satellite architecture, while more technically complex, offers a modular high throughput platform with global coverage. Network planners can use the respective advantages of LEO and GEO satellites to supplement terrestrial 5G networks, where needed.■

References

1. N. Chuberre and C. Michel, "Satellite Components for the 5G System," *3GPP*, January, 2018, Web. https://www.3gpp.org/news-events/1933-sat_ntn.
2. "Concept," *SaT5G Project*, Web. https://www.sat5g-project.eu/concept/.
3. "Communications Infrastructure Upgrade – the Need for Deep Fiber," Deloitte, July 2017, Web. https://www2.deloitte.com/content/dam/Deloitte/us/Documents/technology-media-telecommunications/us-tmt-5GReady-the-need-for-deep-fiber-pov.pdf.
4. "Satellite Reference Use Cases and Scenarios for eMBB," Deliverable D2.1, *SaT5G Consortium*, August 2017.
5. "Study on Using Satellite Access in 5G," *3GPP*, Technical Report 22.822, V16.0.0, June 2018.
6. A. I. Perez-Neira, M. A. Vazquez, M.R. Bhavani Shankar, S. Maleki and S. Chatzinotas, "Signal Processing for High-Throughput Satellites: Challenges in New Interference-Limited Scenarios," *IEEE Signal Processing Magazine*, Vol. 36, No. 4, June 2019, pp. 112–131.
7. "New Services and Applications with 5G Ultra-Reliable Low Latency Communications," *5G Americas*, November 2018, Web. https://www.5gamericas.org/wp-content/uploads/2019/07/5G_Americas_URLLLC_White_Paper_Final__updateJW.pdf.
8. J. Gertner, "The Fall and Rise of Iridium," *The Wall Street Journal*, June 2016, Web. https://www.wsj.com/articles/the-fall-and-rise-of-iridium-1464980784.
9. P. Angeletti, R. De Gaudenzi and M. Lisi, "From 'Bent Pipes' to 'Software Defined Payloads': Evolution and Trends of Satellite Communications Systems," *26th International Communications Satellite Systems Conference*, October 2008.

INVITED PAPER

Selecting Quartz Oscillators with High Frequency Stability vs. Temperature

A. Kotyukov, A. Nikonov, A. Zaslavskiy and Yu. Ivanov
Morion Inc., St. Petersburg, Russia

Frequency stability versus temperature is one of the key parameters of quartz oscillators, with several design approaches used to achieve it (see ***Figure 1***).[1,2] With a simple quartz oscillator (XO), the frequency versus temperature stability is provided only by the quartz resonator itself, primarily by choosing the cut of the quartz crystal. Frequency stability ($\Delta f/f_0$) versus temperature for an XO can reach = ±10 to ±15 × 10^{-6} from -40°C to +85°C. With a temperature compensated quartz oscillator (TCXO), additional components apply a control voltage to a varactor diode that compensates for temperature effects on the frequency. Frequency stability versus temperature for a TCXO can reach ±1 to ±3 × 10^{-7} from -40°C to +85°C. An oven controlled quartz oscillator (OCXO) design places the quartz resonator and all basic circuits inside an oven at constant temperature. Frequency stability versus temperature for an OCXO can reach ±1 to ±5 × 10^{-11} from -40°C to +85°C. Of these three designs, only the OCXO, which has the highest frequency stability versus temperature, is discussed here.

OCXO DESIGN

With the OCXO design, all temperature sensitive elements are located inside an oven and maintained at almost constant temperature (see ***Figure 2***). The temperature inside the oven is set slightly above the upper operating temperature of the OCXO, usually 5°C to 15°C, and it is located near the quartz resonator's lower turnover point or upper turnover point to minimize the frequency variation with temperature (see ***Figure 3***).

The need to maintain a high oven temperature increases the turn-on power consumption; however, as soon as the temperature inside the oven reaches a defined level, the power decreases significantly. Related to this is the warm-up time, which is determined by the time to meet the frequency accuracy specification. Usually, the warm-up time from room temperature ranges from 2 to 5 minutes to achieve an accuracy of ±2 × 10^{-8}.

A basic OCXO provides a frequency stability versus temperature from ±1 × 10^{-8} to ±5 × 10^{-10} depending upon the design. This can be improved through several ways:

- **Double oven design (DOCXO)**—This is an efficient approach usually achieving a frequency stability versus temperature of up to ±1 × 10^{-10}. However, it is relatively large and has a limited OCXO upper operating temperature to maintain a difference between the operating temperature and the oven temperature.
- **Additional temperature compensation**—The frequency versus temperature characteristic of an XO is more or less linear, enabling compensation. The disadvantage of this approach is because the frequency versus temperature characteristic has a rather steep slope, which reduces the improvement that can be achieved. The slope can be reduced using an oven and employing temperature compensation with an OCXO enables up to a 5× increase in stability.
- **Improvement in the basic design**—This results in the best performance yet is the most sophisticated method, involving careful calculation and a multi-iterative process designing the specific type of oscillator to obtain better


MANUFACTURING HIGH QUALITY
INTEGRATED MICROWAVE ASSEMBLIES AND COMPONENTS
LEADERS IN RF AND MICROWAVE
American Microwave Corporation
An Ironwave Technologies Company
MU-DEL ELECTRONICS
AMERICAN MICROWAVE CORPORATION & MU-DEL ELECTRONICS
INTEGRATED ASSEMBLIES
• Eliminate all interconnecting cables
• Solid State Switch Based Assemblies
• Very reliable product in a compact form factor
• Switch Matrices on a Substrate
• Provided excellent repeatability
• Direction Finding and Beam
• Forming Networks
• Has the ability to be remotely controlled by host
• Custom Integrated and Turn Key systems
• Lowered insertion loss
SOLID STATE SWITCHES
• DC to 40 GHz
• SPST to SP128T configurations
Any design can be optimized for specific frequency range, insertion loss, isolation, intercept points, switching speed and VSWR
LOG VIDEO AMPLIFIERS
• Standard products - 50 and 70 dB dynamic range SDLVA & DLVA
• CW immunity circuits available for all models
SOLID STATE VARIABLE ATTENUATORS
• Phase Invariant, Broad Band or Octave Band models available
• Attenuation Ranges 30-120 dB
• 10 MHz to 18 GHz bandwidths availa
• Digital, Analog or Current Controlled Variable Attenuators
• Designed to meet MIL Std 202
(additional screening available)
MULTICOUPLERS
• Renowned for reliability, performance & variety
• Frequency range of HF to Ku Bands
• Ability to be tailored with multi-channels, individual gain controls, remote access, high outputs and up to 64 outputs
• Can be mountable or outdoor weatherproof
RF DISTRIBUTION & SWITCH MATRIX
• Available in up to 24 selectable inputs and outputs
• Basic features include auto signal overload protection, signal communication and complete test signal injection
FREQUENCY CONVERTERS, SYNTHESIZERS, TRANSLATORS
• Covers L to Ka Bands
• High frequency accuracy, low phase noise and excellent frequency stability
• Options include; multi-channel, individual gain control, remote access, high input power, multiple inputs/outputs
POWER PANELS
• Designed to supply and control DC power with coaxial cable to remotely located components
• Available for single or multi-channel
ANTENNA SYSTEM
• Covers L, S and C bands
• Basic features include integrated filtering and LNA packages
FILTER MATRICES
• RF Lumped and Cavity filters covering HF to Ka band
• Band/low/high pass filters and individual components or as arrays
RADAR FREQUENCY GENERATORS & RECEIVERS
• RF Lumped and Cavity filters covering HF to Ka band
• Band/low/high pass filters and individual components or as arrays
AMPLIFIER MATRICES
• LNA, high power and AGC in the HF to Ka bands
IN PURSUIT OF EXCELLENCE THROUGH ENGINEERING
MIL-883 CAPABLE - ISO9001:2015 REGISTERED
ISO 9001:2015 AND AS9100D
WWW.AMERICANMIC.COM | EMAIL: SALES@AMERICANMIC.COM
WWW.MU-DEL.COM | EMAIL: SALES@MU-DEL.COM
7309-A GROVE
.8900

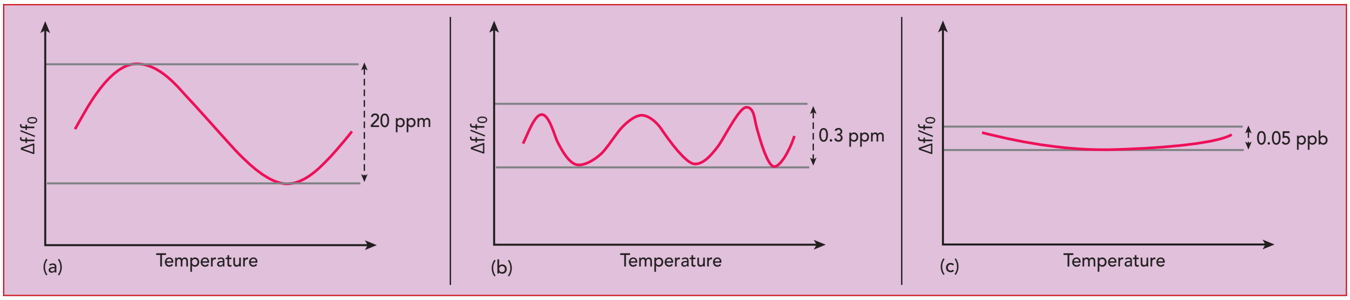

Fig. 1 Typical frequency stability vs. temperature for XO (a), TCXO (b) and OCXO (c) oscillators.

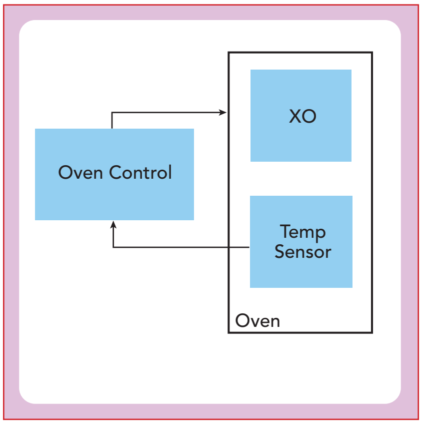

Fig. 2 OCXO block diagram.

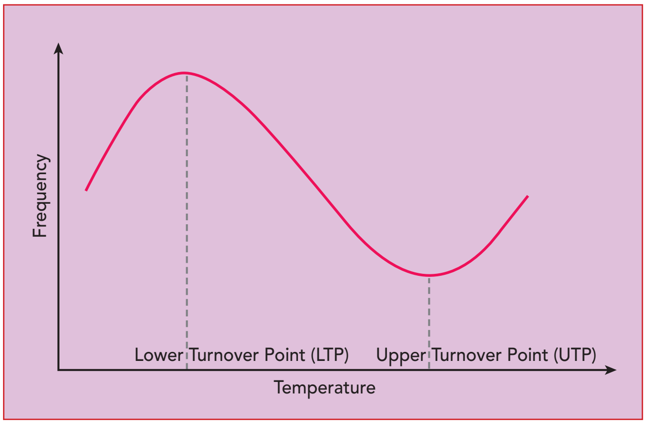

Fig. 3 Typical XO frequency vs. temperature dependency.

frequency stability, typically by decreasing the temperature gradients. The resulting frequency stability versus temperature can be equivalent to a DOCXO while retaining the size—and especially the height—of the basic design.

Obtaining exceptionally high frequency stability versus temperature, as high as 1×10^{-11}, requires using all the above approaches.

OTHER CONSIDERATIONS

During both operation and measurement, additional factors can affect stability, which need to be considered. The higher the OCXO's frequency stability versus temperature, the greater influence these factors will have.

Aging

The frequency of an OCXO changes over time, which is known as aging, making the operating time of the oscillator extremely important. An OCXO operating for several weeks will age around 10^{-11}, while an OCXO that operates for only one day will age around 10^{-10}. This contribution will be noticeable when measuring the frequency versus temperature, especially when it is small and comparable to the aging; so aging must be accounted for when frequency versus temperature is measured.

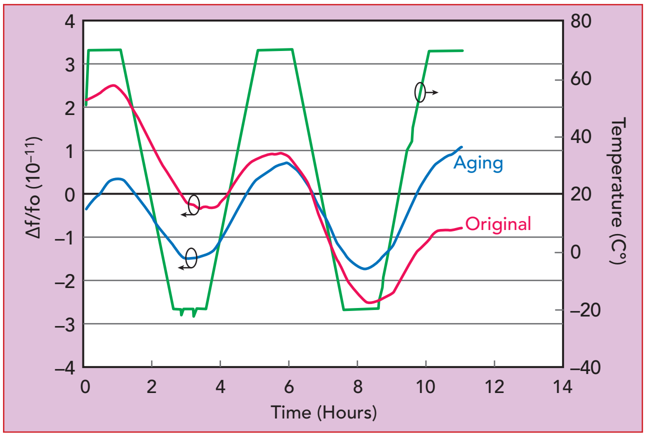

Fig. 4 Frequency vs. temperature cycling test showing OCXO aging.

It is straightforward and necessary to fix the OCXO's frequency at constant temperature. A model of the frequency change over time can be calculated for small time intervals, such as hours, using a simple linear model. Usually, when testing OCXOs with very high temperature stability, several heating and cooling cycles are required to ensure that the OCXO meets the stability requirements. ***Figure 4*** shows an example of aging in the test results of a Morion OCXO.

Frequency vs. Temperature

If additional compensation is used to increase the temperature stability, areas with a steep slope may be present in the final frequency versus temperature characteristics. While this is not very pronounced for OCXOs, it is very noticeable with rubidium oscillators. To illustrate, two frequency versus temperature curves are shown in ***Figure 5***. In Figure 5a, the slope of the frequency change with temperature is relatively small; however, Figure 5b shows an oscillator where a small change in temperature results in significantly more frequency swings, equaling the full range over temperature of the oscillator shown in Figure 5a.

Temperature Shock

Due to the design of the temperature compensation or a "bad" OCXO design, large frequency changes can be observed with rapid temperature changes. This is called temperature shock (see ***Figure 6***). With an OCXO with high temperature stability a change in the shape and magnitude of the frequency versus temperature characteristic can be observed, due to convection inside the OCXO. For a properly

COPPER MOUNTAIN®
TECHNOLOGIES

5 Ways CMT VNAs Work for 5G

1. **Modular Frequency Extension with CobaltFx**
   Configure your 5G Test System to test in the bands you need for a very cost-effective solution.

2. Start with a **9 or 20 GHz Analyzer**

3. Work with CMT engineers for application and **automation support**

4. Implement in **Windows® and Linux® OS** on any computer from desktops to x86 single board computers

5. 4-port measurement at 5G frequencies allow for **fast MIMO antenna feed analysis**

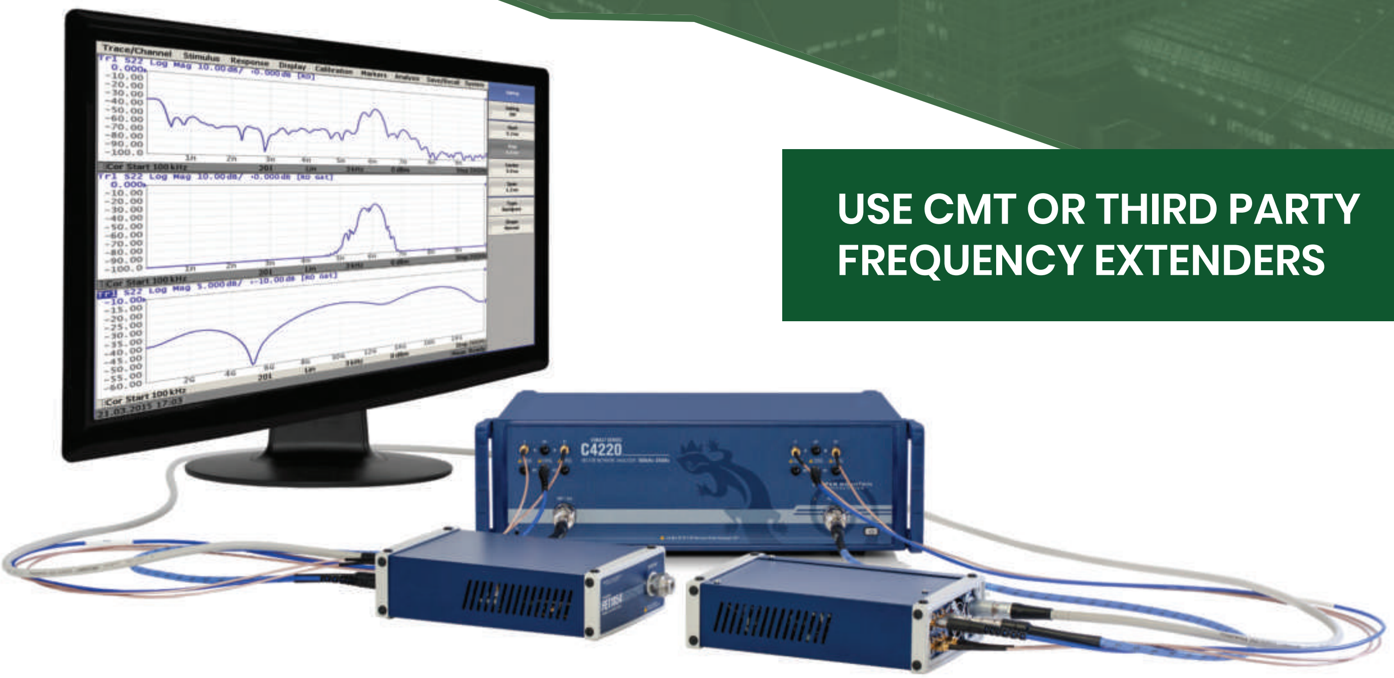

USE CMT OR THIRD PARTY FREQUENCY EXTENDERS

mmWave bands 1.82 mm NMD, WR15, WR12, WR10, WR8, WR6.5, WR5.1, WR4.3, and WR3.4

www.coppermountaintech.com

EXTEND YOUR REACH®

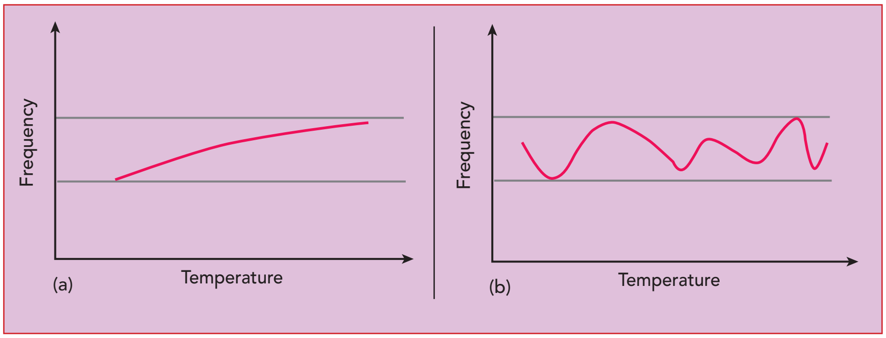

Fig. 5 Frequency vs. temperature for oscillators with linear (a) and highly changing (b) characteristics.

designed OCXO, this dependence should be minimized and evaluated during testing.

Voltage Control

Voltage control directly affects the stability of the OCXO. When considering small instabilities, the contribution due to the presence of frequency adjustment is especially acute. An OCXO without voltage control has better frequency stability versus temperature and better short-term stability than one with it. The frequency stability versus temperature of an oscillator without voltage control can be up to $\pm 1 \times 10^{-11}$, while the stability of an oscillator with voltage control may be only $\pm 2 \times 10^{-11}$. If better frequency stability is needed, an OCXO without frequency adjustment should be chosen for the application, if possible.

Frequency adjustment of the oscillator can be provided either with an analog or digital circuit. Digital voltage control uses a digital-to-analog converter (DAC) with an I^2C or serial peripheral interface. With digital control, degradation of the frequency stability versus temperature is minimal; however, when changing the control code, the short-term stability and phase noise may degrade. Another limitation with digital control is the minimum tuning step, which depends on the bit capacity of the DAC. For a 20-bit DAC, the tuning step is from 5×10^{-13} to 1×10^{-13}. With analog adjustment to adjust the nominal frequency, the control voltage must be applied to the control input and the location of the ground will affect the frequency stability. If a common ground is used (see ***Figure 7a***), the current through the oven heating transistors will raise the voltage on the ground pin of the OCXO, which will add to the control voltage and degrade both the frequency stability versus temperature and the short-term frequency stability. To reduce this source of instability, the common resistance of the supply and control pins must be reduced, which is commonly done using separate grounds for the supply and control circuits (see ***Figure 7b***).

Materials

When different conductors are used, thermoelectric effects at the


Frontlynk®
Bridging Gaps
Multi Coax
Probe Multi Coax up to 67GHz
RF.Microwave Coaxial Connector
& Cable Assembly
1.0mm Series
Connectors, Adaptors, and Cable Assemblies up to 110GHz
1.0mm Connector
DC to 110GHz, VSWR≤1.2
1.35mm Connector
DC to 90GHz, VSWR≤1.2
1.85mm Connector
DC to 67GHz, VSWR≤1.2
2.4mm Connector
DC to 50GHz, VSWR≤1.2
2.92mm Connector
DC to 40GHz, VSWR≤1.15
3.5mm Connector
DC to 34GHz, VSWR≤1.15
1.35mm Series up to 90GHz
Test Cables up to 110GHz
Frontlynk Technologies Inc.
www.frontlynk.com

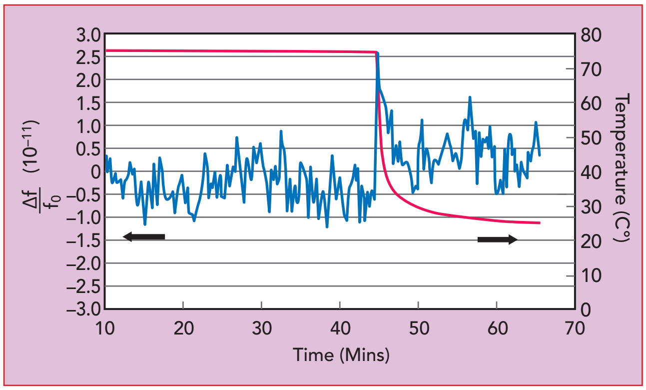

Fig. 6 OCXO designed to minimize frequency changes with temperature shocks.

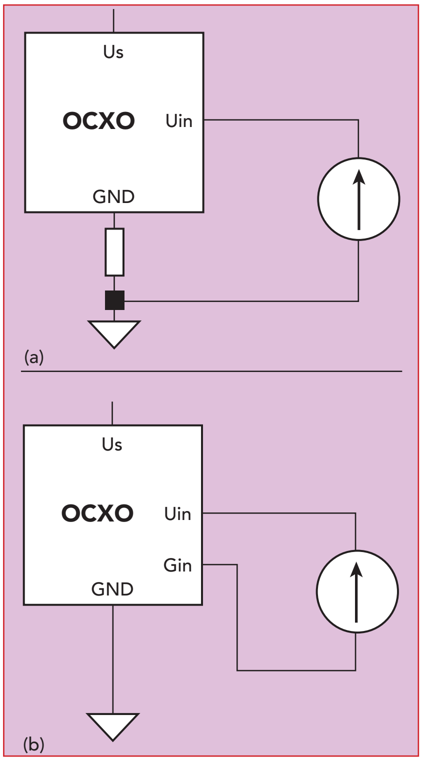

Fig. 7 OCXO designs with analog frequency adjustment using common (a) and separate (b) grounds.

connections can degrade the frequency stability versus temperature.

CONCLUSION

OCXOs with high frequency stability versus temperature can be successfully employed in many areas where very stable frequency sources are needed. They can even compete with rubidium oscillators in some applications, offering smaller size and lower power consumption. The OCXO frequency stability versus temperature characteristic is more linear with a lower slope, so with small changes in ambient temperature, the frequency stability can be better than that of a rubidium oscillator. The only disadvantage with the OCXO is greater aging; in the case of an extremely small change in frequency with a change in temperature, this effect can be compensated.■

References

1. J. R. Vig, "Quartz Crystal Resonators and Oscillators: a Tutorial," *US Army Communications-Electronics Research, Development & Engineering Center* Fort Monmouth, NJ, USA, March 2004.
2. A. Kotyukov, Y. Ivanov and A. Nikonov, "Precise Frequency Sources Meeting the 5G Holdover Time Interval Error Requirement," *Microwave Journal*, Vol. 61, No. 5, May 2018.

Catalog and Beyond

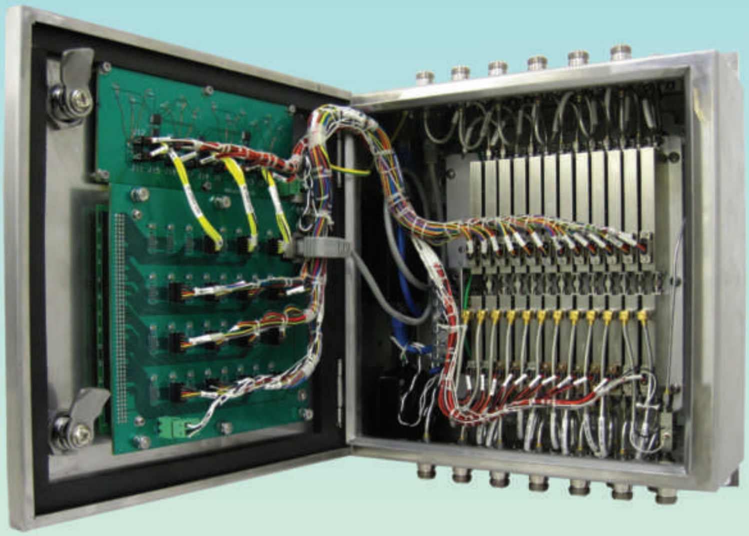

CUSTOM RF/MICROWAVE SWITCH COMPONENTS, ASSEMBLIES & SYSTEMS SINCE 1982

Our catalog of standard components and extensive library of custom designs allows for quick-turn integration of complex assemblies and systems.

Contact us today to discuss your application and our range of solutions.

cmc

Custom Microwave Components, Inc.
www.customwave.com

info@customwave.com
Phone: (510) 651-3434

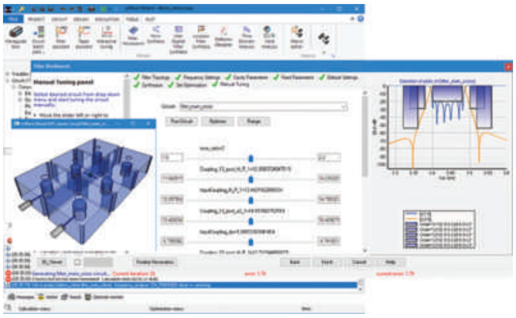

Filter Workbench Streamlines Filter Design for Novice and Experienced Designers

Mician GmbH
Bremen, Germany

Mician's Filter Workbench tool is a quasi-automated filter synthesis add-on to the company's μWave Wizard line of products. Capable of designing and optimizing various physical realizations of microwave filters with moderate relative bandwidths, the tool supports a wide variety of filter designs, from simple waveguide iris filters to more complex geometries such as cross-coupled combline filters. To meet the filter's RF performance requirements, the user can choose tuning coupling elements manually or using an automated mode. The interface provides real-time visual feedback showing the performance as well as a 3D geometric view of the tuned structure.

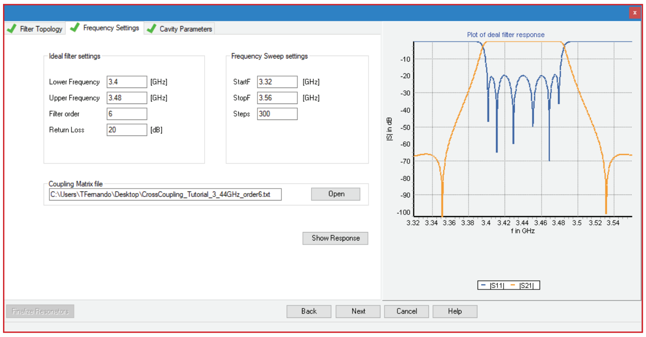

Fig. 1 Setting the frequency range, return loss and order of the ideal filter.

EASY SETTINGS

When launched, the Filter Workbench guides the user through synthesis setup, beginning with selecting a suitable filter topology from a drop-down list. Simultaneously, the physical layout for the topology is shown in an information panel next to the input data template, populated with electrical and mechanical parameters for the filter. Differ-

ent tabs for these entries appear in succession, enabling the designer to proceed to the next tab when all required settings have been entered in the previous tab. While actively editing tabs, explanatory windows provide guidance based on the user's parameters. If an active tab is incomplete or incorrect, the user's attention is directed by a red cross at the top of the tab, which changes to a green check mark once all required fields have been filled out correctly. With the final tab populated, all relevant design inputs such as frequencies, cavity and port parameters and default settings have been entered.

After the filter topology has been selected and the corresponding input mask populated, the required parameters for the ideal filter and frequency sweep settings are entered into the "Frequency Settings" tab. Alternatively, an externally generated coupling matrix in a text file can be imported. Selecting the "Show Response" preview option displays the ideal filter response with options to modify the frequency settings, which immediately changes the displayed preview (see ***Figure 1***).

After the frequency entries are complete, the "Cavity Parameters" tab appears. Data entered on this tab immediately returns information such as the cutoff frequency for the specified geometry, recommended iris thickness (if applicable), recommended resonator diameter for highest Q (if applicable), $\lambda/4$ wavelength and the estimated average resonator height. For combline filters, surface conductivity can be accounted for when determining the cavity Q factor, which will be displayed as the "unloaded Q." This value should closely match the Q used for generating the coupling matrix; otherwise, modifications to the cavity geometries may be necessary. For faster computation, the filter synthesis assumes ideal conducting surfaces. At the conclusion of the synthesis, material parameters can be modified in µWave Wizard to account for limited surface conductivity.

Coax port dimensions are defined in the "Feed Parameters" tab, offering the choice between inductive or capacitive input probes. Based on the port geometries and material parameters, the input port impedance is automatically calculated and displayed. For filters with non-coax input ports, the Feed Parameters tab is disabled.

After the filter topology has been specified, optimization control parameters and physical units can be defined. Modifications to the geometry units affect all input values in all tabs, and project default dimensions for geometry units will be overwritten. Discretization and cutoff settings are initially disabled; once the synthesis based on the initial setup is completed, both options will be enabled, allowing modifications.

SYNTHESIS

After completing the filter synthesis inputs, Filter Workbench

generates an initial filter model using an automated process for determining the initial dimensions for the center frequency and bandwidth. The resulting 3D full-wave model closely resembles the final filter design. In successive steps, this model is used to finalize the coupling element and resonator geometries to meet filter specifications by automatically dividing the model into smaller circuits, each one an individual coupling element (see ***Figure 2***). After completing the initial filter model, tabs for manual or automated fine tuning of the coupling elements appear. At this point, final changes to the tuning goals can be introduced.

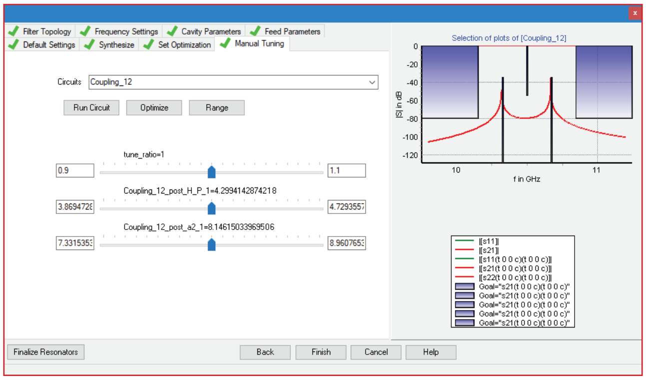

Fig. 2 Tuning individual coupling elements.

Although the filter response of the preliminary model is usually close to the desired performance, Filter Workbench can be used to refine the individual geometries until the filter meets all specifications. The user can choose between template-assisted manual tuning or fully automated fine tuning. In the "Manual Tuning" panel, individual coupling elements can be selected from a drop-down menu and the coupling elements embedded in tuning circuits. The "Run Circuit" command analyzes the selected tuning circuit and displays the actual performance versus the tuning goals. Relevant iris dimensions of each tuning circuit are represented by tunable variables. With the help of sliders on the Manual Tuning tab, the geometries can be decreased or increased from their initial values, manually optimizing the selected circuit until tuning goals are met. After all individual coupling circuits have been manually tuned, the filter response will appear shifted in frequency, because the resonators have not been tuned to account for external loading. This can be corrected by launching the "Finalizing the Resonators" operation.

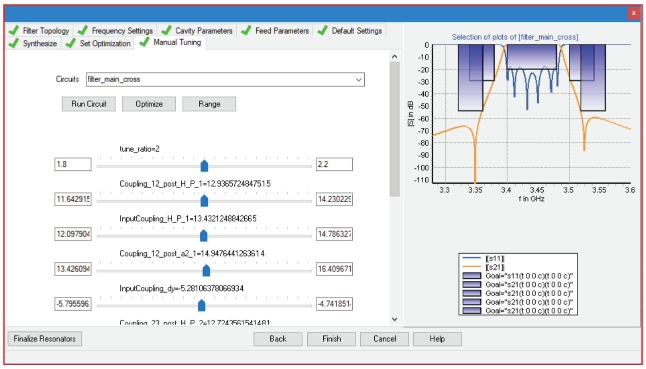

Fig. 3 Performance of a synthesized combline filter meeting all specifications.

With the synthesis process successfully completed, a fully dimensioned µWave Wizard filter model with viable physical dimensions has been created, with subsequent adjustments or additional optimizations possible (see ***Figure 3***).

CUSTOMIZED FILTERS

When selecting a "Customized Filter" topology, Filter Workbench supports the design of filters with arbitrary resonator or iris shapes (see ***Figure 4***). The desired resonator or iris can be created and parameterized either using existing µWave Wizard elements or custom elements generated with µWave Wizard's 3D modeler.

Filter Workbench is ideally suited for casual filter designers or novices with basic knowledge of microwave filter design. The software assists with determining reasonable initial dimensions, then guides the designer to tune the individual components to meet the specifications. Filter Workbench can automatically synthesize a filter with as little user inputs as filter order, bandwidth and return loss. Advanced users can introduce their own topologies and specifications, then have the software provide a physical realization with options for tuning and optimizing. This eliminates the need to create numerous circuits with numerous variables.

Filter Workbench requires an existing installation of µWave Wizard 2020. Evaluation of the filter synthesis tool is free, available by signing up as product tester on Mician's website.

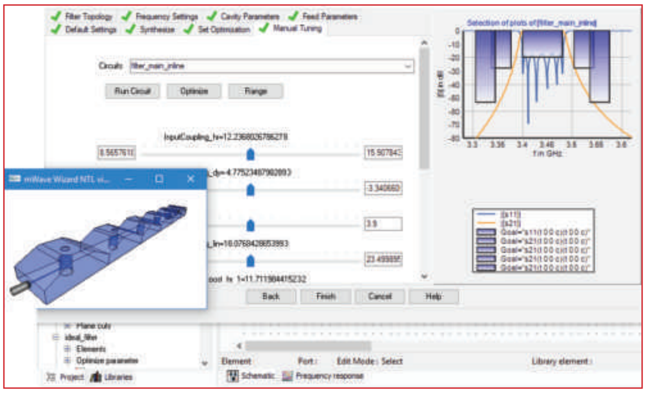

Fig. 4 Custom filter design.

Mician GmbH
Bremen, Germany
www.mician.com

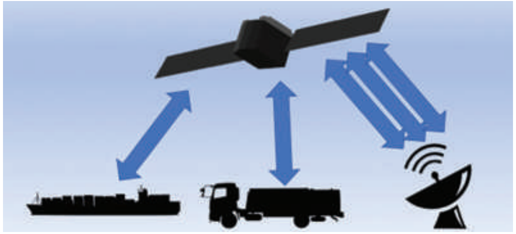

System Simulates 4G/5G Satellite Links, Speeding Development

CommAgility
Loughborough, U.K.

For private satellite communications (satcom) networks, customized LTE has been an option, and 5G is becoming attractive with 3GPP standardization. LTE and 5G offer benefits such as high spectral efficiency, broadband capabilities with high data throughput, all-IP networks and economies of scale. Satcom networks using 5G will begin to be standardized starting with 3GPP Release 17.

With satcom systems, specialized knowledge of the environmental constraints is required to develop reliable systems. The networks need algorithm and protocol adaptations for a range of issues, creating new requirements compared to conventional LTE and 5G terrestrial networks. These include higher latency and interference or multiple parallel channels, particularly where satellites are sharing limited resources. Developing a satcom system using LTE or 5G requires a platform that can simulate and test the real world in a lab.

FLEXIBLE eNodeB

The LTE Reference eNodeB from CommAgility is a pre-integrated, 3GPP-compliant hardware and software system that serves as a key part of such a development system (see ***Figure 1***). The LTE Reference eNodeB provides wireless baseband processing and a 2 × 2 MIMO air interface for radio test systems, small cells and user equipment (UE). The system is based on CommAgility's CA-K2L-RF2 processing board, a low-cost, high performance ARM and DSP processing card with two wideband RF transceiver channels. It also includes CommAgility's PHY and stack software, with example configurations for UE connectivity, and a 4G/5G management tool.

The LTE Reference eNodeB provides a flexible and configurable platform that can be tailored to the needs of a private satcom network, saving development time and reducing risk. It generates the data to be transmitted over a simulated satellite network and handles standard, specialized or advanced LTE and 5G systems beyond Release 15 (see ***Figure 2***). The system gives engineers access to internal eNodeB parameters to change the configuration. For specialized applications, CommAgility can provide source code and test vectors with test cases, customization services and fully integrated applications. The LTE Reference eNodeB handles real world satellite challenges, such as the complications of latency and Doppler shift, by manipulating the PHY source code and providing access to upper protocol layers.

LTE REFERENCE UE

CommAgility also offers an LTE Reference UE. This is a similar system with both hardware and software that can be integrated in a test system for eNodeB and network testing. The LTE Reference UE is based on CommAgility's CA-D8A4-RF4, a baseband processing and RF card for

eNodeB and UE. The card includes a Texas Instruments TCI6638K2K SoC and a Xilinx Kintex-7 FPGA with four flexible wideband RF channels. The RF channels are tunable in pairs over a wide frequency range to cover the LTE and unlicensed frequency bands, with RF bandwidth to 100 MHz to support carrier aggregation and 5G channels. The reference platform is also provided with PHY and stack software and example configurations for UE connectivity.

SIMPLIFYING COMPLEXITY

While platforms such as the LTE Reference eNodeB and UE provide an excellent start to a simulation platform, developing LTE systems can seem overwhelmingly complex, with hundreds of configuration parameters to manage and monitor. As the characteristics of the signal path change, developers need to measure performance metrics and assess the transmission quality users would perceive.

To address this issue, the CommAgility 4G/5G Management Tool enables objective and subjective evaluations of the client user experience. The tool provides a "friendly" and cost-effective graphical interface for monitoring the configuration parameters and data throughput, such as CPU statistics, uplink N+1 histograms, uplink N+1 per PRB, data plane statistics, data plane BLER and control plane. Compatible with CommAgility's 4G/5G protocol stack, LTE Reference eNodeB and Reference UE software, the 4G/5G Management Tool saves effort, time and cost for managing and manipulating hundreds of configuration parameters. The parameters are validated to ensure safe operation and eliminate errors, enabling developers to reduce time to market while maintaining quality.

Together, these products reduce the development complexity and risk for satcom applications, providing the tools to customize LTE and 5G standards to meet the unique needs of satcom links, such as latency and interference.

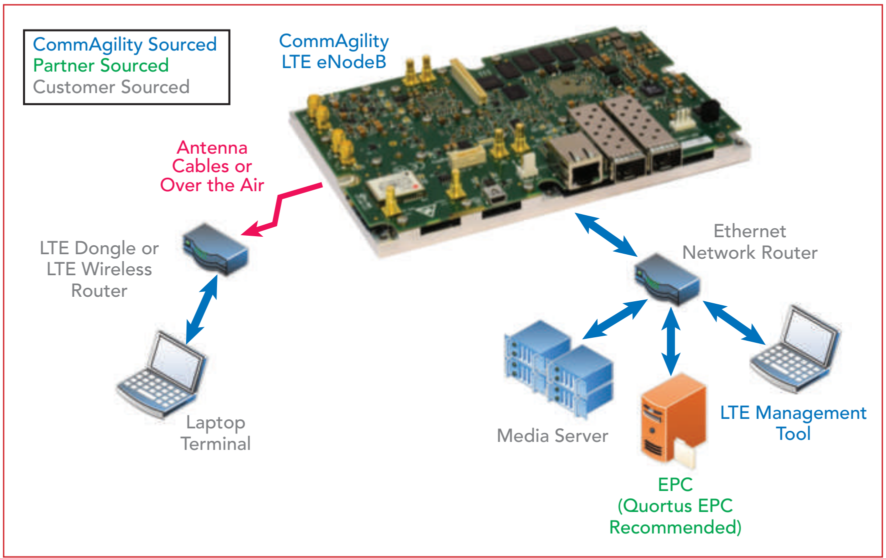

Fig. 1 A satcom development system using CommAgility's LTE Reference eNodeB.

SATELLITE 2020 DEMO

At the recent SATELLITE 2020 conference in Washington, D.C., Wireless Telecom Group (WTG) demonstrated 4G/5G communications for satcom networks using the LTE Reference eNodeB and Management Tool with other WTG products. Featuring signal generation, transport, impairment, monitoring and measurement, the demonstration showed how to overcome the challenges adapting cellular network technology over satellites. Using products from all five WTG companies—CommAgility, Boonton, Holzworth, Microlab and Noisecom—the simulated satcom network demonstrated the transmission and analysis of data over a link (see Figure 2). The effects of latency inherent with GEO satellites, Doppler shifts with LEO satellites, multiple satellite system hops, signal jamming, carrier-to-noise impairments, satellite signal combining and distribution were modeled, controlled and modified by the system, which also measured RF power, signal analysis and link quality.

Suitable for a wide range of wireless applications, the LTE Reference eNodeB and UE from CommAgility provide integrated hardware/software solutions, while the 4G/5G Management Tool streamlines the management of configuration parameters. CommAgility's products, combined with WTG's other solutions, give customers access to the combined expertise and knowledge of the five group companies, enabling fast development and deployment of private and secure satcom networks.

CommAgility
Loughborough, U.K.
www.commagility.com

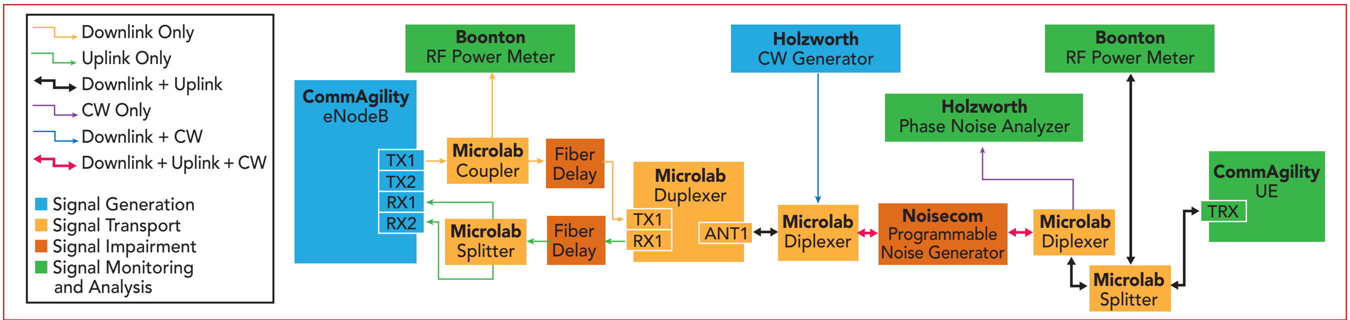

Fig. 2 Satcom test and evaluation system comprising WTG products.

Keeping it down *above 30 GHz...*

Loss is critical in millimeter wave applications,

and **IW** manufactures the range of **lowest attenuation/phase stable** coax to maintain your signal's integrity. From **K-band** to **E-band**, our family of coax was developed using **IW's proprietary EPTFE lamination** process to ensure the lowest cable loss across the mmWave spectrum:

Cable Type	Operating Freq. (GHz)	Atten. (max) dB/ft. dB/m
1801	30	0.49 / 1.62
1701	38	0.57 / 1.88
1571	40	0.64 / 2.09
1501	40	0.75 / 2.46
1401	50	1.02 / 3.34
1251	70	2.14 / 7.02
0471	110	4.95 / 16.23

INSULATED WIRE, INC.
203.791.1999
www.iw-microwave.com
sales@iw-microwave.com

With a broad selection of interconnects including **3.5mm**, **2.92mm**, **2.4mm**, **1.85mm, SMP and SMPM interfaces**, plus jacketing and armoring options, **IW Microwave** delivers reliable **custom cable assembly solutions** to suit a diverse range of applications from **satellite communications systems** to **5G test**.

Talk to us or your local representative about how you can ***get connected*** at **millimeter wave frequencies** with the **lowest attenuation cable** available!

AS9100 Rev. D & ISO9001:2015 certified.

Scan code to find out how you can ***get connected***

We're how the microwave industry ***gets connected!***

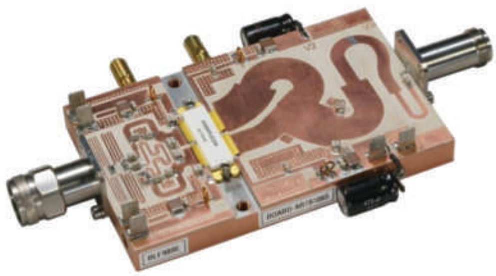

RF Power Solutions for Digital Broadcasting

Ampleon
Nijmegen, The Netherlands

The TV broadcasting industry is undergoing a significant period of change. Across Europe, the rollout of transmitters for second-generation terrestrial digital video broadcasting, designated DVB-T2, continues. In the U.S., to address the looming spectrum crisis caused by 5G, the FCC initiated a spectrum "repack," making the UHF frequency band above 600 MHz available for mobile use and forcing some 1200 broadcasters to change frequency channels. The overall repacking plan is based on 10 phases (see ***Figure 1***), with staggered completion dates designed to minimize interruption to broadcasters during the transition. A large proportion of these broadcasters will upgrade their transmitters to the new ATSC-3.0 standard, so their viewers will not have to rescan channels multiple times. With the 5G rollout, other countries will also face spectrum reallocation, which will extend the demand for new, higher power and more efficient transmitters.

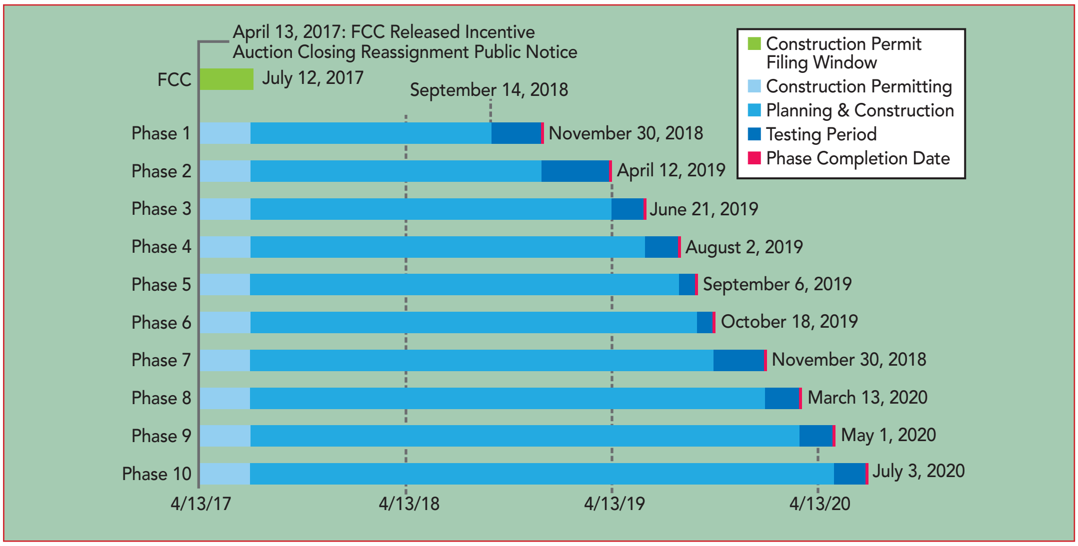

Fig. 1 FCC repack schedule. Source: FCC.

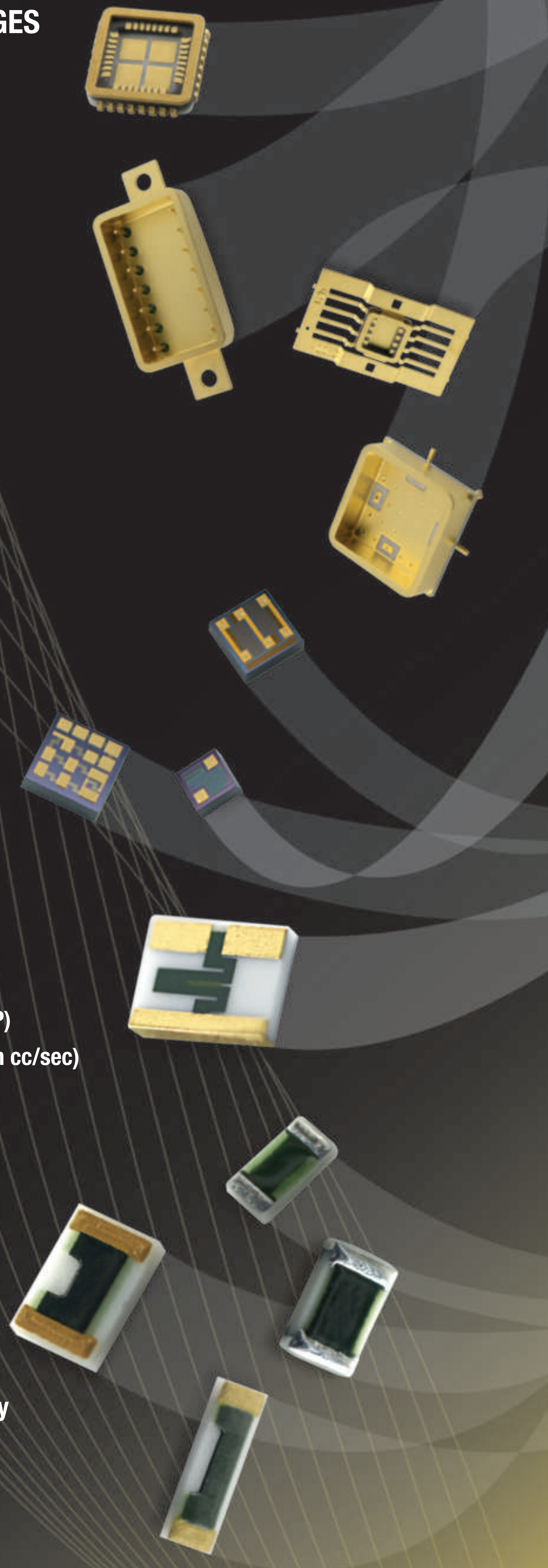

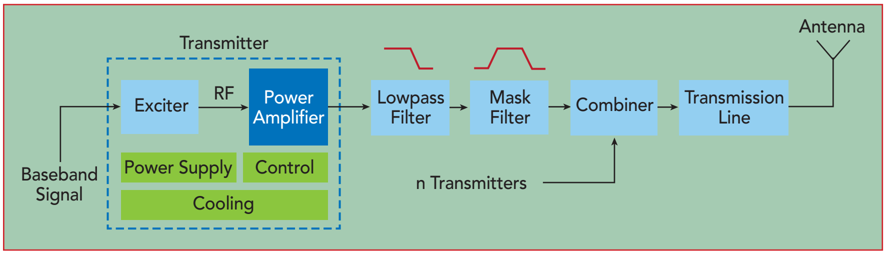

Fig. 2 Typical DTV transmission plant.

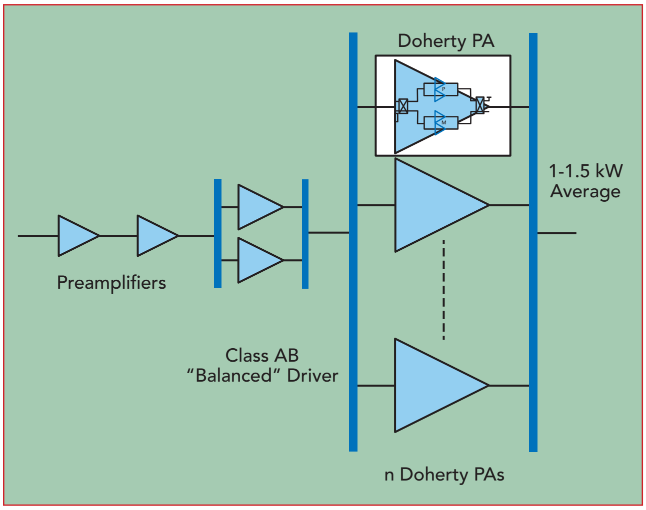

Fig. 3 Typical PA unit.

RFPA REQUIREMENTS

The RF power amplifier (PA) is a crucial component in the transmitter, as a broadcast operator's costs depend on the PA operating efficiently over the broadcast spectrum. The performance requirements for the PA are driven by the DVB-T2 and ATSC-3.0 standards.

DVB-T2—The European Telecommunications Standards Institute adopted the Digital Video Broadcast–Terrestrial (DVB-T) specification in 1997, which was widely deployed and led to the end of analog TV in many countries. With spectrum increasingly scarce in Europe, DVB-T was updated to the more spectrum-efficient DVB-T2 standard in 2009. Using orthogonal frequency division multiplexing (OFDM) modulation with many subcarriers, DVB-T2 is very flexible, with the advantage of enabling re-use of existing antennas. By 2014, DVB-T2 had been deployed in more than 12 countries, and the market research firm Dataxis forecasts 72 percent of European households will have access to DVB-T2 transmissions by 2022.

ATSC-3.0—In January 2018, the Advanced Television Systems Committee (ATSC) released the ATSC 3.0 standard to support newer video technologies, such as HEVC for video channels up to 2160 pixel 4K resolution at 120 frames per second and high dynamic range Dolby AC-4 and MPEG-H 3D audio. ATSC 3.0 and DVB-T2 have many similarities, both using OFDM and offering similar performance and flexibility. While DVB-T2 is widely used, ATSC-3.0 is emerging, and the first TVs capable of receiving ATSC-3.0 transmissions are expected this year.

A typical digital TV transmission chain includes a transmitter with two components: the exciter and the PA (see ***Figure 2***). The input to the exciter is a baseband signal, which modulates the RF carrier before it is amplified by the RF PA. Unlike the time-domain signal envelope for a modulated signal, which shows great variability in envelope peaks, the average power level of the carrier is constant, and the average transmitter output power drives the performance requirements of the TV transmitter. A typical TV station delivers 25 kW average RF power by combining multiple parallel PAs, each with a line-up comprising a pre-driver, a balanced driver and a final stage of four or more PA pallets (see ***Figure 3***).

Since they were first introduced, LDMOS transistors have been the mainstay device technology for the PAs in the broadcast industry. LDMOS has remained the incumbent because it provides high efficiency and high power at an attractive "dollars per watt." The output power performance of LDMOS has improved over the years, from the early days of a few hundred watts to devices capable of delivering greater than 1.5 kW.

As the DVB-T2 and ATSC-3.0 standards define OFDM signals with a high peak-to-average ratio of ~8 dB, the PA must be designed to prevent saturation, which would cause subcarrier intermodulation and out-of-band interference. While the linearity can be achieved by

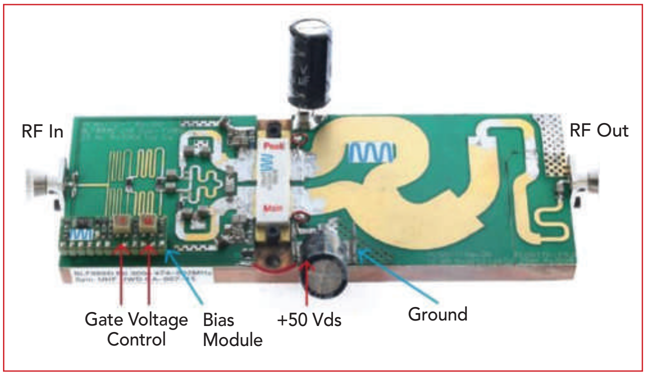

Fig. 4 UWB Doherty PA using the BLF888E.

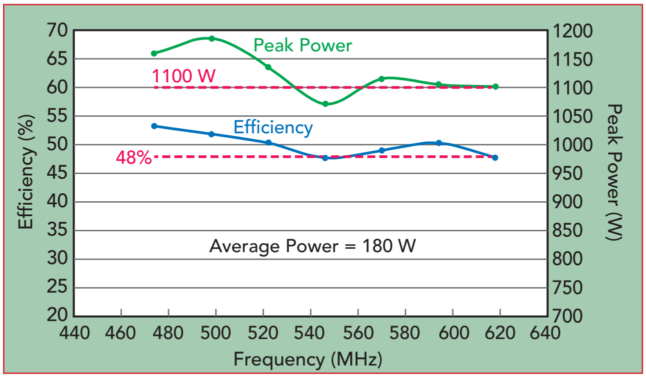

Fig. 5 BLF989E efficiency and power over frequency.

backing off the power of the PA, this approach is not ideal, as it reduces PA efficiency, increasing power consumption and operating cost. Spectrum repacking adds a further design challenge for the PA: during the repacking process, a new transmitter may have to operate at a broadcaster's old frequency before moving to the new one, so the transmitter must operate efficiently across the full UHF broadcast spectrum, from 470 to 806 MHz. The PA designer must maximize the power and efficiency across the full band.

DOHERTY PAS

PA design has been facilitated by two relatively recent developments in PA technology: 1) a new generation of rugged LDMOS transistors with higher power, gain and efficiency; and 2) high efficiency, ultra-wideband Doherty (UWD) circuit architectures, both symmetrical and asymmetrical.

Ampleon has invested significant resources to develop UWD reference designs for the UHF TV broadcast market (see ***Figure 4***). Designs using Ampleon's BLF888 LDMOS transistor, for example, deliver 150 W average DVB-T power from 470 to 700 MHz. The BLF888 family has proven successful addressing both the requirements of ATSC-3.0 and U.S. channel repacking, with many broadcast equipment manufacturers using the devices in their TV transmitters.

Anticipating future demands for more power and efficiency, Ampleon has built upon the success of the BLF888 to introduce its next-generation broadcasting PAs, the BLF989 and the BLF989E. With a DVB-T 8K OFDM signal, the BLF989 achieves the highest narrowband efficiency of 55 percent at an average power level of 200 W (950 W peak) per transistor from 470 to 494 MHz. The BLF989E achieves 180 W average power with a typical efficiency of 50 percent and covers the ultra-wide frequency band from 470 to 620 MHz (see ***Figure 5***). The BLF989E efficiency and power demonstrate how high UWD efficiency can be achieved using an asymmetrical Doherty PA design.

SUMMARY

DVB-T2, ATSC-3.0 and spectrum repacking provide opportunities for manufacturers of broadcast transmitters to meet the needs of TV broadcasters upgrading their systems. OFDM modulation, used by DVB-T2 and ATSC-3.0, challenge the design of the PAs in these transmitters, as higher power must be delivered with high efficiency across the entire UHF broadcast spectrum. Recent advances in LDMOS transistors and UWD architectures are addressing these needs, and Ampleon's UWD high efficiency amplifier solutions are the most cost-effective broadcast PAs available, reflecting innovative engineering to provide the best overall efficiency, bandwidth and reliability.

Ampleon
Nijmegen, The Netherlands
www.ampleon.com

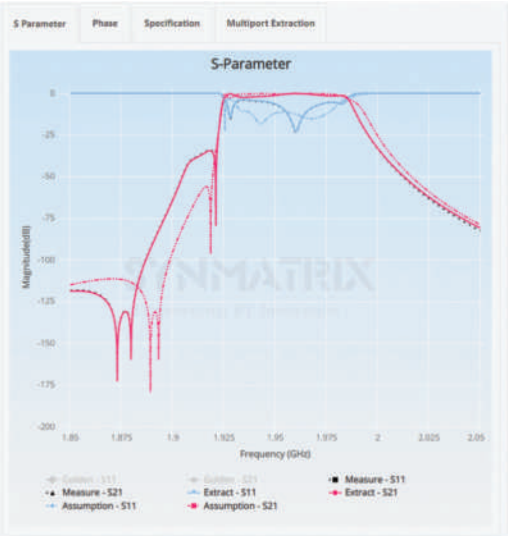

Design Platform Accelerates 5G and mmWave Filter Design

SynMatrix
Richmond Hill, Ontario, Canada

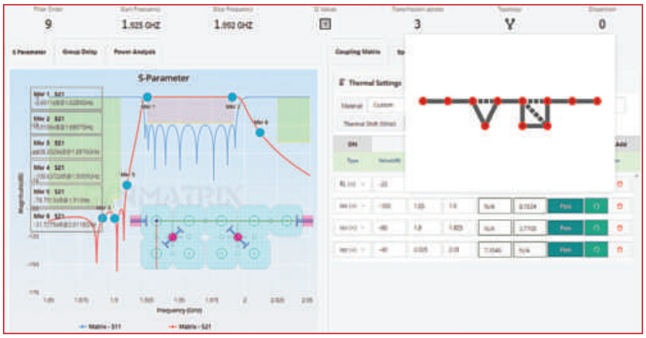

▲ Fig. 1 Advanced coupling matrix synthesis function with specification analysis.

▲ Fig. 2 Computer-aided tuning with error indicators.

With increasing requirements for 5G applications, the demand for RF filter design and production has never been greater. RF/microwave filter design engineering is an iterative and experienced-based process that can be very time consuming for even the most experienced filter design engineers. The product development process requires experience-based knowledge, continuous tweaking and repeated, iterative trials, followed by physically building samples to measure and verify the design's RF performance. For inexperienced designers or more complicated design requirements, additional build cycles are required before reaching an optimized design, extending the R&D cycle time and increasing engineering development costs.

SynMatrix is a cloud-based, intelligent, passive component design platform that can accelerate the RF/microwave filter design process by introducing an accurate and efficient step-by-step method to achieve RF performance goals. The design platform combines proprietary advanced algorithms


ANALOG DEVICES
AHEAD OF WHAT'S POSSIBLE™
PHASED ARRAY RADAR
ELECTRONIC WARFARE
MUNITIONS
Who better to integrate ADI parts **than ADI?**
Our integrated microwave assembly (IMA) solutions build on ADI's high performance semiconductor portfolio while enabling:
Reduced size, weight, and power
Complete system from signal to power
Alleviation of obsolescence issues
Integrate with confidence at analog.com/IMA

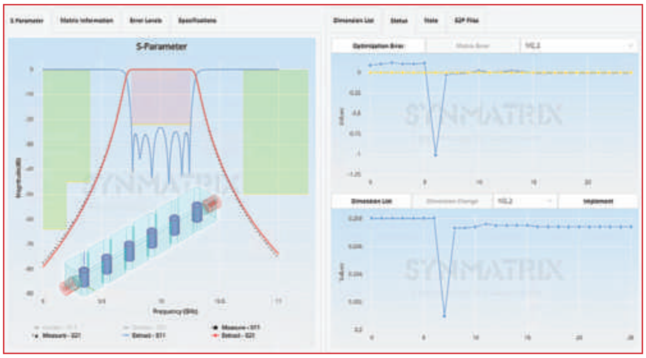

▲ Fig. 3 **HFSS users can use AI-based optimization to automatically tune filters.**

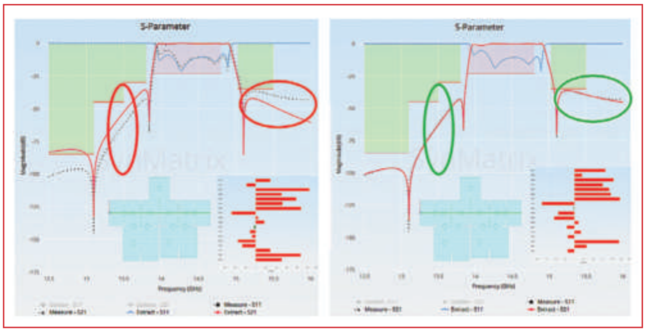

▲ Fig. 4 **The dispersive simulator handles complex structures such as ceramic and waveguide filters and multi-modes with high dispersive or close spurious effects.**

and machine learning technologies with decades of experience in RF/microwave component R&D. Users will dramatically improve the component design simulation and tuning process, armed with a comprehensive set of tools and automation features to help produce designs more accurately and more quickly. A complete line of design structures is available on the platform, including cavity filters, ceramic filters, waveguide, coaxial, LTCC and coplanar microstrip. The design platform was launched in 2019; the latest feature, an intelligent AI-tuning system, was added in February 2020.

The SynMatrix design platform addresses three main elements of the design process:

- Advanced coupling synthesis and comprehensive design analysis (see ***Figure 1***).
- Advanced computer-aided tuning (see ***Figure 2***).
- An AI-optimized tuning system that runs automatically.

The RF/microwave filter design process begins with the product requirements and specification analysis, which can be managed using SynMatrix's advanced matrix synthesis tool. The comprehensive synthesis module includes arbitrary topology synthesis, dispersive effect control, matrix sensitivity analysis, thermal drift margin analysis, peak power handling analysis and matrix optimization. Once the "golden matrix" is established, designers can use advanced algorithms in the computer-aided tuning module, which includes two-port and multi-port tuning techniques and generic optimization, to incorporate dispersive effects and spurious prediction. These features help eliminate repetitive processes to improve development speed and the design accuracy of the end product.

SynMatrix recently released an advanced intelligent AI-tuning feature enabling Ansys HFSS users to access one of the world's first AI-based optimization systems (see ***Figure 3***). SynMatrix directly integrates with HFSS and provides the following benefits:

An advanced intelligent tuning and space mapping design platform in one project workflow—Designers can import Ansys HFSS design parameters directly and automatically into SynMatrix. Once the data is imported, HFSS users can use the user-friendly platform to auto tune and edit the parameters to meet the desired RF design output.

An intelligent AI-tuning tool—The tool uses a machine learning, nonlinear curve-fitting technique, accompanied by an anti-error mechanism with fast convergence. The original and aggressive space mapping functions are also available.

Dispersive simulator—SynMatrix is one of few tools to offer dispersive simulation in the design process. It handles complex structures such as ceramic and waveguide filters and multi-modes with high dispersive or close spurious effects (see ***Figure 4***).

Cloud-based or desktop—Users have the flexibility and convenience of either secure, cloud-based or desktop deployment options.

Compared to other design platforms, few can match the technical array of features available on SynMatrix. Many of the advanced component design functions offered by SynMatrix—arbitrary topology synthesis, RF performance optimization, thermal shift analysis and Monte-Carlo analysis—are not included in many other synthesis tools in the market. SynMatrix's intelligent AI-based optimizer uses reinforcement learning backed by years of practical human experience. This differentiator feature enables filter designers to "auto tune" a design with a click of the mouse, then multi-task while the design is being optimized.

The SynMatrix design platform goes beyond basic filter design: with the Ansys HFSS integration, the combination offers an integrated and comprehensive workflow that can improve efficiency and flexibility to design advanced microwave filters. The platform offers tools to tweak and tune the outputs automatically, greatly reducing the engineering development time to produce designs. With the increasing demand for 5G systems, the corresponding demand for complex RF/microwave filters in these frequency bands will increase substantially. With a design platform like SynMatrix, users have a formidable tool to meet these growing demands.

SynMatrix
Richmond Hill, Ontario, Canada
www.synmatrixtech.com

MiCable

High Accuracy Butler Matrix for WiFi 6E Test

	Model	Frequency Range (GHz)	VSWR Max.(:1)	Insertion Loss* Max.(dB)	Amplitude Bal. Max.(dB)	Amplitude Flatness Max.(dB)	Phase Accuracy Max.(Deg)	Isolation Min.(dB)
4x4	SA-06-51	2.4~2.5	1.4	7.3	±0.5	±0.3	±4	14
		5.18~5.83	1.5	7.7	±0.6	±0.4	±5	13
		5.9~7.25	1.5	7.8	±0.7	±0.5	±6	13
8x8	SA-06-52	2.4~2.5	1.5	11.2	±0.6	±0.4	±8	13
		5.18~5.83	1.5	11.6	±0.8	±0.5	±10	12
		5.9~7.25	1.55	11.8	±0.9	±0.7	±12	12

* Theoretical IL. Included

More Information-
Scan the QR Code

affiliated with SSi Cable Corp.

Fuzhou MIcable Electronic Technology Co., Ltd,
Tel: +86-591-87382856 Email: sales@micable.cn Website: www.micable.cn

One-Port VNA Improves 5G Antenna and Device Measurements

The demand for antennas and other one-port devices for 5G systems requires testing in the sub-8 GHz and 28 to 39 GHz 5G bands. Anritsu's ShockLine MS46131A one-port vector network analyzer (VNA) is the only lightweight, portable solution that uses Extended-K™ ports and guarantees performance to 43.5 GHz. Extending the upper frequency to 43.5 GHz for return loss measurements provides better time domain resolution to ensure signal integrity and optimize material measurements.

Ideal for one-port RF/microwave measurements in engineering, manufacturing and education, the instrument uses Anritsu's patented nonlinear transmission line (NLTL) technology to simplify the VNA architecture, reduce size and enhance measurement accuracy and repeatability. Because of its small size, the one-port VNA can connect directly to the device being tested, which eliminates the need for a test cable, reduces test setup cost and improves the measurement stability and quality.

Two separate ShockLine MS46131A VNAs can be controlled from an external, user PC via USB interface. With no on-board memory, all measurement data is stored on the user's PC, making it easier to analyze and document the measurements, as well as securing the data outside of the instrument. As the entire ShockLine VNA family shares common software, the programs and graphical interface are compatible among all the instruments in the series.

The ShockLine MS46131A VNA is well suited for passive component, cable and antenna testing and troubleshooting, as well as for secure applications.

VENDORVIEW

Anritsu Company
Morgan Hill, Calif.
www.anritsu.com

Liquid Cooled, Hot-Swappable Solid-State PAs Replace Tubes

Empower RF Systems is introducing a technologically advanced, liquid cooled, scalable, solid-state power amplifier (PA) architecture. This solid-state design replaces tube technology, bringing new capabilities to applications needing tens to hundreds of kilowatts of CW and pulsed power. Empower RF's architecture combines four technology advancements.

First, fully digital peak and RMS detection, which provides waveform flexibility and accurate metering to enable asymmetrical and random pulse width and duty cycle operation on pulsed PAs. The short and long pulse capabilities of Empower RF's PAs are from 100 ns to greater than 500 µsec pulse widths with up to 500 kHz pulse repetition frequency and 20 percent duty cycle. Empower RF's CW PAs have the same pulse performance as pulsed amplifiers, with no limit on duty cycle, while the pulsed amplifiers are de-rated for CW operation.

The second advancement combines embedded firmware, software and real time processing and control, bringing multi-use flexibility to any application. Multimode operation, which is user selectable, can be dynamically configured.

Third, the PA design has no single point of RF failure. The layout consists of a system controller in a 3U drawer and up to 16 hot-swappable 2U PA drawers, with each amplifier drawer containing an integrated power supply—with no high voltage power supply in the transmitter. In case of a failure, the output power reduces by only a fractional amount, and the system remains transmitting. The 2U PA drawers are hot-swappable, so a PA can be replaced without turning off the entire rack.

The fourth design element is scalability, which creates an affordable upgrade path to higher power. Hardware is easily added to an existing system: for racks not fully populated, 2U amplifier drawers can be added without tuning, since each PA drawer and the full system rack is digitally controlled to set the phase and gain. For full racks, racks can be added and combined.

VENDORVIEW

Empower RF Systems
Inglewood, Calif.
www.empowerrf.com

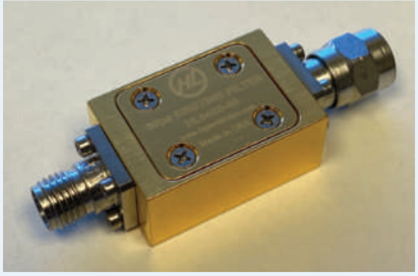

Lowpass Risetime Filters for Digital and Telecom Networks

HYPERLABS has developed a line of lowpass risetime filters for high speed digital networks and telecom systems. Based on a proprietary, absorptive filter design, the HL9450 series achieves very low reflections in- and out-of-band with flat group delay.

The filters have a frequency response like a fourth-order Bessel-Thomson filter. Unlike Bessel-Thomson filters, which filter through reflection, the HL9450 series filters by absorption. The absorptive design enables the filter to provide excellent impedance matching to 50 Ω, with outstanding return loss both within and above the filter passband. The initial HL9450 series comprises risetimes of 60 ps (5.83 GHz 3 dB bandwidth), 100 ps (3.50 GHz), 150 ps (2.33 GHz) and 200 ps (1.75 GHz). Maximum current through the filter is 0.6 A, and the standard housing size is 1.80 in. x 0.60 in. x 0.40 in.

The HL9450 series can be used for compliance testing or data-dependent jitter reduction, such as eye quality management, anti-aliasing filters in digitizing oscilloscopes or limiting the RF bandwidth in a system. In metrology grade test systems, the filters can help detect oscilloscope or sampler risetimes.

To address unique customer needs, HYPERLABS also offers quick-turn custom filters operating to 45 GHz. The design to manufacturing and assembly cycle can be completed within a few weeks for small quantities.

Founded in 1992 and privately owned, HYPERLABS develops ultra-broadband components, including baluns, power splitters and matched pickoff tees with the frequency range to 67 GHz or higher. HYPERLABS' instrumentation line includes the first USB-powered and controlled time domain reflectometry instrument, controlled impedance analyzers, signal path analyzers and samplers, including harmonic mixers.

HYPERLABS INC.
Beaverton, Ore.
www.hyperlabsinc.com

Digitizers for Mechanical Instrumentation

Spectrum Instrumentation has released 11 digitizer products for applications where a sensor converts a mechanical property such as vibration, acceleration, pressure or displacement to an electrical signal. The new digitizers capture and analyze electronic signals from DC to 2 MHz, with signal acquisition rates from 1 kSPS to 5 MSPS at 16-bit resolution. The 11 digitizers are available in two popular formats: PCIe card with two to eight channels or LXI-Ethernet instruments with four to 48 channels.

The four new models of the M2p.591x PCIe series are available with two, four or eight channels and mount directly inside a PC, making it a data acquisition system or data logger. Up to 16 cards can be connected to create larger systems, with as many as 128 fully synchronized channels.

The DN LXI products, part of Spectrum's digitizerNETBOX series, offer similar capabilities as the PCIe cards but connect to a PC or system network with an Ethernet cable. Two digitizerNETBOX sizes are available: the small DN2.591 products, with four, eight or 16 channels, and the larger DN6.591 units, with 24, 32, 40 or 48 channels. The compact DN2.591 digitizers can be deployed almost anywhere, even in mobile applications, with an optional 12/24 V power supply. The high channel density of the DN6.591 units is well suited for setups where multiple signals—coming from arrays of sensors, transducers or antennas, for example—need to be acquired and analyzed.

Spectrum Instrumentation
Grosshansdorf, Germany
www.spectrum-instrumentation.com/en/news

Editor's Note: As this issue goes to press, IMS2020 is scheduled to take place on June 21-26 in Los Angeles. The IMS coverage found in these pages is accurate as of the time of publication and should serve as a useful guide to event activities, even in the case of postponement. Be sure to keep this issue handy.

IMS2020 Conference and Exhibition Overview

IMS2020 Show Coverage
Catch our exclusive conference information, news, social networking, and more at: mwjournal.com/IMS2020

IMS2020 Welcome

Tim Lee, IMS2020 General Chair

Los Angeles and the IMS2020 steering committee are eager to welcome the microwave technical community to the 2020 International Microwave Week. This year's event will take place from Sunday, June 21 through Friday, June 26 and will provide an integrated program including the RFIC Symposium, the International Microwave Symposium (IMS), the 5G Summit and the ARFTG Microwave Measurements Conference. The technical program and industry exhibition will be held at the Los Angeles Convention Center (LACC), located at heart of downtown LA (see ***Figure 1***). The last time IMS was in downtown LA was in 1981.

Fig. 1 Los Angeles Convention Center.

Downtown LA (DTLA) began its renaissance with the opening of the Staples Center in 1999 and has experienced unprecedented growth in attracting business, residents retail and hospitality services. Notable landmarks include the Kodak Theatre (2001), Walt Disney Concert Hall (2003), LA LIVE (2008), the Grammy Museum (2008). This is not your grandfathers' LA (see ***Figure 2***)!

Greater Los Angeles has had a long history in the development of the aerospace industry—that covers the beginning of the aircraft industry, space exploration and microwave engineering. By the end of World War II, 60 to 70 percent of the American aerospace industry was located in Southern California. Major aviation companies included Lockheed, Northrop, Douglas, Rockwell and Hughes Aircraft. Today, in the 21st century, industry leaders like Northrop Grumman, Boeing, Rockwell and Lockheed Martin have joined research labs like HRL Laboratories and Teledyne Scientific and new companies like SpaceX.

In nearby El Segundo, there is the U.S. Los Angeles Air Force Base which is the home for the Space and Missile Systems Center that includes the Global Positioning System,

satellite communications and satellite control networks. We also have the Jet Propulsion Laboratory (JPL) in Pasadena which is the hub of deep space exploration and Earth science missions. Key universities in the region with aerospace and microwave engineering research efforts include UCLA, CalTech, UCSD, UCI and USC. The steering committee, which includes volunteers from most of these organizations, are proud to be your hosts for IMS2020 to provide the best experience for the technical, academic and industry attendees.

NEW THIS YEAR

The 2020 edition of IMS week continues the MTT-S tradition to continue with best practices while adding new features that include:

- Increased coverage of development of technologies for microwave systems like 5G, autonomous vehicles and smart installations for Industry 4.0 and healthcare.
- Reduced pricing for comprehensive Student Superpass that allows admittance to all RFIC, IMS, all workshops, 5G Summit, one technical lecture and ARFTG events.
- Addressing how microwave and wireless technologies can address the broadband digital divide in rural and underserved areas of the world.

INTERNATIONAL MICROWAVE WEEK

The overall format of International Microwave Week remains the same as last year. The RFIC Symposium begins on Sunday with workshops and concludes Tuesday morning. The Three Minute Thesis (3MT®) Competition will be held on Sunday. IMS opens on Monday with a Plenary Session and Welcome Reception. The 5G Summit, again cosponsored by the IEEE Microwave Theory and Techniques Society and the IEEE Communications Society, picks up on Tuesday afternoon and concludes Tuesday evening with a panel session. IMS2020 will run from Sunday through Friday, with the Industry Exhibition open from Tuesday through Thursday. The ARFTG Microwave Measurements Conference will also begin on Friday. In all, we expect more than 9,000 attendees from around the world participating in the technical sessions, workshops and industry exhibition. More than 800 exhibitor booths will showcase the latest developments in microwave hardware, software, components and systems.

Workshops will be held on Sunday, Monday and Friday. Short courses have been replaced by focused technical lectures given by invited subject matter experts on topics that will be of great interest to the technical community. The Opening Plenary Session will be held Monday evening and will feature keynote addresses by Mark Dankberg, chairman of the board and chief executive officer of Viasat Inc. and Doreen Bogdan-Martin, director of telecommunication development at the International Telecommunication Union. The Welcome Reception will immediately follow the Plenary Session in the Petree Plaza area of the LACC. IMS2020 technical sessions will run from Tuesday through Thursday. The Closing Session on Thursday afternoon will feature a keynote address by Hartmut Neven, engineering director of Quantum Artificial Intelligence Lab at Google.

The MTT-S IMS Industry Exhibition is a core foundation of the IMS Week and will take place from Tuesday through Thursday. The industry-hosted reception will be held late afternoon on Wednesday. The exhibition floor will be well organized to provide ready access for attendees to find and engage with exhibitors to learn about new products and services. The MicroApps Theater, the Societies Pavilion and Startup Pavilion will offer the opportunity for learning and engagement with different organizations and sectors. The IMS2020 schedule will include exhibition-only time on Wednesday afternoon to bring focus on the latest products from the microwave industry.

SOCIAL AND NETWORKING OPPORTUNITIES

IMS2020 offers many opportunities for social and networking at the coffee breaks, and evening events for you to catch up with old colleagues or make new ones. The 2020 RFIC and IMS plenary sessions and welcome receptions on Sunday and Monday, respectively, enable informal meet and great opportunities (see ***Figure 3***). Tuesday night there will be the Young Professional social and amateur radio social. On Wednesday evening, the Women in

Fig. 2 Hollywood Boulevard at dusk.

Fig. 3 IMS2019 reception at the Lawn on D in Boston.

Microwaves reception will be held. Within short walking distance of the LACC and IMS2020 hotels are many restaurants and nightspots for informal and private gatherings.

ENJOYING LOS ANGELES

LA is home to renowned museums, unique hotels, diverse experiences, vibrant multicultural neighborhoods and miles of sunny coastlines. Close by to our venue include the Space Shuttle Endeavor, the CA Science Center, Walt Disney Concert Hall, the Getty Center and many art galleries. LA is the entertainment capital of the world. Attractions include Warner Bros Studio Tour and Universal Studio Hollywood. You can hike near the Hollywood sign, discover fossils at the La Brea Tar Pits and find your favorite movie star on the Hollywood Walk of Fame (see Figure 2). The Pacific Ocean is a short drive or ride from downtown using light rail to arrive at Santa Monica or Venice Beach. You can of course shop until you drop—whether on Rodeo Drive, the Arts District, The Grove, Melrose Avenue or Hollywood and Highland. The average temperature in June will be between 16°C to 25°C (or 63°F to 77°F).

Don't forget to visit ims-ieee.org for the most up to date information and to download the IMS Microwave Week Mobile App! We look forward to welcoming everyone in Los Angeles for IMS2020!

2020 RFIC Symposium at IMS2020

Waleed Khalil, RFIC 2020 General Chair, Brian Floyd, RFIC 2020 Technical Program Chair and Osama Shana'a, RFIC 2020 Technical Program Co-Chair

The 2020 IEEE Radio Frequency Integrated Circuits Symposium (RFIC 2020) will be held in Los Angeles, Calif. on June 21-23. Attendees will have the opportunity to interact with world experts, expand their network and leave invigorated with new ideas and a drive to innovate.

The steering committee has implemented important changes for RFIC 2020. In addition to the Emerging Circuit Technology area introduced in RFIC 2019, the symposium is expanding its scope to System Applications and Interactive Demonstrations. This includes papers and presentations on systems and applications in 5G, radar, imaging, terahertz, biomedical, security, IoT and optoelectronic areas. A new Systems and Applications Demonstration Session is being organized to highlight these system papers and provide more engagement opportunities for the audience. Additionally, we continue to expand our focus to include RF and wireless circuits in emerging circuit technology areas.

The RFIC Symposium, in partnership with IMS, offers numerous opportunities for students to enhance career growth, networking and educational experiences. First, the student registration has been streamlined to allow all students to purchase the Student Superpass. This will allow all students to experience every activity within Microwave Week, including a workshop, all three conferences (RFIC, IMS and ARFTG), the 5G forum, a technical lecture and much more, all at a deeply discounted price for IEEE members. Second, RFIC will once again conduct a student paper contest to select the top student papers from the symposium. These top papers will be featured in our Sunday Symposium Showcase. Third, all RFIC students will have the opportunity to apply for and participate in the Three-Minute Thesis (3MT®) program. Fourth, as part of IMS, students can participate in design competitions, the build-a-radar-in-a-day workshop and RF Bootcamp. Finally, MTT-S offers the Ph.D. Student Sponsorship Initiative for new students to become engaged with IMS, providing learning, networking and volunteer experiences along with complimentary registration and accommodations to qualified and selected students.

The 2020 RFIC Symposium will begin on Sunday, June 21, with twelve RFIC focused workshops (seven full-day and five half-day) and one technical lecture. In addition, there will be several joint RFIC/IMS workshops on Sunday and Monday. These workshops cover a wide range of advanced topics in RFIC technology and integrated circuit design, including power amplifiers, 5G systems, coherent optical links, terabit/s networks, quantum computing, imaging radars and much more.

The 2020 RFIC "Technical Lecture" is a 90 minute interactive short course delivered by a distinguished speaker during lunchtime on Sunday, between the morning and afternoon workshop sessions. For 2020, Prof. Peter Kinget from Columbia University, New York, will teach "Taxonomy of RF Receivers: from Basics to Latest Developments." Don't forget to register in advance since we expect a very high attendance and seats will be limited!

Following the full day of Sunday workshops, the RFIC Plenary Session will be held in the evening beginning with conference highlights, the presentation of the Student Paper Awards and the Industry Best Paper Award. The 2020 RFIC Plenary Session will conclude with two visionary plenary talks. Dr. Thomas Cho, executive vice president of Infrastructure & Design Technology Center, System LSI Business, at Samsung Electronics, will share his vision for the future of RFIC in his talk "Is the Third Wave Coming in CMOS RF?," providing a historical perspective and analyzing in-depth the diverse challenges and opportunities looking ahead in RF integrated circuits and systems technology. Bren Professor of Electrical Engineering and Medical Engineering at Caltech, Prof. Ali Hajimiri, will deliver his vision on integrating RFIC with flexible electronics in his talk "The Flexible Future of RF," giving a perspective on a breadth of new applications ranging from wearable RF fabric to instantly deployable communication networks to wireless power transfer systems, to enable a truly wireless ecosystem of the future.

Immediately after the plenary session, the RFIC Reception and Symposium Showcase will follow, with highlights from our industry showcase and student paper fi-

nalists in an engaging social and technical evening event supported by the RFIC Symposium corporate sponsors. You will not want to miss the 2020 RFIC reception!

On Monday and Tuesday, RFIC will have multiple tracks of oral technical paper sessions. Once again, RFIC will schedule special 5G-focused technical sessions on Tuesday morning, which, together with the 5G Summit on Tuesday afternoon and IMS's 5G sessions on Wednesday, will provide attendees with both in-depth and broad perspectives into the latest breakthroughs in 5G circuits and systems. On both Monday and Tuesday, there will be two fascinating lunchtime panels. The Monday panel session titled "HW Startups—No Longer an Oxymoron" will discuss the future of hardware startups with experts from both industry and academia. The panelists will further provide insight on trends for RF hardware and in which field there is still room for the development of hardware startups, especially considering the surge of software and artificial intelligence startups. The Tuesday panel session titled "Automotive Radars and AI: Is My Car Really Safe?" will be held jointly with IMS. Outstanding panelists from academia and both autonomous driving and RF industries will discuss the limitations of existing autonomous driving systems from a wireless technology perspective. They will also provide different views on the way forward and the outlook for the future of assisted cars.

On behalf of the RFIC Steering and Executive Committees, we welcome you to join us at the 2020 RFIC Symposium in Los Angeles, California. Please visit the RFIC 2020 website (http://rfic-ieee.org/) for more details and updates.

ARFTG at IMS2020

Jon Martens and Peter Aaen, ARFTG

ARFTG, the microwave measurements conference, once again caps an exciting and instructive Microwave Week. ARFTG also participates in several co-sponsored and related events during the week to further expand measurements coverage in the community.

With a slightly more relaxed schedule, ARFTG gives an attendee more opportunities to interact one-on-one with colleagues, experts and vendors from the RF and microwave test and measurement community. Whether your interests include high-throughput production or one-of-a-kind metrology, complex systems or simple circuit modeling, small-signal S-parameter or large-signal nonlinear measurements, simpler passive measurements or complex integrated converter analysis, DC or near-optical frequencies, you will find colleagues interested in similar areas and there is probably an expert attending the ARFTG conference.

Fig. 4 An ARFTG conference technical session (Photo courtesy of Lyle Photos).

There is always ample opportunity during extended breaks at every ARFTG conference for detailed technical discussions with others facing similar test and measurement challenges. On Friday, June 26, ARFTG also hosts a separate, vendor exhibit focused on the measurement industry in a more congenial setting. Given the informal and friendly atmosphere, ARFTG attendees often find these interactions are their best source of ideas and information for their projects. Often, someone at ARFTG has already worked through and solved the same problem you are having.

Among the other ARFTG-related events during the week, ARFTG is co-sponsoring two workshops with IMS2020. Workshop WMF, entitled "Calibrated Testbeds for the Characterization, Optimization and Linearization of Multi-Input Power Amplifiers," and workshop WMC, "Platforms, Trials and Applications—The Next Step for 5G and Future Wireless Networks," are scheduled for Monday, June 22 and cover interesting topics in the overlapping areas of communication, subsystem design and measurement. On Wednesday afternoon during the IMS2020 conference, there is also a joint IMS/ARFTG technical session We3C: Advanced Nonlinear Measurement Techniques and Results that covers additional important results. See the full IMS technical program for more details.

Additionally, ARFTG hosts several users' forums that are open to all. For IMS2020, there will be a nonlinear VNA users' forum that discusses the latest techniques and theories for nonlinear measurements and an on-wafer users' forum that deals with issues related to high-frequency on-wafer measurement techniques, calibrations and theory. Both events will be held on the afternoon of Thursday, June 25.

Finally, there is the main one-day ARFTG conference (see ***Figure 4***), where four oral technical sessions take place in a single-track format on Friday, June 26. The theme of the conference is Microwave and mmWave Measurements for the Connected World, and papers on topics related to integrated system and diverse communications system measurements will be presented along with papers in other areas such as nonlinear studies, calibration and de-embedding, on-wafer analysis and mmWave/THz characterization. The conference will open with a keynote talk "Electro-Optic Mapping Techniques for Characterization of Microwave Circuits, Devices and Antenna Systems," presented by Kaz

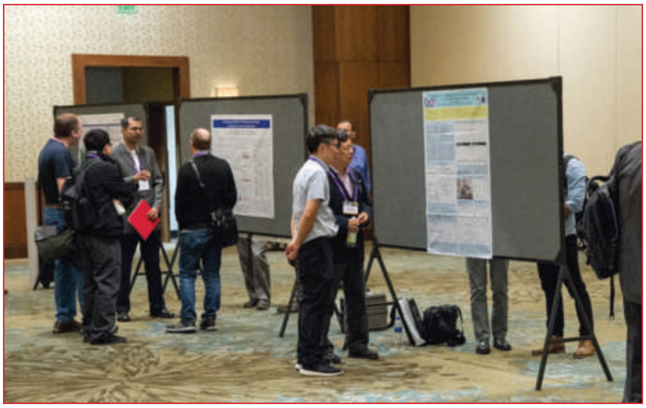

Fig. 5 A combined vendor exhibit and interactive forum session allows for discussions on many relevant measurement topics (Photo courtesy of Lyle Photos).

Sabet of EMAG Technologies Inc. An invited talk entitled "How Did We Get Here? A Short History of VNA Technology" and given by Andrea Ferrero of Keysight Technologies will also be part of the sessions.

There are extended breaks that combine exhibits and an interactive forum to aid networking with vendors and among colleagues (see ***Figure 5***). Integrated within the technical program is a student paper competition to recognize outstanding work in the measurement's arena. This year, ARFTG is a part of the Three Minute Thesis (3MT®) competition along with IMS and RFIC. 3MT® finalists are selected from eligible students and young professionals following acceptance of their papers and subsequent video submissions.

ARFTG has several other programs that occur throughout the year. In addition to the ARFTG conference at IMS, there is a second symposium that takes place in the winter, usually in January and currently co-located with Radio and Wireless Week (RWW). This symposium includes workshops, users' forums, a day-and-a-half conference and a day-and-a-half short course that welcomes experts in the field to teach basic to advanced topics.

ARFTG also has student sponsorship and fellowship programs. The sponsorship program gives financial aid to students presenting at an ARFTG conference, and the fellowship program will give financial aid to support the research of the fellowship competition winner. For more information about these programs, see the ARFTG website at www.arftg.org.

If you are interested in measurements from 1 kHz to 1 THz and beyond, be sure to add the 2020 ARFTG conference to your plans in Los Angeles in June. You will find our atmosphere informal and friendly, which enhances interactions and provides opportunities for you to learn new ideas and discuss your own ideas with colleagues.

5G Summit at IMS2020

The technologies and systems for 5G are now moving to commercial deployment with focus on Stand Alone (SA) networks, mass market for 5G devices and global adoption of mmWave in premium devices and for small cell enhancement and fixed wireless access (FWA). Looking forward, technology research and development needs to focus on MIMO enhancement, V2X and IoT evolution, integration of 5G with Non-Terrestrial Network and new FR3 and FR4 spectrum development. To bring all this into focus, the IEEE Microwave Theory and Techniques Society (MTT-S) is organizing a 5G Summit at IMS2020, with speakers at the leadership level from different companies and industries to discuss 5G related topics, including foundries, standards, mobile networks, MIMO and mmWave systems, RFIC and RFFE.

As part of the IEEE Comsoc 5G Summit series (visit www.5GSummit.org for more details), this summit will

Fig. 6 IMS2019 exhibition hall.

Fig. 7 David Vye, Julie Teinert and Sherry Hess in front of the MicroApps 2019 theater.

provide a platform for leaders, innovators and researchers from both industrial and academic communities to collaborate and exchange ideas regarding 5G and beyond 5G technologies.

Speakers List:

- Dr. Bami Bastani, senior vice president of RF Business Unit at GLOBALFOUNDRIES, "Differentiated End to End Silicon Solutions for the New 5G Reality"
- Dr. Lawrence Loh, corporate senior vice president and CSO at MediaTek, "5G—Evolution or Revolution"
- Dr. Chih-Lin I, China Mobile chief scientist of wireless technology at China Mobile
- Mr. Joel King, senior vice president and general manager at Skyworks, "RF Front-End Evolution from 4G to 5G"
- Dr. Naveen Yanduru, vice president and general manager at Renesas Electronics, "Sub-6GHz and mmWave RFICs for 5G Wireless Infrastructure RF Front Ends"
- Dr. Curtis Ling, co-founder and chief technology officer at MaxLinear, "A Fabless Perspective on 5G Phased Arrays, From Devices to Network Capacity"
- Dr. Shahriar Shahramian, director of Bell Labs, "The 5G Quest: System, Deployment & Application Challenges"
- Dr. Ir. Michael Peeters, program director connectivity at IMEC, "FR 1, 2 ,3, 4 PA and FEM Technology Approaches for 5G and Beyond"

The 5G Summit is open to all IMS and RFIC attendees for a nominal cost, and attendees will be able to register for the 5G Summit using the IMS2020 registration site. The summit will be complemented by a reception for all registered attendees, followed by a rump session to drive a live discussion between the speakers and the audience on the summit presented topics. IMS2020 will be an incredible week that focuses on 5G connectivity and brings together the best engineering minds from systems to hardware.

RF Boot Camp at IMS2020

An introduction to RF basics will be held on Monday, June 22 from 8:00 a.m. to 4:45 p.m. This one day course is ideal for newcomers to the microwave world, such as technicians, new engineers, college students, engineers changing their

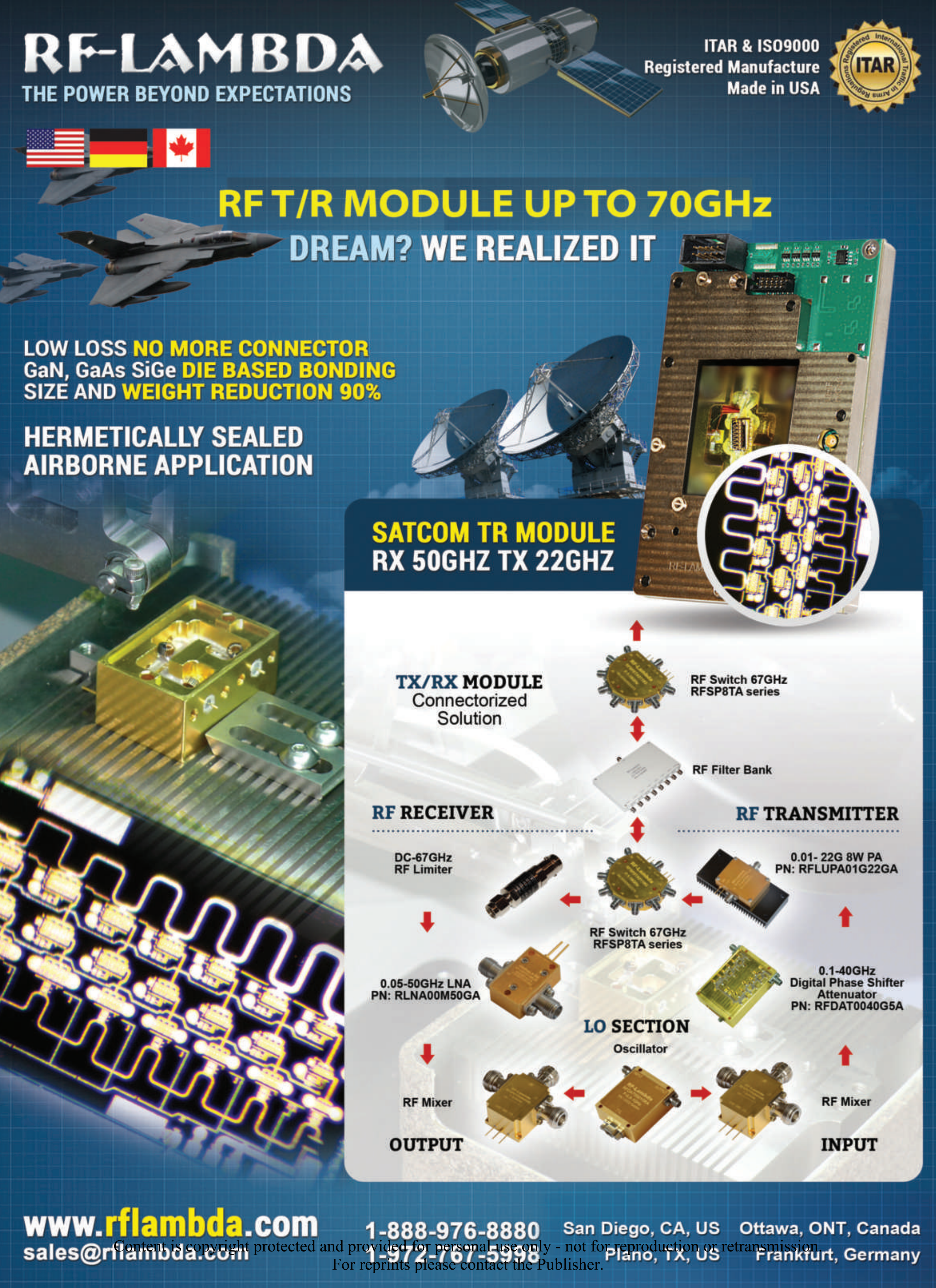
RF-LAMBDA
THE POWER BEYOND EXPECTATIONS
ITAR & ISO9000
Registered Manufacture
Made in USA
ITAR
Registered International Traffic in Arms Regulations
RF T/R MODULE UP TO 70GHz
DREAM? WE REALIZED IT
LOW LOSS NO MORE CONNECTOR
GaN, GaAs SiGe DIE BASED BONDING
SIZE AND WEIGHT REDUCTION 90%
HERMETICALLY SEALED
AIRBORNE APPLICATION
SATCOM TR MODULE
RX 50GHZ TX 22GHZ
TX/RX MODULE
Connectorized
Solution
RF Switch 67GHz
RFSP8TA series
RF Filter Bank
RF RECEIVER
RF TRANSMITTER
DC-67GHz
RF Limiter
0.01- 22G 8W PA
PN: RFLUPA01G22GA
RF Switch 67GHz
RFSP8TA series
0.05-50GHz LNA
PN: RLNA00M50GA
0.1-40GHz
Digital Phase Shifter
Attenuator
PN: RFDAT0040G5A
LO SECTION
Oscillator
RF Mixer
RF Mixer
OUTPUT
INPUT
www.rflambda.com
sales@rflambda.com
1-888-976-8880
1-972-767-5998
San Diego, CA, US
Plano, TX, US
Ottawa, ONT, Canada
Frankfurt, Germany

career path, as well as marketing and sales professionals looking to become more comfortable in customer interactions involving RF and microwave circuit and system concepts and terminology.

The format of the RF Boot Camp is similar to that of a workshop or short course, with multiple presenters from industry and academia presenting on a variety of topics including:

- The RF/Microwave Signal Chain
- Network Characteristics, Analysis and Measurement
- Fundamentals of RF Simulation
- Impedance Matching Basics
- Spectral Analysis and Receiver Technology
- Signal Generation
- Modulation and Vector Signal Analysis
- Microwave Antenna Basics
- RFMW Application Focus

This full-day course will cover real-world, practical, modern design and engineering fundamentals needed by technicians, new engineers, engineers wanting a refresh, college students, as well marketing and sales professionals. Experts within industry and academia will share their knowledge of RF/microwave systems basics, simulation and network design, network and spectrum analysis, microwave antenna and radar basics. Attendees completing the course will earn 2 CEUs.

Given the limited space available for this session, you are encouraged to register early to ensure that a seat is available. These sessions are designed to be interactive, so come prepared to engage the presenters and your other colleagues in the audience with questions and discussions to gain the greatest value from these sessions.

IMS2020 Exhibition

The annual IMS Exhibition is held in conjunction with the IMS, RFIC and ARFTG technical symposia and offers an excellent opportunity for all segments of the microwave community to meet. It is the synergy of the Exhibition in conjunction with the technical symposia that makes Microwave Week the premier international gathering for everyone involved in technologies associated with RF, microwave, millimeter-wave and THz frequencies.

The Exhibition consists of over 600 exhibiting companies who represent the state of the art when it comes to materials, devices, components, and subsystems, as well as design and simulation software and test and measurement equipment (see ***Figure 6***). Whatever you are looking to acquire, you will find the industry leaders ready and willing to answer your purchasing and technical questions.

The Exhibition also includes MicroApps and Industry Workshops presented by IMS exhibitors addressing state-of-the-art products, processes and applications of interest to the microwave community (see ***Figure 7***). *Microwave Journal* will be hosting a special panel session on Tuesday at noon in the MicroApps theater addressing "What is the Best Semiconductor Technology for 5G mmWave Applications?" The panel will discuss and debate RF SOI versus CMOS versus GaAs versus GaN for semiconductor device materials and the tradeoffs for levels of integration, cost, efficiency and thermal considerations associated with various architectures.

Microwave Journal will also be hosting the LinkedIn photo booth at this year's IMS2020. Please stop by for a complimentary professional photo for your bio, resume and professional social media profile. Come to the booth at any time to take advantage of this complimentary service. On Wednesday afternoon during the reception, come meet the editors of *Microwave Journal* for free refreshments at the LinkedIn photo booth. Ask the editors questions about publishing contributed articles and their experiences in the industry.

Exhibition Dates and Hours:
Tuesday, June 23, 9:30 a.m. to 5:00 p.m.; Wednesday, June 24, 9:30 a.m. to 6:00 p.m. (Industry Hosted Reception 5:00 to 6:00 p.m.); and Thursday, June 25, 9:30 a.m. to 3:00 p.m.■

Agile Microwave Technology Inc.
Broadband 15 W Power Amplifier

AgileMwT's broadband 15 W power amplifier operating from 2 to 18 GHz is offered in a compact module configuration. AMT-A0350 provides Psat of 15 W typical with flat small signal gain of 43 dB typical, ±1 dB typical gain flatness with VSWR of 1.8:1 typical. This family of power amplifiers are competitively priced and ship from stock or have short lead times. AgileMwT offers great value with innovative designs.

www.agilemwt.com

Altum RF
GaN Distributed Amplifier

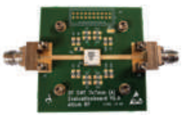

Altum RF's ARF1307C7 is a packaged, GaN distributed amplifier for 2 to 20 GHz applications. The amplifier provides 10 W saturated output power and 17 dB small-signal gain, with 11 dB of power gain and 20 percent power-added efficiency. The ARF1307C7 features a robust, RoHS-compliant, 7 x 7 mm QFN high-performance ceramic package, with excellent thermal and electrical properties. The ARF1307C7 is suitable for higher performance commercial- and defense-related applications, such as test and measurement equipment, EW and commercial or defense radar systems.

www.altumrf.com

American Microwave Corp.
Absorptive/Non-Reflective S25T Switch

VENDORVIEW

American Microwave Corp. announced its latest preliminary product development. AMC Model Number MSN-0518-25T-30DB-HERM-1JV is an absorptive/non-reflective S25T switch that is hermetically sealed with an integral 30 dB coupler on its common port. It works from 0.5 to 18 GHz. Insertion loss of 7.5 dB max and has an isolation of 60 dB min. Switching speed of <2 μSec and a switching transient of <200 mV pk-pk. OIP2 is >+65 dBm and OIP3 >+35 dBm. Output 1 dB compression point of +20 dBm.

www.americanmic.com

Analog Devices
MxFE AD9081/2

VENDORVIEW

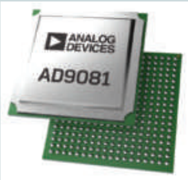

ADI's new AD9081/2 MxFE platform allows manufacturers to quickly prototype and develop massive all digital and hybrid beamforming systems. With a 2.4 GHz channel bandwidth, the new MxFE platform also enables lower SWaP+C multi-antenna phased array radar systems and low-earth-orbit satellite networks. By shifting more of the frequency translation and filtering from the analog to the digital domain, the AD9081/2 provides designers with the software configurability to meet different requirements and achieve quicker time to market.

Navassa ADRV9002

ADRV9002 is first in a new family of integrated RF transceivers (RF to digital) and features two independent transmit paths, two independent receive paths and two independent RF synthesizers on chip. The ADRV9002 operates from 30 MHz to 6 GHz, designed to provide highest dynamic range (150 dB/Hz) and best in class blocker tolerance for narrow and wideband signals from 12 Khz to 40 MHz. The ADRV9002 is a highly versatile transceiver that enables a user to determine performance vs. power consumption and provides many system power saving modes.

ADQUADMXFE1EBZ

Analog Devices has developed a multi-channel RF development platform based on the AD9081 high speed converter. The development platform integrates data converters, RF distribution, power regulation and clocking to provide a 16 channel, direct S-band sampling solution. The AD9081 or mixed signal front end (MxFE) is at the heart of this system-based solution and includes four ADCs, four DACs, and digital up/down converters. The DACs are rated to a sample rate of 12 GSPS and the ADCs are rated to 4 GSPS. Analog bandwidths provide direct sampling and waveform generation through S-band and into low C-band. The board solution contains four of these MxFEs.

www.analog.com

AnaPico Ltd.
Ultra-Agile Vector Signal Generator

The APVSG is an ultra-fast-switching vector-modulated signal source, covering a continuous frequency range from 0.01 to 40 GHz. The standard APVSG enables outstanding ultra-fast CW frequency sweeping, chirping, intra-pulse modulation, pulse shaping, all with very low phase noise. A high performance internal I/Q modulator enables customized modulation waveforms and supports dedicated modulation schemes, including avionics modulation. Now also available as multi-channel version APVSG-X with one to four channels.

www.anapico.com

Anokiwave
Intelligent Array IC Solutions

VENDORVIEW

Anokiwave leads the mmWave market with its Silicon ICs for 5G, SATCOM, and RADAR applications shipping in high volume commercial deployments. Their portfolio of IC options enables intelligent, scalable antenna arrays that can be configured for different use cases, power levels and frequency bands. Anokiwave is the trusted choice of Tier-1 and -2 OEMS worldwide. Visit Anokiwave at booth 1439.

www.anokiwave.com

Anritsu
220 GHz Broadband VNA

VENDORVIEW

The VectorStar™ ME7838G 70 kHz to 220 GHz broadband VNA provides industry-best, single-sweep coverage addressing the need for on-wafer device characterization. The compact, high-performance mmWave module enables direct connection to the probe for accurate, stable results. The ShockLine™ MS46131A 1-port VNA provides unprecedented coverage to 43.5 GHz. Leveraging NLTL technology enhances accuracy and measurement repeatability. Its small size allows direct connection to the DUT, improving measurement stability and simplifying test configurations. Visit Anritsu at booth 1847.

www.anritsu.com

B&Z Technologies Inc.
Low Noise Microwave Amplifier

B&Z Technologies, a state-of-the-art low noise microwave amplifier company based in New York, now offers 18 to 40 GHz amplifiers with less than 2.5 dB noise figure. Standard configuration has typical gain of 34 dB, output 1 dB compression power of +10 dBm, gain flatness of ±2 dB and input/output VSWR of 2.0:1. These can be custom configured for higher gain, higher power or better flatness (up to ±1.5 dB). Its standard co-axial housing can be disassembled also, if needed, to be used as a drop in amplifier.

www.bnztech.com

Cadence Design Systems
Cadence RF/Microwave Solutions
VENDORVIEW

Cadence enables Intelligent System Design™ for 5G with a comprehensive portfolio spanning IP, verification, implementation and mixed-signal/analog/RF. The Virtuoso® RF Solution streamlines the RF design flow with a "golden" schematic that drives layout implementation, simulation, and physical verification. The recent integrations of AWR Corp. and Integrand Software further increase productivity for complex, high-frequency RFIC and application development. Combined with the organically grown Virtuoso, Clarity™, and Sigrity™ solutions, Cadence offers a complete electromagnetic signoff solution.

www.cadence.com

AWR® V15 Software

Cadence announced the latest release of the AWR®Design Environment® platform, V15. This version offers new and expanded capabilities to support power amplifier and antenna/array design, EM modeling and RF/microwave IP integration within heterogeneous systems, enabling designers to better address the design challenges of MMIC/RFIC, package/module, and PCB technologies driven by 5G, automotive, and aerospace and defense application. Discover the power of Cadence with AWR software at IMS2020 at booth 829.

www.awr.com

Cernex
Frequency Multipliers
VENDORVIEW

Cernexwave's CFM series active frequency multipliers cover the frequency range of 10 MHz to 500 GHz. They can be designed to multiply an RF signal 2, 3, 4 or as many as 36 times with its custom multiplier chain assemblies. These multipliers utilize state of the art MIC and MMIC technologies to provide highly stable, reliable and efficient frequency extenders for system applications.

www.cernexwave.com

Charter Engineering Inc.
5G RF Switches from DC–40 GHz

CEI introduces a new series of RF switches operating from DC-40 GHz utilizing 2.92 mm female connectors. The switches feature outstanding characteristics in insertion loss of 0.6 dB max and return loss of 1.50:1 max. The highly repeatable RF switches are targeted to 5G applications and are available in a variety of configurations including failsafe, latching and normally open.

www.ceiswitches.com

Ciao Wireless Inc.
Ultra-Broadband Amplifiers

Ciao Wireless Inc. has introduced its latest product line of ultra-broadband amplifiers covering 2 to 40 GHz, and features an

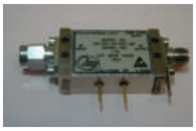

integrated wideband output detector option for communication applications. The series of amps have usable bandwidth over 1 to 40 GHz in most cases. Units are qualified for use in most Hi-Rel and harsh commercial applications.

www.ciaowireless.com

Cicor
Innovative Technology Solutions

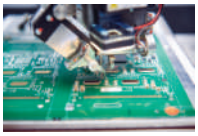

The Cicor Group is a globally active development and manufacturing partner with innovative technology solutions for the electronics industry. With about 2,000 employees at ten production sites, Cicor offers highly complex printed circuit boards, printed electronics, hybrid circuits and substrates as well as comprehensive electronic manufacturing services including microelectronic assembly and plastic injection molding. Cicor supplies customized products and services from design to the finished product from one source.

www.cicor.com

Coilcraft
Ceramic Chip Inductors

Coilcraft 0402CT Series ceramic chip inductors feature a maximum height of just 0.45 mm—a 30 percent lower profile than competitive products. Offered in 23 inductance values from 1.2 to 56 nH (with, 5 percent, 3 percent or 2 percent tolerance), the 0402CT provides excellent Q Factor performance—up to 84 at 2.4 GHz. It also offers self-resonant frequencies as high as 27.5 GHz and current ratings up to 2.3 Amps (Irms).

www.coilcraft.com

Copper Mountain Technologies
SC Series Compact VNAs

The SC Series Compact VNAs deliver lab-grade performance up to 9 GHz with 16 ms measurement speed, 140 dB dynamic range and higher output power. This series combines advanced performance with all the features engineers have come to expect. This innovative approach delivers high measurement accuracy and enables users to take advantage of faster processors, newer computers, and larger displays. Copper Mountain VNAs include excellent customer service, automation support and years of engineering expertise to users.

www.coppermountaintech.com

Crane Aerospace & Electronics
RF Converter Miniaturization Using Multi-Mix®

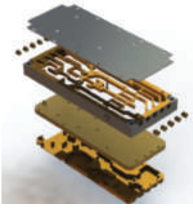

Wideband RF converter assembly in package less than 5"× 2"× 0.5". Offers 5x to 10× reduction over traditional converters—multi-layer multi-mix motherboard with double-sided SMT populated in a lightweight housing frame that provides excellent RF channelization and isolation, four integrated coherent wideband synthesizers, embedded pre-select frequency filters, fast tuning and settling times and low phase noise.

www.craneae.com

CTT Inc.
40 W Multi-Band GaN Power Amplifier

Designed for multi-function, radar, SATCOM and EW system design operating from C-through Ku-bands, this new SSPA offers SWaP solutions for many applications including EW jammers and multi-band mobile SATCOM terminals. CTT's new model AGX/180-4656 covers 3 to 18 GHz with 40 W of CW power output. The compact size of 5.16 in. (L) × 4.90 in. (W) × 0.28 in. (H) offers RF/microwave designers an excellent choice for SWaP solutions in many applications, including EW jammers, and for transmit power in multi-band mobile SATCOM terminals. Visit CTT during IMS2020 at booth 1952.

www.cttinc.com

Custom Microwave Components Inc.
A Non-Blocking Switch Matrix

A non-blocking switch matrix with 72 inputs and 32 outputs is used to configure RF environments for carrier end-to-end backhaul and hand-over testing. Intuitive browser graphical user interface, easy to network and use API to support automated testing. Features include solid-state reliability and repeatability, modular line-replaceable active units with built-in spares, distributed hot-swappable redundant supplies, system health monitoring and reporting, ultra-low operating power (<85 W), ultra-quiet operation with a frequency of 0.7 to 3.0 GHz (optional 0.7 to 6.0 GHz), and insertion loss of 30 dB max. Visit Customave at IMS2020 booth 1304.

www.customwave.com

dB Control
High-Power Amplifiers

dB Control offers six mmWave high-power amplifiers, including the dB-3201H microwave power module. This wideband MPM features a 30 to 38 GHz frequency range and 125 W of continuous wave power. It is designed for electronic countermeasures and electronic warfare applications so military personnel can experience faster exchanges of data and enhanced situational awareness. The dB-3201H enables additional channels of communication to combat congestion across traditional C-, X- and Ku- and lower Ka-band frequencies. Visit during IMS2020 at booth 801.

www.dBControl.com

Delta Electronics Mfg. Corp.
SMPM-T Connectors

Delta's SMPM-T connectors have a threaded retractable nut combined with SMPM Mil-STD-348 female interface, giving these connectors superior mechanical and electrical performance. These connectors are the perfect choice for applications requiring frequencies up to 40 GHz in demanding environments, involving vibration and/or temperature extremes. Centerline to centerline spacing can be as low as 5 mm, and Delta's unique tooling options allow for simple mating and un-mating of the threaded interface. SMPM-T are available for both 0.047" and 0.086" cable termination options.

www.Deltarf.com

Empower RF Systems Ultra-Broadband Amplifier

VENDORVIEW

This versatile single band CW SSPA is equally suited for RF and microwave digitally modulated communications and product testing. Utilizing 50 VDC GaN devices its class AB design is heavily biased towards class A and delivers exceptional EVM performance. Included for semiconductor test is a pulse modulated mode and a gated pulsed mode, with accurate metering in both cases. Control and monitoring is via touchscreen LCD or peer connected PC/browser with no software to install. **www.EmpowerRF.com**

Eravant (formerly SAGE Millimeter)

Horn Antenna

SAF-2434231535-328-S1-280-DP is a dual polarized, broadband scalar feed horn antenna assembly with orthomode transducer that covers several popular 5G bands in the frequency range of 24 to 42 GHz. The OMT provides high port isolation and cross-polarization cancellation. Integrated OMT enables the antenna to separate a circular or elliptical polarized waveform into two linear, orthogonal waveforms or vice versa. The horn exhibits 15 dBi gain and a 3 dB beamwidth of 35 degrees with -25 dB sidelobe levels.

Solid State Power Amplifier

SBP-3233831838-KFKF-E1-HR is Eravant's solid state power amplifier solution for high power radar and communication system applications. In 5G, common radar and communication frequency band, this GaN power amplifier delivers +38 dBm linear output power with 18 dB gain. Even for large signals, this amplifier provides good gain flatness across the frequency range of 32 to 38 GHz. The DC power requirement for the amplifier is +30 VDC/2 A. The amplifier employs Uni-Guide™ port configuration, which allows easy port orientation settings. **www.eravant.com**

GLOBALFOUNDRIES

8SW RF SOI for 5G/4G LTE Smartphones

Manufactured by GLOBALFOUNDRIES®, 8SW RF SOI offers best-in-class performance for LNAs, switches and tuners in front-end modules for premier sub-8 GHz 5G and 4G LTE smartphones. Industry leaders are taking advantage of differentiated GF 8SW solutions to help bring these sleek new devices to market faster—devices that deliver an enhanced, more immersive user experience by enabling faster download speeds, more reliable connectivity for fewer dropped calls and higher quality connections, even at the network edge.

www.globalfoundries.com

Gowanda Components Group
Expanded Conicals

Gowanda's newest broadband conical series—surface mount C102SM and C182SM and flying lead C102FL and C182FL—offer inductance ranges from 0.47 μH to 10.7 μH, DCR ohms from 0.19 to 7.10 and current rating mA DC from 150 to 815. They also meet outgassing requirements per ASTM E595 with a TML of 1 percent max. These conicals are designed for use in broadband communication applications for bias T's, high frequency, microwave circuitry, RF test set-ups, test and measurement and transmission amplifiers. GCG booth 2214.

www.GowandaComponentsGroup.com

Herotek
26 to 40 GHz Amplifier

Herotek offers a wideband mmWave amplifier. Model A2640205010A operates from 26 to 40 GHz and matched for low VSWR. It has gain of 20 dB with max gain variation of ±2.5 dB, noise figure of 5 dB, P1dB output of +10 dBm and current draw of 180 mA at +12 V bias. This amplifier comes in a hermetically sealed package with removable connectors for drop in assemble and designed for both military and commercial applications.

www.herotek.com

Holzworth Instrumentation
50 GHz Real Time Phase Noise Analyzer

VENDORVIEW

Holzworth will unveil the HA7063A 50 GHz downconverter during IMS2020. The HA7063A integrates seamlessly with the HA7063 Series Real Time Phase Noise Analyzer products to cover 10 MHz to 50 GHz. The advanced heterodyne downconversion architecture provides optimal measurement noise floors and extremely fast acquisition speeds. Holzworth analyzers are the only industry solutions that fully integrates additive/residual measurement capabilities that span above 18 GHz (to 50 GHz) as well as the critical ability to measure the instrument's true noise floor.

www.holzworth.com

HYPERLABS
Ultra-Broadband DC Blocks

HYPERLABS' wideband component portfolio now includes ultra-broadband DC blocks covering the range from 20 kHz to over 67 GHz. The HL9430 Series will be offered at upper frequency ranges of 40, 50 and 67 GHz. These DC blocks have less than 1 dB insertion loss (typical) within the pass band with a smooth roll-off beyond the cutoff frequency. See these and all of its other ultra-broadband components at IMS2020, booth 1954.

www.hyperlabsinc.com

Insulated Wire (IW)
Cables

To support high power applications including EMC test, semiconductor processing, broadcast and other applications requiring high power signal transmission, IW's 4806 and NEW 7506SP provide a flexible, low loss/phase stable alternative to solid wall cables. Using expanded PTFE dielectric for extremely low loss and phase stability over temperature, 4806 has been demonstrated to out-perform other manufacturer's products at equivalent line sizes. Customer testing has proven 4806 capable of handling 17 KW at 13.56 MHz for semiconductor and EMC testing and other high power commercial and military applications.

www.iw-microwave.com

Integra Technologies
GaN/SiC RF Power Transistor

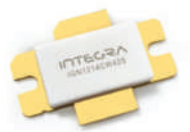

Integra Technologies Inc. (booth 1207) announced its latest GaN/SiC RF power transistor, the IGN1214CW425. Designed using Integra's patented Thermally Enhanced GaN/SiC Technology, the IGN1214CW425 operates instantaneously from 1.2 to 1.4 GHz delivering 400 W CW at 40 V drain with >15 dB of power gain at 70 percent efficiency under CW operating conditions. This product sets a new industry benchmark for CW efficiency and performance, enabling the next generation of multi-mode radar performance.

www.integratech.com

JQL Technologies Corp.
Surface Mount Isolator/Circulator

VENDORVIEW

JQL has developed the smallest surface mount isolator/circulator for 5G application. Their 7 mm package is the best choice for 3.5 and 4.9 GHz bands with robust RF performance. For higher frequency, JQL offers true surface mount microstrip isolators/circulators with no need of any additional biased steel plate for installation. The new solution covers S, C, X, K, Ku and Ka-bands. JQL's smallest 5.2 mm package for X-band delivers 250 W power handling.

www.jqlelectronics.com

K&L Microwave
Bandreject Filter

K&L Microwave's D5CTN-4000/6000-100MHz-O/O-MQI is a digitally controlled tunable bandreject filter with a tuning range of 4 to 6 GHz. The novel design approach extends the passband significantly below the tuning range achieving 3 to 6 GHz as a passband with 1.5 dB max insertion loss. With five resonant sections selectivity reaches a 100 MHz, 40 dB bandwidth. Convenient USB control and a +12 VDC supply power make this bandreject filter an excellent option for lab testing environments.

www.klmicrowave.com

KRYTAR
Ultra-Broadband mmWave/Microwave/RF Components

VENDORVIEW

KRYTAR specializes in the manufacture of ultra-broadband mmWave, microwave and RF components and test equipment for commercial and military applications. The product line includes directional couplers, directional detectors, 3 dB hybrids, MLDD power dividers/combiners. Products cover DC to 110 GHz offering solutions for many applications including warfare (EW) systems and commercial wireless applications including mmWave, 5G, SATCOM, radar, signal monitoring and measurement, antenna beam forming and EMC testing environments. KRYTAR's new dual-directional coupler, model 510050010, exhibits excellent coupling over the 10 to 50 GHz frequency (X through Q-bands).

www.krytar.com

LadyBug Technologies

True-RMS Power Sensor

LadyBug's fully self-contained, thermally stable LB5944A True-RMS power sensor. The power sensor offers 44 GHz frequency coverage and an 86 dB dynamic range and is fitted with a 2.4 mm male connector. Optional autonomous mode with non-volatile storage for over 50 million measurements is available. Once setup, the sensor only requires power to make and store accurate NIST traceable measurements with no power meter or computer. Ask for a demonstration of the company's exclusive Unattended Operation (Option UOP) feature at IMS2020.

www.ladybug-tech.com

Logus Microwave

WR10 Ultra-Light Waveguide Switch

The LOGUS WR10 Ultra-Light Waveguide Switch operates across the 75 to 110 GHz band and boasts a maximum VSWR of 1.20:1, insertion loss of 0.40 dB maximum and a minimum isolation of 50 dB. The switching time is 50 ms maximum and it is available with indicators, TTL interface control and three or four port configurations. The Ultra-Light Series from Logus can be an airborne application constructed and is also available from WR10 thru WR112 and Double-Ridge WRD180 through WRD750.

www.logus.com

LPKF Laser & Electronics

ProtoMat S64

The allrounder in printed circuit board processing. Suitable for almost all in-house prototyping applications. The high speed of the low-maintenance milling spindle guarantees the production of fine structures down to 100 µm and allows the production of multilayers. The extensive equipment, including dispenser and vacuum table, makes the LPKF ProtoMat S64 the perfect addition to any development environment.

www.lpkfusa.com

MCV Microwave

mmWave Ceramic Filters 30 to 70 GHz

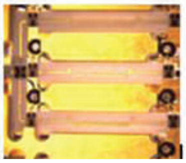

MCV Microwave is now offering mmWave filters to 5G communications, satellite internet/network services, space, aerospace, defense and military industries. These miniature surface mount bandpass filters exhibit excellent passband insertion loss and rejection. A typical 29 GHz filter has less than 2 dB insertion loss and over 15 percent bandwidth with 20 to 30 dB near band rejection.

www.mcv-microwave.com

Micable Electronic Technology Co. Inc.

High Accuracy Butler Matrices

SA-6-51 and SA-6-52 is 2.4 to 7.1 GHz 4 × 4 and 8 × 8 butler matrix respectively. SA-6-51 has insertion loss 7.8 dB max, VSWR 1.5:1 max, isolation 13 dB min, rating input power 5 W CW, phase accuracy ±4° at 2.4 to 2.5 GHz, ±5° at 5.18 to 5.83 GHz, ±6° at 5.9 to 7.1 GHz, amplitude balance ±0.7 dB max, size 101.6 × 106.7 × 16.5 mm, weight 410 g. SA-6-52 has insertion loss 11.8 dB max, VSWR 1.55:1 max, isolation 12 dB min, rating input power 5 W CW, phase accuracy ±8° at 2.4 to 2.5 GHz, ±10° at 5.18 to 5.83 GHz, ±12° at 5.9 to 7.1 GHz, amplitude balance ±0.9 dB max, size 205.7 × 205.7 × 16.5 mm, weight 1375 g.

Ultra-Wideband Two Way Power Divider/Combiner

Model P02N005500 is two way 0.5 to 50 GHz DC pass through power divider/combiner, it has 4.2 dB max insertion loss, 16 dB min isolation, 1.7:1 max VSWR, ±0.4 dB amplitude balance and ±6 ° phase balance. The input power as the power divider is 20 W average. As a combiner, it can stand for 5 W average input power. The size is 149.2 × 26.4 × 12.7 mm (5.87 × 1.03 × 0.50 in.), weight is 150 g max and the operating temperature is -54° to +85°C.

www.en.micable.cn

MICIAN

µWave Wizard

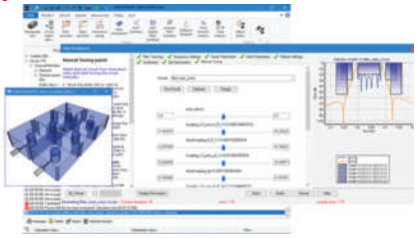

Mician's µWave Wizard products are powerful tools for synthesis, analysis and optimization of microwave assemblies. The software's hybrid EM solver guarantees fast and accurate simulation of passive components, feed networks and antennas. Typical applications include horn and reflector antennas, feed clusters, OMTs, polarizers, circulators, waveguide and combline filters, multiplexers, couplers and more. Integrated COM/VBA interfaces support external control and third-party add-ons. A new add-on feature for µWave Wizard is Mician's Filter Workbench, a novel synthesis tool for the design of Chebyshev and quasi-elliptic function filters.

www.mician.com

Micro Lambda Wireless

Single Slot PXI Frequency Synthesizer

The MLMS-Series frequency synthesizer is a new smaller and lower cost frequency synthesizer designed to fit into a single slot PXI chassis. Dimensions measure 2.5" × 2.5" × 0.65" tall. Standard frequency models are available covering 250 MHz to 6 GHz, 2 to 8 GHz, 6 to 13 GHz and 8 to 20 GHz. Applications include wide band receivers, automated test systems, telecom, satcom, UAV's and drones, as well as a variety of military and commercial test applications.

www.microlambdawireless.com

Milliwave Silicon Solutions

3D DUT Positioner

The MilliBox GIM01 Positioner is a cost effective test tool specially designed for mmWave over-the-air (OTA) measurements. Features include ±180 degree horizontal and ±180 vertical, better than 1-degree resolution, 11 cm DUT maximum width, 0.5 kg maximum DUT weight, 75 deg/sec rotational velocity, laser guided alignment, tangle-free wiring, open software controller interface over USB and is the best for device and module characterization. MilliBox products are cost effective test tools and accessories specially designed for mmWave OTA measurements.

www.millibox.org

Mini-Circuits

Four-Way Divider

VENDORVIEW

Mini-Circuits' model ZC4PD-V1854+ is a four-way, 0-deg. power splitter/combiner with broad frequency range of 18 to 50 GHz. The 50 Ω DC-pass splitter/combiner handles as much as 16 W input power as a power divider with low insertion loss and excellent amplitude and phase unbalance. The typical insertion loss (above the 6 dB power split) is 1.1 dB from 18 to 40 GHz and 1.6 dB from 40 to 50 GHz with typical isolation of 29 dB from 18 to 40 GHz and 30 dB from 40 to 50 GHz.

MMIC Transformer

Mini-Circuits' model MTY2-243-D+ is a miniature GaAs MMIC 2:1 impedance transformer for use from 10 to 24 GHz. Supplied in die form, the 50 Ω balun transformer is fabricated by heterojunction-bipolar-transistor (HBT) process. It handles as much as 1.25 W (+31 dBm) input power with low insertion loss and minimal amplitude and phase unbalance. The typical insertion loss is 1 dB from 10 to 20 GHz and 1.3 dB from 20 to 24 GHz.

Tiny LTCC Filter

Mini-Circuits' model LFCW-6000+ is a low-temperature-cofired-ceramic (LTCC) lowpass filter (LPF) with passband from DC to 6 GHz. The typical passband insertion loss is 1.6 dB, with typical passband VSWR of 1.50:1. The stopband rejection is typically 42 dB or more from 8.2 to 14 GHz, typically 35 dB from 14 to 18 GHz, and typically 15 dB from 18 to 26.5 GHz. The stopband VSWR is typically 20.0:1 from 8.2 to 26.5 GHz.

SPDT Switch Die

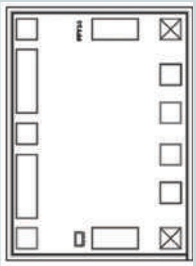

Mini-Circuits' model M3SWA-250DRBD+ is a GaAs MMIC single-pole, double-throw (SPDT) absorptive switch die with internal driver for DC to 4.5 GHz. Well suited for communications, defense and test applications, the tiny switch features typical "on" time (from 50 percent control to 90 percent RF) of 14.4 ns and typical "off" time (from 50 percent control to 10 percent RF) of 11.3 ns; rise and fall times are typically 4.6 ns. Insertion loss is typically 1.4 dB or better across the full frequency range.

LTCC Bandpass Filter

Mini-Circuits' model BFCN-1052+ is a LTCC bandpass filter (BPF) with passband from 9.70 to 11.95 GHz. Passband insertion loss is typically 1.6 dB with typical passband VSWR of 1.90:1. The lower stopband extends from DC to 8.4 GHz, with typical rejection of 38 dB from DC to 8.1 GHz and 32 dB from 8.1 to 8.4 GHz. The upper stopband spans 14 to 44 GHz, with typical rejection of 28 dB from 14 to 28.5 GHz and 25 dB from 28.5 to 44 GHz.

Absorptive Attenuator Die

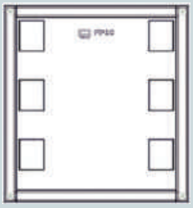

Mini-Circuits' KAT-1-D+ series of attenuator die includes models with fixed values of 0 to 10 dB in 1 dB steps as well as attenuation values of 12, 15, 20 and 30 dB for wideband applications from DC to 43.5 GHz. Well suited for mmWave applications including in 5G cellular wireless communications circuits and systems, the RoHS-compliant attenuator dice feature a contiguous ground plane for ease of installation. The typical VSWR is 1.10:1 from DC to 26.5 GHz and 1.30:1 from 26.5 to 43.5 GHz.

Monolithic Amplifier Die

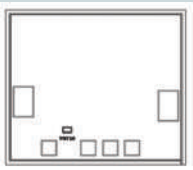

Mini-Circuits' model PHA-83W-D+ is a high-dynamic-range monolithic amplifier die for wideband 50 Ω applications from 50 MHz to 8 GHz. Based on GaAs pseudomorphic high electron mobility transistor semiconductor technology, the RoHS-compliant amplifier delivers typical small-signal gain of 15.7 dB that is flat within ±1.4 dB across the frequency range. The high dynamic range is marked by a typical output third-order intercept point of +35.5 dBm and typical output power at 1 dB compression of +23.3 dBm.

Hand-Formable Cable

Model 141-7SBSM+ is a 7 in. long cable assembly based on Mini-Circuits' Hand-Flex™ coaxial cable. It is hand formable without special tools and an ideal replacement for custom-bent 0.141 in. diameter semi-rigid cable assemblies in 50 Ω applications from DC to 18 GHz. It features an SMA male connector (with anti-torque nut) at one end and SMA female bulkhead connector at the other end. The RoHS-compliant cable has a minimum bend radius of 8 mm for tight fits.

RF Transfer Switch Matrix

Mini-Circuits' model RC-3MTS-18 is a broadband switch matrix consisting of three independently controlled electro-mechanical transfer switches, each covering DC to 18 GHz. It can be operated under USB or Ethernet control and is rated for 10 million switch cycles. It handles 10 W typical power with 0.25 dB or less typical insertion loss. Typical isolation is 76 dB or more from DC to 18 GHz with 25 ns typical switching speed. Typical VSWR is 1.15:1 or better.

Highpass Filter

Mini-Circuits' model ZHSS-K11G+ is a suspended substrate stripline filter with high-rejection stopband of DC to 8.5 GHz, transition band of 8.5 to 11 GHz, and low-loss passband of 11 to 40 GHz. The RoHS-compliant coaxial filter achieves typical stopband rejection of 80 dB from DC to 6.5 GHz and 60 dB from 6.5 to 8.5 GHz for effective separation of signals below 8.5 GHz from higher microwave and mmWave signals through 40 GHz, such as in satellite communications and 5G wireless communications systems.

www.minicircuits.com

Modelithics
COMPLETE Library™
VENDORVIEW

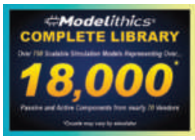

Modelithics® COMPLETE Library™ reaches a milestone with over 18,000 passive and active components for more than 750 scalable simulation models from nearly 70 vendors. COMPLETE Library is an indispensable collection of highly scalable models for capacitor, inductor and resistor families as well as non-linear diodes and transistors and system level components. All models are highly accurate and well documented. Compatible with six popular EDA tools. Free trials available, including vendor sponsored trial libraries.

www.Modelithics.com

Morion Inc.
Ultra-Stable 10 MHz OCXO

Ultra-Stable 10 MHz OCXO: MV336M Type Morion's MV336M is an ultra precision 10 MHz OCXO with phase noise of <-93 dBc/Hz at 0.1 Hz and -120 dBc/Hz at 1 Hz. Short-term stability (ADEV) is <1E-13 at 1 second and <3E-13 until 100 sec which is accompanied by temperature stability of <4E-11 vs. -10…+70 deg C. The MV336M is housed in a 92 x 80 x 50 mm package and operates at 12 V.

www.morion-us.com

Networks International Corp.
Thin Film Filters

Network International's engineering expertise in hi-reliability RF products and integrated assemblies includes a specialty in Thin film filters that span from 1 to 20 GHz. These high performance filters are built on industry standard substrates such as alumina and titanate, offering a compact package size with low profile of < 0.08 in. The filters also offer high selectivity and out of band rejection of > 60 dB. These filters can be customized to meet passband requirements from 1 to 60 percent and meet a wide range of environmental requirements as well.

www.nickc.com

Noisecom
Programmable Noise Generator

The new RFX7000B programmable noise generator can generate complex, custom noise signals up to 40 GHz in a single, 1U rackmountable form factor. Built on the technology of the popular Noisecom UFX7000A benchtop platform, the RFX7000B delivers the performance and capabilities system designers and engineers to stress test wireless/5G, military and satellite communication systems. This new 1U form factor makes it easier than ever before to add customizable RF and microwave noise generation to a communications or ATE system.

www.noisecom.com

Passive Plus Inc.

RF/Microwave Passive Components

Passive Plus Inc. (PPI) High-Q/Low ESR capacitors are offered in multiple case sizes, dielectrics and various terminations and include RoHS compliant and non-magnetic finishes. Data sheets and S-parameters are available. PPI specializes in High-Q, low ESR/ESL capacitors, broadband capacitors, single layer capacitors, non-magnetic resistors (high power and thin film) and trimmer capacitors.

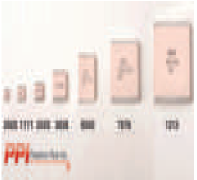

www.passiveplus.com/hiqproducts.php

Pasternack

VENDORVIEW

mmWave Waveguide Antennas

Pasternack has expanded its offering of mmWave waveguide antennas to address the growing number of 5G and other high-frequency applications. Pasternack's line of mmWave waveguide antennas has added 54 new models and now covers broad operating frequency ranges from 1.7 to 220 GHz, provides nominal gain ranging from 0 to 40 dBi, and features a variety of different waveguide sizes.

Waveguide Shorts and Shims

Pasternack has just released a new line of waveguide shorts and shims that are ideal for use in satellite communication, radar, wireless communication and test and instrumentation applications. Pasternack's new line of waveguide shorts and shims consists of 36 models available in waveguide sizes ranging from WR-430 to WR-10. This new line provides superior RF performance and is ideal for use in RF test and measurement applications.

www.pasternack.com

Pixus Technologies

Ruggedized Software Defined Radio

Pixus Technologies will be featuring a rugged version of the Ettus Research (a National Instruments brand) ×310 SDR. The Pixus RX310 is IP67 weatherproof in a rugged fanless enclosure. The solution is ideal for field testing and deployment for drone detection/takeover, wireless/wideband prototyping, SIG/INT, RADAR and other applications. The company will also be showing various OpenVPX chassis configurations geared for VITA 67 RF and SOSA/HOST applications. Visit the Pixus at booth 723.

www.pixustechnologies.com

The IEEE Microwave Theory and Techniques Society (MTT-S), along with the International Microwave Symposium and Microwave Week (IMS, RFIC and ARFTG) 2020 organizers are closely monitoring the Coronavirus (COVID-19) pandemic relying upon authoritative sources for guidance such as the the Centers for Disease Control and Prevention (CDC) and the World Health Organization (WHO). The health, safety, and well-being of our global community is of paramount importance.

IMS2020 and Microwave Week, scheduled for 21-26 June 2020 in Los Angeles, is continuing with the planning process. We know it is important to keep the lines of communication open and will provide updates as soon as they become available.

We are committed to providing the best attendee experience possible and encourage you to check out the technical programs on the IMS, RFIC and ARFTG websites.

Updates will be posted at https://ims-ieee.org/travelandsafety and we will provide as much advance notice of our plans as possible.

We appreciate the continued patience and support of our authors, exhibitors, and attendees as we navigate these unprecedented times.

Thank you,

IMS Microwave Week Response Team
IMS2020information@gmail.com
RFIC2020info@gmail.com
Chairs@arftg.org

WWW.IMS-IEEE.ORG

LOS ANGELES CONVENTION CENTER

Symposium Dates: 21-26 June 2020 • Exhibition Dates: 23-25 June 2020

Follow us on:

IEEE

#IMS2020

MTT-S

IMS2020 and RFIC 2020 Keynote Speakers

RFIC Plenary Session Speaker
Sunday, 21 June 2020

Dr. Thomas Byunghak Cho – *EVP Samsung Semiconductor*

"Is the Third Wave Coming in CMOS RF?"

RFIC Plenary Session Speaker
Sunday, 21 June 2020

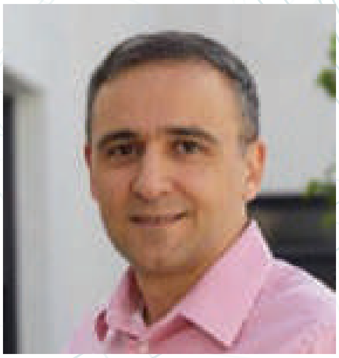

Prof. Ali Hajimiri – *Bren Prof. of Elect. Eng. and Medical Eng., Caltech*

"The Flexible Future of RF"

IMS Plenary Session Speaker
Monday, 22 June 2020

Doreen Bogdan-Martin – *Director, Telecommunication Development, International Telecommunication Union*

"Can Digital Technologies Really Change the World?"

IMS Plenary Session Speaker
Monday, 22 June 2020

Mark Dankberg – *Chairman of the Board and Chief Executive Officer, Viasat, Inc. .*

IMS Closing Session Speaker
Thursday, 25 June 2020

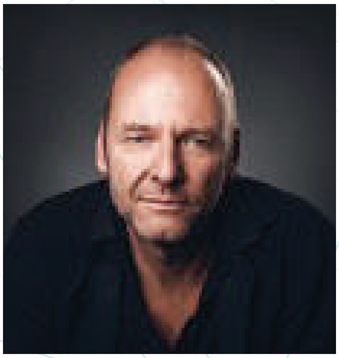

Hartmut Neven – *Engineering Director, Quantum Artificial Intelligence Lab, Google*

"The Road Ahead for Quantum Computing"

For the latest on IMS and Microwave Week visit www.ims-ieee.org

RFIC Technical Sessions, Monday, 22 June 2020

All technical sessions will take place at the Los Angeles Convention Center (LACC)

Time					402AB	403A	403B	404AB
08:00 – 09:40					**Session Mo1A** High Spectral Purity Phase-Locked Loops	**Session Mo1B** Microwave and mmWave Radar Systems	**Session Mo1C** Circulators and Full-Duplex Transceivers	**Session Mo1D** Switches and Delay Elements for Receiver Front-Ends
09:40 – 10:10	AM Coffee Break							
10:10 – 11:50					**Session Mo2A** Reconfigurable RF Front-End Blocks	**Session Mo2B** Millimeter-Wave Circuits in D and E Band for High Data-Rate Wireless Links	**Session Mo2C** Digital Power Amplifiers	**Session Mo2D** Novel RF Devices and Modeling Approaches
13:40 – 15:20					**Session Mo3A** RFIC Systems and Applications I: Biomedical and Radar Systems	**Session Mo3B** Millimeter-Wave Transceivers and Building Blocks	**Session Mo3C** mmWave Power Amplifiers	
15:20 – 15:50	PM Coffee Break							
15:50 – 17:20					**Session Mo4A** RFIC System and Applications II: Wideband Wireless Communication and Quantum Computing	**Session Mo4B** Millimeter-Wave and Terahertz Circuits and Systems for Sensing and Communications	**Session Mo4C** High-Performance Frequency-Generation Componentss	

Also on Monday: Workshops, Technical Lectures, RF Boot Camp, RFIC Panel Session, IMS Plenary and Welcome Reception

For the latest on IMS and Microwave Week visit www.ims-ieee.org

RFIC and IMS Technical Sessions, Tuesday, 23 June 2020

All technical sessions will take place at the Los Angeles Convention Center (LACC)

Time	406AB	408A	408B	409AB	402AB	403A	403B	404AB
08:00 – 09:40	**Session Tu1E** Novel Components, Waveguides, and Methods for Radiating Structures	**Session Tu1F** High Power Amplifiers for HF Through S Band	**Session Tu1G** Innovative RF Switches and Applications	**Session Tu1H** Advances in RF and Microwave CAD Techniques	**Session Tu1A** mmWave Signal Generation	**Session Tu1B** 5G Focus Session on Advances in Mixer-First Receivers	**Session Tu1C** Linearization and Efficiency Enhancement Techniques	**Tu1D** Mixed-Signal and Power Management Techniques for RF Transceivers
09:40 – 10:10	AM Coffee Break							
10:10 – 11:50	**Session Tu2E** Advances in Microwave to Terhertz Photonics and Nanotechnology	**Session Tu2F** Power Amplifiers for S and C Band	**Session Tu2G** Filters Based on Micro-machined Acoustic or Electromagnetic Structures	**Session Tu2H** Advances in Electromagnetic Modeling Techniques	**Session Tu2A** Ultra-Low Power Transceivers	**Session Tu2B** 5G Focus Session on Millimeter-Wave Components and Systems	**Session Tu2C** Sub-6 GHz Receiver Front-End Circuits	
	402AB	403A	403B	404AB	406AB	408A		409AB
13:40 – 15:20	**Session Tu3A** Integrated Millimeter-Wave Transmission Lines	**Session Tu3B** Advances in Low Noise Circuits for Quantum Computing, Scientific Sensing, and Broadband Communications	**Session Tu3C** Advanced Mixed-Signal Transmitter and Optical Driver ICs towards 100Gbit/s	**Session Tu3D** Microwave Characterization of Liquid and Biological Materials	**Session Tu3E** Acoustic Devices for Ultra-high Frequency Applications and RF Filter Synthesis	**Session Tu3F** Broadband, High-Performance GaN and GaAs Power Amplifiers		**Session Tu3H** Advances in Microwave Semiconductor Devices
15:10 – 15:55	PM Coffee Break							
15:50 – 17:30	**Session Tu4A** Innovative Wave Transmission, Manipulation and Generation	**Session Tu4B** High-Performance Low-Noise Amplifiers	**Session Tu4C** Advanced Design Techniques for Voltage Controlled Oscillators	**Session Tu4D** Microwave Systems and Methods for Permittivity Measurements	**Session Tu4E** Nonlinear Circuits & Systems	**Session Tu4F** Innovations in Broadband Millimeter-wave Power Amplifiers		**Session Tu4H** Advanced Transistor Modeling and Characterization

Technical Track Key: Field, Device and Circuit Tech. | Passive Components | Active Components | Systems & Applications | Emerging Technical Areas | Focus or Special Sessions | RFIC Sessions

Also on Tuesday: IMS Exhibition, IMS Student Design and Student Paper Competitions, Panel Session, Technical Lectures, Startups 101 Panel Session, 5G Summit, MicroApps, Industry Workshops, YoPros Networking Event, Amateur (HAM) Radio Event

For the latest on IMS and Microwave Week visit www.ims-ieee.org

IMS Technical Sessions, Wednesday, 24 June 2020

All technical sessions will take place at the Los Angeles Convention Center (LACC)

Time	402AB	403A	403B	404AB	406AB	408A	408B
08:00 – 09:40	**Session We1A** Non-Planar Filters I	**Session We1B** Advances in Wireless Sensors	**Session We1C** Millimeter-Wave and Terahertz Transmitter Components	**Session We1D** Novel Microwave Technologies for Biomedical Sensing	**Session We1E** High Frequency Non-Reciprocal Techniques using Novel Material, Device and Circuit Approaches	**Session We1F** Advances in 5G Millimeter-wave Systems and Architectures	**Session We1G** Emerging Next Generation GaN RF Technologies for 5G and MMW Applications
09:40 – 10:10	AM Coffee Break						
10:10 – 11:50	**Session We2A** Non-Planar Filters II	**Session We2B** Advances in Radar and Backscatter Sensor Systems	**Session We2C** Millimeter-Wave and Terahertz Transmitter and Receiver Systems	**Session We2D** Advancement of Biomedical Radar and Imaging	**Session We2E** Recent Advances in Compact and High Performance Planar Filter Design and Realization	**Session We2F** 5G Arrays and Beamformers	**Session We2G** Load Modulated Power Amplifiers
13:40 – 15:20	**WEIF1: Interactive Forum Session**						
15:10 – 15:55	PM Coffee Break						
15:50 – 17:30	**Session We3A** Recent Advances in Passive Components	**Session We3B** Advanced Nonlinear Measurement Techniques and Results	**Session We3C** Millimeter-Wave and Submillimeter-Wave Components	**Session We3D** Millimeter Wave Radar Vibrometry: Technical Advances and New Phenomenology	**Session We3E** Tunable and Active Filters	**Session We3F** Beamforming for Satellite Communications and Sensors	**Session We3G** Digital Predistortion and Supply Modulation

Technical Track Key: Field, Device and Circuit Tech. | Passive Components | Active Components | Systems & Applications | Emerging Technical Areas | Focus or Special Sessions

Also on Wednesday: IMS Exhibition, IMS Interactive Forum, IMS Panel Session, Technical Lectures, MicroApps, Industry Workshops, Women in Microwave Networking Event, Industry Hosted Reception, MTT-S Awards Banquet

For the latest on IMS and Microwave Week visit www.ims-ieee.org

IMS Technical Sessions, Thursday, 25 June 2020

All technical sessions will take place at the Los Angeles Convention Center (LACC)

Time	408A	403B	404AB	406AB	408A	408B
08:00 – 09:40	**Session Th1B** Late-breaking News in Silicon Technologies and Circuits	**Session Th1C** Advanced Radar Systems for Automotive and Vehicular Applications	**Session Th1D** Chip-Scale Interconnects and Packaging Technologies	**Session Th1E** Advances in RF Energy Harvesting	**Session Th1F** Phased Arrays and Beamformer Technologies	**Session Th1G** Advanced Silicon PAs for 5G and Automotive Applications
09:40 – 10:10	AM Coffee Break					
10:10 – 11:50	**Session Th2B** Late-breaking News from the Terahertz Frontier	**Session Th2C** Networked and Distributed Radar and Imaging Systems	**Session Th2D** 3D Packaging and Additive Manufacturing	**Session Th2E** Novel Applications of Wireless Power Transfer	**Session Th2F** In-Band Full-Duplex Cancellers and Transceivers	**Session Th2G** Phased Array and Beamformer Integrated Circuits
13:40 – 15:20	**Session Th3B** Robert J Trew: More than 50 Years of Service to the Microwave Community"	**Session Th3C** Emerging Technologies for Radar Detection, Tracking, and Imaging	**Session Th3D** Late-breaking News in Millimeter-Wave Communication and Radar Systems	**Session Th3E** Late-breaking News in III-V MMICs		**Session Th3G** Phased Array Silicon Components

Technical Track Key: Field, Device and Circuit Tech. | Passive Components | Active Components | Systems & Applications | Emerging Technical Areas | Focus or Special Sessions | Late Breaking News

Also on Thursday: IMS Exhibition, MicroApps, Industry Workshops, IMS Panel Session, Technical Lectures, MTT-S Student Awards Luncheon, IMS Closing Session and Reception

For the latest on IMS and Microwave Week visit www.ims-ieee.org

5G Summit, Tuesday, 23 June 2020

The technologies and systems for 5G are now pushing for commercial deployment with focus on Stand Alone (SA) networks, mass market for 5G devices, and global adoption of mmWave in premium devices and for small cell enhancement and fixed wireless access (FWA). Furthermore and looking beyond 5G, technology research and development needs to focus on MIMO enhancement, V2X and IoT evolution, integration of 5G with Non-Terrestrial Network, and new FR3 & FR4 spectrum development. This year's 5G summit will provide a platform for leaders, innovators, and researchers from both industrial and academic communities to collaborate and exchange ideas regarding 5G and beyond 5G technologies.

The 5G Summit will be open to all attendees for a nominal cost and will be complemented by a reception for all registered attendees, followed by a rump session to drive a live discussion between the speakers and the audience on the summit presented topics.

For speaker list visit, www.ims-ieee.org/5g-summit.

Panel Sessions, Monday, 22 June 2020 - Thursday, 25 June 2020

- **HW Startups – No Longer an Oxymoron?**
- **Automotive radars and AI: Is my car really safe?**
- **Who needs RF when we can digitize at the antenna?**
- **Persuasive Presentations: Getting your message across and getting results**
- **Should my car kill me or you?**
- **Connecting the Unconnected Enabled by Wireless Broadband Technologies**
- **Connecting the Unconnected Enabled by Wireless Broadband Technologies**

Technical Lectures, Sunday, 21 June 2020 - Thursday, 25 June 2020

- **"Fundamentals of Phased Arrays"** - Marinos Vouvakis - *University of Massachusetts Amherst*
- **"Quantum Computing: an RF Control Perspective"** - Evan Jeffrey - *Google Inc.*
- **"N-Path Mixers and Filters: Concept, Theory and Applications"** - Alyosha Molnar - *Cornell University*
- **"Trends in Automotive Radars: Waveform, System Implementation, and IC Technologies"** - Cicero Vaucher - *NXP Semiconductors*
- **"Silicon-based Millimeter-Wave Phased Array Design"** - Bodhisatwa Sadhu - *IBM T. J. Watson Research Center*
- **"Understanding Oscillator Phase Noise and Locking"** - Ali Hajimiri - *Caltech*
- **"Intuitive Microwave Filter Design with EM Simulation"** - Daniel Swanson - *DGS Associates, LLC*
- **"Taxonomy of RF Receivers: From Basics to Latest Techniques"** - Peter Kinget - *Columbia University*

Workshops, Sunday, 21 June 2020 - Friday, 26 June 2020

Please visit https://ims-ieee.org/technical-program/workshops-and-short-courses?date=2020-06-21 for the latest Workshop and Technical Lecture information.

IMS Microwave Week Mobile App:

The IMS Microwave Week app is now available in the Apple App store and Google Play store. Install the app on your Android or iOS device to view the full schedule of Workshops, Technical Lectures, IMS and RFIC Technical Sessions, ARFTG, Panel Sessions, Social Events and Exhibition information. On-site during Microwave Week you will be able to download IMS and RFIC papers and presentations, locate exhibitors, upload photos and explore all that Los Angeles, CA has to offer! Download today!

Apple App Store

Google Play Store

Exhibition Overview:

The Exhibition consists of over 600 exhibiting companies who represent the state of the art materials, devices, components, and subsystems, as well as design and simulation software and test/measurement equipment. Whatever you are looking to acquire, you will find the industry leaders ready and willing to answer your purchasing and technical questions.

Exhibition Dates and Hours

Tuesday, 23 June 2020	09:30 to 17:00
Wednesday, 24 June 2020	09:30 to 17:00
Exhibit-Only Time:	13:30 to 15:10
Industry Hosted Reception:	17:00 to 18:00
Thursday, 25 June 2020	09:30 to 15:00

MicroApps

The Microwave Application seminars (MicroApps) offered Tuesday, 23 June through Thursday, 25 June 2020, provide a unique forum for the exchange of ideas and practical knowledge related to the design, development, production, and test of products and services. MicroApps seminars are presented by technical experts from IMS2020 exhibitors with a focus on providing practical information, design, and test techniques that practicing engineers and technicians can apply to solve the current issues in their projects and products.

Industry Workshops

The Industry Workshops are 2-hour industry-led presentations featuring hands-on, practical solutions often including live demonstrations and attendee participation. These Workshops are open to all registered Microwave Week attendees at a nominal charge.

For more information on MicroApps and Industry Workshops please visit www.ims-ieee.org/exhibition.

Use promo code IMS2020MWJ to register for the Exhibition for FREE!

Register Today!

www.ims-ieee.org

Key Deadlines:

Early Bird Registration Deadline: 26 May 2020
Advance Registration Deadline: 19 June 2020
Housing Bureau Deadline: 31 May 2020

For the latest on IMS and Microwave Week visit www.ims-ieee.org

The IEEE Microwave Theory and Techniques Society (MTT-S), along with the International Microwave Symposium and Microwave Week (IMS, RFIC and ARFTG) 2020 organizers are closely monitoring the Coronavirus (COVID-19) pandemic relying upon authoritative sources for guidance such as the the Centers for Disease Control and Prevention (CDC) and the World Health Organization (WHO). The health, safety, and well-being of our global community is of paramount importance.

IMS2020 and Microwave Week, scheduled for 21-26 June 2020 in Los Angeles, is continuing with the planning process. We know it is important to keep the lines of communication open and will provide updates as soon as they become available.

We are committed to providing the best attendee experience possible and encourage you to check out the technical programs on the IMS, RFIC and ARFTG websites.

Updates will be posted at https://ims-ieee.org/travelandsafety and we will provide as much advance notice of our plans as possible.

We appreciate the continued patience and support of our authors, exhibitors, and attendees as we navigate these unprecedented times.

Thank you,

IMS Microwave Week Response Team
IMS2020information@gmail.com
RFIC2020info@gmail.com
Chairs@arftg.org

WWW.IMS-IEEE.ORG
LOS ANGELES CONVENTION CENTER
Symposium Dates: 21-26 June 2020 • Exhibition Dates: 23-25 June 2020

Follow us on:

IEEE

#IMS2020

MTT-S

Planar Monolithics Industries Inc.

Absorptive Switch

VENDORVIEW

Planar Monolithics Industries Model Number: P16T-100M52G-100-T-DEC is a 0.1 to 52 GHz, SP16T absorptive switch. This model offers a typical insertion loss of 16 dB while maintaining a typical isolation of 70 dB. It operates at 20 dBm CW, 100 ns switching speed and is controlled with TTL logic. Power requirements are +12 VDC at 800 mA max, -12 VDC at 720 mA max. Other features include 2.4 mm connectors, nickel plated finish and 12.00" × 5.50" × 0.65" package size.

www.pmi-rf.com

Qorvo

High Performance GaN PA's

Qorvo released the QPA261x GaN power amplifier family. These high performance GaN on SiC PAs are packaged in a 5 x 5 mm plastic QFN, with tight lattice spacing for phased array radars. The QPA2610 (8.5 to 10.5 GHz) has > 2 W of saturated output power and 23 dB of large-signal gain, 47 percent PAE. The QPA2611 (8 to 12 GHz) provides > 5 W of saturated output power, 26 dB of large-signal gain, 42 percent PAE. The QPA2612 (8 to 12 GHz) has > 12 W of saturated output power and 23 dB of large-signal gain and 40 percent PAE.

Broadband Driver Amplifier

The CMD305C4 is a broadband MMIC driver amplifier housed in a leadless 4 × 4 mm surface mount package. The CMD305C4 is ideally suited for EW and communications systems where small size and low power consumption are needed. The broadband device delivers 18.5 dB of gain and +21 dBm saturated output power at 23 percent PAE from a single 5 V supply. The CMD305C4 is a 50 ohm matched design eliminating the need for external DC blocks and RF port matching.

Broadband Low Noise Amplifier

The CMD316C3 is a broadband MMIC low noise amplifier housed in a leadless 3 x 3 mm surface mount package. The CMD316C3 is ideally suited for EW and communications systems where small size and low power consumption are needed. The broadband device delivers greater than 20 dB of gain with a corresponding output 1 dB compression point of +15 dBm and a noise figure of 2 dB. The CMD316C3 is a 50 ohm matched design eliminating the need for external DC blocks and RF port matching.

www.qorvo.com

Reactel Inc.
Filters, Multiplexers and Multifunction Assemblies
VENDORVIEW

Reactel will feature its full line of filters, multiplexers and multifunction assemblies covering up to 50 GHz at IMS2020. Supporting military, commercial, industrial, medical and research needs, Reactel can design a unit that is right for you. From small, lightweight units suitable for flight or portable systems to high power units capable of handling up to 25 kW, connectorized or surface mount, large or small quantities—their talented engineers can design a unit specifically for your application.

www.reactel.com

RelComm Technologies Inc.
Terminated Coaxial Relay

RelComm Technologies provides a high performance 1P3T to 1P6T, 50 ohm, 2 W terminated coaxial relay configured with 'SMA' type connectors having excellent RF performance to 18 GHz. The relay measures 2.25" sq. × 2.00" tall and is fitted with a standard DE9P header for ease of wire up. Operating temperature range is -30° to +75°C. The relay is available in latching with auto re-set and failsafe configurations. Standard operating voltages of 12, 24 and 28 VDC. This product is fully RoHS compliant.

www.relcommtech.com

Remcom Inc.
XFdtd's Superposition Simulation
VENDORVIEW

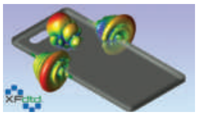

Designing high-frequency MIMO and 5G devices requires intensive, yet efficient, analysis. Beamforming applications increase complexity due to hundreds or even thousands of beam states that must be analyzed. XFdtd leverages the EM principle of superposition to quickly analyze port phase combinations with a single simulation and identifies the ones that maximize far zone coverage in each direction. As a result, the design workflow for MIMO beamforming array analysis is greatly simplified and streamlined. Visit Remcom's booth for a demonstration of XFdtd's new features!

www.remcom.com

RFHIC Corp.
Pulsed, GaN Solid-State Power Amplifier Module

RFHIC Corporation will showcase its latest 1.2 kW, L-Band GaN solid state power amplifier designed for various radar applications at IMS2020. The RRP131K0-10 delivers a high efficiency of 50 percent efficiency with a duty cycle up to 20 percent. The PA is fabricated with RFHIC's groundbreaking GaN on SiC HEMT, providing high breakdown voltage and wide bandwidth. RFHIC's RRP131K0-10, power amplifier delivers the industry's leading SWaP-C (size, weight, power and costs), enabling next-generation development in the field of high-power radar solutions.

www.rfhic.com

RFMW
28 GHz Power Divider Goes SMT
VENDORVIEW

RFMW announced a portfolio of devices designed for mmWave 5G radio applications. Created by Knowles—DLI, the portfolio includes filters, broadband couplers and Wilkinson power dividers. Patented ceramic substrate materials exhibit excellent temperature stability and high K factor enabling off the shelf solutions with small size and high performance. For example, the 25 to 32 GHz PDW06984 power divider has maximum excess insertion loss of 0.7 dB while consuming just 2.5 mm of board space, ideal for ultra-compact phased array antenna applications.
www.rfmw.com

RFMW/Qorvo
22 GHz Bandwidth Distributed Amplifier
VENDORVIEW

RFMW announced design and sales support for a wide bandwidth, distributed amplifier from Qorvo (Custom MMIC). The CMD284P4, GaAs MMIC distributed amplifier is housed in a leadless, 4 × 4 mm plastic surface mount package for ease of installation. Operating from DC to 22 GHz and delivering 17 dB of gain, the device offers 19 dBm P1dB and noise figure of 2.5 dB at 10 GHz. Matched to 50 ohms, the CMD284P4 eliminates the need for external RF port matching.
www.rfmw.com

Richardson RFPD
Power Amplifier

The CMPA2738060F is a 50 V GaN-on-SiC MMIC power amplifier covering the extended range S-Band radar band of 2.7 to 3.8 GHz. The two-stage PA offers 34 dB of gain and 60 W peak power over the entire band. The highly integrated PA includes two gain stages with internally matched 50 ohms input and output, which provides ease of use. The combination high power density, efficiency and reliability of GaN, with the high integration makes this a versatile option for compact phased array/AESA radar systems.
www.richardsonrfpd.com

RLC Electronics
Miniature SPDT Switch

RLC Electronics introduced an addition to their miniature SPDT switch product line.

This switch is offered in a unique package with connectors in a "T" configuration for ease of connection/mating at the system level, and is a perfect drop-in replacement for pin diode switches. The switch is offered in both surface mount and connectorized versions and operates from DC to 18 GHz. Standard options available include indicators and TTL drivers. The switch measures 1" × 1" × 0.90".
www.rlcelectronics.com

Roos Instruments
Cassini Spyder Modular ATE Platform

Move 5G test from the lab into production with the Cassini Spyder modular ATE platform. Combining production speed with a scalable instrument and device interface architecture, Spyder provides seamless multi-function test from DC to 100 GHz. Integrated instrument and device interface calibration software delivers VNA accuracy right to the device under test. Visit us at IMS2020.
www.roos.com

Rosenberger Hochfrequenztechnik GmbH & Co. KG
PIM Test Solutions for 5G Technology

Rosenberger develops and provides low-PIM components as well as PIM test solutions for 5G technologies. The portfolio includes new rack PIM analyzers for production/lab environments, portable desktop analyzers, PIM site analyzers for measurements on site, and band filter units for 600 MHz and 3,500 MHz measurements. The portable desktop analyzer offers high flexibility for measurements in production lines, R&D and test labs. Rosenberger rack analyzers are designed to make PIM tests in production or test lab environments as modular, precise and efficient as possible.
www.rosenberger.com

Samtec Inc.
50 GHz Microwave Cable Solution

Samtec announced a new high-performance cable assembly with performance up to 50 GHz using both male and female 2.40 mm connectors. The RF23C Series uses cable manufactured in their Wilsonville, Ore. facility, which is a flexible low-loss alternative to RG405 semi-rigid cable. According to their on-line characterization report, 12 in. assemblies typically exhibit less than 1.3:1 VSWR and just over 2 dB of insertion loss up to 50 GHz.
www.samtec.com

Signal Hound
Spectrum Analyzers

Signal Hound's latest device, the SM200C, maintains the dynamic range, phase noise, 1 THz/s sweep speed, and 100 kHz to 20 GHz tuning range that made the SM200B so popular, but now includes a full 160 MHz IBW available for calibrated I/Q data streaming, plus device control via 10 GbE SFP+ connection. No longer limited by the length of a cable, the SM200C is perfect for secure environments where USB is prohibited.
www.signalhound.com

Signal Microwave
Edge Launch Drop-in Replacement Connector

Signal Microwave's line of 2.92 mm, high performance, edge-launch connectors was designed for the thinner substrates being used today, typically between 5 and 10 mils thickness (0.127 to 0.254 mm) with dielectric constants from 3.0 to 3.5. Previously, high frequency board materials were around 30 mils thick, and the dielectric constants were lower, from 2.0 to 2.5. Signal Microwave can provide design support to optimize the interface on the board for best performance.
www.signalmicrowave.com

Skyworks
Front-End Module

Skyworks' SKY66404-11 2.4 GHz front-end module (FEM) is designed for Zigbee®, Thread and Bluetooth® (including low energy) ultra-low power IoT applications. Featuring high-performance in a compact package, SKY66404-11 provides increased efficiency, and more than 4× range extension over previous models. This FEM is ideal for applications spanning sensors, beacons, smart meters and thermostats, wireless cameras, smoke and CO detectors, and wearables including medical devices.
www.skyworksinc.com

Southwest Microwave Inc.
Board-Launch Connectors

Southwest Microwave offers high frequency vertical launch and end launch connectors that deliver unrivaled mechanical and electrical performance up to 110 GHz. For

design assistance to ensure optimal connector performance, including printed circuit board layout and 3D models for mechanical layout, visit Southwest Microwave at IMS2020 booth 2329.
www.southwestmicrowave.com

Spacek Labs
High-Power Amplifier SP392-35-33

Spacek Labs' solid-state, high-power amplifier, Model SP392-35-33, has excellent performance characteristics from 36 to 41 GHz. With a saturated output power greater than 33 dBm it is ideally suited for markets such as 5G. The unit has a nominal gain of 38 dB with VSWR less than 2:1 using 2.92 mm coaxial connectors. The amplifier requires a bias voltage of +8 VDC with 2.4A quiescent current and ~ 4A at 1 dB gain compression.
www.spaceklabs.com

SV Microwave
Waterproof Interconnects

SV Microwave offers a wide range of IP67 and IP68 waterproof interconnect products designed to withstand rigorous environments and harsh elements. SV's line of waterproof adapters include hermetically sealed connectors to 1×10 to 8, making them ideal for high pressure, vacuum applications and the prevention of liquid or gas leakage.
www.svmicrowave.com

Teledyne e2v
Microwave Data Converters

Join us at IMS2020 to see Teledyne e2v's demonstration of a recently announced microwave data converter enabling multi-band direct conversion up to Ka-Band and to see a demonstration of the company's advanced data converter synchronization techniques allowing accurately synchronized sampling of microwave antenna arrays. The Teledyne e2v EV12DS480 is the world's first K-Band capable DAC and it will be running a live demo displaying direct to Ka-band performance. Talk with Teledyne technical representatives about simplifying your microwave transmit systems using the EV12DS480.
www.teledyne-e2v.com

Times Microwave Systems
TLMP Connector

Harsh conditions demand a more rugged, durable design than the typical SMP/SMPM connectors. The Times Locking Miniature Push-On (TLMP) is ready to take on the challenge. TLMP connectors operate at up to 60 GHz. An interface O-ring provides a superb environmental seal. Designed with overlapping outer shields, the TLMP has improved electromagnetic interference (105 dB vs. 65 dB for similar), making it a durable, highly shielded alternative to SMP/SMPM designs.
www.timesmicrowave.com

Z-Communications
X-Band Surface Mount DRO

VENDORVIEW

The DRO11750A is a high performance

dielectric resonator VCO operating in the X-band with exceptional phase noise performance. It is designed to cover 11.75 GHz within 0 to 12 V of tuning and provides -104 dBc/Hz phase noise at 10 kHz offset. It operates off a 5 VDC supply while consuming 23 mA and delivers 0±3 dBm over -40° to 85°C. The DRO11750A can integrate into any radar system. Call Z-Communications to learn how this DRO can fit into your next project.
www.zcomm.com

NEW PRODUCTS

FOR MORE NEW PRODUCTS, VISIT WWW.MWJOURNAL.COM/BUYERSGUIDE
FEATURING VENDORVIEW STOREFRONTS

American Technical Ceramics
Ultra-Broadband Capacitor

ATC's new 560L ultra-broadband capacitor is manufactured with highest quality materials to provide reliable and repeatable ultra-broadband performance from 16 KHz through 40+ GHz. It exhibits ultra-low insertion loss, flat frequency response and excellent return loss and is ideal for D.C. blocking, coupling, bypassing and feedback applications requiring ultra-broadband performance. The 560L is a one-piece orientation-insensitive 0402 SMT package, fully compatible with high speed automated pick-and-place manufacturing. It is designed to meet the most stringent requirements of ultra-broadband applications.
www.atceramics.com

Berex
Front-End RFIC

The BFM4120 is a compact, multi-function front-end radio frequency integrated circuit (RFIC) intended for 802.15.4 ZigBee™/Thread, Bluetooth® Smart and proprietary ISM wireless protocol systems in the 2.4 GHz band. The BFM4120 is optimized for battery operation with enhanced efficiency, operating over a wide voltage supply range from 1.8 to 3.6 V, suited for a wide array of applications including battery-powered wireless systems, IoT/MK2M connectivity, industrial wireless sensor networks and wireless sensor nodes and networks.
www.berex.com

Comtech PST, Hill Engineering
Broadband Limiter

COMTECH PST, Hill Engineering announced the release of a surface mount technology, high power broadband limiter, which is capable of running from 0.1 GHz to 18 GHz. This solid-state, pin diode RF limiter is perfect to protect your receiver circuitry from the errant signal. The product is small in size, 0.65" × 0.7" and light weight, making it perfect for airborne applications.
www.comtechpst.com

Comtech PST
Solid-State Power Amplifier

COMTECH PST proudly introduces its latest development for the TWT/MPM replacement market covering the full 2000 to 6000 MHz band providing programable power control (in 0.1 dB Steps) up to 75 W linear power in a small, compact 6.75" × 3.5" × 1.7", 2.5 lbs. module. Designed for S & C Band datalink applications on UAV, fixed wing and rotary wing platforms. This solid-state power amplifier features highly efficient and reliable GaN solid-state technology, with >20 K hours mean time between failures, built in monitoring/protection circuits and operates from +28 VDC input.
www.comtechpst.com

Exceed Microwave
Group Delay/Phase Equalizer
VENDORVIEW

Do you ever have too much group delay variation in your passband? Exceed Microwave's waveguide group delay equalizer can distort the group delay with minimum impact on the amplitude. Provide us with the shape of your current group delay and we will inversely match the shape to help flatten out the overall group delay response.
www.exceedmicrowave.com

Fairview Microwave
High Frequency Bends, Twists and Straight Sections
VENDORVIEW

Fairview Microwave Inc. has introduced a new line of waveguide transmission components that are ideal for radar, satellite communication and airport security system applications. Fairview's new waveguide bends, twists and straight sections feature high frequency ranges from 90 to 220 GHz in three waveguide bands. These include waveguide sizes of WR-8, WR-6 and WR-5 and UG-387/U mod round cover style flanges.
www.fairviewmicrowave.com

Metropole Products Inc.
MUOS

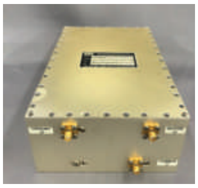

Upgrade your legacy UHF SATCOM to include MUOS, with the FMA-123. This compact unit has performance compatible with MUOS requirements, proven both in field and shipboard operations. Metropole also offers a host of other MUOS compatible units, to include low noise amplifiers, bandpass filters and diplexer/preamplifiers, just to name a few. Metropole Products can help you incorporate MUOS into your system.
www.metropoleproducts.com

MiniRF Inc.
Two Way Splitter
VENDORVIEW

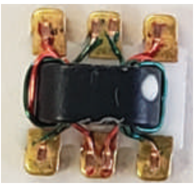

Featuring 1.8 GHz bandwidth and a minimum 30 dB isolation for 75 ohm applications with low insertion loss, this low cost miniature component splits/combines RF wideband signals while maintaining high RF performance. MiniRF offers highly repeatable performance with a low cost, surface mount component. These parts designed to operate over extreme temperature range -40° to 85°C with minimal variation. Do not delay and have mismatched signals in your circuit, contact us or RFMW for evaluation samples and support.
www.minirf.com

Narda Safety Test Solutions
Real Time Receiver

When connected to Narda's powerful real time receiver SignalShark, the ADFA 2 can precisely and reliably localize signals between 10 MHz and 8 GHz. This newly developed automatic DF antenna delivers extraordinarily stable measurement results in milliseconds. Additionally, it is insensitive to reflections. Its wide frequency range means that direction finding at low and high frequencies is covered equally. This makes the ADFA 2 particularly interesting for use by mobile network providers and regulatory authorities, as well as for military applications.
www.narda-sts.com

E LEARNING CENTER

Presented by: Microwave Journal

Webinars

NOW

5/6

TECHNICAL EDUCATION TRAINING

Optimizing Peak-to-Average Power Ratio for Wireless Systems

Sponsored by: Boonton, Tabor Electronics

5/13

TECHNICAL EDUCATION TRAINING

The Rebirth of HF

Sponsored by: Rohde & Schwarz

Now On Demand

Small Satellite System Architectures: Designing for Testability

Sponsored by: Rohde & Schwarz

Presented by:
Matt Hammond, NewSpace and Satellites Business Development Manager, Rohde & Schwarz

microwavejournal.com/events/1948

Practicalities of Building a 28 GHz Small Cell

Sponsored by: Knowles

Presented by:
Tim Brauner, Product Manager, Microwave Products Group, Knowles Precision Devices

microwavejournal.com/events/1947

Register to attend at mwjournal.com/webinars

FEATURED

e-Books

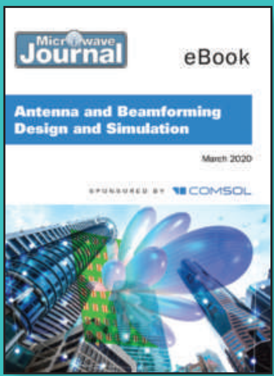

mwjournal.com/ebooks

New**Products**

RFE Inc.

V-Band Down-Converter

VENDOR**VIEW**

RFE Inc. has designed a convenient, cost-effective solution for translating 51 to 59 GHz signals into the 10 to 160 MHz domain. The incoming signals are converted to the IF Band using double-sided down-conversion. The down-converter can be tuned to any input center frequency in the range of 51 to 59 GHz by changing the mixer LO frequency from 12.75 to 14.75 GHz.

www.rfe-mw.com

Sanan Integrated Circuits

High-Performance GaAs Technology

New to Sanan IC's P15 family of high-performance 6" GaAs PHEMT foundry technologies, the P15EP1 is integrated with 0.15 µm gate length E-mode transistors (85 GHz FT, 155 GHz Fmax) for mmWave and 0.5 µm E-mode/D-mode devices for single-die logic implementation. Sanan IC also launched a family of GaAs PIN diodes, including the PINAB11 which features a 1.2 µm I-layer and 4 µm air bridge, and the polyimide-based PINPI11, a 3 µm I-layer suitable for RF switches and broadband limiters.

www.sanan-ic.com

Spinner GmbH

Compact Splitters

VENDOR**VIEW**

Spinner GmbH's new splitters and tappers have all of the ports in the same axis. This lets them be easily and securely installed in limited space. Finally, an end to symmetrical splitters with ports pointing in up to five different directions. More than anything, these splitters are characterized by compactness. They are significantly smaller than similar assemblies, making them easy to install in narrow conduits. Like their larger cousins, they support frequencies up to 3800 MHz and their power ratings are also respectable at up to 300 W.

www.spinner-group.com

Wright Technologies

Broadband LNA

Wright Technologies' improved broadband LNA Models ASL18B and ASL20B are 1 to 18 GHz, and 1 to 20 GHz LNA's that offer great broadband noise figures. The typical noise figure is below 2 dB while the maximum measured noise figures are at 2.5 dB and below. The available gain blocks are +25 dB at 120 ma. and +40 dB at 180 ma. The output P1dB is +17 dBm minimum and +19 dBm typical. The 3KK package dimensions are small and robust for a compact LNA.

www.wrighttec.com


ES MICROWAVE LLC.
Since 1985 we have offered our custom design filters and sub-assemblies in combline, interdigital and suspended-substrate technologies.
Broadband
Suspended-Substrate
Filters, Diplexers, Triplexers, Quadruplexers, Quintuplexers, Sextuplexers...
DC-40 GHz Filters
Multiplexers &
Switch Filter Banks
ES Microwave, LLC
8031 Cessna Avenue, Gaithersburg, MD 20879
P: 301-519-9407 F: 301-519-9418
www.esmicrowave.com

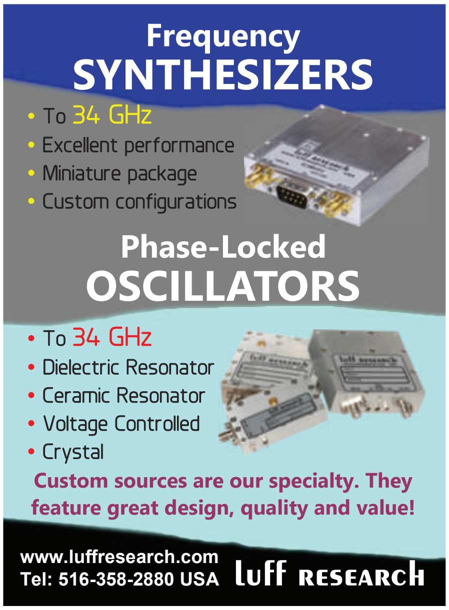
Frequency
SYNTHESIZERS
• To 34 GHz
• Excellent performance
• Miniature package
• Custom configurations
Phase-Locked
OSCILLATORS
• To 34 GHz
• Dielectric Resonator
• Ceramic Resonator
• Voltage Controlled
• Crystal
Custom sources are our specialty. They feature great design, quality and value!
www.luffresearch.com
Tel: 516-358-2880 USA
luff RESEARCH


Coatings For
EMI/RFI Shielding
Electrically Conductive
Elastomeric Systems
• X5SC
silver filled
• X5N
nickel filled
• X5G
graphite filled
MASTERBOND®
www.masterbond.com


FEATURED eBooks
Microwave Journal
eBook
Design Techniques and Considerations for GaAs and GaN RF and Microwave Devices
April 2020
qorvo
Check out this month's featured eBooks, online at
mwjournal.com/ebooks

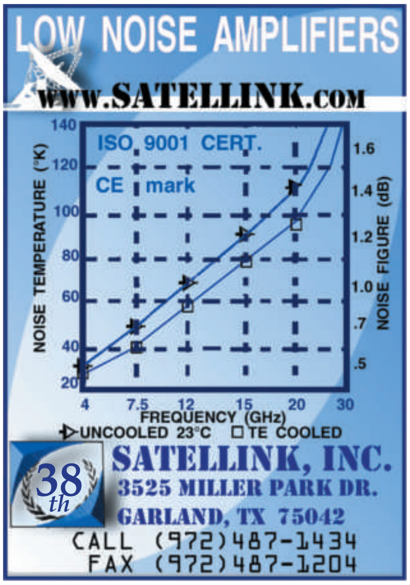
LOW NOISE AMPLIFIERS
WWW.SATELLINK.COM
ISO 9001 CERT.
CE mark
NOISE TEMPERATURE (°K)
NOISE FIGURE (dB)
FREQUENCY (GHz)
UNCOOLED 23°C
TE COOLED
38th
SATELLINK, INC.
3525 MILLER PARK DR.
GARLAND, TX 75042
CALL (972)487-1434
FAX (972)487-1204


SECTOR MICROWAVE
Don't sweat over your switching needs.
Our Waveguide and Coaxial switches are COOL!!
smi
(631)242-2300 PHONE (631)242-8158 FAX
WWW.SECTORMICROWAVE.COM


FEATURED eBooks
Microwave Journal
eBook
Antenna and Beamforming Design and Simulation
March 2020
COMSOL
Check out this month's featured eBooks, online at
mwjournal.com/ebooks

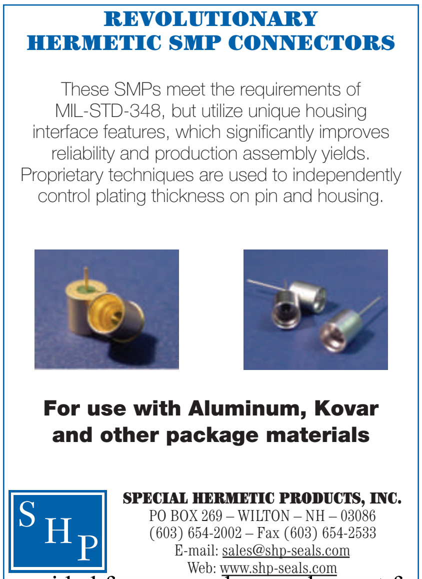
REVOLUTIONARY
HERMETIC SMP CONNECTORS
These SMPs meet the requirements of MIL-STD-348, but utilize unique housing interface features, which significantly improves reliability and production assembly yields. Proprietary techniques are used to independently control plating thickness on pin and housing.
For use with Aluminum, Kovar and other package materials
SHP
SPECIAL HERMETIC PRODUCTS, INC.
PO BOX 269 – WILTON – NH – 03086
(603) 654-2002 – Fax (603) 654-2533
E-mail: sales@shp-seals.com
Web: www.shp-seals.com

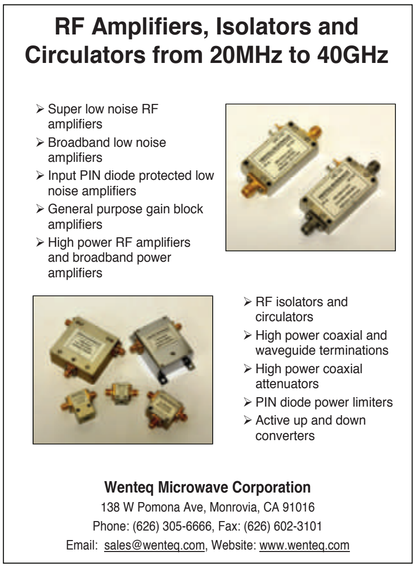
RF Amplifiers, Isolators and Circulators from 20MHz to 40GHz
➤ Super low noise RF amplifiers
➤ Broadband low noise amplifiers
➤ Input PIN diode protected low noise amplifiers
➤ General purpose gain block amplifiers
➤ High power RF amplifiers and broadband power amplifiers
➤ RF isolators and circulators
➤ High power coaxial and waveguide terminations
➤ High power coaxial attenuators
➤ PIN diode power limiters
➤ Active up and down converters
Wenteq Microwave Corporation
138 W Pomona Ave, Monrovia, CA 91016
Phone: (626) 305-6666, Fax: (626) 602-3101
Email: sales@wenteq.com, Website: www.wenteq.com

Implementing Full Duplexing for 5G

David B. Cruickshank

This exciting new book examines the feasibility of using a method of doubling the capacity of cellular networks by simultaneously transmitting and receiving signals at the same frequency, a process known as full duplexing (FD). To realize FD, changes in the hardware of the cell-base stations, relaying equipment, "hot spot" access points and mobile phones are necessary to prevent the hardware's transmitters from interfering with their own receivers. This requires looking at how to separate the strong transmitted signal from the very weak received signal, a process requiring both hardware (analog) changes and more complex digital signal processing. Different ways of achieving that goal are examined. The book reviews the merits of hardware changes involving new duplexing components that may be different depending on the frequency band and cell hardware being used.

Developing FD systems in 5G LTE cellular communications and what can be achieved with ferrite-based circulators in terms of size reduction and performance enhancement, especially at millimetric frequencies, is considered. The relative merits of ferrite and non-ferrite circulators are compared in terms of their fundamental materials and device technologies, such as isolation, insertion loss, bandwidth and non-linearity. FD in the entire 5G cell is also examined and its resulting range of equipment and device communication. This includes fronthauling, more sophisticated back and fronthauling, backhaul beam switching, and cell extenders and relays, all of which could involve FD.

To order this book, contact:

Artech House
www.artechhouse.com
Email: artech@artechhouse.com
US 800-225-9977
UK +44 (0)20 70596 8750

ISBN: 978-1-63081-695-7
300 pages
$159
£138

Use code CRU25 to receive 25% discount on this title! (expires 06/30/2020)


REGISTRATION NOW OPEN
EDI CON
2020
Electronic Design Innovation Conference
电子设计创新大会
COMING THIS FALL
China National Convention Center, Beijing, China
GO TO EDICONCHINA.COM TO REGISTER
5G/Advanced Communications
mmWave Technologies
Amplifier Design
EMC/EMI
Low Power RF and IoT
Front End Design
Power Integrity
Radar and Defense
RF and Microwave Design
Signal Integrity
Simulation and Modeling
Test and Measurement
www.ediconchina.com

Advertising**Index**

EXHIBITORS ARE HIGHLIGHTED IN GREEN

Advertising**Index**

Sales Representatives

Microwave Journal

Eastern and Central Time Zones
Carl Sheffres
Publisher
(New England, New York, Eastern Canada)
685 Canton Street
Norwood, MA 02062
Tel: (781) 619-1949
FAX: (781) 769-5037
csheffres@mwjournal.com

Michael Hallman
Associate Publisher
(NJ, Mid-Atlantic, Southeast, Midwest, TX)
4 Valley View Court
Middletown, MD 21769
Tel: (301) 371-8830
FAX: (301) 371-8832
mhallman@mwjournal.com

Pacific and Mountain Time Zones
Brian Landy
Western Reg. Sales Mgr.
(CA, AZ, OR, WA, ID, NV, UT, NM, CO, WY, MT, ND, SD, NE & Western Canada)
144 Segre Place
Santa Cruz, CA 95060
Tel: (831) 426-4143
FAX: (831) 515-5444
blandy@mwjournal.com

International Sales
Richard Vaughan
International Sales Manager
16 Sussex Street
London SW1V 4RW, England
Tel: +44 207 596 8742
FAX: +44 207 596 8749
rvaughan@horizonhouse.co.uk

Germany, Austria, and Switzerland (German-speaking)
WMS.Werbe- und Media Service
Brigitte Beranek
Gerhart-Hauptmann-Street 33,
D-72574 Bad Urach
Germany
Tel: +49 7125 407 31 18
FAX: +49 7125 407 31 08
bberanek@horizonhouse.com

France
Gaston Traboulsi
Tel: 44 207 596 8742
gtraboulsi@horizonhouse.com

Israel
Dan Aronovic
Tel: 972 50 799 1121
aronovic@actcom.co.il

Korea
Young-Seoh Chinn
JES MEDIA, INC.
F801, MisahausD EL Tower
35 Jojeongdae-Ro
Hanam City, Gyeonggi-Do
12918 Korea
Tel: +82 2 481-3411
FAX: +82 2 481-3414
yschinn@horizonhouse.com

China
Shenzhen
Michael Tsui
ACT International
Tel: 86-755-25988571
FAX: 86-755-25988567
michaelt@actintl.com.hk

Shanghai
Linda Li
ACT International
Tel: 86-021-62511200
lindal@actintl.com.hk

Beijing
Cecily Bian
ACT International
Tel: +86 135 5262 1310
cecilyb@actintl.com.hk

Hong Kong, Taiwan, Singapore
Mark Mak
ACT International
Tel: 852-28386298
markm@actintl.com.hk

Japan
Katsuhiro Ishii
Ace Media Service Inc.
12-6, 4-Chome,
Nishiiko, Adachi-Ku
Tokyo 121-0824, Japan
Tel: +81 3 5691 3335
FAX: +81 3 5691 3336
amskatsu@dream.com

Ed Kiessling • Traffic Manager • 685 Canton Street, Norwood, MA 02062 • Tel: (781) 619-1963 FAX: (781) 769-6178 • ekiessling@mwjournal.com

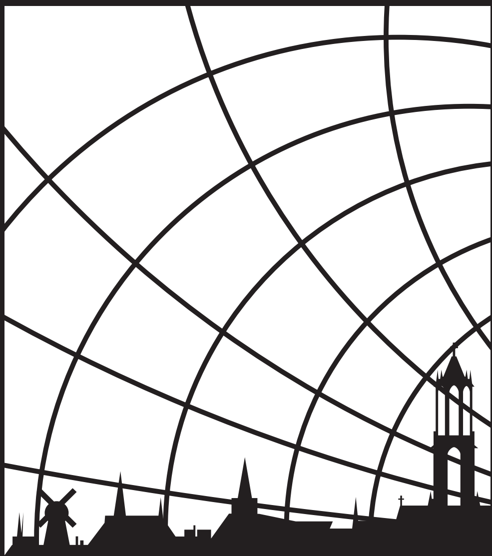

FABS and LABS

Cobham Advanced Electronic Solutions' Radar & EW Microelectronics

Meeting the growing A&D demand

Cobham Advanced Electronic Solutions Radar & EW Microelectronic Solutions facility is located in San Diego occupying 188,000 square feet of space with its seven buildings across the campus. The facility currently employs more than 1,000 people while running two shifts. The recently renovated and upgraded buildings were designed using Lean 3P (Production Preparation Process) principles to meet the growing demands of the U.S. air and surface fleet plus the research and development of next generation systems.

The large facility designs and manufactures a wide range of technology from custom MMICs to highly integrated digital receiver/exciter (DREX) RF/digital subsystems with sophisticated built in calibration functions. Their DREX products are designed utilizing a mix of direct analog and Direct Digital Synthesis (DDS) techniques that realize very fast settling time performance that are also phase coherent. These DREX products have low phase noise and spurious performance that enable the most sophisticated radars to be built.

Cobham's front-end diplexer and filters are combined with high power switches and limiters to produce antenna switching modules that protect high sensitivity receivers from a variety of undesired jamming techniques. Their high isolation filter products are used in wide bandwidth fast switching filter banks that enable low spurious frequency multiplier local oscillator generators to be produced. These low phase noise, low spurious signal generators enable advanced EW, radar and space platforms. They also produce front-end protection line replaceable units (LRUs) that allow sensitive systems to operate in the presence of jamming, as well as integrated high performance RF/microwave filters; all providing state-of-the-art phase noise and spurious performance. These are produced for a wide range of end markets including shipboard radar, aircraft (radar and EW), missiles and space. Many products are designed for demanding environmental conditions, temperature extremes, high shock and vibration applications and radiation (space/hypersonics).

The facility has more than 140 engineers performing RF/microwave/mmWave, MMIC, mechanical, digital and software design and development. They also have many engineers involved in process development, manufacturing and industrial engineering, and vertically integrated manufacturing development. The facility supports many processes including machining, plating, laser welding, substrate fabrication (thin film and Duroid), custom capacitor and inductor design and fabrication, surface mount assembly (pick and place, reflow, automated optical inspection), MIC chip and wire assembly (five assembly cells), automated epoxy and die placement, automated wire/ribbon bonding and hybrid/MIC automated optical inspection. They have 500+ tune and test benches, 16,000+ test assets and an environmental test facility. The location is certified to the AS9100 and MIL-PRF38534, Class H standards.

Cobham Advanced Electronic Solutions has been producing filters and integrated microwave assemblies for space applications for more than 20 years. The company is now combining their latest developments in multi-chip module (MCM) packaging and mmWave technology with their legacy technology to produce new products for emerging LEO and MEO space systems. Built on their legacy of radar and EW marque programs, the company is also developing technology in the areas of mmWave, Flip chip MCM, MMIC (GaN, SiGe, SOI) to support emerging platform capabilities in space, hypersonics and advanced EW.

Cobham Advanced Electronic Solutions' San Diego facility is constantly pushing A&D technology forward with the development of new advanced high frequency products and developing new processes and designs to meet the military's future needs. They are exploring new areas like hypersonics and low-cost space products as they continue to innovate.

www.cobhamaes.com

WERLATONE®

TEST & MEASUREMENT DIRECTIONAL COUPLERS

Up to 1000:1 Bandwidth ✦ Low Insertion Loss ✦ Covering DC to 6.5 GHz

Model	Type	Frequency (MHz)	Power (W CW)	Coupling (dB)	Insertion Loss (dB)	Mounting Style	Size (inches)
C1979	Dual	0.01-100	10000	60	0.10	LC-Female	12.0 x 6.0 x 4.5
C6021	Dual	0.01-1000	500	40	0.45	N-Female	6.7 x 2.27 x 1.69
C5725	Dual	0.1-1000	500	40	0.50	N-Female	5.2 x 2.67 x 1.69
C9688	Dual	1.0-1000	800	40	0.50	N-Female	6.0 x 2.2 x 2.2
C11744	Dual	20-1000	200	40	0.50	SMA-Female	1.75 x 1.16 x 0.56
C7734	Dual	30-2500	100	43	0.35	N-Female	3.5 x 2.6 x 0.7
C8188	Uni	30-3000	20	20	2.40	N-Female	6.0 x 1.5 x 1.1
C3910	Dual	80-1000	200	40	0.20	N-Female	3.0 x 3.0 x 1.09
C3908	Dual	80-1000	1500	50	0.10	7/16-Female	3.0 x 3.0 x 1.59
C7711	Dual	100-3000	100	40	0.35	N-Female	3.0 x 2.2 x 0.7
C7058	Bi	200-2000	200	10	0.30	N-Female	6.4 x 1.6 x 0.72
C8060	Bi	200-6000	200	20	1.10	SMA-Female	4.8 x 0.88 x 0.5
C7248	Bi	300-3000	100	6	0.35	N-Female	6.0 x 2.0 x 0.85
C8000	Bi	600-6000	100	30	0.40	SMA-Female	1.8 x 1.0 x 0.56
C10462	Dual	700-4200	250	40	0.20	N-Female	2.0 x 2.0 x 1.06
C10536	Dual	700-4200	1000	50	0.20	7/16-Female	2.15 x 2.0 x 1.36
C10006	Dual	700-4200	2000	50	0.20	7/16-Female	3.0 x 3.0 x 1.59
C10799	Dual	700-6000	100	40	0.20	N-Female	2.0 x 2.0 x 1.06
C10117	Dual	700-6000	250	40	0.20	N-Female	2.0 x 2.0 x 1.06
C10526	Dual	700-6000	300	40	0.20	N-Female	2.0 x 2.0 x 1.06
C10364	Dual	700-6000	500	50	0.20	7/16-Female	2.15 x 2.0 x 1.36
C10614	Dual	700-6000	500	60	0.20	7/16-Female	2.15 x 2.0 x 1.36
C10996	Dual	700-6000	700	50	0.20	7/16-Female	2.15 x 2.0 x 1.36
C11555	Dual	700-6000	1000	50	0.20	7/16-Female	2.15 x 2.0 x 1.36
C10695	Dual	700-6500	500	50	0.20	7/16-Female	2.15 x 2.0 x 1.36
C8644	Bi	1800-6100	60	20	0.40	SMA-Female	1.1 x 0.75 x 0.48
C10746	Dual	2000-6500	500	50	0.20	7/16-Female	2.15 x 2.0 x 1.36

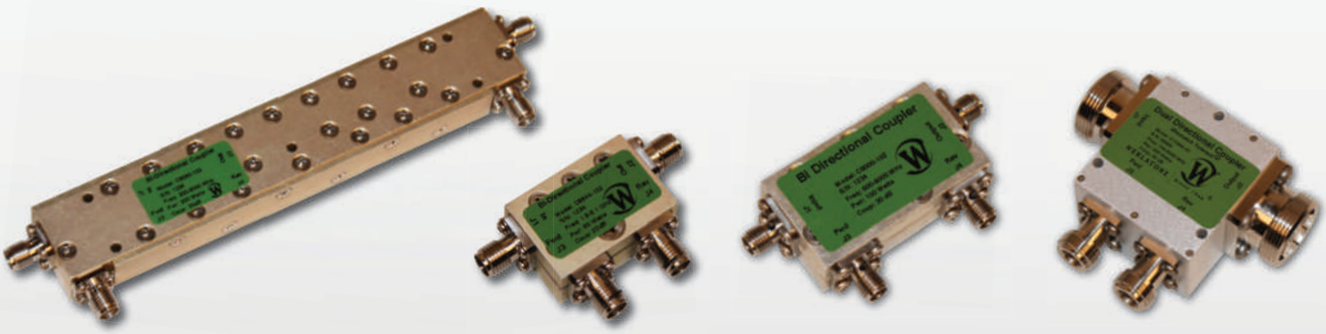

Werlatone, Inc. 17 Jon Barrett Road Patterson, NY 12563 T 845-278-2220 sales@werlatone.com www.werlatone.com all around you

A Comprehensive Guide to mmWave Solutions

A CURATED SELECTION OF ARTICLES:

- Featured GaN & GaAs products
- Tech briefs for high-performance GaN & GaAs design
- Tech requirements for defense & aerospace applications

Qorvo's New Products for mmWave Applications

Setting the New Standard for Innovation and Performance

CMD304
Distributed amplifier
- Frequency range: DC-67 GHz
- Package: Die

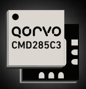

CMD285C3
Voltage variable attenuator
- Frequency range: DC-20 GHz
- Package: 3x3 mm QFN

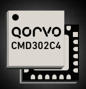

CMD302C4
SP4T Non-reflective switch
- Frequency range: DC-20 GHz
- Package: 4x4 mm QFN

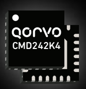

CMD242K4
Distributed amplifier
- Frequency range: DC-40 GHz
- Package: 4x4 mm QFN

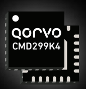

CMD299K4
Low noise amplifier
- Frequency range: 18-40 GHz
- Package: 4x4 mm QFN

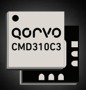

CMD310C3
Sub-harmonic mixer
- Frequency range: 20-32 GHz
- Package: 3x3 mm QFN

CMD297P34
Analog phase shifter
- Frequency range: 5-18 GHz
- Package: 3x4 mm QFN

CMD312
Fundamental mixer
- Frequency range: 4-28 GHz
- Package: Die

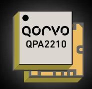

QPA2210/QPA2210D
7W Ka-band GaN PA
- Frequency range: 27-31 GHz
- Package: 5x5 mm QFN/Die

QPA2211/QPA2211D
14W Ka-band GaN PA
- Frequency range: 27-31 GHz
- Package: 15x15 mm Cu Bolt Down/Die

QPA2212/QPA2212D
25W Ka-band GaN PA
- Frequency range: 27-31 GHz
- Package: 15x15 mm Cu Bolt Down/Die

QPA2610
2W X-band GaN PA
- Frequency range: 8.5-10.5 GHz
- Package: 5x5 mm QFN

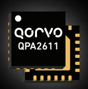

QPA2611
5W X-band GaN PA
- Frequency range: 8-12 GHz
- Package: 5x5 mm QFN

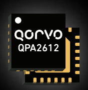

QPA2612
12W X-band GaN PA
- Frequency range: 8-12 GHz
- Package: 5x5 mm QFN

Connect with Qorvo®

Sign-up to stay in the loop on Qorvo's latest news.

www.qorvo.com/go/subscribe

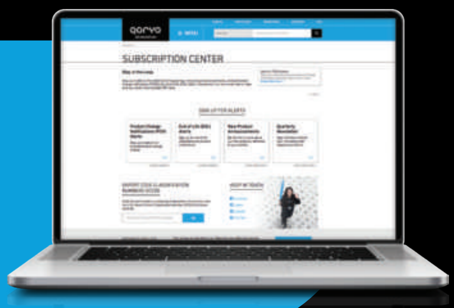

Ka-Band Satcom Trends and Power

The ever-expanding appetite for data is driving strong growth in satellite communications (satcom), especially in higher-frequency bands. But, instead of concentrating on the lower frequency ranges, many companies are focusing on higher frequency Ka-band which provides more allocated spectrum for applications such as internet access and 5G.

Operating in Ka-band creates new challenges in RF power amplification due to an increase in video bandwidth requirements and the need for high linear power to support multi-carrier systems. Thanks to advances in semiconductor technology, GaN PAs have increased performance and are now an attractive alternative to high-power vacuum tube amplifiers.

This article provides insights into current satcom trends and approaches to Ka-band power amplification.

Satcom's Changing Role in Global Communications

Satcom equipment plays a vital role in the daily lives of people across the world. It supports a broad variety of applications in telecommunications, weather monitoring, aeronautical communications, maritime and military uses, as well as navigation. Satcom in commercial aviation has satisfied the need to be always connected with in-flight connectivity services.

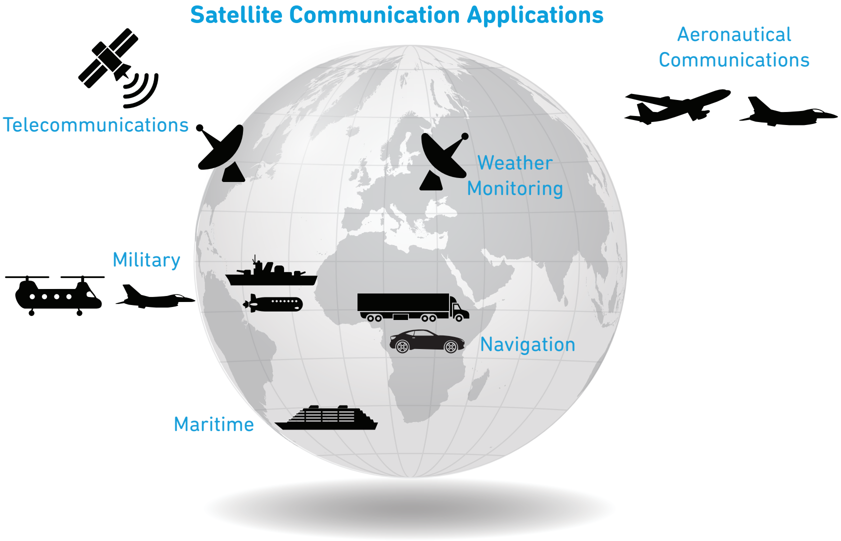

The explosive growth in consumer data traffic, 5G, big data and artificial intelligence will further propel the global expansion of satellite systems and services – according to Strategy Analytics – which forecasts the market will grow at 5.4% a year to reach more than $93.6 billion in 2028.

This growth is driving change across the satcom landscape, with some companies planning huge constellations of high-throughput satellites to support the demand.

Ka-Band's Leading Role in Satcom

Responding to the increasing demand, the satcom industry has moved to higher-frequency bands, where more bandwidth is available. In the Ka-band, 3.5 GHz of bandwidth is available for satcom – over 4x more than in other commonly used bands. It's become widely used, especially for uplink (earth-to-satellite) connectivity.

The below table describes the bands used in the Satcom industry. In the Ka-band, many high-profile users include startups like Elon Musk's SpaceX and Amazon's Project Kuiper. These two organizations are planning to launch thousands of small satellites to provide high-speed internet access to consumers and businesses worldwide – including coverage for remote and underserved areas that are beyond the reach of other broadband services. Moreover, there are other organizations following a similar path to take advantage of the new revenue streams opened by the satcom market.

Satcom Bands

Satcom Frequency Band	Satcom Frequency Range	Satcom Bandwidth	Description
C-Band	5.85-6.425 GHz	575 MHz	Primarily used for satellite communications, full-time satellite TV networks or raw satellite feeds.
X-Band	7.9-8.4 GHz	500 MHz	Used for satcom uplink, military satcom. Also used in radar applications.
Ku-Band	13.75-14.5 GHz	750 MHz	Used for satcom uplink. Fixed satellite services & broadcast satellite services.
K-Band	17.3-21.2 GHz	3,900 MHz	Used for satcom downlink. Fixed satellite services & broadcast satellite services.
Ka-Band	27.5-31 GHz	3,500 MHz	Used for satcom uplink, military satcom, 5G telecommunications.

Because the Ka-band supports many revenue streams like stationary and mobile equipment, including satellite gateways, airborne and marine systems, and portable satcom man-packs, it is a key band to exploit.

Ka-Band Uplink Power Amplification Challenges

Ka-band transmission creates RF power amplification challenges: satcom equipment must be capable of transmitting at high power over wide bandwidth while maintaining high linearity. Also, the modulation schemes are increasing to enable more transmission data bits per second. Traditionally, QPSK modulation satisfied the tradeoff of data throughput versus signal noise. However, the recent push for higher modulation schemes in the 16 to 64 quadrature amplitude modulation (QAM) is driving the need for higher performance linear amplification.

Traditionally, traveling wave tube amplifiers (TWTAs), a type of vacuum tube, have been the mainstay for power amplification in satcom applications because of their ability to produce high power while maintaining high efficiency.

Advances in GaN semiconductors are changing that trend. This is in part due to RF performance improvements, though it is also attributed to robustness and reliability in comparison to tube amplifiers. Solid state power amplifier customers combine many of the latest GaN power amplifiers to achieve 100W+ of RF output power, making GaN an attractive alternative instead of TWTAs.

The figure to the right shows a typical satcom RF configuration using a GaN PA.

VSAT - Ka-Band

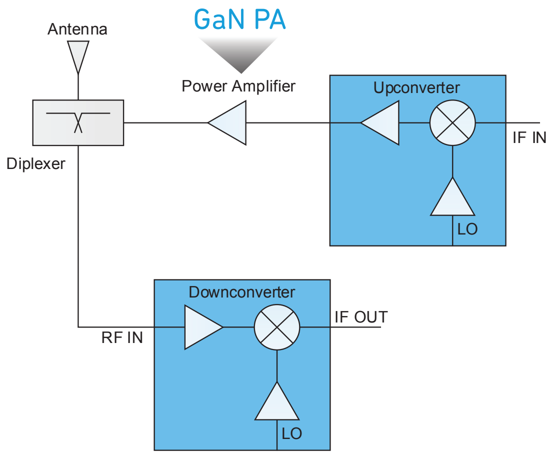

LEOs and Phased Arrays

GaN PAs are also well matched to a major change in satcom architecture: the shift from single antennas to phased arrays of multiple antennas. This change is taking place both on satellite and within ground terminals.

Some of the most ambitious new applications use thousands of satellites in low earth orbit (LEO) – 100-500 miles above earth's surface – much closer to earth than most traditional satellites. See figure on the following page. A big advantage of LEO is lower latency – roughly 20 ms round-trip – which is vital for applications like internet access.

LEO satellites orbit the earth much more rapidly than satellites at higher orbits – traveling from horizon to horizon in only 15 minutes. To maintain continuous communication links with these satellites, earth-based equipment must track them as they zoom across the sky.

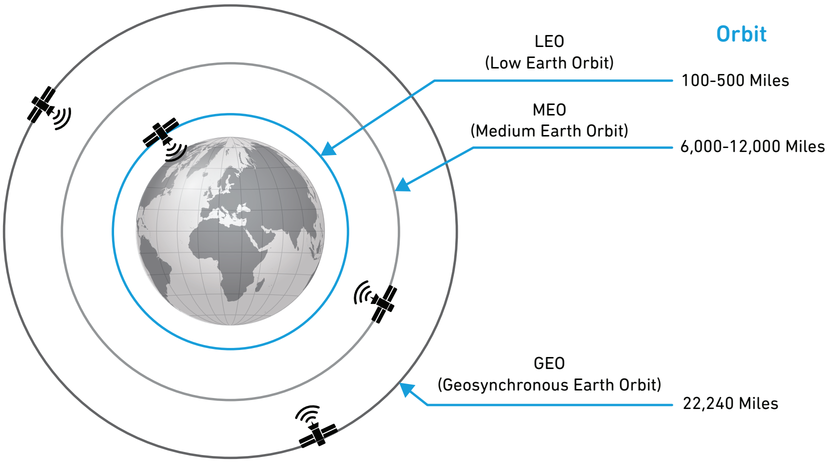

This creates a new challenge. Traditionally, earth-based satcom equipment has used mechanically steered antennas to track satellites. But this approach isn't practical for LEO satellites due to the potential wear-and-tear on a system that has to sweep from horizon to horizon every 15 minutes; the maintenance and upkeep for the equipment needed to support very large LEO constellations would likely break the bank.

Electrically steered phased arrays avoid this problem, because they eliminate the need for mechanical movement to track satellites. Instead, these phased array systems have many small antennas that can continuously change the direction of the signal by adjusting the phase of the individual antennas within the array.

While designs based on a single TWTA were well suited to high-power single-antenna systems, designs based on GaN PAs are a natural match for multi-antenna phased arrays. GaN also makes it possible to build a system that's lower-cost, lighter and more compact.

Designing the Future: More Linear Power, Higher Frequencies and Even Greater Bandwidth

Looking to the future, satcom architectures are in a state of change. Higher linear power over wider bandwidths is the present trajectory in the Ku/K/Ka-bands. System operators are moving even higher in frequency to V-band (40-75 GHz) where bandwidth is even greater than Ka-band. As Ka-band was once a frontier in satcom, it is now an established and strong market segment with many operators and equipment providers. V-band is viewed as the new frontier in satellite communications. With the continued innovation we have seen across the satellite industry, the duration from adoption to maturity in V-band could be faster than anyone expects. It is expected that GaN will play in this higher frequency market as well.

Qorvo GaN technology is rapidly evolving to address the satcom market. Successive GaN generations offer increasing linear power output, with improvements in efficiency, enabling equipment manufacturers to use GaN PAs for more high-power applications that traditionally would have required TWTAs. The growing power capability per GaN PA also means equipment makers can build amplifiers with fewer GaN devices, resulting in a lower-cost solution to deliver the required power. More powerful devices help to make systems smaller, simpler to build and more reliable.

Qorvo offers a wide range of GaN devices for satcom ground-based applications and satellites. Some newly developed products recently added to our portfolio are shown below.

Part Number	Features	P_{SAT}	PAE	Small Signal Gain
QPA2210/QPA2210D	27-31 GHz	> 38.4 dBm	> 32%	25 dB
QPA2211/QPA2211D	27-31 GHz	> 41.5 dBm	> 34%	26 dB
QPA2212/QPA2212D	27-31 GHz	> 43.4 dBm	> 25%	22 dB

Foundry or Research Laboratory?

Where Innovation Comes to Life.

Qorvo's 30 Years of Foundry Service Produces Market-Changing Defense and Small Business Innovations

Maintaining a US based foundry is critical for the DoD, our country's defense primes and our key partnerships because it continues to fuel new technology, innovations and maturation of processes. Advancing technologies and manufacturing products in high volume not only helps drive costs down but brings new technologies into the commercial space – as we are seeing with 5G.

We sat down with Senior Director of Research Vijay Balakrishna to discuss Qorvo's foundry, its history and why it has a crucial role in the company's strategy.

Q1: Qorvo's Legacy in RF Innovations – Particularly its Foundry Services – has a Considerable History. Tell us about the Key Milestones.

Qorvo has been a main supplier of gallium arsenide (GaAs) for multiple markets since 1985. Our GaAs (III-V) semiconductor roots stem from several technology companies that came together to form Qorvo.

Altogether, it's been more than three decades of supporting a wide variety of customers with foundry services. We provided GaAs MESFET in the 1980s, pHEMT in the 1990s, gallium nitride (GaN) in the 2000s and we've continued advancing GaAs and GaN technology. Some may think of GaAs as antiquated but really, it's all around us, in airplanes and satellites for example, and just as necessary as ever – even for future 5G technology. We have also expanded foundry services to acoustic filters – surface and bulk acoustic wave (SAW, BAW) filter technologies – benefiting both the defense and commercial markets.

The Qorvo Manufacturing facility in Richardson, TX is fully accredited by the US DMEA as a Category 1A "Trusted Source".

Back in 2005, we worked with the defense advanced research projects agency (DARPA) on its wide bandgap semiconductors RF program (WBGS-RF) to advance critical GaN transistor technology for X-band radar and wideband EW applications. Since then, we've met challenging wideband monolithic microwave integrated circuit (MMIC)-level performance metrics in power, efficiency and bandwidth. Besides being the first to release the 0.25-micron GaN technology (GaN25) in 2008, and offering it as a foundry service in 2009, we were also the first to reach a 65-volt process for GaN. From UHF to Q-band, Qorvo's GaN product line has continued maturation, achieving manufacturing readiness level (MRL) 10 through the DoD's Title III GaN program.

Q2: Since the Merger Between TriQuint and RFMD, there have been some Misperceptions that Qorvo No Longer has an Open Foundry. Is the Foundry Open?

Yes, the foundry is open to strategic customers. We typically work with large defense companies and government research organizations, and we also work with small businesses and universities on research ideas. We engage with many labs, like DARPA, that pursue challenging initiatives and advanced functions that involve creating new designs, running tests and exploring "what if" scenarios on particular technology nodes.

When we have the availability, we're open to working through new designs and innovations and produce both custom and standard products. We also provide wafer and chip options for prototyping.

Q3: What are the Driving Factors of Qorvo's Foundry Services?

Working in lockstep with our customers affords us a hands-on perspective regarding new technology needs and use cases – from 3-5 years to 10 years and beyond. They're the canary in the coal mine, giving us the inside view into future research and shaping the products we develop.

For instance, DARPA's advanced research projects look at needs 10-20 years out. They're driving technology and programs with the future in mind. One example – what do we do with silicon (Si) after Moore's Law, how do we get more out of our chips?

The Army, Air Force, Navy and other research labs look 5-10 years out; the defense primes work approximately three years out. For small businesses and universities, it's hard to say. Their timelines really vary, depending on the customer and the needs of the industry.

Q4: You've Talked about the Technologies – GaN, GaAs, and the BAW/SAW Acoustic Filters – Produced in the Foundry. Why do your Foundry Customers come to Qorvo?

We see our customers evaluating four key services:

For our defense and DoD-based customers, US-based foundries are a critical resource. These organizations are looking for a secure, trusted environment in which to design, develop and test new ideas and technologies. We're proud to offer a DoD-accredited Trusted Source (Category 1A) facility, that has achieved manufacturing readiness level (MRL) 10.

Another service that we offer is a wide breadth of technology with the scalability to meet customer needs. We're one of the few companies that can scale rapidly to manufacture GaAs, GaN and BAW acoustic filters. The ability to scale also provides the benefit of driving production costs down.

In addition to providing quality and reliability, we do cost walkthroughs with our customers to make their solutions affordable. They give us a price point; we make recommendations on how to achieve their cost targets. We work with our customers to reduce test times, improve yields and deliver additional services or packaging. We also discuss specifications and volume needs to drive the costs to the next level of assembly.

Last but not least, we're the only vertically integrated foundry of its kind. This means we offer additional services like packaging, on-wafer tests, visual inspections, and extended foundry services all under one roof. Offering this variety of services is unique – including the ability to process wafers, die, components, packaging, provide consulting, run testing, grow the epitaxy.

Q5: Earlier you Mentioned that Qorvo Provides a Variety of Extra Services for Strategic Foundry Customers. What are some of these Services?

Our services are bucketed into a few different categories:

One is assembly and packaging technologies. Many customers prefer integrated, cost-effective packaging designs – so we offer various high-reliability RF packaging options including ceramic, plastic epoxy packaging, military-grade and high-grade custom metal packaging – all produced in house. Our automated microwave module assembly (AMMA), located in our Texas facility, is where we perform assembly functions. With the addition of die-attach equipment, we fabricate, test, package and ship die-level devices to customers from one secure location.

Another is design consulting. We have world-class researchers and designers available to engage with our customers. It's common that we may recommend small changes to design or custom testing to improve circuit performance or reduce variations and sensitivity. We offer consultations on electronic parameters and can adjust manufacturing characteristics, such as how we test and analyze a new product. We talk with our customers in great detail about our processing capabilities, to understand their needs and provide guidance regarding which processes will work best in their design.

Another service offered is technical assistance – various options in our processes and data acquisition analysis for customers to make better choices with their circuits. For example, the types of transistors, number of capacitors, allowable configurations for interconnect, different capabilities for on-wafer tests, inspection criteria, delivery characteristics are all areas we may offer insight. Our customer base produces highly differentiated products and we help them achieve that.

At times, our customers are looking for a secure foundry space in which they can either choose to develop new designs and technologies, while still maintaining their own IP – with the option to utilize Qorvo senior research fellows and designers for their expertise, or not.

Q6: What are some Significant Technologies that the Foundry has Produced?

One significant achievement is when we were working with a large defense prime contractor on an emergent need for the US Army. We were able to quickly ramp to scale, successfully respond to our customer's needs, and field the technology, thus, working to save lives in Afghanistan.

Another example is within space communications, most recently New Horizons. That mission was notable because it sent the first high-resolution pictures of Pluto and its moons back to Earth, nine years after launching. There's some remarkable history here – including that our space-qualified technology accompanied other explorations like the Curiosity Rover on Mars and the Cassini-Huygens spacecraft near Saturn as well.

We've had more than 250,000 Qorvo components launched in space, for more than three decades – aboard orbital payloads, such as communications and navigation satellites, including programs which support broadband data, telecommunications and global positioning services.

Qorvo has pioneered and perfected many of today's processes with GaN, GaAs and other materials that enable the most powerful RF modules on the market. Notably, GaN – matured through a defense funding model – is now extending data rates and operating frequencies for commercial 5G networks, more than ever envisioned for mobile wireless communications. These foundry-produced innovations are possible due to years of tests, proven reliability in harsh environments, and focus on quality. With a thriving foundry, and more than three decades of innovation under its belt, we're always looking to the future and new research developments.

Qorvo's headquarters in Greensboro, NC is also a design, sales, support center and GaAs/GaN manufacturing facility.

GaN-on-SiC is Driving Advances in Radar Applications

New and increasingly sophisticated threats are driving requirements for radar systems that deliver more instantaneous bandwidth, greater resolution, longer range and multi-beam function.

Traditionally, radar systems have had short pulse widths, narrow instantaneous bandwidths and relatively small duty cycles (e.g., 100 us pulse width and 10% transmit duty cycle). Today, there are requirements across all radar bands for 3x to 5x longer pulse widths and ≥ 50% duty cycle. In some cases, the requirements have been for near-continuous wave operation. Radar system requirements are pushing for more RF output power per element with minimal change in cooling requirements.

To support these system level requirements and reduce system operating costs, the RF hardware must have higher transmit output power and power-added efficiency (PAE), better thermal dissipation and lower receive path noise figure.

How These System Requirements Relate to the RF Module

A challenge for the component supplier is translating system-level needs to component-level capabilities. Generally, higher transmit power and lower receive noise figures equate to greater range and higher resolution – the radar can "see" a smaller target farther away and give the operator more time to react.

The downside of higher power along with near-continuous wave operation is more dissipated heat. In order to reduce the impact of increased heat on performance, the components must have better thermal dissipation and higher PAE. The desire for increased instantaneous bandwidth means more complex design, increased losses and sacrifices in performance that could be achieved in a narrower frequency band application.

Component Technologies

A mix of LDMOS (lower frequency operation), GaAs, SiGe and GaN products are being used in radar systems. LDMOS technology is mature, has high PAE and power density for the transmit path, and good thermal dissipation, but generally only supports relatively narrowband operation at S-band and below. LDMOS generally has lower recurring costs for the component level but requires board-level matching and additional surface mount components. Fully matched LDMOS components for radar applications are rare on the open market.

SiGe technologies allow for large-scale integration of RF and DC functions, low power operation, small component size and wide bandwidths, higher frequency bands and lower recurring costs. In contrast, SiGe has low power density and high non-recurring costs. In the receive path, SiGe components have higher noise figures than both GaN and GaAs technologies. The SiGe technology is well suited for low-power, shorter-range radar applications, signal control functions, large-scale phased arrays and/or high-volume applications.

Mature GaAs high electron mobility transistor (HEMT) technologies can support the bandwidth and the higher frequency bands, but have lower power density compared to GaN. GaAs HEMT remains a viable solution for both transmit and receive components where lower transmit power per element is viable and receive chain noise figure is key.

GaAs HEMT gate lengths continue to decrease, allowing for lower noise figures, which improves the radar resolution, range and sensitivity. Smaller gate lengths may improve RF performance, but the cost is ESD sensitivity and input power survivability. When higher transmit power is required, the GaAs HEMT device solution is to increase gate periphery by adding gates or by increasing the individual gate width. Increasing individual gate widths will limit the operating band of the device and stress the manufacturability of the product. Adding gates to the FET stack complicates the matching circuit, increases design and manufacturing risks and adds insertion loss.

GaN-on-SiC HEMT technologies have higher power density compared to GaAs HEMT, support wider bandwidths in all the operating bands of interest, use a thermally superior substrate (SiC) and are quickly being adopted by the radar markets as the PA solution of choice.

With the higher power density, matching circuit combining structures are simpler and lower loss vs. GaAs HEMTs. Like LDMOS, GaN operates at higher voltages compared to GaAs and SiGe. GaN-on-SiC HEMTs are viable solutions for high input power, robust LNAs. The noise figure of the GaN device is the similar to a GaAs LNA with an input protection limiter.

Qualitative Technology Comparison

	GaN-on-SiC	GaAs	LDMOS	SiGe
Function	Tx PA & Rx LNA	Tx PA, Rx LNA, RF signal control	Tx PA	Rx LNA & RF signal control
Operating Voltage	High	Low	High	Low
Power Density	High	Low	High	Low
Operating Frequency	All bands	All bands	S-band and below	All bands
Bandwidth	Wide	Wide	Narrow	Wide

The Need for a New Approach

To meet new radar system demands, the products being designed today must meet tougher size, weight, power and cost (SWaP-C) requirements, and have higher PAE, lower channel temperatures and lower noise figures. SWaP-C is especially important in air and space-based systems where physical space and weight are at a premium.

Higher PAE translates to less prime power, lower cooling requirements and lower operating costs. Specifically, in X-band, there are products now on the open market that are pushing >40% higher efficiency with 3 GHz of bandwidth. At L- and S-band radar frequencies, PAEs were in the 50% to 60% range for a discrete GaN HEMT – now products are pushing to 75% and higher. Multi-stage S-band MMICs are approaching 60% efficiency. In the past, these products were not available commercially due to technologies and design capabilities.

The SiC substrate used for GaN is the ideal enabler for the transmit portion of next-generation radars. SiC has higher thermal conductivity when compared with GaAs or Si. GaN-on-SiC transistors can operate at a higher channel temperature than GaAs or LDMOS transistors for the same mean-time-to-failure value.

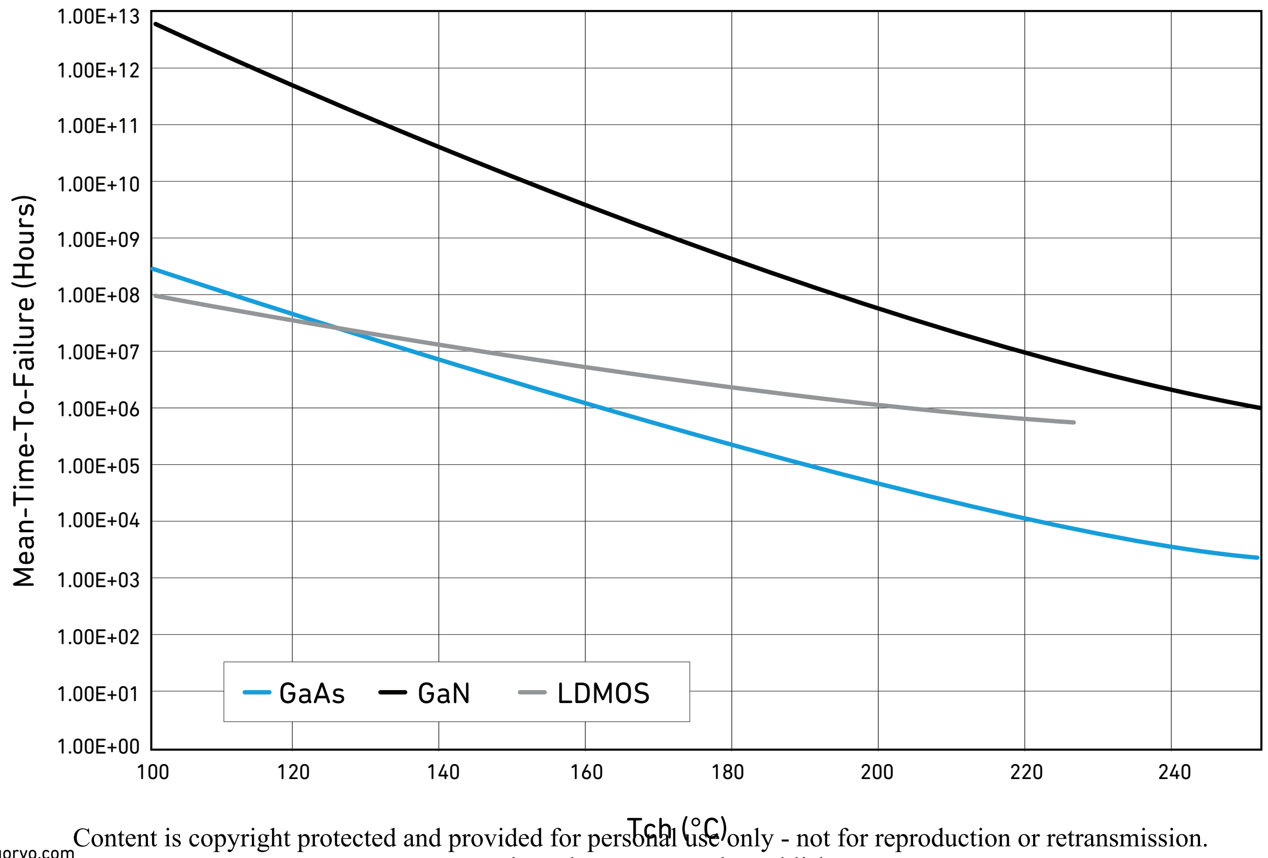

GaN transistors have operating voltage capability that is 2-5X higher than GaAs transistors. GaN operates between 20V and 50V. Higher operating voltages mean lower I^2*R losses are possible. Higher voltage operation also means fewer voltage step conversions between the power supply and the RF devices. These advantages translate to size reductions, less weight, fewer components, lower cost and increased system performance.

GaN offers a 3-5X increase in power density versus GaAs and even greater increase vs. SiGe. Increased power density means fewer components and size reductions.

From a radar antenna pattern perspective, when the equivalent isotropically radiated power (EIRP) remains constant, the PA power per channel increases as the number of elements in the array decrease. More transmit power can translate to fewer elements, smaller size and less complexity.

Use of GaN-on-SiC technology also opens the door to a range of manufacturing options with SWaP-C benefits:

- High thermal conductive materials for die attach and assembly, for increased thermal dissipation (weight and power)
- Direct Cu attach vs. CuMoly or CuW composites, for the highest thermal conductivity is possible

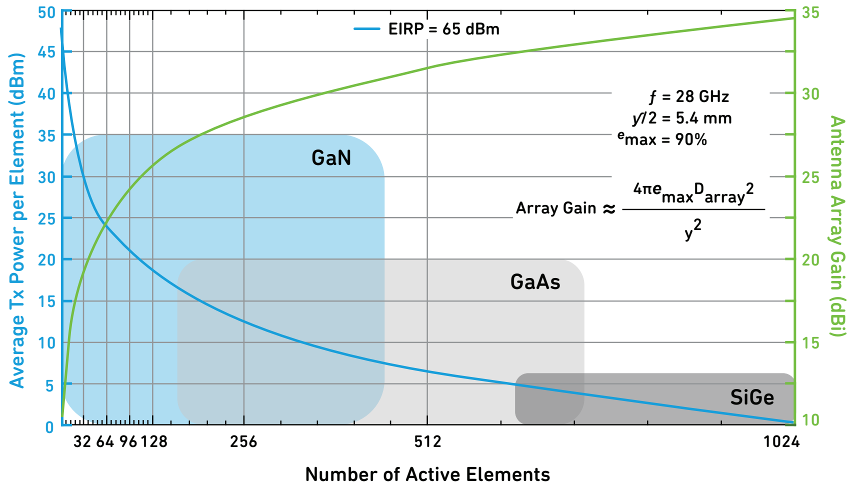

Integration of the PA and LNA into a single, front-end module (FEM) further reduces unit size and number of components. For example, designers working with traditional radar architectures often have five to seven components per channel plus all of the associated peripheral resistors and capacitors.

Replacing the traditional RF Tx/Rx module with an integrated GaN-only FEM or GaN/GaAs FEM reduces the number of components to one. This is a significant change in the BoM complexity of the board, simplifying designers' efforts to place the component closer to the antenna to reduce loss and provide higher dynamic range. Designers can create higher-density arrays and achieve greater range for the same power budget.

When the FEM is combined with a SiGe or GaAs "core" circuit, further component count reduction can occur. The core chip can replace the phase, attenuation and control circuits for one or more radar elements, depending on the radar architectures. It is feasible to see a greater than 50% component reduction for a 4-channel sub-array with the right combination of GaN, GaAs and SiGe.

Below are a few examples from Qorvo of newer GaN-on-SiC products where high PAE, continuous wave operation and SWaP-C were primary design requirements in order to support next-generation military and civilian radar applications:

The Qorvo QPA1022 high-performance power amplifier supports X-band phased arrays. Built on the company's 0.15 um GaN-on-SiC process (QGaN15), this amplifier is an integrated, 4x4x0.85 mm package that can support tight lattice spacing requirements for phased array radar applications. In this PA, GaN technology enables best-in-class PAE of 45% at 4 watts RF power in the 8.5-11 GHz range. This is an increase in efficiency by 8% over previous products while providing 24 dB large signal gain.

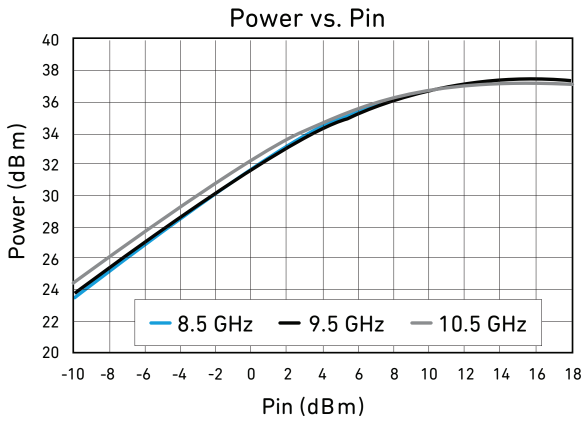

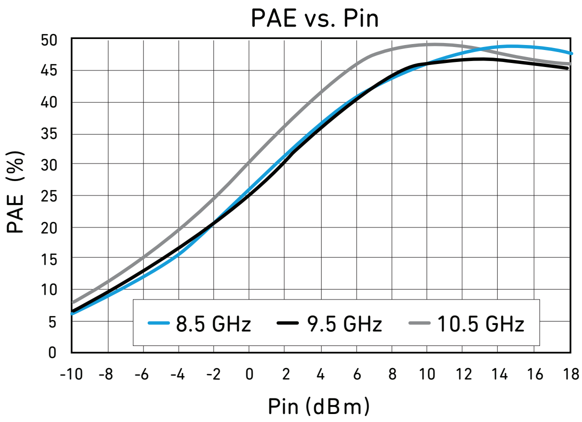

The Qorvo QPD1006 supports 1.2-1.4 GHz frequency L-band applications and is capable of continuous wave operation at high voltages – 45V CW and 50V pulsed. Since it is fully matched to 50-ohms at the input and output, it supports a smaller module design and fewer components on the system board vs. the typical footprint for an unmatched FET design. The design has 55% drain efficiency for CW operation; 62.2% pulsed operation, with > 300 W CW power and > 450 W pulsed power.

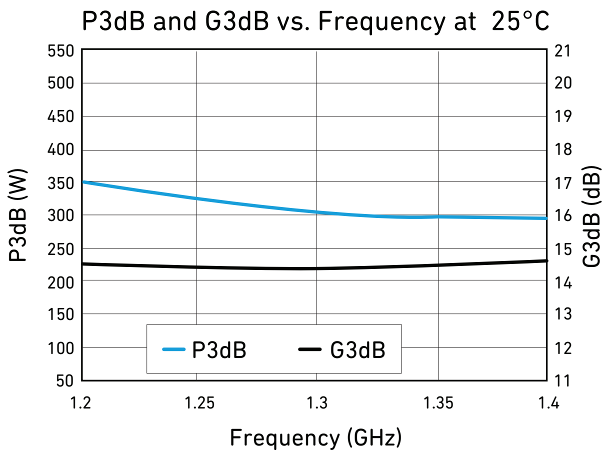

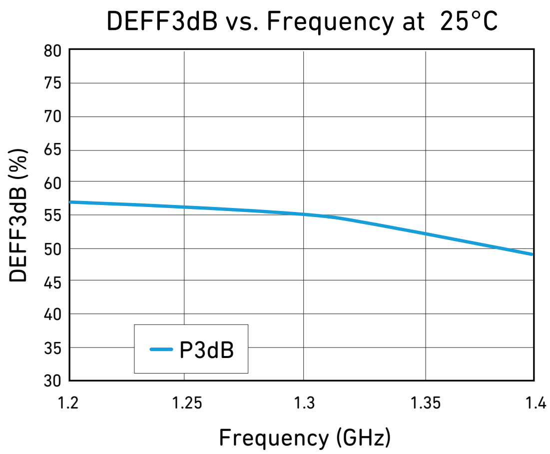

Looking Ahead

To meet and defeat a new generation of threats, defense radars must leverage sophisticated RF technology to achieve higher efficiencies and greater bandwidth.

Designers are turning to GaN technology to deliver these operational enhancements, as well as SWaP-C improvements that are critical in the harsh, space-constrained environments where these systems operate. While GaN may be a relatively young technology compared to others, it continues to mature as a process and adopted for radar applications.

Further, marrying GaN PAs with GaAs LNAs into single front-end modules creates highly integrated, multifunction components that provide advanced capabilities. System operating and manufacturing costs reduce as component count reduces and PAE increases. These capabilities translate into maximum power with minimum heat, higher reliability and lower cost of operation.

Model-Based GaN PA Design Basics

GaN Transistor S-Parameters, Linear Stability Analysis & Resistive Stabilization

Introduction

S-parameter matching is used to maximize gain and gain flatness in simple linear RF/microwave amplifier designs. This same S-parameter data is used to develop matching networks that address amplifier stability. This article discusses the importance of using modeling for basic S-parameter and stability analyses in the GaN PA design process. It introduces the use of models and resistive stabilization techniques to help avoid device instabilities that can affect nonlinear and linear simulations.

In this article, we focus our attention on a simple two-port stability analysis derived from linear S-parameter calculations. We will use a nonlinear Qorvo GaN power transistor model from the Modelithics Qorvo GaN Library, in combination with simulation templates and keysight advanced design system (ADS) software.

Stability Explained

Stability refers to a PA's immunity from possible spurious oscillations. Oscillations can be full power, large-signal problems, or subtle spectral problems that might go unnoticed if not properly analyzed. Even unwanted signals outside your intended frequency range can cause system oscillations and gain performance degradation.

There are two types of stability and measures to analyze PA stability in your system.

- Conditional stability – a system design that is stable when the input and output see the intended characteristic impedance Z0 (50 ohms or 75 ohms) but may be subject to oscillations (exhibiting a negative resistance at the input or output port) for some other input or output impedance.

- Unconditional stability – a system that is stable in any possible positive real impedance inside of the Smith Chart. Note, that any system design can oscillate if it sees a real impedance that is negative (outside the Smith Chart). But generally speaking, if a system is defined as unconditionally stable, it is stable at all frequencies (where the device can have gain) and all positive real impedances.

Measures of stability

Let's begin with the well-known "k-factor" and stability measure "b" to determine frequency ranges that cause instability at a given bias. These are given by the following equations[1]:

$$k = \{1 - |S_{11}|^2 - |S_{22}|^2 + |S_{11}*S_{22} - S_{12}*S_{21}|^2\} / \{2*|S_{12}*S_{21}|\}$$

and

$$b = 1 + |S_{11}|^2 - |S_{22}|^2 - |S_{11}*S_{22} - S_{12}*S_{21}|^2$$

Unconditional stability is indicated by k > 1 and b > 0.

However, because this criterion requires two parameters to check for unconditional stability, a more compact formulation is given with the following "mu-prime" parameter[2]:

$$mu\_prime = \{1 - |S_{22}|^2\} / \{|S_{11} - conj(S_{22})*Delta| + |S_{21}*S_{12}|\}$$

If mu_prime > 1, it indicates unconditional (linear) stability.

Matching and tuning to attain stability

As noted above, S-parameter data is used to develop matching networks to attain amplifier stability. Figure 1 shows a single-stage amplifier configuration and the key parameters that affect gain and stability. In the unconditional stability region, maximum gain is achieved by setting Γ_s and Γ_L to conditions attaining a simultaneous conjugate match at both ports.[1]

Single-stage amplifier configuration showing key parameters affecting gain and stability calculations

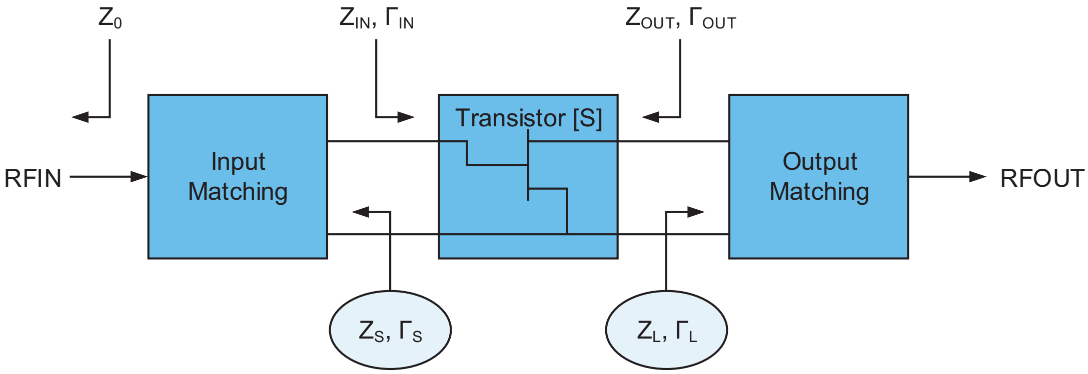

Figure 1.

Linear Stability Analysis

Stability measurements of untuned transistor

Let's consider an example. Figure 2 shows a simulation setup for linear S-parameter analysis of the nonlinear model for Qorvo's T2G6003028-FS GaN HEMT device, included in the Modelithics Qorvo GaN Model Library.

Setup with no stabilization added

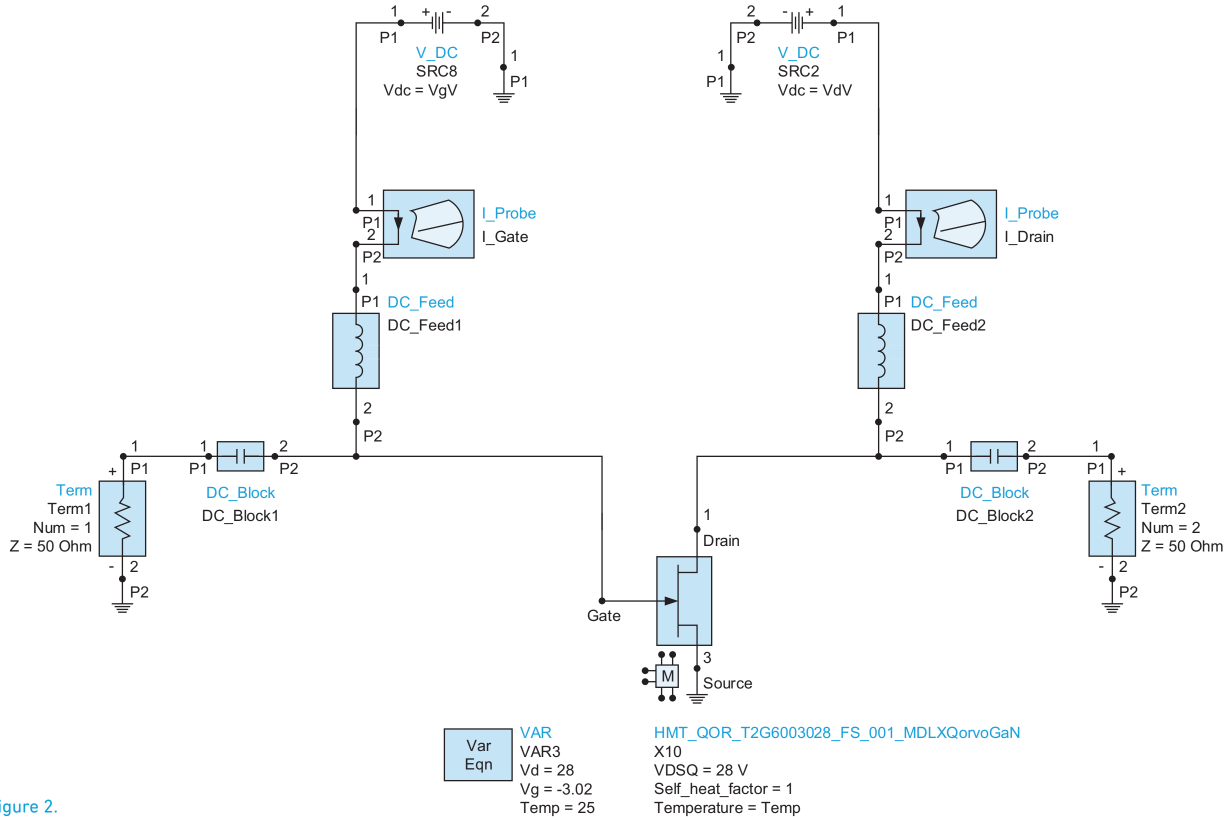

Figure 2.

Note: Bias condition for all simulations in this note is set to Vds = 28 V, Vgs = -3.02 V, which corresponds to a drain current of approximately 200 mA.

In the schematic above, icons represent parameters that can be calculated from device S-parameters, including stability k, b and mu_prime. The “MaxGain1” parameter is the maximum available gain. The “MaxGain1” parameter calculates the maximum available gain for frequency ranges where the device is unconditionally stable, and displays a value that is termed the maximum stable gain. This is calculated as simply |S21|/|S12| for regions of conditional stability.

Figure 3 shows the MaxGain1 parameter, the 50 ohm gain (S_{21} in dB) and stability factor k, measure b and mu_prime calculated from the schematic of Figure 2 (at m5). This plot shows that the stability measure b is > 0 and stability factor k > 1. The stability measurement parameters show a clear break point at about 1.85 GHz (m5). This is the transition frequency between conditional and unconditional stability regions. For 3.5 GHz the maximum gain indicated by this simulation parameter is approximately 18.4 dB (marker m3 in Figure 3). Note: The maximum available gain goes to 0 dB at about 10.4 GHz; this frequency is referred to as the maximum frequency or f_{max}. It is also a good practice to analyze stability from a very low frequency to at least f_{max}, which is why the frequency range for this example was set to sweep from 25 MHz through 12 GHz.

From this analysis, we can conclude the following:

- The device is unconditionally stable above 1.85 GHz.
- Frequencies below 1.85 GHz device are conditionally stable.

These S-parameters produced from the schematic simulation (Figure 2) are show in Figure 4. S_{11} and S_{22} are displayed on Smith Charts, while polar charts are used for S_{21} and S_{12}.

Notice the large difference between the gain for 50 ohm input and output ($|S_{21}|$ in dB) and the MaxGain1 value. This is due to the mismatch associated with S_{11} and S_{22} in a 50 ohm system.

Gain and maximum gain (left) and stability metrics (right)

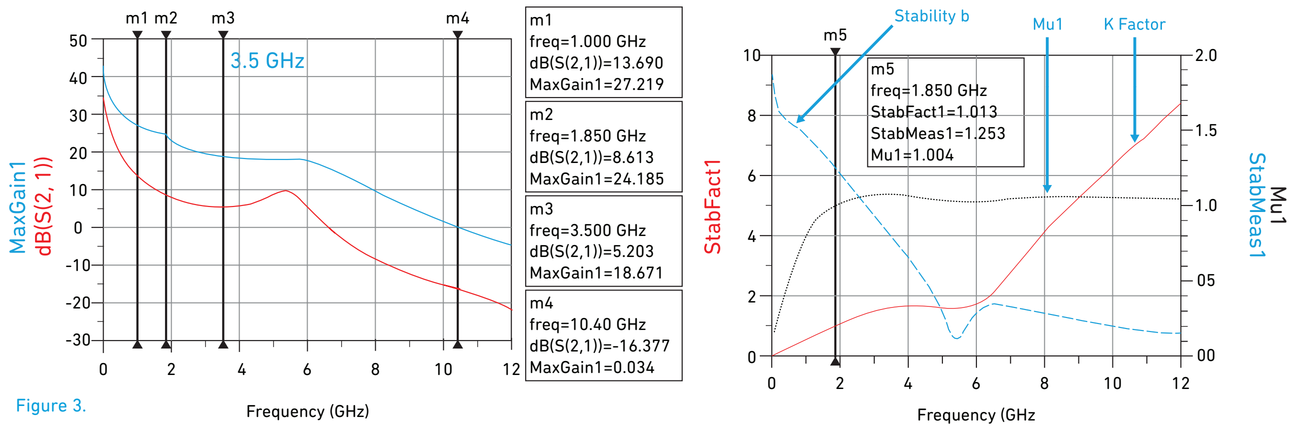

Figure 3.

Plotting the stability circles in the input and output planes provides additional insight. Also included in the schematic of Figure 2 are the icons for “S_StabCircle” and “L_StabCircle”, which correspond to calculations of stability circles in the input and output planes.

The meanings of these circles can be described as follows. In the case of the input stability circle at 25 MHz, indicated by marker 14 in Figure 5, each point along that circle represents a Γ_s value that will result in a Γ_{out} value equal to 1 according the following relation.

$$\Gamma_{out} = S_{22} + S_{12}{}^*S_{21}{}^*\{ \Gamma_s / (1-S_{11}{}^* \Gamma_s)\}$$

Eq. 1

S-parameters plotted from setup of Figure 2

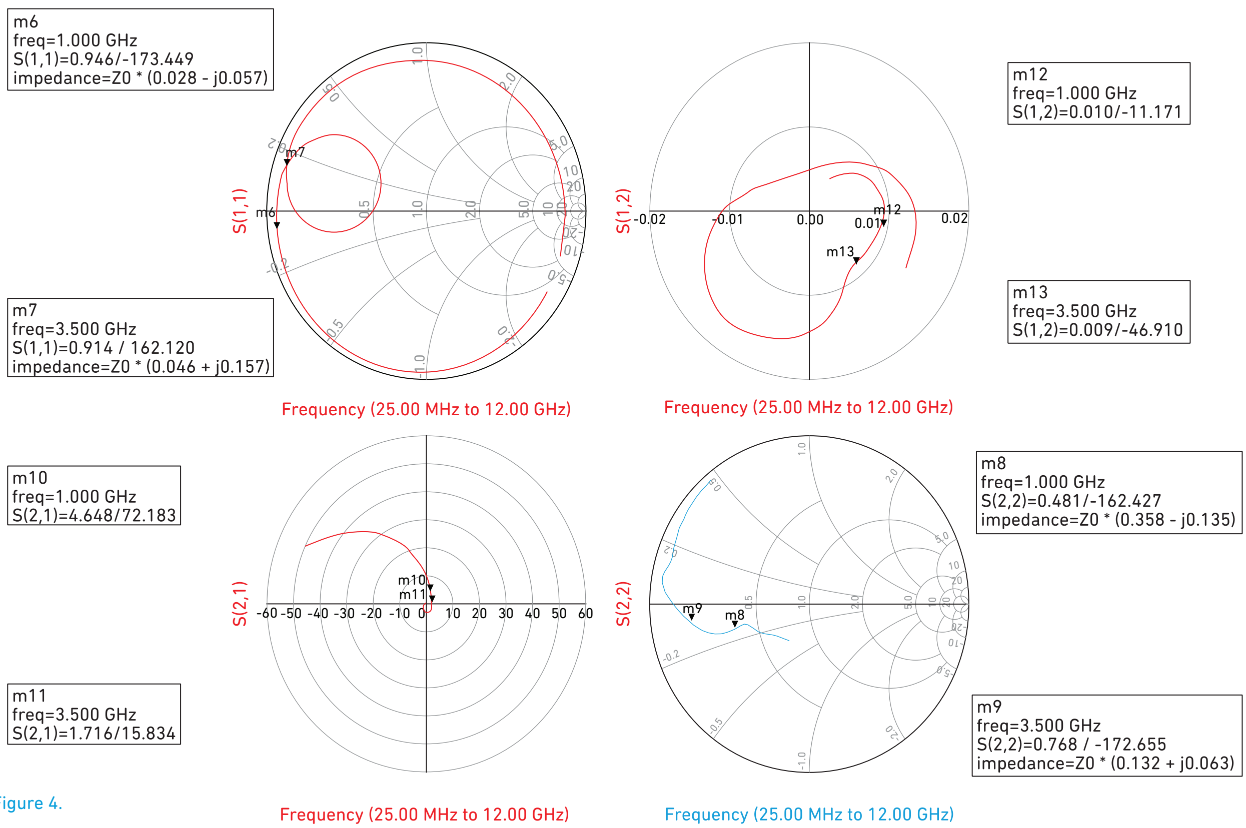

Figure 4.

This circle sets a boundary between $\Gamma_{out} < 1$ and $\Gamma_{out} > 1$, the significance of which is that $\Gamma_{out} > 1$ corresponds to a negative resistance at the output port, which is a condition that can lead to an oscillation. The question then becomes whether the inside or outside of the circle is the unstable ($\Gamma_{out} > 1$) region. A quick check in the case of $\Gamma_s = 0$, which is the 50 ohm point. Note from Eq. 1, for this case $\Gamma_{out} = S_{22}$, which is less than 1 at all frequencies being analyzed here. From this, we can conclude the outside of the circle is the stable region and the inside is the unstable region.

The explanation of the output stability circles is basically the same, except here we are plotting circles of points for Γ_L for which $\Gamma_{in} = 1$, according to the Eq. 2. By a similar argument, we can conclude that it is the inside of the circles plotted on the right side of Figure 5 that correspond to the unstable regions. Note - the frequency plan of Figure 2 was reduced to show fewer circles in Figure 5 for clarity.

$$\Gamma_{in} = S_{11} + S_{12} * S_{21} * \{\Gamma_L / (1 - S_{22} * \Gamma_L)\}$$

Eq. 2

Stability circles - the source (left plot) and load (right plot) reflection coefficient reference planes

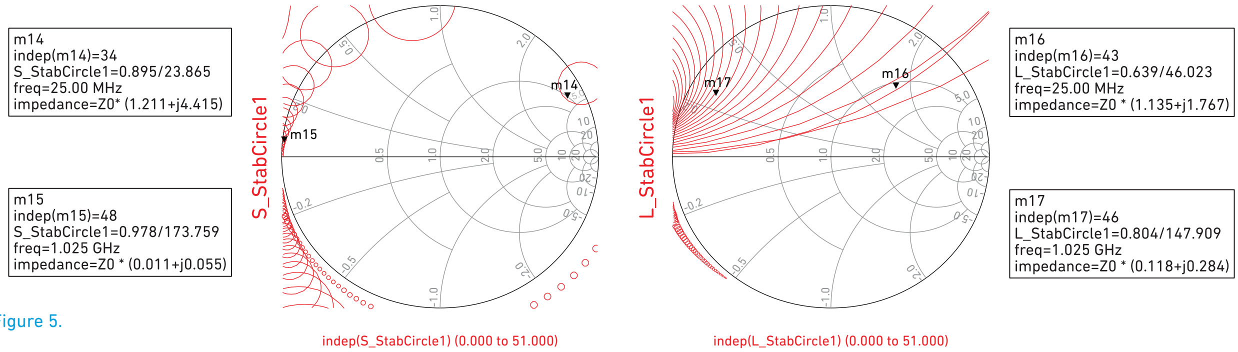

Figure 5.

Linear Stability Analysis

So, what if a device does not meet the requirements for unconditional stability, like in our example for frequencies below 1.85 GHz?

There are multiple matching methods to help stabilize your circuit. In this article we describe two methods. One is resistive and the second is frequency-dependent stabilization.

- Resistive: uses matching resistors to provide stabilization
- Frequency-dependent: uses resistors, inductors and capacitors to provide stabilization

Resistive stability for microwave PA design

Matching resistors can be employed in our example to help stabilize high-gain, low-frequency transistors in most microwave applications. These resistors can be series or shunt at the input or the output, can be in the parallel feedback loop, or included in the bias networks. For PAs, we want to maximize output power, so it's best to avoid resistors in the output network. Feedback amplifiers are outside the scope of this post, so we will concentrate on the series and shunt resistors in the input network.

Figure 6 shows where both series and shunt resistors have been added in the input network. The values are tuned to achieve unconditional stability over the entire 0.025 to 12 GHz frequency range. The resulting stability measurements are plotted in Figure 7. These show the transistor has unconditional stability over the entire frequency range. Note, however, fmax dropped from 10.3 GHz to about 8.75 GHz. Comparing the maximum gain estimation in Figure 7 (design frequency of 3.5 GHz [12.3 dB]) with Figure 3 achieved without this stabilization (18.4 dB), we can see we have incurred a 6 dB degradation in maximum available gain. This is caused by adding a purely resistive input stabilization network. The S-parameters of the resistively stabilized device are displayed in Figure 8, with the overlaid S-parameters of the non-stabilized device. We can see that S_{11} and S_{12} have been affected over the entire frequency range, and S_{21} is also reduced with only minimal change in S_{22}. It is gratifying to observe in Figure 9 that with the resistive stabilization network added, the stability circles are now all outside of the Smith Chart in both the source and load-planes.

Setup with resistive stabilization

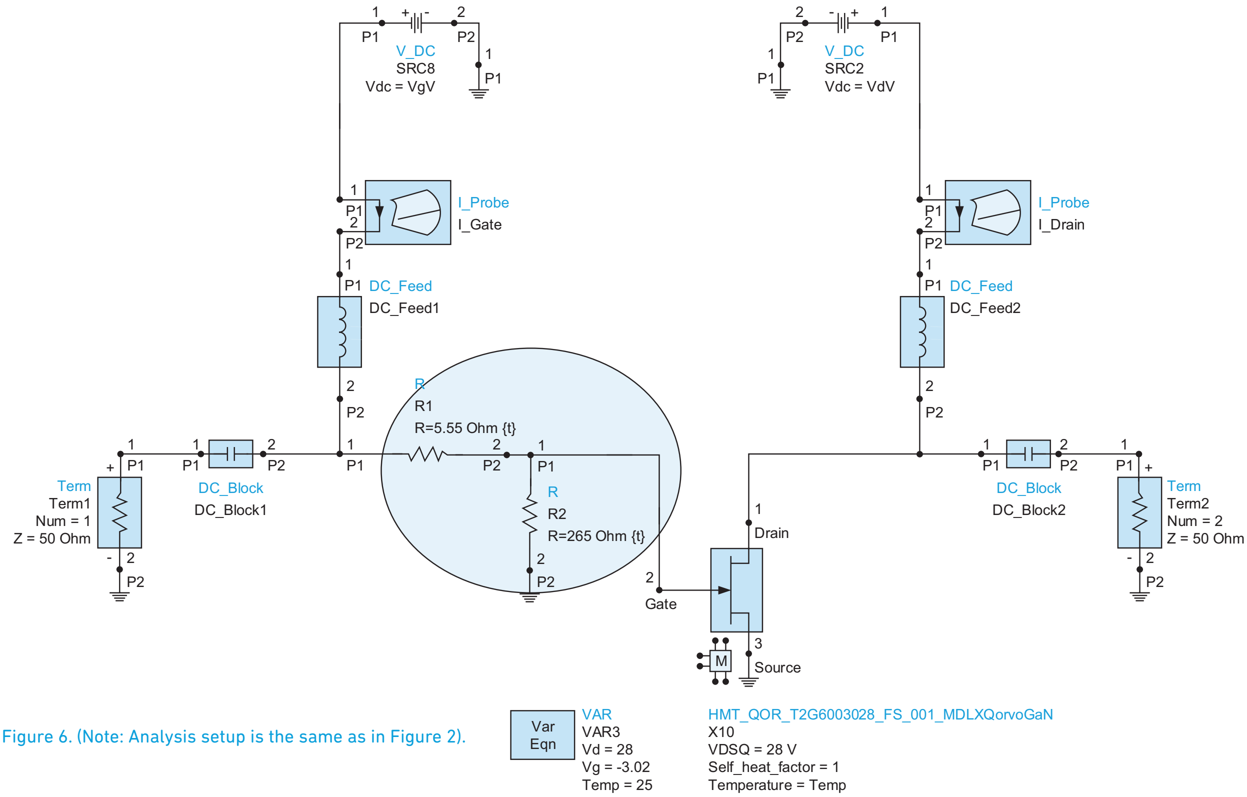

Figure 6. (Note: Analysis setup is the same as in Figure 2).

Resistively stabilized - gain and maximum gain calculated by ADS (left) and stability metrics (right)

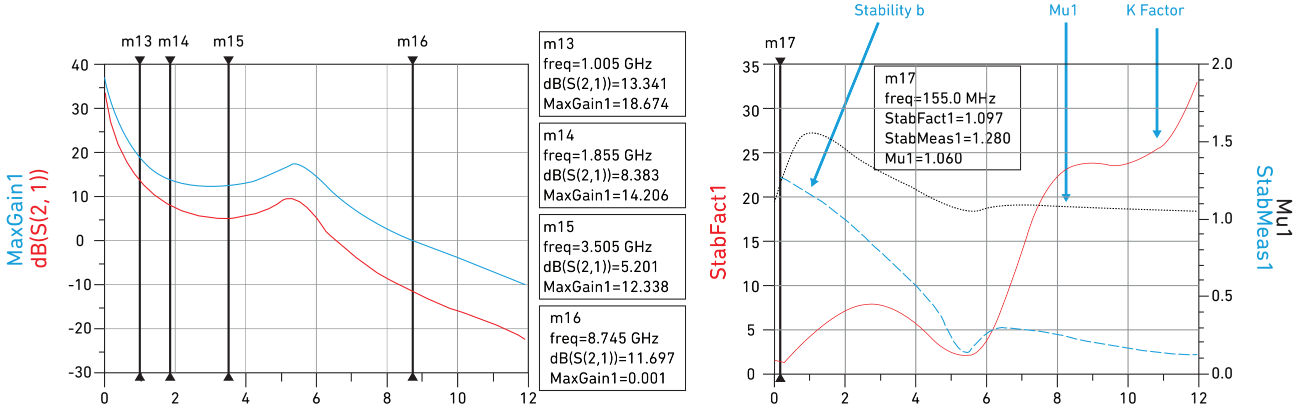

Figure 7.

S-parameters for resistively stabilized schematic versus the non-stabilized device

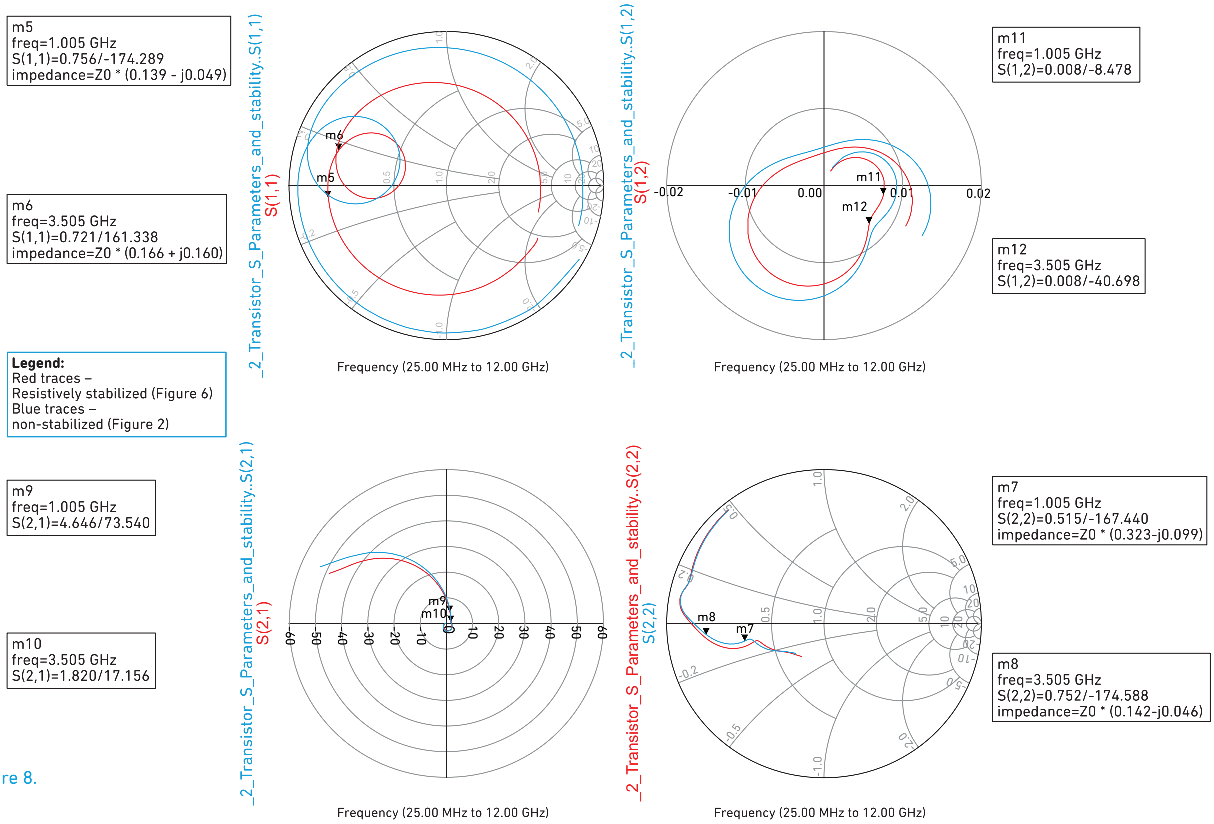

Figure 8.

Stability circles - the source (left plot) and load (right plot) reflection coefficient reference planes for resistively stabilized device (Figure 6)

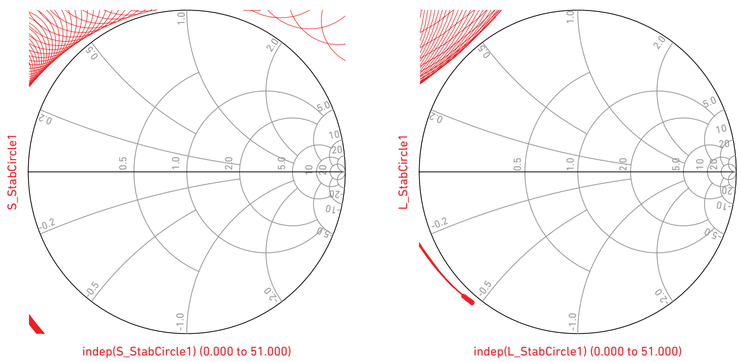

Figure 9.

Frequency-dependent resistive stability

If the design frequency is above 1.85 GHz (e.g., 3.5 GHz), we can implement a frequency-dependent resistive approach using the series-shunt stabilization network. Let's see if we can mitigate the above gain penalty using this approach.

In Figure 10, a resistor (R1) has been incorporated into a modified gate bias network. Additionally, a capacitor (C3) has been placed across the series stabilization resistor (R1). The value of this capacitance can be tuned to adjust what frequency the series resistor (R1) is - effectively shorting it out (making it not "seen"). This can help increase the available gain.

Setup with frequency-dependent stabilization

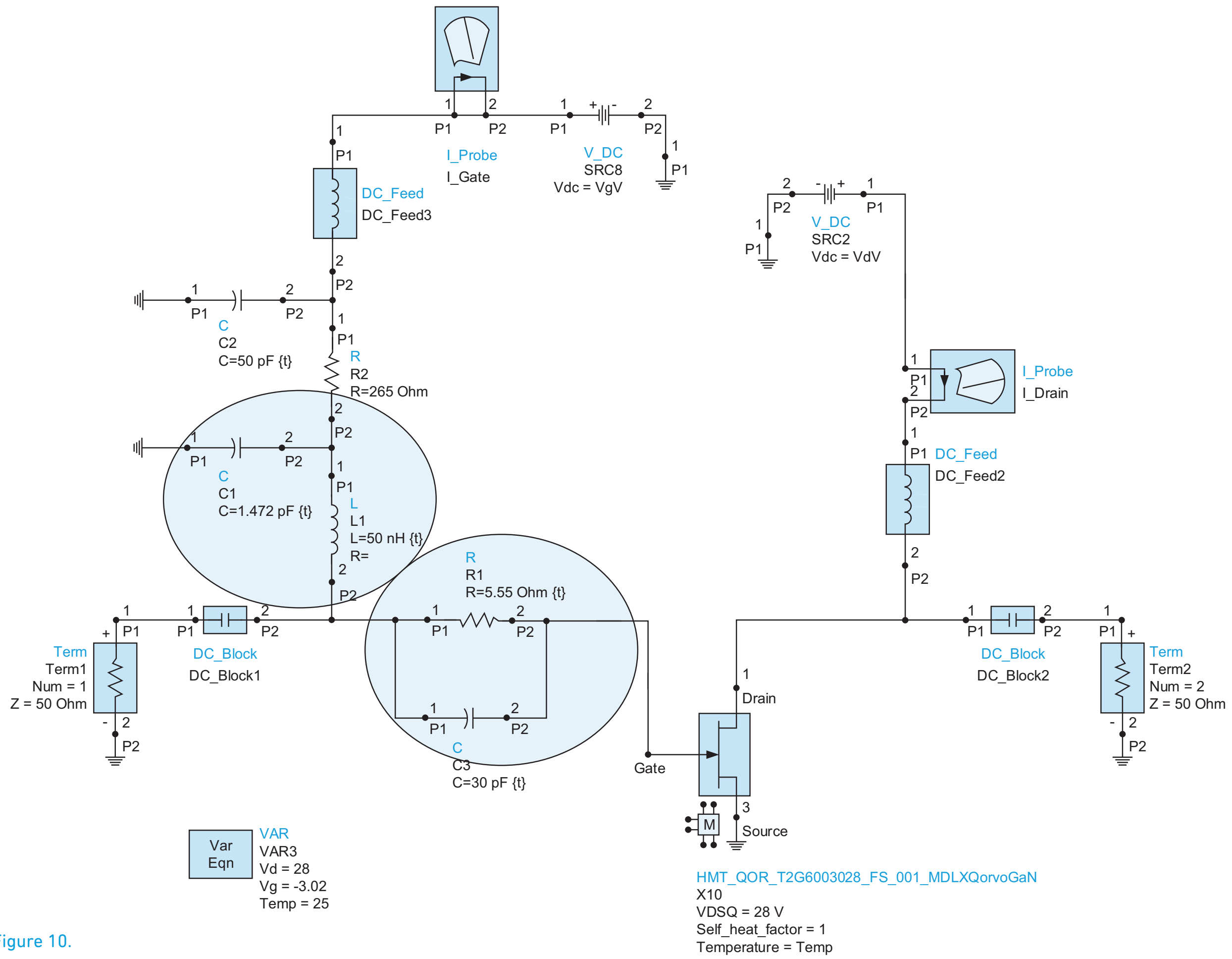

Figure 10.

The inductor (L1) and capacitor (C1) are used to create a low-pass filter. This prevents the resistor (R1) from being seen at higher RF frequencies, or lower frequencies for stabilization. The gain, stability and S-parameter analysis for this solution is shown in Figure 11, Figure 12 and Figure 13. As shown, the frequency-dependent stability network provides unconditional stability across the full frequency range, while reducing the impact on maximum available gain at 3.5 GHz. Note the gain at 3.5 GHz is now reduced by only about 1 dB compared to the non-stabilized device, and also the f_{max} is about the same as the non-stabilized device (~10.4 GHz). In examining the S-parameter comparison to the non-stabilized device as shown in Figure 12, we see that, in contrast to the resistively stabilized device, the S-parameters are not altered over the entire frequency range, but rather only at lower frequencies, as desired. Figure 13 just confirms that none of the stability circles overlap with the Smith Chart in either the source or load planes as expected for an unconditionally stable circuit.

Frequency-dependent gain and maximum gain (left) and stability metrics (right)

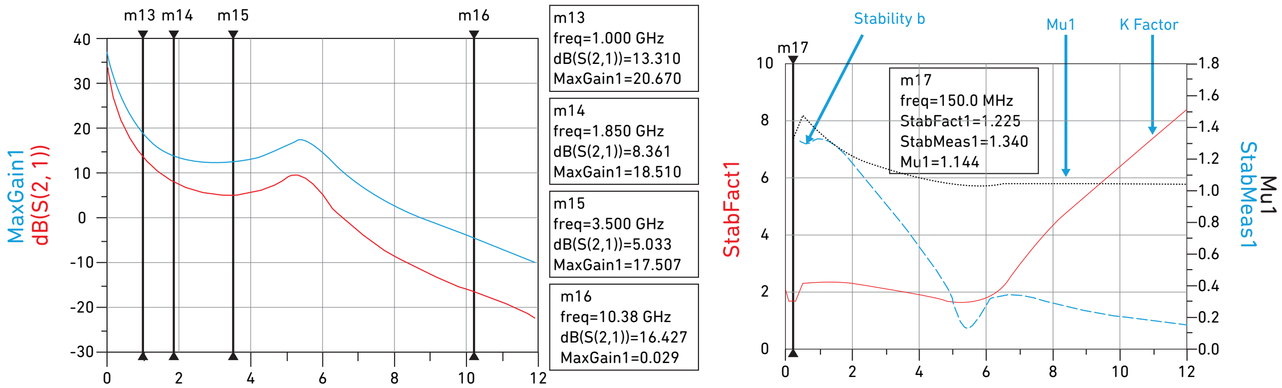

Figure 11.

S-parameters for frequency-dependent stabilized schematic versus the non-stabilized device

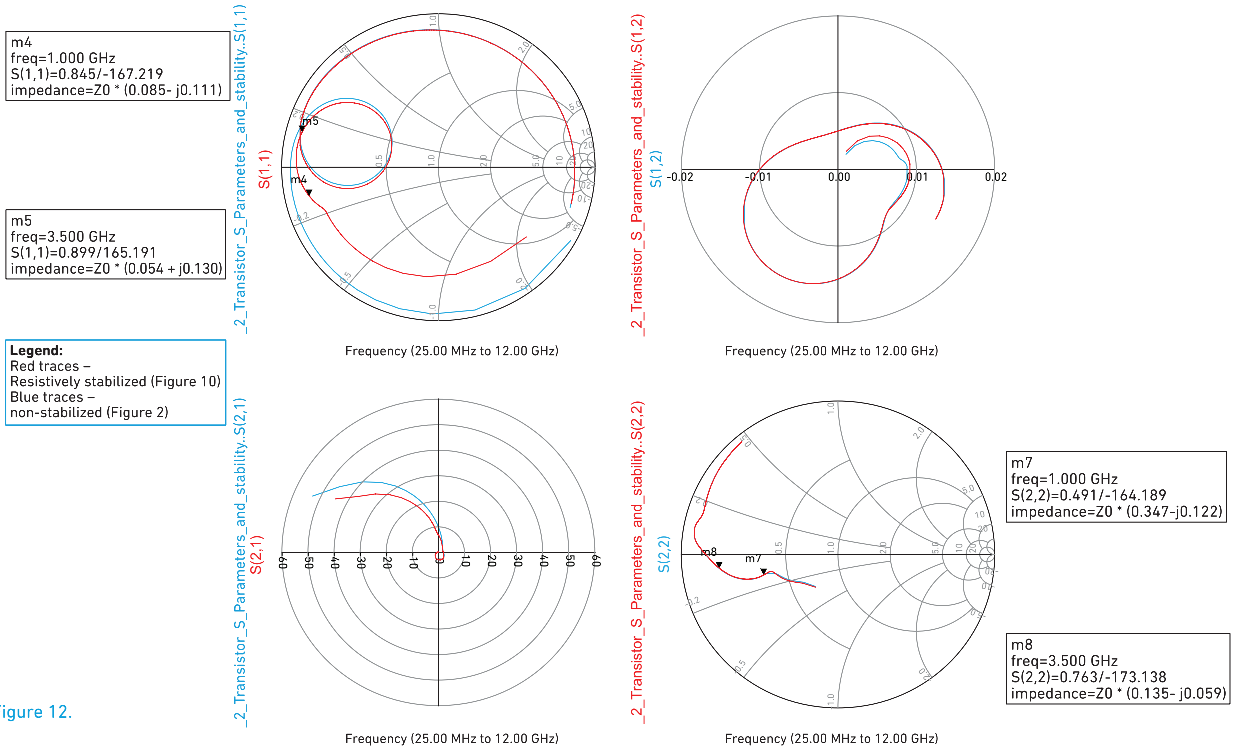

Figure 12.

Stability circles - the source (left plot) and load (right plot) reflection coefficient reference planes for frequency-dependent stabilized device (Figure 10)

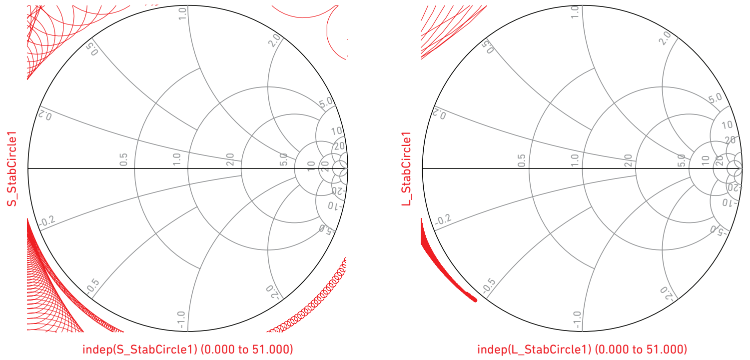

Figure 13.

Key Results

So what are the key findings? As shown in the below data, stability and gain are optimized when using frequency-dependent stability.

No stabilization: 18.373 dB maximum available gain at 3.5 GHz – Figure 3
- Unconditionally stable above 1.85 GHz
- Conditionally stable below 1.85 GHz

Resistive stability applied: 12.334 dB maximum available gain is at 3.5 GHz – Figure 7
- Unconditionally stable over entire 0.025 to 12 GHz frequency range
- 6 dB maximum available gain degradation

BEST RESULT: Frequency-dependent stability applied – 17.5 dB maximum available gain at 3.5 GHz – Figure 11
- Unconditionally stable over entire 0.025 to 12 GHz frequency range
- Increase in maximum available gain of 5.166 dB above resistive stability

Summary

Modeling helps address common design problems such as stability prior to testing your application on the bench. By accurately modeling and implementing stability techniques, we can match and tune for optimal S-parameter performance while maintaining unconditional stability.

As a final note, the stabilization networks explored here used ideal lumped elements. In an actual microwave design, you will need to include microstrip interconnects and accurate parasitic models for all RLC components, whether you are doing a MMIC design or a board-based hybrid design with lumped elements.

How GaN is Changing the Satcom RF Front-End

Introduction

Solid-state technologies such as GaN are transforming satcom. GaN's advantages of high RF power, low DC power consumption, high reliability and smaller size (which reduces system weight) are opening new markets and revolutionizing the RF front-end (RFFE) in existing satcom applications.

For many years the TWTA and GaAs were the go-to RFFE technologies for power amplification in satcom – with TWTAs used for high-power applications and GaAs employed in lower-power applications and as a pre-driver. But the situation has changed rapidly in recent years, due to advancements in GaN. Now, GaN and GaAs semiconductor technologies are becoming the go-to solutions; GaN has been replacing TWTAs due to its high-power performance and reliability combined with a small form factor. GaN and GaAs are enabling a wide variety of commercial and military satcom applications, such as 5G backhaul, ultra-HD TV transmission, satcom-on-the-move, internet access for aircraft passengers, and manpack (portable) terminals.

GaN Advantages

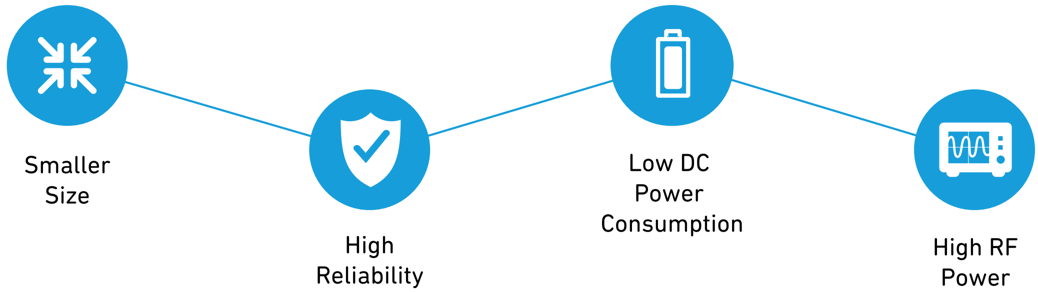

Satcom Trends

Satcom equipment plays vital roles in the global communications ecosystem and the daily lives of people across the world. It supports a broad and expanding variety of applications in telecommunications, weather monitoring, aeronautical communications, maritime applications, military uses and navigation (see Figure 1). According to MarketsandMarkets research, the satcom equipment market is projected to grow at about 8.5% a year to reach $30B by 2022. Strategy Analytics forecasts spending on global military communications systems and services will grow to over $36.7 billion in 2026, representing a CAGR of 3.5%.

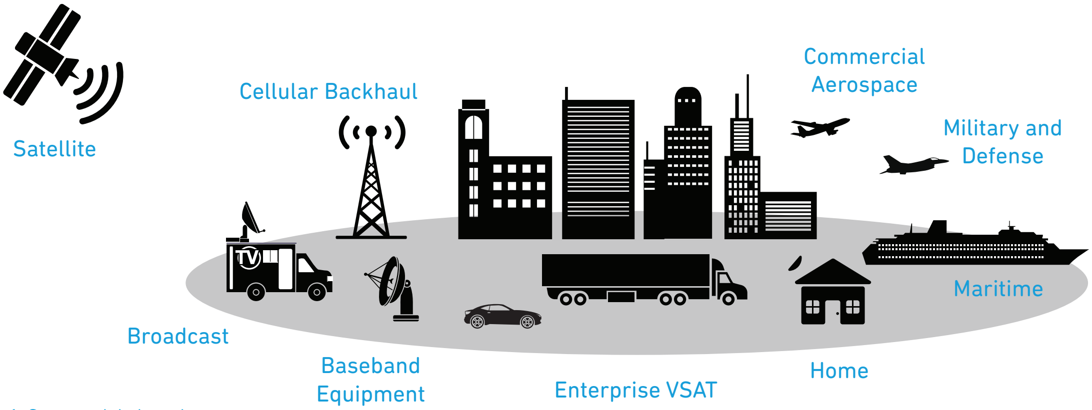

Figure 1. Satcom global markets.

Several broad trends are creating new and more challenging requirements for the RFFE in satcom equipment. The increasing use of smaller satellites and portable, mobile satcom devices is driving a need for more compact, lightweight components with lower power consumption. Additionally, components need to handle much greater bandwidth and data throughput to support advances such as 5G, ultra-HD TV, un-interrupted and secure communications. There's also pressure, to reduce development costs and increase reliability.

These trends are propelling the transition from TWTAs to solid-state devices that support higher data throughput and smaller form factors. Though GaAs and Si have been used in some systems, GaN offers significant advantages for high-power amplification in satcom applications. Its high saturation velocity, high breakdown voltage, and thermal conductivity result in an order of magnitude improvement in power density and high reliability under thermal stress. As a result, GaN is uniquely suited to the high-power requirements of satcom, very small aperture terminal (VSAT), point-to-point (PtP) and base station applications, as shown in Figure 2.

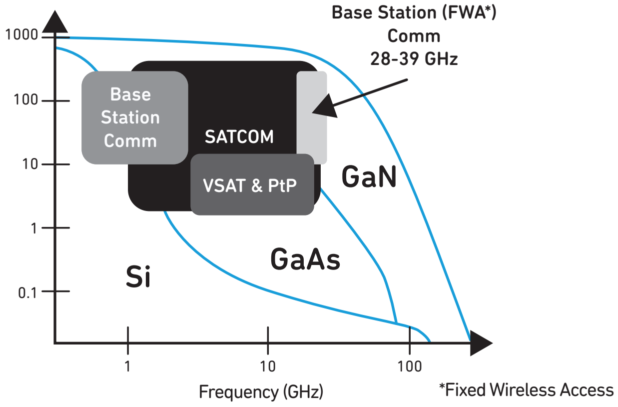

Figure 2. Suitability of semiconductor technologies to different applications.

GaN's potential for the space and satellite communications sectors is only beginning to be realized. The high RF power, low DC power consumption, lightweight, small form factor and high reliability will enable manufacturers to downsize the RFFE. For example, GaN is expected to facilitate weight reduction in satellites and aeronautic applications.

Frequency Bands

The satcom industry has progressively moved to higher-frequency bands to support growing demand for bandwidth, including the X, Ku, K, and Ka-bands as shown in Figure 3. GaN easily supports high throughput and wide bandwidth across these higher frequencies. Today, many of the same satcom components are used across multiple military, space and commercial applications in these bands.

IEEE Microwave Band	Frequency Range	Description
L-Band	1-2 GHz	Global positioning system (GPS) carriers and also satellite mobile phones, some communications at sea, land and air
S-Band	2-4 GHz	Weather radar, surface ship radar, and some communications satellites
C-Band	4-8 GHz	Primarily used for satellite communications, for full-time satellite TV networks or raw satellite feeds
X-Band	8-12 GHz	Primarily used by the military, also used in radar applications
Ku-Band	12-18 GHz	Used for satellite communications, fixed satellite services and broadcast satellite services
K-Band	18-26 GHz	Used for fixed satellite services and broadcast satellite services
Ka-Band	26-40 GHz	Communications satellites, uplink in either the 27.5 GHz and 31 GHz bands, and high-resolution, ctlose-range targeting radars on military aircraft

Figure 3. IEEE microwave bands.

Replacing TWTAs

Until recently, TWTAs were the mainstay in many satcom applications because solid-state devices weren't capable of producing similar power levels. However, power combining techniques now make it possible to generate much higher power using GaN, enabling the replacement of TWTAs with more-reliable solid-state devices.

The GaN power-combining approach aggregates the output power from several single power amplifier MMICs using fully isolated coupling networks. An example is Qorvo's Spatium®, which is a spatial combining product that uses a patented spatial combining technique to offer high RF power, high efficiency and broadband operation. Spatium uses broadband antipodal fin-line antennas as the launch to and from the coaxial mode, splitting into multiple microstrip circuits (see Figure 4). It then combines the power from these circuits after amplification with a power MMIC. A typical Spatium design combines 16 devices, with a combined loss of 0.5 dB. Spatium is used in Ka-band satellite earth stations that operate at 100 Watts and 27-31 GHz, covering both military and commercial bands. Within these stations, it is used in the transmitter side at the antenna hub in block up-converters (BUCs).

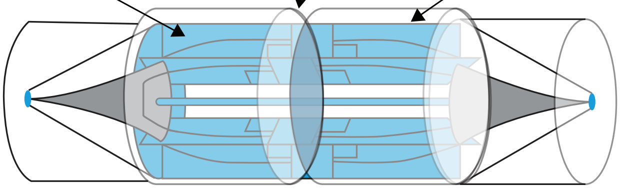

Figure 4. Spatium spatial combining patented design.

This solid-state power-combining approach offers several performance advantages over TWTAs.

- TWTAs need to warm up before they can attain stable RF performance. Warming the tube can take a few minutes. Mitigating the problem requires backup systems running in hot standby. This results in large energy costs. These back-up systems are not required when using Spatium, as no warm up is required.
- TWTAs require high voltage power supplies, typically in the multi-kV range, thus increasing system power consumption. GaN devices do not require high-voltage power supplies.
- Solid-state GaN generates lower noise and has better linearity than TWTAs. Noise figures for medium power TWTAs can be around 30 dB, versus about 10 dB for a solid-state GaN MMIC PA. Another operational benefit of the GaN transmitter is the reduced harmonic content in the output signal.

GaN Advantages for Satcom

GaN offers a range of other advantages over both TWTAs and other solid-state technologies for satcom applications.

Reliability and ruggedness. Reliability is extremely important in satcom applications. GaN offers much higher reliability than TWTAs for several reasons. With TWTAs, a failure in the tube causes a total performance breakdown. In contrast, a spatial combining technique like Spatium increases robustness and reliability. The failure of one transistor does not mean the entire unit shuts down; instead it continues to function using the remaining GaN amplifier MMICs. Each solid-state device is also highly reliable: although the lifetime of a transistor is limited due to electromigration, time-to-failure is typically over 100 years.

The higher power-efficiency of GaN also reduces heat output, which further contributes to higher reliability. Furthermore, wide-bandgap GaN tolerates much higher operating temperatures, so the cooling requirements in compact areas may be relaxed without compromising performance and reliability. This reduces the need for cooling fans and heatsinks, which reduces the weight and size of satellites and therefore the cost of launching them into orbit.

Small, lightweight devices. Weight and size are becoming critical factors in satcom applications, with the trend to smaller satellites and the growth of other on-the-move satcom applications. GaN's high-power output and on-resistance and breakdown voltage allows satellites and other applications to reach target power output levels with smaller devices. Higher power density results in less weight and size per given unit of power output. The high breakdown field allows higher voltage operation and increased efficiency and helps to ease impedance matching requirements, reducing the need for tuning components and helping to decrease board size.

Low current consumption means lower operating costs and less heat to dissipate. Lower currents also helps to reduce system power consumption and demand on power supplies. The result is reduced expense for manufacturers and operators.

Reducing the thermal rise in a system makes it easier to increase performance and cuts cost for the application. Because GaN technology is highly power-efficient and tolerates higher operating temperatures, GaN technology can help system designers work within tighter thermal related margins, allowing extra performance to be delivered from the RFFE.

Frequency bandwith. Increased bandwidth is being used across the entire communications industry to provide greater capacity to support the ever-growing number of users and insatiable demand for data. The high-power density of GaN and its lower gate capacitance enables greater operational bandwidth and higher speeds. Today's GaN modules and power amplifiers deliver broadband operation to support the unprecedented bandwidth requirements of 5G and other emerging applications.

Integration is now appearing in satcom RFFEs. Demand for smaller solutions for aeronautic applications and satellites is prompting suppliers to replace large multi-technology discrete RF front-ends with monolithic fully integrated solutions. GaN manufacturers are catching this wave, and are developing fully integrated solutions that combine the transmit and receive chain in a single package. This will further reduce system size, weight and time to market for manufacturers.

Key GaN Satcom Applications

GaN is making its way into many commercial and military satcom applications, including satellites, manpack, satcom-on-the-move, commercial aircraft, and very small aperture terminal (VSAT) terminals. In the space industry, GaN is replacing Si and GaAs due to advantages such as size, weight and efficiency. The smaller die size of a GaN device, compared to Si, enables performance improvements in power-switching applications. Parasitics such as output capacitance and layout inductance are reduced, resulting in lower switching insertion loss and higher-frequency operation.

Moreover, new all-electric satellites are currently under study. GaN will be a key enabler in these developments as size reduction, weight and low power consumption are important for success. Some GaN suppliers like Qorvo have space-qualified their technology, underlining the clear opportunities for GaN in this sector.

GaN is also poised to transform the lower-power VSAT satcom sector. The use of VSAT systems is expanding: they are employed for a wide variety of applications including fixed and portable wideband systems for consumer, commercial, defense and maritime communications, as well as transaction processing, data acquisition and remote monitoring. GaN is replacing and teaming up with traditionally all GaAs systems used in VSAT due to its ability to provide higher output power, which supports higher speeds and increased bandwidth allowing greater data throughput. This accelerates demanding applications, such as commercial two-way data transfers of video and other large files. GaN also outperforms Si in PA-related applications.

GaN's reliability under harsh environmental conditions is also important in this sector. VSAT devices are typically used in environments where they are subjected to harsh conditions. Advances in thermal management using unique packaging are further enhancing GaN's high reliability under these conditions. A two high-level VSAT applications using GaN PA are shown in Figure 5.

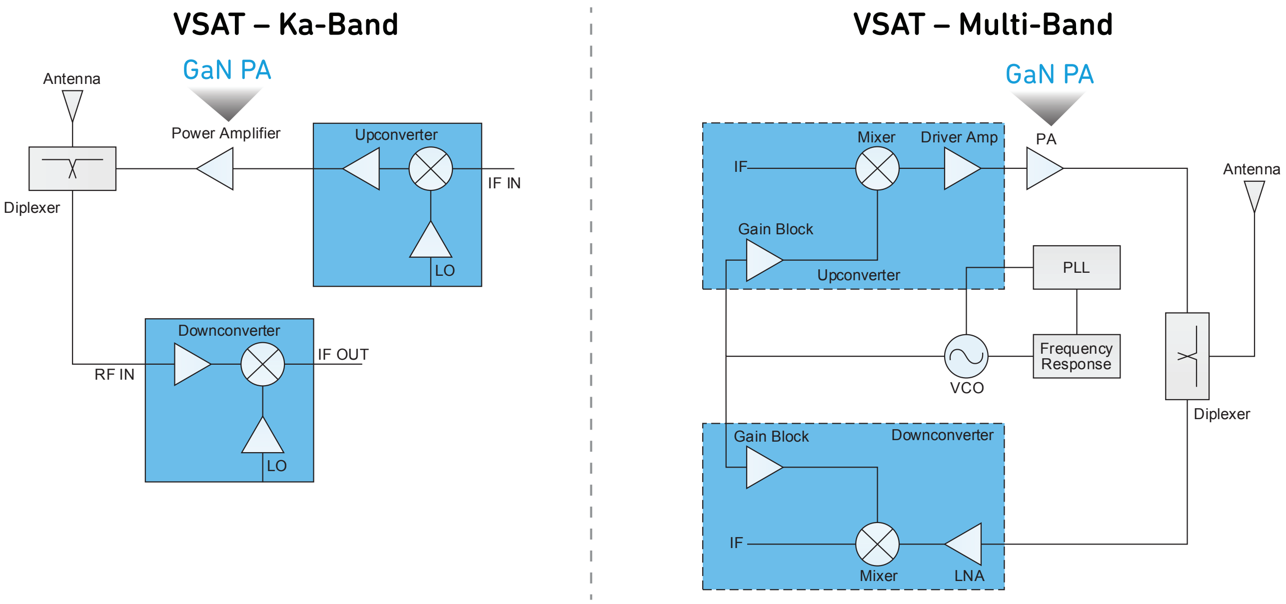

Figure 5. Satellite terminal system, VSAT block diagrams.

Conclusion

GaN is transforming the RF front end across multiple satcom application sectors. GaN is replacing incumbent technologies such as TWTAs, GaAs, and Si, because it is more reliable, more efficient, smaller, and offers higher power density and lower power consumption. Satcom manufacturers are using GaN to improve current satcom products – and to explore new developments and potential new applications.

Reaching New Levels of Linearity in Passive Mixers with GaN Technology

When microwave engineers hear the word GaN, one thought usually comes to their minds: power amplifiers. Due to its physical properties of high-breakdown voltage and high-thermal conductivity, GaN is ideally suited over its GaAs counterpart for the development of highly efficient, highly effective power amplifiers. Until now, the benefits of GaN technology beyond amplification have not been pursued.

Over the past year, Qorvo has been investigating the use of GaN for passive mixers. As a result of this work, we have discovered the high-linearity properties of GaN amplifiers do indeed translate to mixers. This realization has let us develop a new family of ultra-linear mixers operating from 1 to 20 GHz. With these mixers, microwave engineers can now approach levels of linearity that used to seem impossible.

Current State of Affairs

The passive, high-frequency mixer market of today is dominated by circuits constructed from various GaAs processes including MESFET, pHEMT and HBT. A key linearity-performance criterion used to judge different mixers is the third-order intercept point (IP3), as the higher the IP3, the better the linearity. One key factor that can influence the IP3 is the LO drive level. Many GaAs mixers achieve an IP3 that is only slightly higher than the LO drive level. To examine this phenomenon, we define the new metric, Linear Efficiency, which is the difference between IP3 and LO drive level. In Table 1 below, we summarize the linear efficiencies of some commercially available mixers.

In this table, we note that many of the mixers have a linear efficiency of 3 to 8 dB, with no clear dependence on frequency or process. Such linearity performance has been relatively unchanged over the past twenty years, when GaAs-based MMIC mixers were first introduced into the marketplace. Since then, system linearity requirements have only increased. Today, microwave engineers are routinely asking for mixers with IP3 levels above 30 dBm, if not 40 dBm. Based on the information in Table 1, GaAs-based mixers would require extraordinary amounts of LO power, greater than 30 dBm, to achieve these high-linearity levels. Such a cost is usually prohibitive in most systems, and is one reason why highly linear GaAs mixers have not been introduced to the market.

Technology	Topology	LO, RF Freq. (GHz)	IF Freq. (GHz)	Conv. Gain (dB)	LO Drive (dBm)	Input IP3 (dBm)	Linear Efficiency (dB)
pHEMT	Double Balanced	2.5-7	DC-3	-9	13	18	5
pHEMT	Double Balanced	3-10	DC-4	-9	17	24	7
pHEMT	Double Balanced	3.5-8	DC-1.6	-7	13	17	4
MESFET	Double Balanced	5.5-14	DC-6	-7.5	15	21	6
HBT	Double Balanced	6-14	DC-4.5	-6.5	13	16	3
HBT	Double Balanced	16-26	DC-9	-6.5	13	17	4
MESFET	Double Balanced	18-32	DC-8	-9	13	19	6
HBT	Double Balanced	20-32	DC-10	-7	13	18	5
pHEMT	Double Balanced	24-40	DC-17	-8	13	21	8

Table 1. Summary of some commercially available, passive, double-balanced GaAs MMIC mixers, including their linear efficiencies.

GaN to the Rescue

As developers of passive GaAs mixers, we at Qorvo have studied this problem in detail and asked what GaN can do to help solve this problem. One compelling feature of GaN processes is that they can generally support two types of mixing elements: a 2-terminal Schottky diode, and a 3-terminal FET. Each of these mixing devices offers its own unique benefits for increased linearity through physical properties and topology choice. Consider the 2-terminal GaN Schottky diode. In Figure 1, we present a typical DC I-V trace for a GaN diode as compared to a typical GaAs pHEMT diode.

In this figure, we note the pHEMT diode has a turn-on voltage of approximately 0.8 V, whereas the GaN diode has a turn-on voltage closer to 1.1 V. A higher turn-on voltage translates directly into a higher IP3 level, but at a cost of more LO drive. However, as we will see, the GaN diodes deliver a much higher LO efficiency than their GaAs pHEMT counterparts. Although not shown, a similar trend can be seen in the three terminal GaN FET devices, which have a more negative pinch-off voltage and higher breakdown voltage than their GaAs counterparts. Such performance allows for higher levels of linearity in passive mixers, again at the cost of higher LO drive.

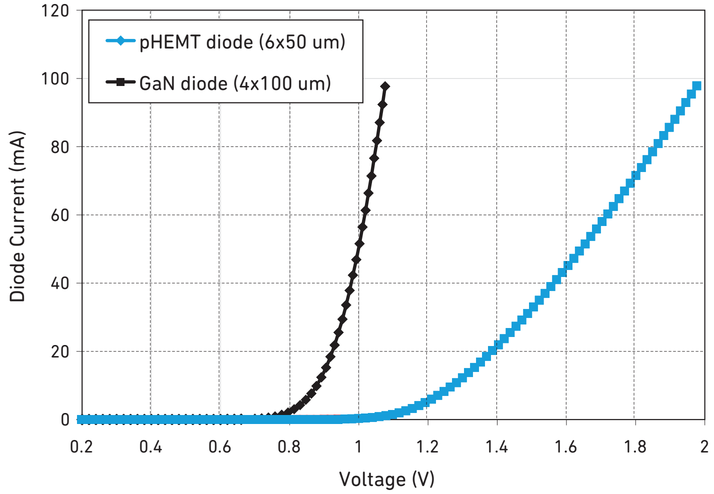

Figure 1. DCI-V comparison of a typical GaAs pHEMT diode vs. a GaN diode.

GaN Mixer Higher Linearity and Superior Efficiency

As the result of design and manufacturing process improvements and enhancements, Qorvo has been successful in developing a family of highly linear mixers with input IP3 levels well above 30 dBm and linear efficiencies of greater than 10 dB. A summary of these designs is shown below in Table 2.

In the sections below, we take a closer look at three of the most recent mixers, which are bolded in the table below.

Technology	Topology	LO, RF Freq. (GHz)	IF Freq. (GHz)	Conv. Gain (dB)	LO Drive (dBm)	Input IP3 (dBm)	Linear Efficiency (dB)
GaN	Diplexed FET	1.4-2.6	DC-0.8	-8	21	35	14
GaN	**Diplexed FET**	**2.6-3.8**	**DC-1.1**	**-8**	**22**	**37**	**15**
GaN	Double Balanced	6-11	DC-5	-6	19	30	11
GaN	**Double Balanced**	**7-13**	**DC-1.5**	**-8**	**22**	**35**	**13**
GaN	**Single Balanced**	**13-19**	**DC-2**	**-9**	**24**	**34**	**10**

Table 2. Summary of GaN mixers developed by Qorvo, showing very high linear efficiencies.

S-band GaN FET Mixer (3-Terminal Device)

The first design is a 3-terminal FET mixer as shown in Figure 2. The mixer has an operational bandwidth of 2.6 to 3.8 GHz and an IF response from DC to 1.1 GHz.

In this figure, we note the LO is applied to the gate through a filter network, whereas the RF/IF is applied to the drain via a diplexer constructed from a spiral transformer. The transformer does not introduce any balance into the circuit, but does allow for an enhanced isolation of the signals. Additional filtering elements in the signal path provide further port-to-port isolations.

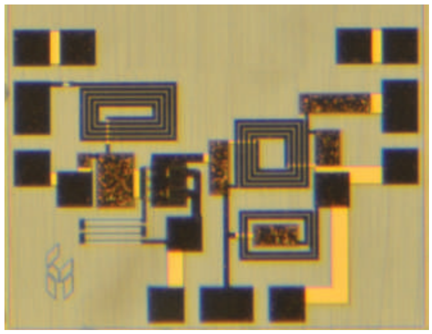

Figure 2. Die photograph of the S-band GaN FET mixer.

In Figure 3, we present the conversion gain for the S-band mixer as a function of frequency. Here, the mixer was measured as a downconverter with a fixed IF frequency of 100 MHz, USB. We note the mixer has a conversion gain of approximately -8 dB across the operating bandwidth when driven by an LO signal greater than 20 dBm.

In Figure 4, we present the input IP3 of the S-band mixer at a number of LO drive levels. We note that at a drive level of +26 dBm, the input IP3 averages around +40 dBm, which demonstrates a linear efficiency of nearly 14 dB.

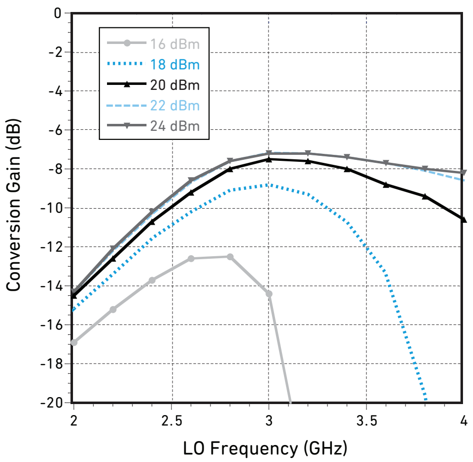

Figure 3. Conversion gain of the S-band GaN mixer. IF=100 MHz USB.

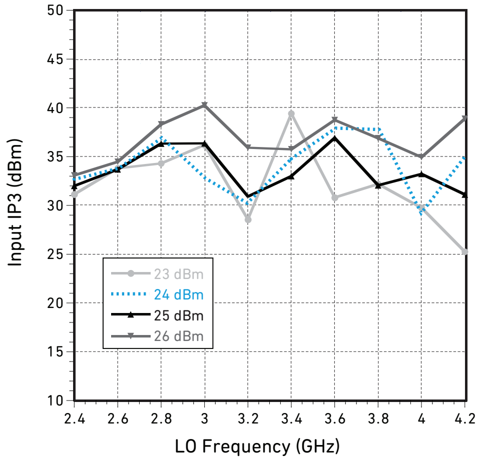

Figure 4. Input IP3 for S-band GaN mixer. IF=100 MHz USB.

X-Band GaN Diode Mixer (2-Terminal Device)

The second mixer is a double-balanced, diode-based mixer, as shown below in Figure 5. The operational bandwidth of this mixer is 7 to 14 GHz with an IF response range of DC to 1.5 GHz.

In this figure, we note the LO and RF signals are fed to the diode ring through spiral balun transformers, while the IF signal is extracted from the centertap of the RF balun. Additional matching and filter elements are also added to each of the ports to optimize the performance.

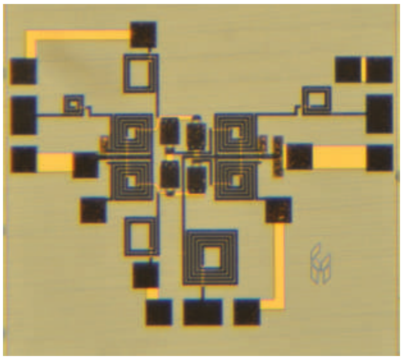

Figure 5. Die photograph of the X-band GaN diode mixer.

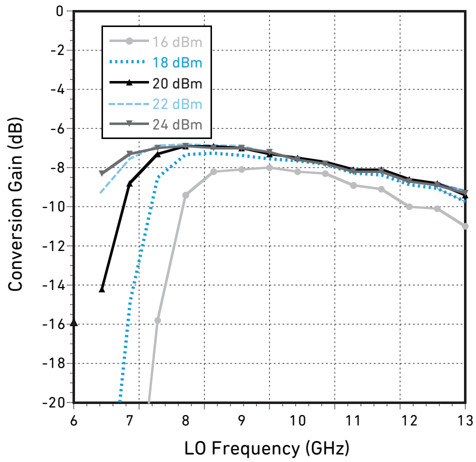

Figure 6. Conversion gain of the X-band GaN diode mixer. IF=100 MHz LSB.

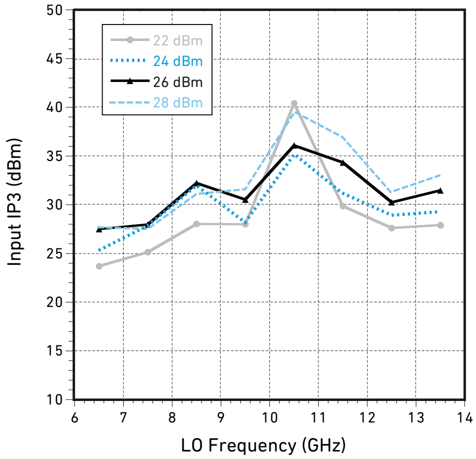

Figure 7. Input IP3 for X-band GaN diode mixer. IF=100 MHz LSB.

In Figure 6, we present the conversion gain of the X-band mixer versus frequency. Here, the mixer was configured as a downconverter with a fixed IF frequency of 100 MHz LSB. We note the mixer has a conversion gain of approximately -8 dB across the operating bandwidth when driven with an LO drive level greater than 16 dBm.

In Figure 7, we present the input IP3 of the X-band mixer at a number of LO drive levels. We note that at drive levels above +22 dBm, the input IP3 is +30 to +38 dBm, which demonstrates a linear efficiency of 8 to 12 dBm.

Ku-band FET Mixer (3-Terminal Device)

Our third mixer is a single-ended, cold FET mixer, as shown below in Figure 8. The operational bandwidth of this mixer is 13 to 19 GHz with an associated IF response range of DC to 2 GHz.

In this figure, we note the LO is applied to the gate of the GaN FET through a filter network, whereas the RF and IF signals are applied to, and extracted from, the drain through high pass (RF) and low pass (IF) networks. These filter networks provide the isolation in the mixer, as the topology has no inherent balance. The source of the FET is grounded.

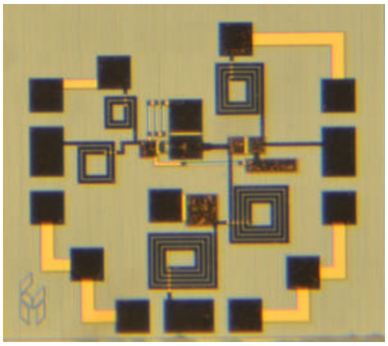

Figure 8. Die photograph of the Ku-band single-ended GaN FET mixer.

In Figure 9, we present the conversion gain of the Ku-band mixer versus frequency. Here, the mixer was configured as a downconverter with a fixed IF frequency of 100 MHz USB. We note the mixer has a conversion gain of approximately -9 dB across the operating bandwidth for LO drive levels above +22 dBm.

In Figure 10, we present the input IP3 of the Ku-band mixer at a number of LO drive levels. We note the input IP3 increases as the LO drive level increases, up to a measured value of +35 dBm. This does not appear to be the ultimate limit. Unfortunately, we were constrained in LO drive during this measurement and were unable to generate higher power. Regardless, the Ku-band FET mixer demonstrates a linear efficiency of 8 to 10 dB.

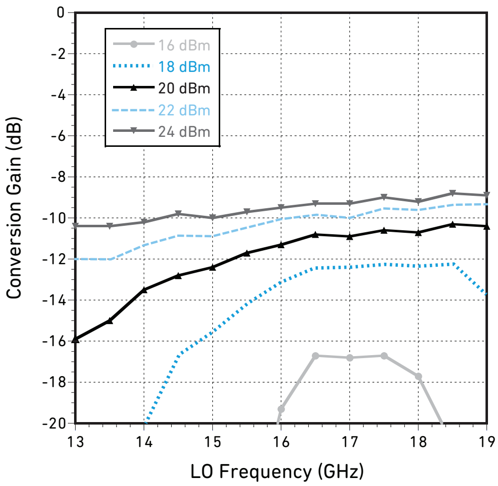

Figure 9. Conversion gain of the Ku-band GaN FET mixer. IF=100 MHz USB.

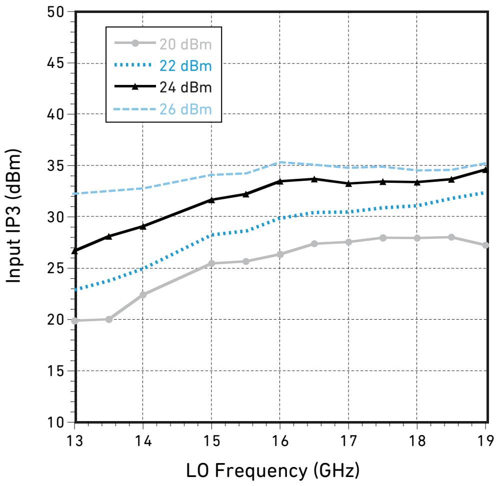

Figure 10. Input IP3 for the Ku-band GaN FET mixer. IF=100 MHz USB.

Where Do We Go From Here?

Based on the results for these three examples, it is clear that GaN mixers can deliver linear efficiencies that are much higher than their GaAs counterparts. The use of 2-terminal or 3-terminal mixing devices offers a wide range of mixer topology possibilities, thus allowing GaN mixers to be optimized for many different microwave systems. At Qorvo, we have already begun developing GaN mixers to cover more of the frequency spectrum, while still retaining very high linear efficiencies. We expect these mixers will soon find their way into radar communications and instrumentation systems near and far.

5 Key MMIC LNA Choices That Can Make or Break A Receiver Design

Introduction

Low noise amplifier (LNA) MMICs are a critical component in virtually all radar, wireless communication and instrumentation systems. There are a wide range of options and tradeoffs an engineer must consider when picking an LNA MMIC for a particular system design. The noise figure is often the feature of primary focus, as noise figure defines the sensitivity of the receiver – a critical system requirement. After noise figure, other project specific needs related to performance and size, weight, power and cost (SWaP-C) are then considered. Often these features are not heavily weighted, but they can make a big difference in advanced microwave applications.

The goal of this article is to describe additional selection criteria commonly overlooked during the initial evaluation phase of an LNA. Keeping these additional parameters in mind may help an engineer save time during the design cycle, save money during assembly, and enhance a product's competitive advantage, leading to valuable contract wins.

Pinpointing the LNA in the Microwave Signal Chain

Receiver sensitivity and signal-to-noise (SNR) are two of the most critical electrical performance considerations for modern wireless communications, radars, instrumentation, and satellite communications. Largely, the noise performance of the receiver is defined by the performance of the LNAs used in these circuits.

Phased array and AESA radar systems are being retrofitted into both commercial and military aircraft. They employ dozens of low noise amplifier MMICs that are relied on for receiver sensitivity and optimal SNR.

Advanced applications, such as electronically steered arrays (AESAs) for military applications and phased array antennas for 5G wireless communication systems, require massive numbers of T/R modules, with each receive channel requiring an LNA.

In radar systems, wideband LNAs can be used in the receiver modules, and their performance will impact the range and accuracy of the radar system.

To choose the best overall LNA designers should consider the importance of these five additional characteristics after they've identified the frequency band and noise figure combination required.

1. Input Power Survivability

Specifically in military and aerospace radar and communications applications, where electronic countermeasures (ECMs) may be used to overwhelm a receiver, a receiver must be capable of withstanding high levels of input power for varying intervals of time. Active or passive jamming can cause levels of noise and frequency bursts that couple large amounts of microwave energy into a receiver. Moreover, in many systems there is often a high-power transmitter in close proximity to the receiver, which can also lead to substantial power into the receiver front end.

Many of the latest applications, such as wideband and multi-band communications transceivers, and Low probability of intercept/low probability of detection (LPI/LPD) radar (often employing frequency hopping) use extremely wide bandwidths of spectrum for transmission and reception. These factors lead to greater noise power coupled into the receiver, and less protection from the aggressive filtering possible in narrowband receivers. If the amount of noise or interference exceeds certain limits, a receiver may be overloaded and unable to function as designed.

If the receiver is exposed to these power levels for too long, the components within a receiver may suffer accelerated aging, performance degradation, or outright destructive failure.

A common method to reduce the impact of critically high input powers to a receiver is to include a limiter or circulator on the input of a receiver chain. An unfortunate side effect of adding anything prior to the LNA in the receiver is the degradation of the overall system noise figure.

This circuit will reduce the sensitivity of the receiver, which may shorten communications range, throughput, radar range and accuracy, and cause delays in acquiring mission critical information. For example, a superior system noise figure of 1 dB can rise to 2 dB or more when a limiter is added.

Ratings of a Typical LNA MMIC

Parameter	Rating
Drain Voltage, V_{dd}	5.0 V
RF Input Power	+20 dBm
Channel Temperature, Tch	150° C
Power Dissipation, Pdiss	540 mW
Thermal Resistance	120° C/W
Operating Temperature	-40 to 85° C
Storage Temperature	-55 to 150° C
ESD Sensitivity (HBM)	Class 1A

Conditions of a Typical LNA MMIC

Parameter	Min	Typ	Max	Units
Vdd	2.0	3.0	4.5	V
Idd	–	52	–	-mA

Understanding and carefully operating LNA MMICs to their specified maximum power ratings and operating conditions is critical to ensuring reliability and long life.

Therefore, it is very important to consider an LNA's highest input power handling (or input survivability) when choosing a component. Most LNAs can handle only 10 dBm pulsed on their input, but some can now survive 20 dBm continuously and 23-25 dBm pulsed. Such protection levels can in many cases eliminate the limiter.

2. Gain Flatness and Gain Stability Over Temperature

Gain flatness with frequency is essential for wideband communications systems to achieve the required inter-symbol-interference (ISI) levels of complex digital modulations schemes. Similarly, gain flatness can impact the range performance of radar systems. Equalizers are often employed to compensate for the gain slope of typical LNAs. It is important to note many LNA suppliers use different bandwidths to characterize gain flatness, often without indicating what the gain flatness is across the entire band.

Another factor to consider about LNA performance, which is often omitted from datasheets, is the gain stability over temperature (Figure 1.). In applications such as aerospace communications and satcom, the operating temperature variations can exceed 180° F within a short time window.

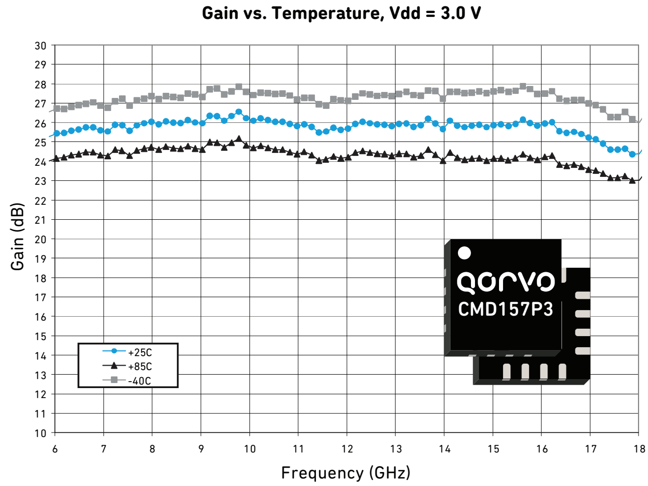

Figure 1. This 6-18 GHz LNA exemplifies how gain flatness and gain stability over temperature are possible in a single device.

Temperature changes that are significant can affect an LNA by more than just changing the noise figure of the device and system; they can vary the frequency dependent gain of the LNA. For example, large phased array antennas may have thousands of TR modules, with many of the modules exposed to a variety of temperature gradients. If the communications system relies on gain stability throughout the TR modules, and the LNA's gain variation over temperature is too large, the system may suffer a loss in performance that impacts the bottom line of the deployment.

Recognizing this, system designers should opt for LNA designs that exhibit both superior gain flatness and gain stability over temperature.

3. Supply Voltage

Properly biasing a MMIC amplifier is critical to achieving adequate device performance. Depending upon the particular LNA design, the biasing circuitry could be composed of a positive and negative biasing circuit with temperature compensation. With such a dual bias scheme, the positive and negative voltage supply must be provided in the correct sequence, or else device failure can result.

When designing at a system level for a large RF or microwave assembly, many different voltage supplies may be required. Certain design constraints may also limit the noise and stability performance of those power supplies, which may impact the practical LNA performance due to limited power supply rejection ratio (PSRR). To avoid this, additional circuitry may be used to condition the voltage supplies for a given LNA MMIC. Each of these circuits and connection points introduces a potential failure mode to the voltage supplies, and thus impacts system reliability. These supply-voltage circuits also consume valuable assembly real estate and power, contribute to the overall size/weight of the assembly, add costs, and of course, consume design and test time.

In order to reduce the infrastructure necessary to integrate a MMIC LNA into a microwave assembly, Qorvo has applied innovative circuit-design techniques. The approach has resulted in MMICs which only require a single positive voltage supply enabling a wide range of voltage input options for greater flexibility. All of the necessary circuitry to properly bias these LNAs is integrated into the MMIC itself. Ultimately, when your MMIC requires only a single positive supply voltage it reduces your bill-of-material, overall system complexity, failure modes, and overall system SWaP-C.

4. Power Consumption

For many ground-based and stationary RF communications and radar systems, the power consumption of an LNA is not a significant consideration. However, the latest AESAs, phased-array antennas, and multi-input multi-output (MIMO) RF systems may require tens, hundreds and even thousands of LNAs integrated into T/R modules. Many satcom, military, automotive and 5G wireless communication systems are also looking to these extremely complex antenna transceiver systems to solve the performance challenges innate in transmitting and receiving at high microwave and millimeter-wave frequencies.

As launching satellites costs thousands to tens of thousands of dollars per kilogram, reducing the weight of a satellite system can directly influence the cost-per-bit of high-speed satellite communication services.

In mobile platforms, including aerospace and satellite communications, power constraints are a system-wide limitation that often dictate what solutions can be used. Moreover, for these applications, the power requirements of the components directly lead to the overall size and cost of the power generation circuits, and hence, the total system SWaP-C. Some systems may have a power budget limit, and performance sacrifices must be made to meet that limit. With the importance of reliable communications in the modern battlefield, time to market may be impacted in order to design within the power budget while producing dependable communications.

An example of this concept is seen with satellite communications. The power required by a phased-array antenna must be generated by solar cells mounted on the satellite, which is one of the largest contributing factors of a satellite's weight and size.

At Qorvo, we have analyzed each of our LNA designs to ensure that their power consumption (bias current and bias voltage) is as efficient as possible. MMICs designed in this way also derive the benefit of lower power draw. They are also typically smaller, demonstrate better temperature performance, and provide improved SNR at lower power levels.

5. Value of Time Saved in the Development and Production of Your System

The SWaP-C parameters of an LNA are important in the component selection cycle. In addition, an often neglected factor is savings in time. Such time factors include design, assembly, test, qualification, support, and documentation. Choosing less efficient LNA MMICs, which might increase one or more time element, can cause project delays and cost overruns. Therefore, selecting LNAs that exhibit characteristics discussed in this brief will save time in addition to size, weight, power and cost.

Conclusion

Real-world receiver design challenges are often impacted by what is not featured in a product datasheet. Considering more than just noise figure when selecting an LNA therefore can make or break a project. Giving serious thought to survivability, gain flatness/stability, supply voltage, power consumption, and the impact of time hold the keys to success in modern radar, satcom and communications systems.

Addressing Phase Noise Challenges in Radar and Communication Systems

Introduction

Phase noise is rapidly becoming the most critical factor addressed in sophisticated radar and communication systems. This is because it is the key parameter defining target acquisition in radars and spectral integrity in communication systems. There are many papers detailing the mathematical derivation of phase noise but few mention the reasons for its importance. In this Tech Brief, we discuss the importance of phase noise, and what can be done to lessen its effects in microwave systems.

What is Phase Noise?

Phase noise is commonly used as a measure of frequency stability within an oscillator. This noise is inherently different than the general background noise of any electrical system, which is defined as kTB, where k is Boltzmann's constant, B is the bandwidth, and T is the temperature. Instead, phase noise is a secondary effect directly related to the topology and construction of the oscillator. A pictorial representation of phase noise is given below in Figure 1.

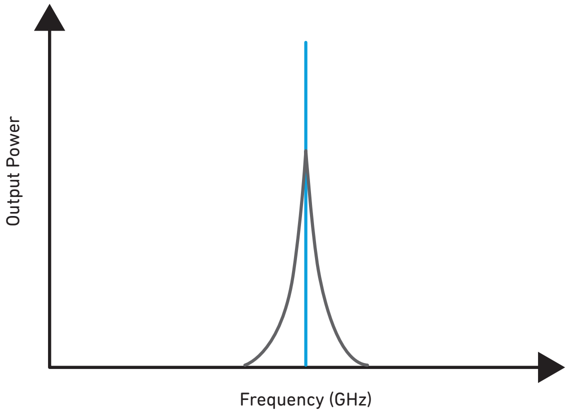

Figure 1. Pictorial representation of an ideal signal (blue) and a signal with phase noise (grey).

In this figure, we have plotted the output power of an oscillator versus frequency. The ideal oscillator is shown in blue, which only outputs power at a single, fixed frequency. The grey curve, however, is the output of an oscillator with phase noise, which shows up as power across a spectrum of frequencies very close to the desired output. These skirts, as they are called, are always present and are due to thermal noise within the active devices of the oscillator. The power level of the red skirts is dependent upon the quality of the oscillator and is measured in dBc/Hz at an offset frequency from the desired signal (typically called the carrier).

Why Do We Care About Phase Noise?

Phase noise can affect the performance of many different microwave systems. In this article, we discuss two in particular: direct down conversion receivers and radars.

Direct downconversion is a type of receiver in microwave communication systems. One benefit of direct downconversion is the simplicity of the circuit, which is essentially a single mixer driven by a local oscillator (LO) to convert the input RF signal to a baseband (very low frequency). This baseband signal is then directly applied to an analog-to-digital converter for processing. A common term for this architecture is "RF in, bits out". One problem with direct downconversion, though, is that the input RF signal can be very close in frequency to the LO, which makes the conversion process susceptible to phase noise, especially if the signal strength is low.

In radar systems, the problem is similar in nature. Radar systems operate by transmitting a pulse at one frequency, and then measuring the frequency shift of the returned pulse, as the shift is related to the velocity of the object being imaged through the Doppler effect. Objects moving very slowly will generate a return pulse very close in frequency to the transmitted pulse, and if the cross section of the object is also very small, the power level of this received signal will be also very low. Ultimately this return pulse has to be converted to baseband in order to recover the velocity information, and phase noise can obscure the data.

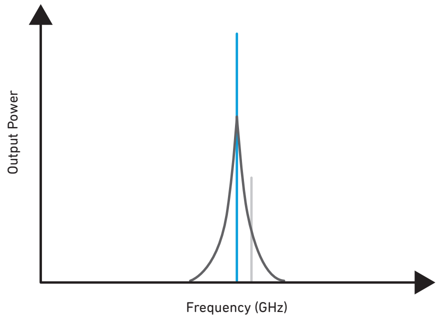

Figure 2. Pictorial representation of an ideal LO signal (blue), an LO signal with phase noise (grey), and an RF signal close in frequency (light grey) we wish to convert to baseband.

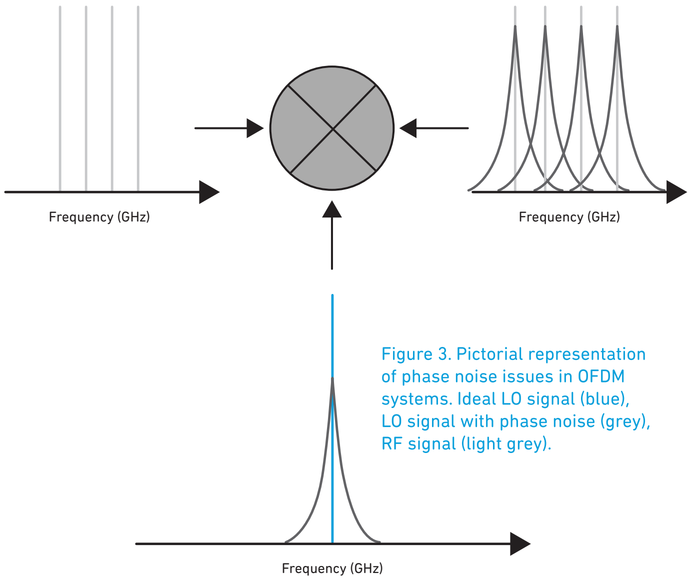

Figure 3. Pictorial representation of phase noise issues in OFDM systems. Ideal LO signal (blue), LO signal with phase noise (grey), RF signal (light grey).

A pictorial representation of the dilemma faced by direct conversion receivers and radar systems is shown in Figure 2. In this figure, we can see that if the power level of the RF signal we wish to convert falls below the phase noise spectrum of the LO signal, we will be unable to recover any baseband information, as the signal will be in the noise. Therefore, reducing the phase noise will increase our receiver sensitivity.

In Figure 3, we present a second pictorial example of how phase noise can negatively impact a conversion, this time of a multi-carrier orthogonal frequency-division multiplexed (OFDM) signal.

In this figure, we note that if the phase noise of the LO is too high, then the noise will be converted into adjacent channels of the baseband data, thereby ruining the integrity of the information.

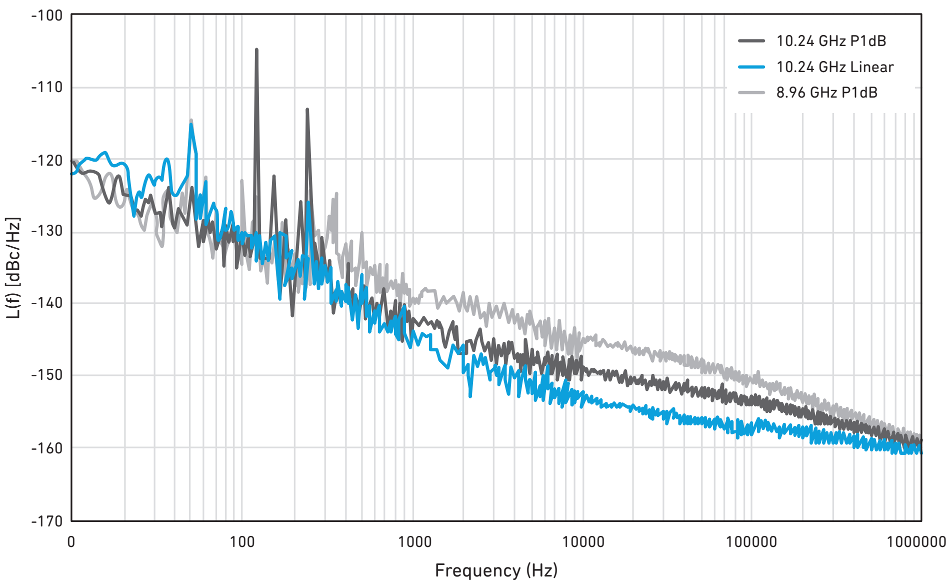

Figure 4. CMD167 LNA phase noise.

Amplifiers and Phase Noise

One obvious place to limit phase noise is in the choice of oscillator. This problem can be addressed by spending considerable time and money to design or procure a low noise oscillator. However, most oscillators do not generate enough output power, and indeed let us assume that for a particular application, the oscillator output of +5 dBm needs to be amplified to a level of +15 to +17 dBm, in order to drive the LO port of a mixer. The question then becomes, does the amplifier affect the phase noise of the LO signal?

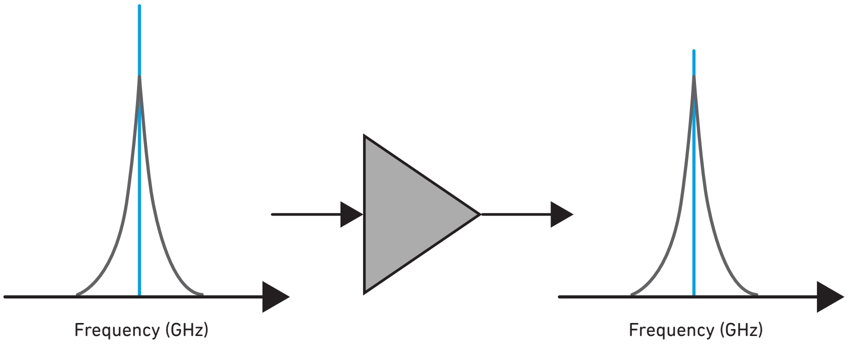

Figure 5. Pictorial representation of the degradation of phase noise due to an amplifier. The skirts of the input signal on the left are increased after passing through the amplifier, with the output spectrum on the right.

In an ideal situation, the answer would be "no," as the amplifier would simply raise desired LO signal and the skirts by the same level. However, in reality, microwave amplifiers add noise of their own to any signal, and herein lies the problem. All electronic devices exhibit a phenomenon called 1/f noise or "pink noise", which is noise power that is added to an input signal spectrum but falls off proportionally to the inverse of the offset frequency. In Figure 4, we present the phase noise of the CMD167, a low noise amplifier covering the 10 to 17 GHz range, versus offset frequency away from the desired signal. The phase noise of the incoming signal has been canceled out, so this plot represents the noise generated by the amplifier.

In Figure 4, we note the phase noise falls off linearly on the logarithmic scale with increasing frequency offset, which is characteristic of 1/f noise. If this noise level is higher than the phase noise of the input signal, then the amplifier noise would dominate the output noise spectrum. In our example, this means the low phase noise of the oscillator would be replaced by the higher phase noise of the amplifier, thereby defeating the purpose of the low phase noise oscillator. A pictorial representation of this phenomenon is shown in Figure 5.

One obvious question is, can anything be done to lower the phase noise of amplifiers? The answer lies in device physics. The 1/f noise is caused by random and thermal charge movement in the channel of an active device. The CMD167, for example, is manufactured on a GaAs pHEMT process with a gate length of 0.13 um. The FET devices on this process typically have a high 1/f corner due to their high electron mobility. GaAs bipolar devices, on the other hand, tend to have lower electron mobilities, which means a much lower 1/f noise, so they are considerably better for phase noise than their FET counterparts. Therefore, one solution to lowering the additive phase noise is to use a GaAs HBT process.

At Qorvo we have used our extensive knowledge of amplifier design techniques to create a family of new low phase noise amplifiers (LPNAs) on a GaAs HBT process operating from 6 to 40 GHz. In Table 1, we present the summary characteristics of these new amplifiers.

Product	Frequency (GHz)	Saturated Output Power (dBm)	Phase Noise (dBc/Hz@10 kHz offset)
CMD245	6-18	20-22	-165
CMD246	8-22	18-20	-165
CMD247	30-40	15	<-160

Table 1: Summary of Qorvo's new LPNAs die. SMT packaged versions are also available.

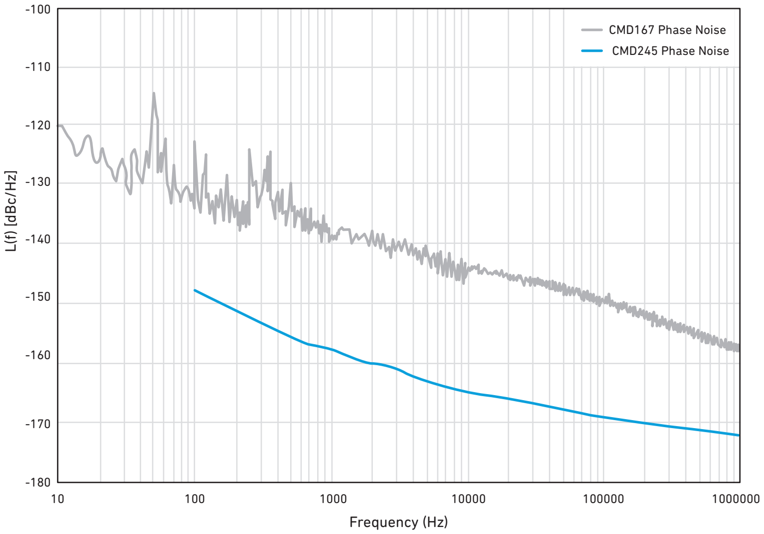

Figure 6. Phase noise of the CMD245C4 low phase noise amplifier vs CMD167 LNA.

In Figure 6, we present the phase noise versus offset frequency for the CMD245 amplifier as housed in a 4 mm QFN-style package, relative to the CMD167 HEMT LNA shown previously. We note the phase noise of the CMD245C4 is 15 to 20 dB lower than the CMD167 pHEMT LNA.

Other Components and Phase Noise

Other components besides oscillators and amplifiers can contribute to phase noise, including frequency multipliers. Many microwave systems utilize a lower frequency oscillator that is then multiplied to produce a higher frequency. One common approach for multiplication is to use a harmonically terminated amplifier to generate the required output frequency. Unfortunately, such an approach will then add the amplifier's phase noise to the multiplied signal, which will degrade the phase noise of the original oscillator.

A second approach is to use passive multiplication, which has the potential to add minimal additional phase noise to the multipliers signal (aka doublers). Qorvo, has also created a family of passive HBT style frequency multipliers which do not add to the phase noise of the input signal. In Table 2, we present a summary of these multipliers.

Product	Output Frequency (GHz)
CMD225	8-16
CMD226	14-22
CMD227	16-30

Table 2: Summary of Qorvo's passive multiplier die family. SMT packaged versions are also available.

Realizing the SWaP-C Benefits of Designing with Positive Gain Slope MMIC Amplifers

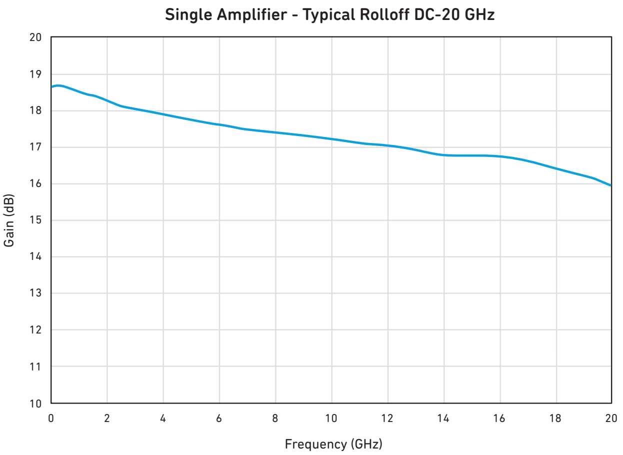

Figure 1. Frequency response of a typical distributed amplifier.

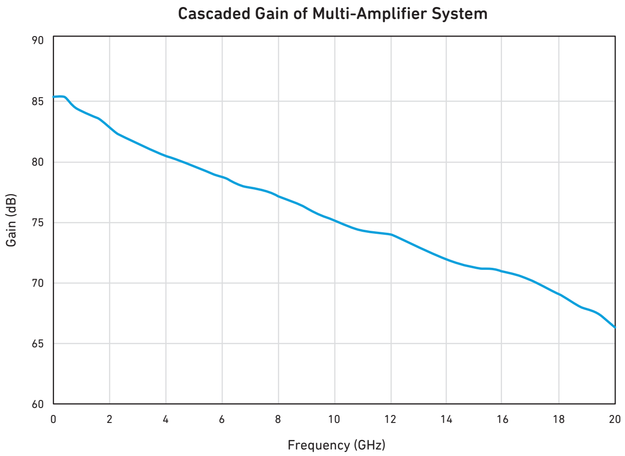

Figure 2. Frequency response of a typical wideband lineup.

Introduction

Modern wideband microwave systems often require a flat overall gain response with respect to frequency. Achieving this performance can be difficult, however, since most wideband microwave components exhibit a negative gain slope as the frequency increases. In this technical brief we discuss a means of achieving a flat system response using distributed amplifier MMICs which exhibit positive gain slope characteristics.

Figure 1 shows a typical wideband distributed amplifier response. As a standalone component its negative gain slope of approximately 3 dB is not a limiting factor. Unfortunately for designers of wideband microwave systems, a single amplifier rarely meets the overall system requirements. A wideband system will typically incorporate multiple amplifiers, passive elements and transmission lines in the signal chain. This cascade of elements with a negative gain slope versus frequency can quickly become a serious problem for the designer.

Figure 2 shows the frequency response of five typical microwave amplifiers in cascade with passive components and transmission lines, and demonstrates that while a single amplifier only had a gain delta versus frequency of 3 dB peak to peak, this cascaded lineup has a gain delta of greater than 20 dB from DC to 20 GHz.

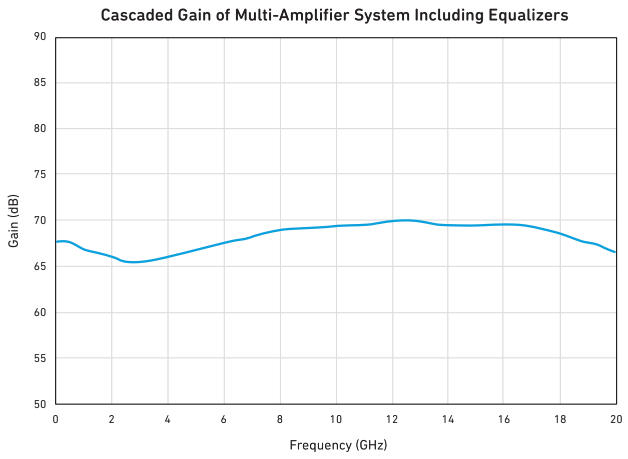

Figure 3. Frequency response of a wideband lineup including equalizers.

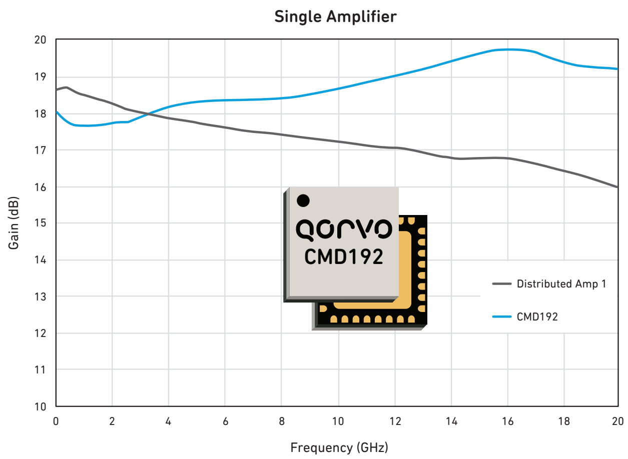

Figure 4. CMD192 vs. a typical distributed amplifier.

Traditional Methods for Flattening out the Gain

The most common solution to this problem is to add passive equalization to flatten the response across the frequency band. While this technique can solve the problem of flatness, it can also introduce three major concerns.

1. The first is the need for additional components that will increase the size and cost of the overall system. This is true whether building a discrete equalizer using resistors, inductors and capacitors, or buying an off-the-shelf die or surface-mount equalizer.

2. The second concern is the additional loss these components will add, which will undoubtedly have a negative impact on system sensitivity and noise.

3. Finally, these components require careful selection and analysis as they will also affect the power handling and linearity of the overall system.

Figure 3 shows the frequency response of the system once equalizers have been added to flatten the response. The equalizers selected were commercial off-the-shelf equalizers available in die form with less than 0.1 dB of loss at 20 GHz. Since each equalizer contributes roughly 3.5 dB of equalization over the band from DC to 20 GHz, five equalizers were used to balance the negative gain slope of the five amplifiers and the added passive components. This added up to 20 dB of loss at the low end of the frequency range while minimizing the impact at high frequency.

While this approach does provide a flat gain response versus frequency, it is not ideal due to the additional unwanted loss and other system concerns previously discussed.

Utilizing the Natural Behavior of a MMIC with Positive Gain Slope

As a more elegant solution to this problem, wideband microwave system designers should consider using positive gain slope distributed amplifier MMICs, which effectively create the necessary equalization in each stage without the need for additional components. As one example, consider the positive gain slope of Qorvo's CMD192.

In Figure 4, we first compare the gain of a single CMD192 versus the typical distributed amplifier of Figure 1. The nominal gain of each amplifier is around 18 dB, however the typical distributed amplifier shows approximately 3 dB of negative gain slope across the band while the CMD192 exhibits a positive gain slope of greater than 1.5 dB across the same band, which results in a gain differential of greater than 3 dB at 20 GHz.

The benefit of this positive gain slope becomes apparent when the CMD192 is cascaded in a system.

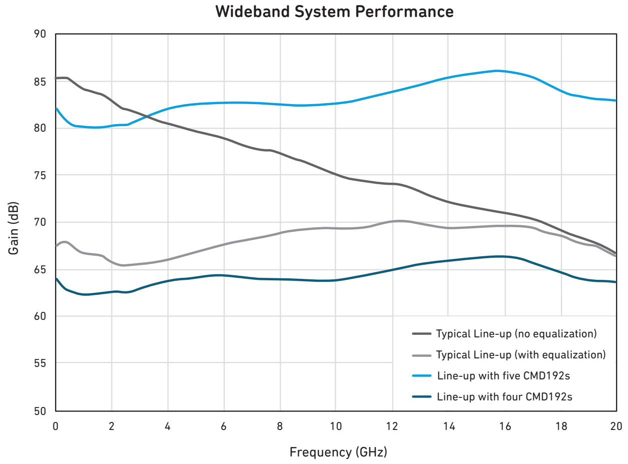

Figure 5. Overall system performance including equalization.

In Figure 5, we compare the overall gain of a few cascaded systems, including one comprised of five typical distributed amplifiers, one with five distributed amplifiers and equalization, one with five CMD192s and one with just four CMD192s. The solutions using CMD192s require no equalization, which results in approximately 15 dB more gain than the equivalent system built with the negative gain slope amplifier when using five stages. For this reason, an equivalent system can be created using only four CMD192s, further reducing the total component count. In either case, since no equalization is needed, the system complexity, cost and size of implementation are greatly reduced.

Conclusion

In this tech brief, we discussed the need for flat gain in wideband microwave systems. Typically, this performance is achieved using equalizers to cancel the effects of negative gain slope components, however, a more efficient solution utilizes positive gain slope amplifier MMICs that eliminate the need for equalization. This approach reduces the size, weight and cost of the system directly through elimination of a series of now unnecessary passive components. In addition, for systems that require multiple amplifier stages, the elimination of additional loss could reduce the total number of gain stages required. This will decrease a microwave system's power consumption in addition to reducing size, weight and cost, and help you achieve your SWaP-C goals.

See Table 1 below for a list of Qorvo's positive gain slope amplifiers as well as a switch with positive gain slope that can also be used to eliminate an equalizer.

Part Number	Function	Frequency (GHz)	Gain (dB)	P1dB (dBm)	Bias (V)	Current (mA)	Package
CMD192/C5	Distributed Amp	DC-20	19	24.5	5-8/-1	200	Die/5x5 mm
CMD240/P4	Distributed Amp	DC-22	15	19	5-8/-0.65	80	Die/4x4 mm
CMD241/P4	Distributed Amp	2-22	13.5	21	5-8/-0.65	74	Die/5x5 mm
CMD244	Distributed Amp	DC-24	18	25	5-8/-0.65	185	Die
CMD246/C4	Low Phase Noise Amp	8-22	17	13	3-5/3	48	Die/4x4 mm
CMD275P4	Low Phase Noise Amp	DC-26.5	16	18	5/3	74	4x4 mm
CMD195/C3	Switch (SPDT)	DC-20	-2	25	0/-5	0	Die/3x3 mm

Table 1. Positive gain slope components from Qorvo.

Understanding the Phenomenon of High-Power Pulse Recovery in GaN LNAs

Introduction

The GaN HEMT is well known for its use in microwave and millimeter-wave power amplifiers due to its high breakdown voltage and ability to handle high RF power. Recently, GaN technology has also been used to create low noise amplifiers (LNAs) in the microwave region, as the noise properties of GaN are similar to other semiconductor materials, most notably GaAs [1-2]. In many microwave systems, LNAs are subject to unwanted high input power levels such as jamming signals. One of the features of LNAs made from GaN is the ability to withstand these input power levels without the need for a limiter, due to the inherent robustness of the device [2]. Indeed, this is one reason GaN LNAs are supplanting their GaAs counterparts, since GaAs LNAs typically require a front-end limiter, which adds to the cost and degrades the performance of the LNA.

Despite the ability to operate without a limiter, GaN LNAs, however, are not completely immune to the effects of high input power. The problem occurs when both a high-power jamming signal and the desired signal are input to the GaN LNA, and then the jamming signal is suddenly turned off. Under this scenario, the GaN amplifier does not recover immediately, as there is some residual distortion of the desired signal before normal operation returns. This phenomenon is known as pulse recovery time and is fast becoming an important parameter with regards to LNAs in general.

Past researchers have studied pulse recovery times in GaN LNAs, although this work has been limited in scope. One study presented recovery times of less than 30 ns in some amplifiers [3-4], but these measurements only utilized a coherent jammer, and the overall number of measurements was limited. A second investigation of pulse recovery time was performed on a GaAs LNA with a limiter [5]. The limiter not only effected the small signal performance, but it also increased the recovery time when high power was applied. Further research has been performed on the degradation of GaN HEMT noise performance after exhibiting DC and RF stress, which can cause forward gate current and damage the gate device [6]. However, this work did not explicitly address pulse recovery times in LNAs. Other papers have similarly analyzed the survivability of GaN amplifiers to high input power overdrive [7-10], but again this work offers little understanding of pulse recovery times. A summary of the relevant previous work is shown below in Table 1.

Reference	Jamming Signal	Frequency	Incident Power of Jammer	Duration of Jammer
[3]	Coherent	8 GHz	+39 dBm	250 ns -3 us
[4]	Coherent	3 GHz	+20 to +33 dBm	250 ns -3 us
[5]	Non-Coherent	12 GHz (jammer) 7 GHz (signal)	+40 dBm	10 us
This work	Non-Coherent	8.5 GHz (jammer) 7.5 GHz (signal)	+15 to +27 dBm	1, 2, 4, 6, 10, 100, 200, 400, 600 us

Table 1: Summary of previous work.

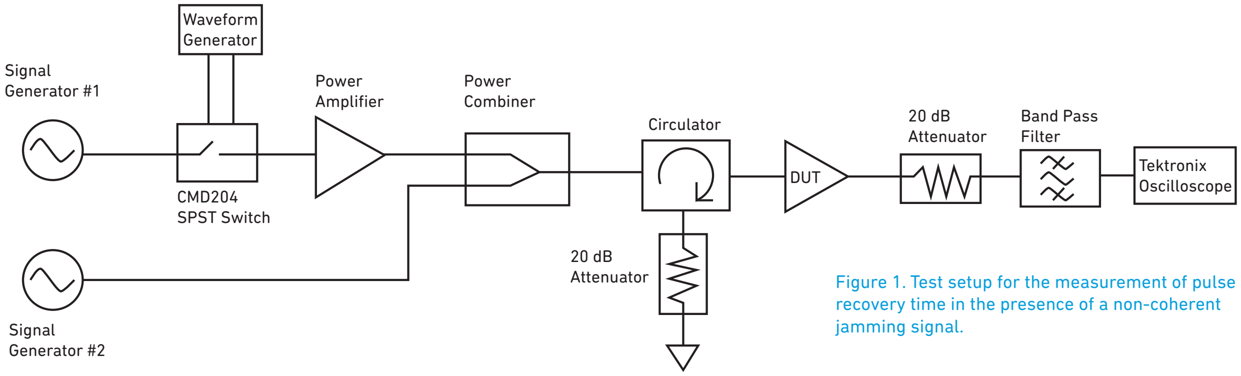

Figure 1. Test setup for the measurement of pulse recovery time in the presence of a non-coherent jamming signal.

Interferer Power (dBm)	Pulse Width (us)	Pulse Repetition (Hz)	Interferer Energy (uJ)
17	6	500	0.30
15	10	500	0.32
23	2	500	0.40
20	4	500	0.40
17	10	500	0.50
27	1	500	0.50
20	6	500	0.60
26	2	500	0.80
23	4	500	0.80
20	10	500	1.00
27	2	500	1.00
23	6	500	1.20
26	4	500	1.59
23	10	500	2.00
27	4	500	2.00
26	6	500	2.39
27	6	500	3.01
26	10	500	3.98
27	10	500	5.01

Table 2: Summary of test conditions - short pulses.

Interferer Power (dBm)	Pulse Width (us)	Pulse Repetition (Hz)	Interferer Energy (uJ)
15	100	100	3.16
17	100	100	5.01
15	200	100	6.32
20	100	100	10.00
17	200	100	10.02
15	400	100	12.65
15	600	100	18.97
23	100	100	19.95
20	200	100	20.00
17	400	100	20.05
17	100	100	30.07
26	600	100	39.81
23	200	100	39.91
20	400	100	40.00
27	100	100	50.12
20	600	100	60.00
26	200	100	79.62
23	400	100	79.81
27	200	100	100.24
23	600	100	119.72
26	400	100	159.24
27	400	100	200.47
26	600	100	238.86

Table 3: Summary of test conditions - long pulses.

Measurement Test Setup

A functional description of the test setup is shown above in Figure 1. This setup uses two signal generators, where the first (labeled as #1) provides the out-of-band interfering signal at 8.5 GHz, and the second (#2) provides the desired continuous wave (CW) in-band signal at 7.5 GHz. The interfering RF signal from #1 is pulsed using a single pole single throw (SPST) switch controlled by a square wave with a low duty cycle. We chose to pulse the signal path, as opposed to the bias circuitry of the interferer amplifier, due to the fast rise/fall time of the SPST, which is on the order of 1.8 ns. Additionally, pulsing the power supply caused high levels of ringing to appear at the output. The interfering signal was amplified by an external PA and then added to the desired signal with a passive power combiner. We utilized a circulator, terminated in a 20 dB pad and a high-power 50 Ohm load, between the combiner and the device under test (DUT) in order to prevent any high-power mismatch signal from reflecting back into the PA. The output of the DUT was then attenuated with an additional 20 dB pad, sent through a band pass filter with a pass band of 7.25 to 7.75 GHz, and then input into a digitizing oscilloscope. The filter attenuates the interfering signal to allow for an accurate measurement of the pulse recovery time.

Finally, we utilized two different oscilloscopes for the measurement. A Tektronix digital serial analyzer oscilloscope was used to measure the recovery time for the shorter pulse widths, while a Hewlett Packard Digitizing Oscilloscope was used to measure the recovery time when longer pulses were used.

The test procedure consisted of varying the pulse width and the input power of the interfering signal, while keeping the power of the desired signal constant at -10 dBm. A summary of the test conditions including pulse widths, repetition rates, and power levels of the interfering signal are presented in Table 2 (short pulses of 1 to 10 us), and Table 3 (long pulses of 100 to 600 us). In these tables we note the input power of the interfering signal was varied between 15 and 27 dBm, with the total energy delivered to the DUT being the important parameter of concern. All measurements with short pulses were performed on the Tektronix oscilloscope, whereas the long pulse measurements were performed on the Hewlett-Packard oscilloscope.

Measurement Results

In this section we present the measurements of pulse recovery time for a commercially available GaN MMIC amplifier with a 5 to 9 GHz bandwidth [11]. The amplifier was assembled into a metal housing, with 2.4 mm connectors used to interface with the test equipment. Three separate units were tested, with the results being consistent among all units. Therefore, we present the results for one unit in the interest of brevity.

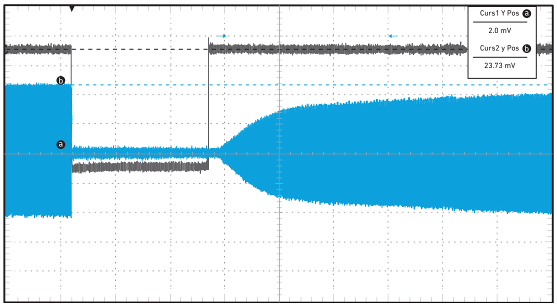

Figure 2. Typical oscilloscope trace for the measurement of pulse recovery time. Desired signal in blue, interferer pulse in magenta.

We begin, in Figure 2, by presenting an example of a pulse recovery time measurement. In this figure, the interferer pulse is shown in magenta, whereas the desired signal is shown in red. We can see that desired signal is heavily distorted when the interferer is activated, and then recovers once the interferer is disengaged. The recovery is measured as the rise time from 10% to 90% of the signal level.

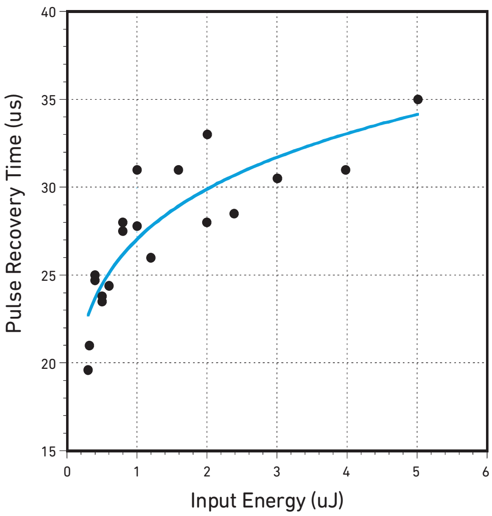

Figure 3. Recovery time versus input energy for short pulses (<= 10 us).

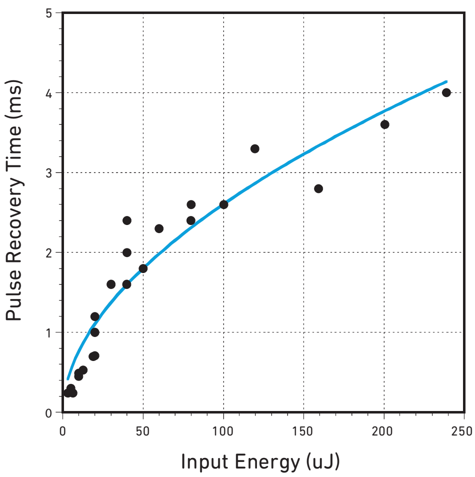

Figure 4. Recovery time versus input energy for long pulses (>= 100 us).

In Figure 3, we present the pulse recovery times versus input energy under short pulse conditions. We note the recovery time appears to increase monotonically with increasing input energy, though the relationship appears to be nonlinear. Indeed, we curve fit the data to a radical function. The form of this function is given below in Eq. 1, where y is the pulse recovery time, x is the input energy, C is a constant, and m is the radical order.

$$y = C \times \sqrt[m]{x} \quad (1)$$

One feature of this equation is that it predicts a recovery time of 0 us when the incident energy is 0 uJ. For the short pulses results as shown in Figure 2, C = 27, and m = 0.145.

In Figure 4, we next present the pulse recovery times versus input energy under long pulse conditions. We note the recovery time increases monotonically with increasing energy, and follows the same trend as the short pulses, with the same governing trend as described by Eq. (1). However, the fitted results give different constants in Eq. (1) for the long pulses, with C = 0.224 and m = 0.53.

In considering the results for short pulses versus long pulses, we did notice that the recovery time was not solely dependent on the incident energy. Indeed, there were two sets of short pulse and long pulse measurements with the same incident energy, but much different recovery times. These results are presented below in Table 4.

In this table, we note that the longer pulses with lower power had a much longer recovery time than the shorter pulses with higher power, even though they had near identical incident energy. Therefore, it appears that pulse recovery time, while being dependent on incident energy, is also dependent on the incident action (energy times duration, uJ-us) of the interfering signal. This is an interesting phenomenon we will explore in future work.

Conclusion

In this article we presented a methodology for measuring the pulse recovery times of GaN low noise amplifiers in the presence of high power, out-of-band jamming signals. Pulse recovery time is becoming an important metric for assessing system performance. In our examination of a commercially available 5 to 9 GHz GaN LNA, we considered jamming signals that operated under short pulse (< 10 us) and long pulse (> 100 us) conditions. We found that in each case, the recovery time was mathematically related to the input energy through a radical relationship. However, the pulse recovery time also appears to be a function of the input action (uJ-us), as short and long pulses with the same incident energy had recovery times that were different by an order of magnitude. In the future, we will explore this phenomenon through more measurements of GaN low noise amplifiers.

Interferer Power (dBm)	Pulse Width (us)	Interferer Energy (uJ)	Interferer Action (uJ-us)	Recovery Time (us)
15	100	3.162	316.228	240
26	10	3.981	39.811	31
17	100	5.012	501.187	300
27	100	5.012	50.119	35

Table 4. Summary of short and long pulse recovery measurements with equal incident energies.

References

"On the Measurement of Pulse Recovery Times in Gallium Nitride Low Noise Amplifiers" by Nicholas Novaris, Paul Blount, and Charles Trantanella of Custom MMIC. Copyright (c) 2017 European Microwave Association.

[1] C. Trantanella and P. Blount, "The End ofthe Limiter as We Know It?" Microwave Product Digest (July 2015): 8, 28, 30.

[2] C. Trantanella and P. Blount, "Low Noise GaN Amplifiers with Inherent Overdrive Protection," Microwave Journal 58, no. 5 (May 2015): 78-88.

[3] A. Liero, M. Dewitz, S. Kuhn, N. Chaturvedi, J. Xu, M. Rudolph, "On the Recovery Time of Highly Robust Low-Nose Amplifiers," IEEE Trans. Microw. Theory Tech., vol. 58, no. 4, pp. 781-787, Nov. 2010.

[4] O. Axelsson, N. Billstrom, N. Rorsman, M. Thorsell, "Impact of Trapping Effect on the Recovery Time of GaN Based Low Noise Amplifiers," IEEE Microw. Wireless Components Letters, vol. 26, no. 1, pp. 31-33, Nov. 2016.

[5] J. Looney, D. Conway, I. Bahl, "An Examination of Recovery Time of an Intergrated Limiter/LNA," IEEE Microw. Mag., vol. 5, no. 1, pp. 83–86, Mar. 2004.

[6] O. Axelsson, M. Thorsell, K. Andersson, N. Rorsman, "The Effect of Forward Gate Bias Stress on the Noise Performance of Mesa Isolated GaN HEMTs," IEEE Trans. On Device and Materials Reliability, vol. 15, no. 1, pp. 40-46, Nov. 2015.

[7] M. Rudolph, R. Behtash, R. Doerner, K. Hirche, J. Wurfl, W. Heinrich, Trankle, "Analysis of the Survivability of GaN Low-Noise Amplifiers," IEEE Microw. And Theory Tech., vol. 55, no. 1, pp. 37-43, Nov. 2007.

[8] C. Andrei, O. Bengtsson, R. Doerner, S.A. Chevtchenko, W. Heirrich, Rudolph, "Dynamic Behaviour of a Low-Noise Amplifier GaN MMIC under input power overdrive" European Microwave Conference, pp. 231-234, Sept. 2015.

[9] K. Lee, J. Rhee, K. Ko, "Damage Modeling on a Radar affected by High Power Electromagnetic Pulse" IEEE Pulsed Power Conference, pp. 1-4, 2005.

[10] J.H. McAdoo, W.M. Bollen, R.V. Garver, "Single-Pulse RF Damage of GaAs FET Amplifiers" IEEE MTT-S International Digest, vol. 1, pp. 289-292, 1988.

[11] CMD218 datasheet, http://www.custommmic.com/uploads/pdf/cmd218-5-9-ghz-gan-low-noise-amplifiermmic.pdf (accessed February 8, 2017).

Simplify Amplifier Biasing Using Positive Bias pHEMT MMICs

In modern telecommunication systems, the range of parameters an engineer must consider while optimizing a design is staggering. Not only must electrical specifications be achieved, but physical and thermal constraints must be given special attention and significant design effort, especially since they are often at odds with overall system requirements.

As a result, any design technique that aids in reducing system complexity – without reducing performance – can eliminate costs, failure modes, and waste in the design cycle. The use of enhancement mode pseudomorphic high-electron-mobility-transistors (E-pHEMT) in MMICs is one such promising technique, for it may directly address a well-known design challenge. Specifically, that of sequencing in amplifier biasing, as demonstrated in Figure 1.

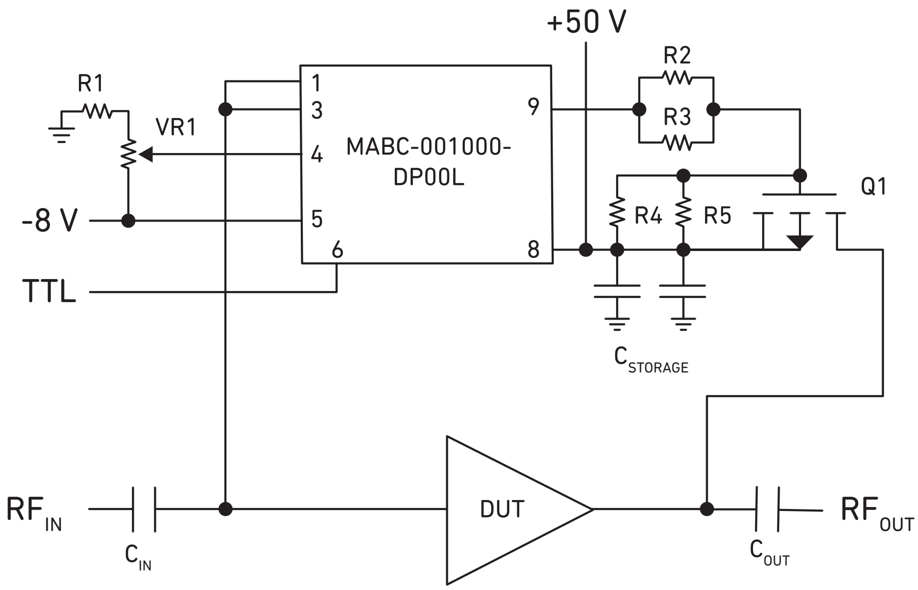

Figure 1. Amplifier bias controllers/sequencer modules are generally complex and expensive circuitry to purchase or develop in-house.

Traditionally, amplifiers constructed from depletion mode pHEMTs (D-pHEMT) and HEMT require sequencing circuits to ensure the bias voltages are energizing the transistors in the proper order. A typical bias timing scheme is shown below in Figure 2.

Failure to bias such an amplifier in the correct manner, often results in transistor damage. For instance, the device channel is normally conductive and will sink large levels of current, if not first biased into pinch-off mode. A depletion mode device also requires that RF power to be applied after the device has entered the appropriate portion of the sequence, and must also be powered down with the exact reverse sequence. Any deviations in the timing sequence could induce damage to the amplifier.

The timing problem becomes even more complicated when the microwave system contains multiple D-pHEMT amplifiers, such as phased array radars. Not only does the sequencer have to control hundreds, if not thousands, of amplifiers in parallel, but any delays or offsets in the bias scheme could have profound impact on the overall sensitivity of the radar.

A solution to this vexing problem can be found in physics. Many MMIC processes now offer both D-pHEMT transistors and enhancement E-pHEMT devices on the same substrate. In terms of RF performance, these transistors are comparable – and in some instances, E-pHEMT amplifiers can outperform their D-pHEMT cousins in maximum gain, noise figure, and linearity.

Typical Bias Timing Scheme using D-pHEMT or HEMT Amplifiers

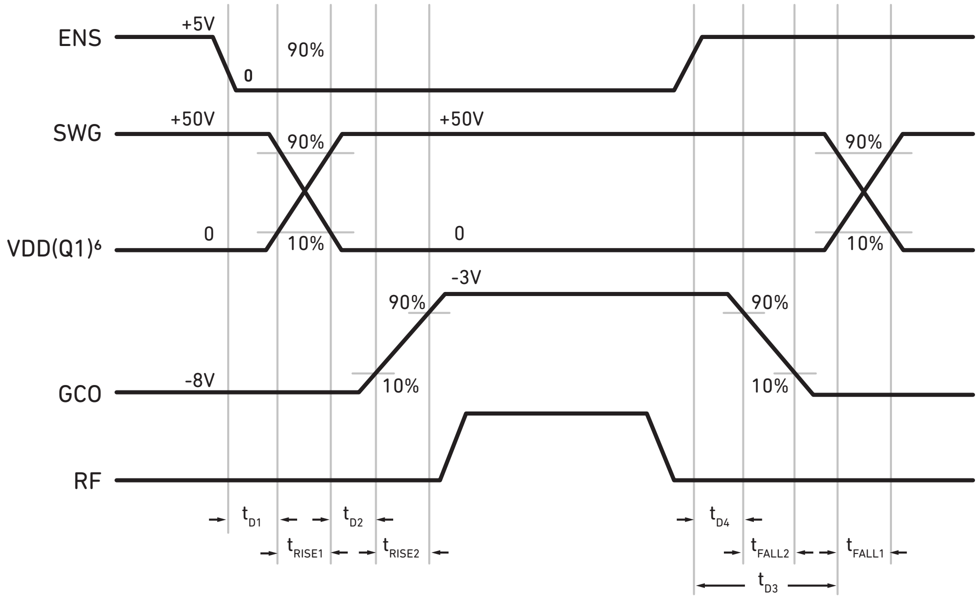

Figure 2. As dual bias amplifiers require a precise sequence before energizing each port, timing diagrams and activation sequences require digital controllers to prevent damage from improper sequencing.

Unlike depletion mode devices, E-pHEMT transistors are normally non-conductive, and will ultimately reduce current when both the drain and the gate are biased (regardless of sequence). As a result, the sequencer circuit can be eliminated altogether.

The savings generated by removing the sequencer can be enormous. For example, positive bias techniques enable a reduced bill of materials, a simplification of the circuitry, and a reduction the number of extraneous noise sources. These eliminations allows the designer to focus on more important aspects of the system, such as optimizing the RF signal chain at large.

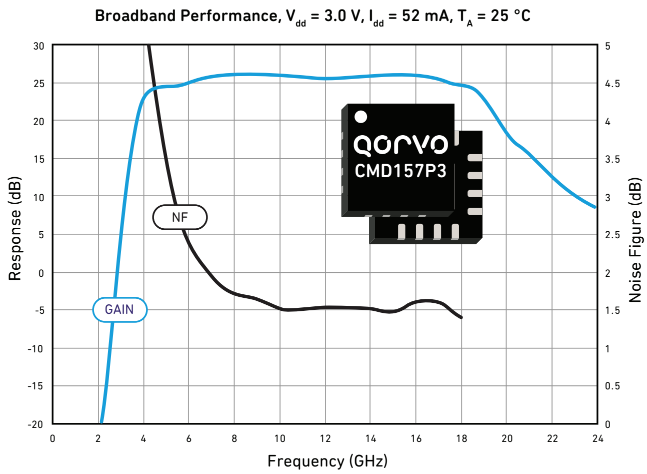

Figure 3. A perfect combination of high gain and high linearity can be achieved with E-pHEMT amplifiers.

The use of E-pHEMT devices by designers of power amplifiers (PAs) and low noise amplifiers (LNAs) is in its infancy, as such devices have only recently been made available from a number of semiconductor manufacturers. However, Qorvo has been a pioneer in this area and currently offers dozens of standard, off-the-shelf PA and LNA components built with E-pHEMT technology.

In many of these designs, the high gain and high linearity E-pHEMT amplifiers have matched – and even exceeded similar depletion mode designs.

Conclusion

Not only can E-pHEMT amplifiers reduce cost and complexity, they can also improve performance.

all around you